Universitat Autònoma de Barcelona

Application of Quality by Design and Near Infrared Spectroscopy in Manufacturing and Control of Freeze-Dried Drug Products

Glòria Clua Palau

Universitat Autònoma de Barcelona

Application of Quality by Design and Near Infrared Spectroscopy in Manufacturing and Control of Freeze-Dried Drug Products

Glòria Clua Palau

PhD THESIS

Programa de Doctorat de Química

Director: Prof. Santiago Maspoch Andrés

Departament de Química

Facultat de Ciències

2018

Memòria presentada per aspirar al Grau de Doctor per **Glòria Clua Palau**

Glòria Clua Palau

Vist i plau,

Prof. Santiago Maspoch Andrés

Bellaterra, 4 de Juny de 2018

Aquest projecte de recerca s'ha elaborat en col·laboració amb l'empresa Laboratorios Reig Jofre en el marc del Pla de Doctorats Industrials, convocatòria DI 2014.

Responsable i tutor del projecte a l'empresa:

Dr. Enric Jo Cardoso

Bellaterra, 4 de Juny de 2018

“We are just an advanced breed of monkeys on a minor planet of a very average star. But we can understand the Universe. That makes us something very special”

Stephen Hawking

Agraïments

Aquesta tesi doctoral s'ha realitzat gràcies al finançament de les següents institucions i empreses:

- *Ajut de Doctorat Industrial concedit per l'Agència de Gestió d'Ajuts Universitaris i de Recerca (AGAUR) del Departament d'Empresa i Coneixement de la Generalitat de Catalunya (2014 DI 12)*
- *Departament d'Innovació, Universitats i Empresa de la Generalitat de Catalunya*
- *Projecte CTQ 2016-79696-P (AEI/FEDER, EU), concedit al grup de Quimiometria Aplicada del Departament de Química de la Universitat Autònoma de Barcelona, Bellaterra (2014 SGR 00249 – 2017 SGR 280)*
- *Laboratorios Reig Jofre, Sant Joan Despí, Barcelona.*

Juntament amb la col·laboració i recolzament de molts professionals i amics.

Des que vaig començar aquesta aventura, pensava que escriure els agraïments de la tesi em suposaria un moment trist i melancòlic. Però, de fet, fer un tomb pels últims tres anys i mig de la meva vida, m'està resultant molt enriquidor. A més, he decidit escriure'ls quan encara em queden petits detalls per a finalitzar la redacció del treball, cosa que m'està ajudant a agafar forces i motivació per valorar i estimar cada pàgina que composa aquesta tesi.

No crec gaire en el destí, però si en les decisions, guiades primerament pel cor però també recolzades per l'hipotàlem, el lòbul frontal i el sistema límbic. Si, en el fons soc biòloga humana, però m'agrada aprendre de totes les àrees del coneixement encara que acabin esdevenint, gairebé sempre, reptes personals.

Al llarg dels últims anys m'he qüestionat vàries vegades si iniciar el projecte de tesi doctoral havia estat una bona decisió. Doncs bé, arribats a aquest punt, no tinc cap dubte sobre la meva resposta. Haver conegut i treballat amb grans professionals, tan del sector industrial com acadèmic, i haver compartit aquesta experiència amb els companys de laboratori i empresa, ha estat tot un plaer i només tinc paraules d'agraïment i estima per a tots ells.

Vull agrair d'una manera molt especial i sincera al Professor Santiago Maspoch, per haver acceptat la direcció de la tesi i per a tot el seu recolzament i confiança en el meu treball. Gràcies per haver-me guiat en tot aquest camí i per totes les aportacions de gran valor que han permès el desenvolupament de la tesi. Gràcies Santi, de tot cor.

De la mateixa forma vull agrair al Dr. Enric Jo que acceptés la tutoria d'aquesta tesi. Tot i la seva ocupada agenda, sempre ha trobat un espai per oferir-me la seva visió científica i empresarial sobre la importància del projecte. Moltes gràcies per obrir-me la porta a Reig i confiar en mi.

Voldria agrair molt sincerament als responsables del Servei d'Anàlisi Tèrmic i Calorimetria del IQAC, Dr. Josep Carilla i Dra. Sònia Pérez, i al director tècnic del Servei de Difracció de Raigs X de la UAB, Dr. Ángel Álvarez, per a la seva orientació constant i l'ajuda tècnica, que han estat essencials en el desenvolupament d'aquesta tesi. També, i de manera molt afectuosa, al Professor Jordi Coello, per tot els seu esforç, compromís i dedicació en el projecte de tesi. Gràcies per tot el coneixement que m'has transmès Jordi!

D'altra banda, voldria transmetre un immens GRÀCIES als meus companys de feina del Laboratori de Liofilització i companys de despatx al llarg d'aquest període de tesi. Ells han viscut el meu dia a dia, tan les celebracions com les angoixes, i sempre m'han recolzat. Moltes gràcies a la Laia Garcia, Anna Flo, Anna Anglada, Carmen Blanes, Laura Rioja, Pere Armengou, Emma Romeu, Gemma Martínez, Cristina Cañadas i Miquel Viñas. En especial vull agrair al meu responsable a l'empresa, Sasha Nikolic, per ensenyar-me tot el que sé sobre liofilització i per tots els seus consells, confiança i paraules de suport. Després de llargues reunions, queixes, llàgrimes, alegries,... sento que sempre has estat allà per escoltar-me, gràcies per tanta paciència.

No vull oblidar-me de tot el personal dels diferents departaments de Reig: control de qualitat, producció, garantia de qualitat, transferència tecnològica, informàtica, investigació i desenvolupament..., sense la seva ajuda aquesta tesi no hagués estat possible. L'Alba i la Montse, dues peces clau que sempre m'han ajudat amb els anàlisis al laboratori. A tots els tècnics de control, en especial a la Montse Andreu i a la Mònica Montes, per a la seva disposició, comprensió i capacitat de reorganització.

Tot i que no tinc espai suficient per agrair de manera personal a molts treballadors i amics de l'empresa, no voldria deixar-me a la directora de producció, Nerea Garcia, i a la directora de garantia de qualitat, Maria Jesus Alonso. Nerea, el viatge a Cuba em va permetre conèixer la gran persona que ets i volia agrair-te totes les paraules d'afecte i suport, sobretot en l'últim tram de la tesi. Maria Jesus, molts gràcies per a la teva col·laboració, en especial en la correcció i comentaris en l'etapa de redacció, que m'han permès millorar la feina. En definitiva, voldria donar les gràcies a tot el personal de Reig, que són el cor i motor de l'empresa, i han fet que treballant amb ells em senti com a casa.

Però, a la recepta de la tesi li falta un ingredient fonamental: els meus companys de laboratori a la Universitat. Estimats amics, amb vosaltres he compartit intenses jornades de feina amenitzades amb l'estoneta del cafè, reunions de grups, alguns sopars, rialles...., en definitiva, sou genials! Vull donar les gràcies a la Vanesa, en Dong, en Diego, l'Aira, la Judit Brassier, la Judit Puig, l'Èlia, en Carlos, la Laia i la Desirèe.

Per últim, vull agrair molt especialment a la meva família i amics per tot el seu suport emocional i per haver estat al meu costat durant la realització d'aquest treball. De fet, més que un agraïment, podria ser una disculpa... ja que com bé diuen, qui més t'estima et farà plorar. Lara, Victor, Alba, Laura i

Oriol, sou amb qui més confio, gràcies per estar amb mi sempre. Un dels més grans tresors que m'emporto de l'etapa de la tesi ets tu, Laia Garcia, t'has convertit en una gran amiga i confident, gràcies per no deixar-me caure.

Papes, Anna, cosins, tiets i avis, gràcies per a l'empatia, paciència i estima. Iaia Sión, gràcies per ser el meu referent a la vida i per mimar-me tant, fins i tot des del cel. A la meva família política, al meu primer nebot, l'Arnau, gràcies per estar al meu costat. I, al meu company de vida, Sergi, no tinc paraules per expressar tot el que sento. Per estar sempre quan t'he necessitat, per compartir-ho tot amb mi. Ho saps, oi?, jo també.

I finalment, t'agraeixo a tu, tesi, l'oportunitat que m'has donat per madurar com a científica i també de créixer com a persona. He començat els agraïments explicant que no crec gaire en el destí, però si en les decisions... doncs, ara espero que la meva següent decisió sigui igual d'encertada.

Us estimo molt a tots.

Glòria.

Index

Chapter 3. Freeze-drying of Pharmaceuticals

Chapter 4. Near Infrared Spectroscopy

Materials and methods

Results and Discussion

Chapter 7. Freeze-Drying Cycle Development and Qualification

List of Abbreviations and Acronyms

Absorbance	Abs
Active Pharmaceutical Ingredient	API
Alternative hypothesis	H_a
American Society for Testing and Materials	ASTM
Analysis of Variance	ANOVA
Anderson-Darling	AD
Centre of Excellence in Lyophilisation	CoEL
Chamber Pressure	P_{ch}
Classical Least Square	CLS
Coefficient of correlation	r
Coefficient of determination	R^2
Collapse temperature	T_{co}
Confidence Interval	CI
Critical Material Attribute	CMA
Critical Process Parameter	CPP
Critical Quality Attribute	CQA
Cross Validation	CV
Decision Limit	LD
Derivatives	Der
Design of Experiment	DoE
Design Space	DS
Differential Scanning Calorimetry	DSC
European Medicines Agency	EMA
European Pharmacopoeia	*Ph. Eur.*
Eutectic temperature	T_e
Failure Mode and Effects Analysis	FMEA
Far-InfraRed	FIR
Food and Drug Administration	FDA
Fourier Transform	FT
Freeze-Drying Microscopy	FDM
Gas Chromatography	GC
Glass transition temperature of the dried solid	T_g
Glass transition temperature of the maximally freeze-concentrated solution	T_g'
Good Manufacturing Practices	GMPs
High Performance Liquid Chromatography	HPLC
Infrared	IR
Injectable Freeze-dried Product A	IFDA
Injectable Freeze-dried Product B	IFDB
International Council for Harmonisation	ICH
International Organization for Standardisation	ISO
International Society for Pharmaceutical Engineering	ISPE
International Union of Pure and Applied Chemistry	IUPAC
Inverse Least Square	ILS
Karl Fischer	KF

Kubelka-Munk	K-M
Least Square Regression	LSR
Light Emitting-Diodes	LED
Limit of Detection	LOD
Limit of Quantitation	LOQ
Low Temperature X-Ray Powder Diffraction	LT-XRPD
Lower Capability Confidence Interval Bound	LCCB
Lower Control Limit	LCL
Lower Specification Limit	LSL
Lyophilization technology Hub	LyoHUB
Mannitol Hemihydrate	MHH
Mean Square Error	MSE
Mean Square Error of Cross-Validation	MSECV
Mean Square Error of Prediction	MSEP
Mid Infrared	MIR
Multiple Linear Regression	MLR
Multiplicative Scatter Correction	MSC
Near infrared Spectroscopy	NIRS
Near-infrared	NIR
Nonlinear Iterative Partial Least Squares	NIPALS
Normal Operating Range	NOR
Null hypothesis	H_0
Number of objects	N
One Variable at a Time	OVAT
Orthogonal Signal Correction	OSC
Out of Specifications	OOS
Parenteral Drug Association	PDA
Partial Least Square	PLS
Pirani/Baratron Ratio	P/B
Powder Diffraction Files	PDF
Predicted Residual Error of Sum of Squares	PRESS
Pressure	P
Pressure Rise Test	PRT
Primary Drying	PD
Principal Component Analysis	PCA
Principal Component Regression	PCR
Principal Components	PC
Process Analytical Technology	PAT
Process Capability	C_p
Process Capability Index	C_{pk}
Process Performance	P_p
Process Performance Index	P_{pk}
Process Performance Qualification	PPQ
Product Quality Lifecycle Implementation	PQLI
Product Quality Review	PQR
Product Temperature	T_p
Proven Acceptable Ranges	PAR

Pseudounivariate Limit of Detection	LOD_{pu}
Quality Assurance	QA
Quality by Design	QbD
Quality Control	QC
Quality risk management	QRM
Quality Target Product Profile	QTPP
Real-Time Release Testing	RTRT
Reconstitution time	RT
Reig Jofre	RJ
Relative Standard Deviation	RSD
Relative Standard Error	RSE
Relative Standard Error of Calibration	RSEC
Relative Standard Error of Cross-Validation	RSECV
Relative Standard Error of Prediction	RSEP
Research & Development	R&D
Residual Moisture Content	RMC
Resistance Temperature Detectors	RTD
Risk Priority Number	RPN
Root Mean Square Error	RMSE
Root Mean Square Error of Calibration	RMSEC
Root Mean Square Error of Cross-Validation	RMSECV
Root Mean Square Error of Prediction	RMSEP
Savitzky-Golay	SG
Secondary Drying	SD
Shelf Temperature	T_{shelf}
Spanish Agency of Medicines and Medical Devices	AEMPS
Standard Deviation	std
Standard Error of Calibration	SEC
Standard Error of Cross-Validation	SECV
Standard Error of Prediction	SEP
Standard Error of the Laboratory	SEL
Standard Normal Variate	SNV
Statistical Process Control	SPC
Temperature	T
Thermogravimetric analysis	TGA
Tunable Diode Laser Absorption Spectroscopy	TDLAS
United States Pharmacopoeia	USP
Univariate Limit of Detection	LOD_u
Universitat Autònoma de Barcelona	UAB
Upper Control Limit	UCL
Upper Specification Limit	USL
Water for injection	WFI
X-Ray Powder Diffraction	XRPD

Content Summary

Every industrial manufacturing process of a pharmaceutical drug product must be validated before it can be launched into the market. The validation procedure consists in ensuring that a process is capable of consistently delivering high quality products. Recently, global health authorities and regulators are communicating their expectations for risk and science-based justification for process validation, changing to a new landscape focused in a product lifecycle concept. Then, the process validation approach links product and process development, qualification of the manufacturing process, and maintenance of the process in a state of control during routine commercial production.

In this sense, a true lifecycle approach requires gathering useful knowledge about the product and the process from the very beginning, which is the philosophy of Quality by Design. In brief, Quality by Design states that quality, safety, and efficacy are built into the product instead of tested at the end of the process. The key is to obtain a better understanding of the process, its sources of variation and how to control them, and the correlation between process performance and product quality.

This thesis describes the application of Quality by Design for the development and qualification of the freeze-drying process of two drug products developed in Laboratorios Reig Jofre. In fact, the complete study at industrial scale has been done with one of the products, which is commercialized in two strengths (1 g and 500 mg), while only the studies at laboratory scale had been executed for the other product.

The freeze-drying process is used to transform solutions of active ingredients, with or without excipients, in more stable solid products. This process is divided in three main stages: freezing, primary drying and secondary drying. Firstly, sample is completely frozen prior to primary drying, where the ice formed is removed by sublimation. Finally, secondary drying is carried out at elevated temperatures to remove most of the unfrozen water by desorption. From an economical point of view, freeze-drying is an expensive process with a relatively long processing time. Of the three steps in freeze-drying, primary drying is the longest one, and hence, optimization of this step is the focus in industry.

Understanding the physical properties of substances that are freeze-dried is a key part in developing a successful freeze-drying process, because there is no universal "safe" recipe that will work with every product. Therefore, it is strictly necessary to characterize the thermal properties and the structure of both, the solution and the freeze-dried product, to develop a suitable freeze-drying process.

An important part of the process qualification is the level of sampling. In the freeze-drying unit operation, extensive sampling was needed to guarantee the homogeneity of the drying process. For instance, the number of samples could represent approximately 1% or even more than 5% of a batch of tens of thousands of units. This large number of samples cannot be analysed by the conventional Karl

Fischer method. Consequently, a non-destructive and fast near infrared spectroscopy method was developed to determine the residual moisture content of those samples.

This PhD manuscript has been organised in an introduction composed by five chapters, and an experimental section divided in two chapters with four subsections or parts in each. In the introduction, a brief explanation of the pharmaceutical industry organization and the regulatory framework is provided, specifically for the manufacturing of sterile injectable freeze-dried products. Furthermore, the main components of Quality by Design are explained, as well as the theoretical principles of the freeze-drying process, equipment, development strategies and a description of the quality attributes of this kind of products, with more-emphasis in the residual moisture content (RMC). The introduction also contains a brief description of the near infrared spectroscopy method, and the applications thereof in the pharmaceutical industry. In the last chapter of the introduction, some basic principles of multivariate calibration analysis and design of experiments are also given to introduce the chemometric tools used to analyse the freeze-drying and near infrared spectral data.

As stated before, the experimental section is divided in two chapters (chapter 7 and chapter 8). First, the freeze-drying processes for both drug products were developed at laboratory scale. The second study consists in the development and validation of quantitative near infrared models for residual moisture content prediction in one of the studied drug product, concluding with its applications in the analysis of production samples.

In chapter 7, the development strategy of the freeze-drying process started with the definition of the quality target product profile and critical quality attributes and process parameters for each product. Then, a risk assessment was used to prioritise the parameters for the design of a flexible and robust freeze-drying process for each product. Characterization studies of both formulations were performed to define their thermal fingerprint using a variety of analytical techniques, such as differential scanning calorimetry, freeze-drying microscopy or X-ray powder diffraction. Then, the influence of shelf temperature and chamber pressure on some product quality attributes and process efficiency was studied through a Doehlert design. As no restriction was found for the temperature and pressure ranges studied, the entire experimental region was considered as the process design space in both products. After that, the operational conditions for production manufacturing were selected focusing on process time reduction while preserving the quality of the product.

When sufficient amount of knowledge was gained, the process was scale-up and qualified at industrial scale, for both strengths of the drug product. Then, representative samples from these industrial batches were put into stability studies at different storage conditions, to guarantee that the product will be safe and effective throughout its shelf life. In addition, a laboratory scale batch with parameters set at outer limits of the design space was executed and included in the stability program to expand the studied

region and try to find the edge of failure. Until now, 12 month of stability data have been analysed, and all batches complied with product quality specifications.

In chapter 8, the feasibility of using near infrared spectroscopy for the intended purpose was assessed using risk analysis tools and risk mitigation studies. The effect of several high-risk variables, such as age of samples, duration of NIR spectra acquisition and sample temperature, was evaluated. In addition, it was necessary to optimise and validate the reference Karl Fischer method to obtain accurate, precise and reliable results of individual vials and not pooled samples.

After that, calibration models were developed using partial least square regression, and they were validated in compliance with current pharmaceutical guidelines. Specific models for each strength were first developed, and later, with the final aim of obtaining the most simple and robust model with an acceptable predictive ability, a single model useful for both strengths was built up. During method validation, special attention was placed in the estimation of the limit of detection, because when dealing with small concentrations of a component, like in the case of water in freeze-dried vials, the measurement and reference errors could have a large impact on the predicted result. Therefore, different statistical estimations were used to determine the limit of detection.

Finally, the combined NIR model was applied for two objectives: a) to assess the residual moisture variability among different positions, shelves, and industrial freeze-dryers, and, then, establish the correct sampling plan for routine production, b) to evaluate the potential application of the near infrared spectroscopic procedure to predict the residual moisture content of samples under stability studies. Its application represents a great benefit for the industry, reducing the number of samples in stability programs as well as the use of the same vial for other analysis, which, in turn, allows correlating different quality attributes of the same freeze-dried vial.

Finally, the entire experimental work was included in a variation of the drug product dossier, which was submitted to the Spanish Agency of Medicines and Medical Devices (AEMPS). A significant reduction in the classification of the requested variations was achieved, and, after six months, the variations were approved, and the process is currently implemented in routine production.

Objectives

The objectives of this thesis can be framed in two large subsets, which are obviously related although they are presented separately:

1. The first objective was to set up a methodology for the development and validation of industrial freeze-drying processes following the quality by design principle. This general objective can be broken down into the following partial objectives:
    a. Comprehensive revision of the manufacturing process of two freeze-dried drug products and definition of critical quality attributes and process parameters using risk analysis tools.
    b. Understand and evaluate the different source of variations that could significantly affect the process and the product.
    c. Thermal and structural characterization of both, the freeze-dried solid and the solution of the two formulations under study.
    d. Use of robust experimental designs to study the primary drying stage of the freeze-drying process and definition of the optimal freeze-drying process conditions which maximizes the sublimation rate while preserving the quality of the product.
    e. Estimation of the design space for the primary drying stage and study the impact of secondary drying temperature and drying time in the quality of the product.
    f. Freeze-drying process scale-up and qualification at industrial scale, and application of process control tools to study whether the process is under statistical control.

2. The second objective was to set up and validate an *off-line* near infrared method for the quantitative determination of residual moisture content directly through the intact freeze-dried vials. Partial goals derived from this objective are:
    a. Validation of the reference Karl Fischer method.
    b. Feasibility study using risk analysis to understand the effect of external variable on the performance of the near infrared spectroscopic procedure.
    c. Development and validation of near infrared methods for each of the different strengths of the drug product and for a single model which combines both strengths, following specific pharmaceutical guidelines and protocols.
    d. Application of the combined near infrared model for the qualification of the freeze-drying process for the residual moisture content attribute, for the study of the homogeneity of the drying stage as a function of the position of the vials inside the industrial freeze-dryers, as well as for the analysis of samples undergoing stability studies.

INTRODUCTION

Chapter 1

Sterile Manufacturing of Injectable Drug Products

1. Pharmaceutical industry

Pharmaceutical industry is comprised of companies engaged in researching, developing, manufacturing and distributing drugs for human or veterinary use. In this field, drugs are defined as any substance intended for use in the diagnosis, cure, mitigation, treatment or prevention of diseases, as well as any substance (other than food) intended to affect the structure or function of the body.

More specifically, drug product refers to the finished dosage form that contains at least one drug substance or Active Pharmaceutical Ingredient (API), generally, but not necessarily, in association with other substances named excipients. The latter are inactive substances but provide important properties to the drug product such as stabilization, improvement of quality attributes or drug delivery, among others.[1]

1.1. Laboratorios Reig Jofre

The present Industrial Doctorate's project has been performed in a pharmaceutical company named Laboratorios Reig Jofre (RJ). In brief, RJ is a Spanish company founded in 1929. Its business is divided into the development of antibiotics and injectable products, consumer healthcare products and therapeutic-specialization products in the areas of dermatology, gynaecology, and respiratory system. RJ has 927 employees and 4 manufacturing sites in Europe: one located in Malmö (Sweden), one in Barcelona and two in Toledo (Spain). RJ has direct sales in 6 countries in Europe and over 130 commercial partners in 64 countries worldwide.

The principal specialization in the RJ's industrial plant in Barcelona is the production of sterile drug products, specifically injectable freeze-dried products. It began in 1978 with the acquisition of the first freeze-dryer and continued with a further investment in 2009, to build a second manufacturing plant of sterile drug products. Nowadays, RJ has started an ambitious plan for a short-term exponential growth in the sterile manufacturing area with the aim to get a leader position in the market of sterile freeze-dried pharmaceuticals worldwide.[2] One of the pillars of the company is the Centre of Excellence in Lyophilisation (CoEL) located in Barcelona. This centre is focused on the formulation characterisation for freeze-drying processes development and the continuous improvement of routine manufacturing, in both cases, applying the Quality by Design (QbD) approach. The work included in the present thesis has been conducted in the CoEL department in collaboration with the Quality Control (QC) and the Research & Development (R&D) departments.

The following sections point out information regarding the studied drug products, its manufacturing process, and how its quality is controlled and assured. At the end of the chapter, a summary of the regulatory framework associated with sterile freeze-dried drug products is also included.

2. Injectable freeze-dried product

Sometimes, the only formulation strategy that result in an adequate stability of liquid formulations is water removal.[3] In drug products for parenteral use, this is usually achieved by means of freeze-drying, which is explained in more detail in Chapter 3.

According to European Pharmacopoeia (*Ph. Eur.*) Monograph 0520 [4], freeze-dried products for parenteral use are considered as powders for injections or infusions. The latter are defined as solid, sterile substances distributed in their final containers that, when shaken with a specific volume of a prescribed sterile liquid rapidly form clear solutions or uniform suspensions.

Figure 1.1 provides a representation of different types of primary packaging of injectable freeze-dried drug products. The selection of the primary package is of great importance because it provides protection to the sterile product throughout the shelf life. The most common used containers are glass vials. Furthermore, an elastomeric closure system with an aluminium cap is needed to seal the containers and secure the tightness of the vial. Specific stoppers are used in freeze-dried products characterized by a window hollow to enable solvent to escape during the freeze-drying process.[5]

Figure 1.1. Representation of different types of packaging of freeze-dried drug products (left) and the rubber stopper specific for freeze-dried products (right).

Injectable freeze-dried products are manufactured in sterile conditions. Due to this fact, these type of products are characterised by the following primary properties of sterile products[6]:

1. Safety: freedom from adverse toxicological concerns.
2. Sterility: freedom from microbiological contamination.
3. Nonpyrogenic: free of pyrogenic contamination.
4. Particle-free: freedom from visible particle contamination and below a specification limit for sub-visible particle contamination.
5. Chemical, physical and microbiological stability.
6. Compatibility with formulation, package and other diluents for reconstitution.
7. Tonicity: isotonic with biological fluids.

It is responsibility of the pharmaceutical industry to guarantee the proper achievement of all those properties and to ensure that every product meets quality specifications. According to European commission Volume 4 of Good Manufacturing Practices (GMPs) Annex 1 "Manufacture of sterile medicinal product"[7], it is recommended to study and control the manufacturing process of these pharmaceutical preparations. Careful attention should be placed in several factors, such as: facility design, equipment selection, sterilization procedures, cleaning requirements, management of personnel, environmental and particulate monitoring and detailed in-process controls.

3. Sterile manufacturing process

All pharmaceutical manufacturing operations are complicated, but sterile manufacturing is subject to special requirements to minimise risks of microbiological, particulate and pyrogen contamination.

Unit operations involved in the manufacturing of injectable freeze-dried products include: compounding or dissolution, filtration, filling, freeze-drying, closing and sealing, inspection, labelling, and final packaging for distribution. A typical process flow is shown in Figure 1.2. Due to the sterility requirement, processing also includes cleaning, sanitising or sterilising containers, equipment and facilities to validated specifications.[6,7]

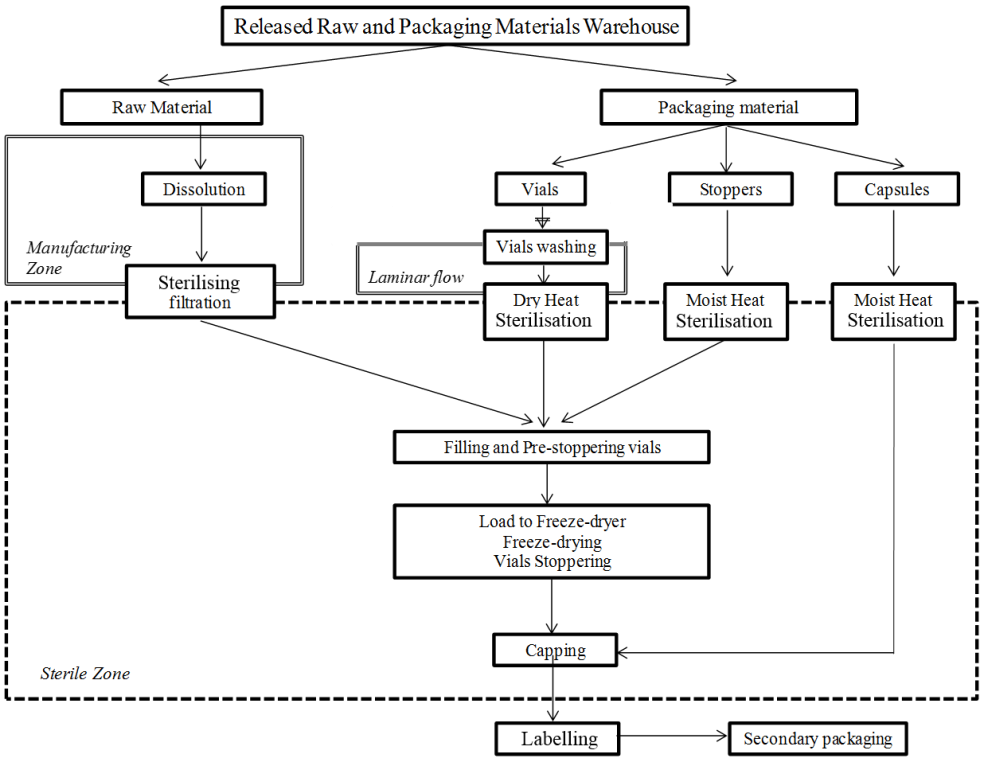

Figure 1.2. Manufacturing process flow for a freeze-dried formulation.

It is important to note that sterile products can be sterilized either by terminal sterilization technologies or by filtration followed by aseptic processing. The sterile freeze-dried products manufactured in the RJ

industrial plant are aseptically processed which means that components of the final product are separately sterilised, and then put together under aseptic conditions.[6,7]

In general terms, the production of an injectable freeze-dried product comprises the steps represented in Figure 1.3. Raw materials (APIs and excipients) are tested according to its quality specifications and only approved materials can enter to weighing rooms. Then, the weighted raw materials are transported to the compounding area. The purpose of compounding is to formulate together the API, excipient and solvent components. For aqueous injectables, water for injection (WFI) should be used as solvent. Raw materials are added into the compounding tank and mixed to obtain a homogenous solution. Moreover, it is important to determine the optimal order of addition of ingredients to ensure complete solubilisation of components with minimal API degradation. Additional water is added to achieve the desired concentration.[5,6]

Then, the solution is sterilised by passing it through a 0.22 µm filtration membrane. The primary purposes of filtration are to clarify, i.e. remove all visible particulate matter, and to sterilise the solution. Filters are selected based on three primary factors: microbial retention, product compatibility, and low extractables. Sterile filtration has limited effect on endotoxin reduction, so it is necessary to ensure that the upstream solution has a low bioburden to minimise the formation of endotoxins.[8]

Once filtered, the sterilised solution enters to the aseptic area and it is contained in a holding tank prior to the filling process. Before that, container and closure components are prepared. Vials are first washed to remove extraneous particulates and, later, subjected to dry heat depyrogenation to inactivate bioburden and degrade endotoxins. Stoppers are washed, and moist heat sterilised. During the filling process, the sterile solution is filled into the washed and depyrogenated glass vials, followed by the partial application of the sterilised stoppers. Once filled and partially stoppered, vials are accumulated in trays which are loaded onto the shelves of the freeze-dryer.

Following the freeze-drying process, shelves are hydraulically lowered to fully insert stoppers into the vials. After that, all vials are unloaded and placed into a capping line for sealing with aluminium caps in order to assure the long-term integrity, and therefore, maintain the sterility of the drug product.[6,8]

After the closure of the primary package, the intermediate product is obtained. Every single unit must be inspected for visible foreign particulate matter and any other defect. After labelling and secondary packaging, the finished product is obtained ready for storage and distribution. However, before that, samples are taken for final testing to verify that the batch meets the final product specifications and it can be released to the market.[5]

Finally, to be confident that quality is attained in the finished product, the responsibility is divided appropriately into Quality Assurance (QA) and QC departments.

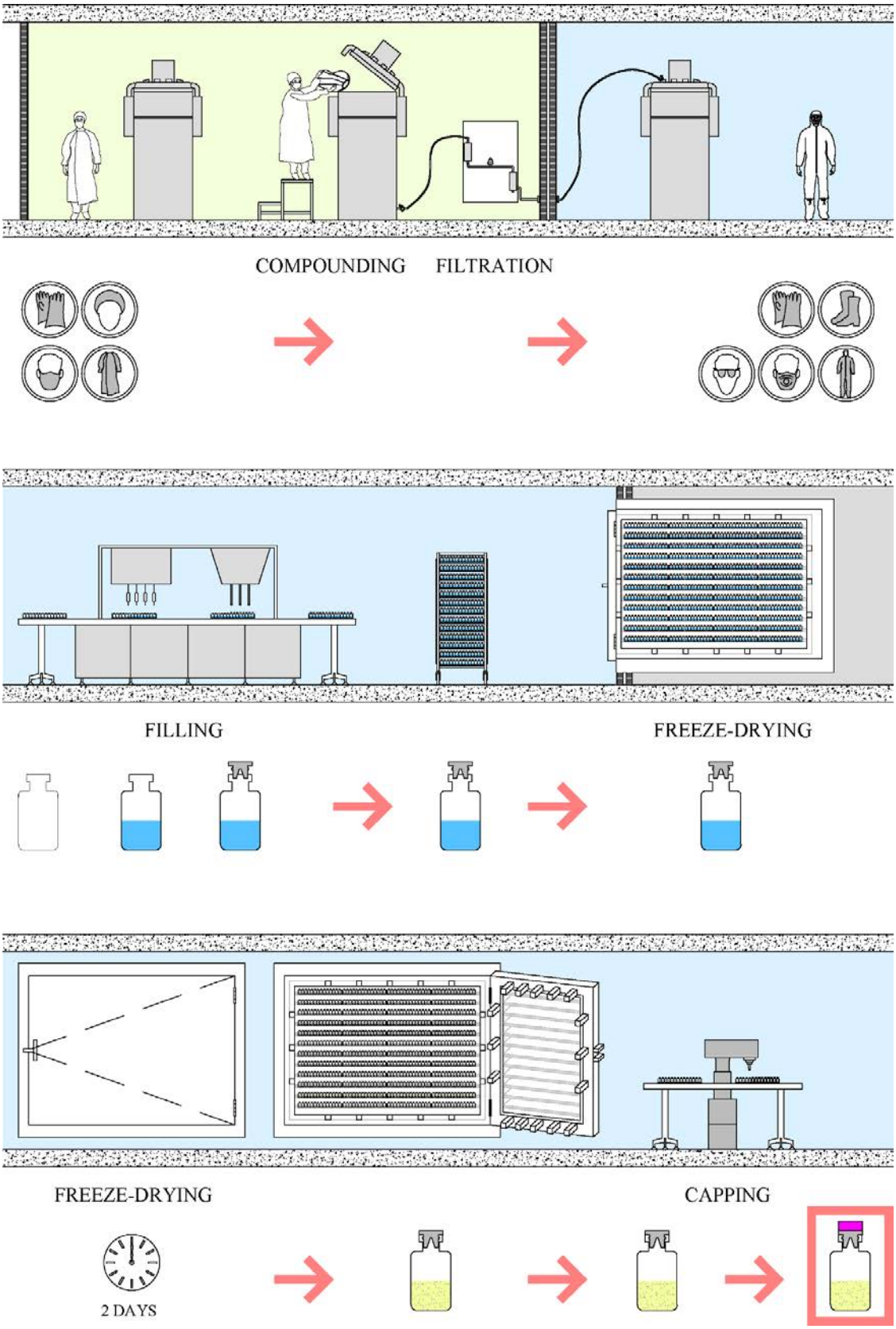

Figure 1.3. Process diagram of the unit operations for the sterile manufacturing of an injectable freeze-dried product. Excipients and active ingredients are mixed, the solution is prepared and filtered. Then, it is filled into vials and loaded into the freeze-dryer. After the freeze-drying cycle, vials are unloaded, capped, and are tracked throughout the packaging and delivery processes. Background colours differentiate between the manufacturing zone (green) and aseptic zone (blue).

4. Quality control

QC is responsible for reviewing the batch history and executing the in-process controls, the finished product testing and the environmental monitoring.

In-process controls are those operations within a manufacturing process where a critical parameter is controlled to an acceptable range, or an analytical assay is conducted to determine proper conditions prior to progressing to the next step. Examples of in-process controls are: pH, clarity, appearance, bioburden, filter integrity, fill weight, etc. Appropriate specifications for in-process controls are needed to ensure batch-to-batch reproducibility.[6]

For finished product testing, an appropriate number of samples are removed using a statistically valid sampling plan and analysed to verify that the product meets the quality criteria, and it can be released for commercial use.[6,7]

Furthermore, stability studies of the finished products during process qualification or as ongoing verifications are performed by QC as well. The results of such stability testing shall be used in determining appropriate storage conditions and expiry dates for the drug products.[6]

5. Quality assurance

QA covers all the studies and plans developed for ensuring quality in a product. In the last twenty years, quality systems have evolved from principles of "product testing" to "process design".[9] Accordingly, an effective Pharmaceutical Quality System should include the following objectives:

a) Establishment, implementation, and maintenance of a set of processes that provide a product with the desired quality to meet the needs of patients, health care professionals and health authorities.
b) Establishment and maintenance of a state of control using effective process performance and product quality monitoring systems.
c) Promotion of continual improvement of product quality and manufacturing processes that includes, for example, reduction of variability and innovation.

The major elements of the pharmaceutical quality system are: process performance and product quality monitoring system, knowledge management[a] review, corrective action/preventative action system, and change management system. In addition, quality risk management[b] (QRM) should be used to provide science and risk-based decisions related to product quality and process design.[6,10]

[a] Knowledge management is a systematic approach to acquire, analyse, store and disseminate information related to products and manufacturing processes.

[b] QRM is a systematic process for the assessment, control, communication, and review of risks to the quality of the drug product.

6. Regulatory framework

Injections[11] and parenteral preparations[4] are general chapters in the United States Pharmacopoeia (USP*)* and the *Ph. Eur.,* respectively. Both represent the reference documents in each country or region, regarding the standards and quality specifications of this type of products.

However, the basic requirements for the manufacturing, packaging and distribution of finished pharmaceutical products, in a global perspective, are described in the GMPs regulations. Compliance to current GMPs ensures that pharmaceutical products taken by or administered to humans and animals meet or exceed minimum requirements of the following five attributes: safety, identity, strength, purity, and quality.[6] GMPs were first proposed by the United States government in 1963, and they are found in the Code of Federal Regulations Part 210 and Part 211.[12] Besides, the European Union GMPs are described in "EU Guidelines to Good Manufacturing Practice: Medicinal Products for Human and Veterinary Use"[7], whose first edition was published in 1989 in which the Annex 1 about the manufacture of sterile medicinal products was included.

GMPs are continuously evolving, from concepts focused on products and processes to current focus in quality systems.[6] The first evidence of this change of paradigm came from Food and Drug Administration (FDA), with the announcement of the initiative of "Pharmaceutical current GMPs for the 21st Century"[13] in August 2002. The idea was to create a new scientific framework based on quality systems and risk management approaches to find ways of mitigating risk while facilitating continuous improvement in pharmaceutical manufacturing. More recently, in December 2017, European Union released an updated draft of Annex 1 where the need for effective quality system and QRM implementation is remarked.[14] All these initiatives are great examples of the agencies position around GMPs.

Once GMPs became official, the industry found that more help was required to better understand how the agencies were interpreting the regulations. Thus, guidance documents began to be issued, giving the industry more specific information on agencies expectations, especially in areas of validation and documentation.[6] As examples for sterile products, FDA and European Medicines Agency (EMA) published guidelines on the sterilization of medicinal products.[15,16]

In this view, two important guidance on Process Analytical Technology (PAT) and Quality systems[17,18] were released by FDA in 2004 and 2006 respectively. These documents actively support the use of PAT tools as an improvement on finished product testing and provides a contemporary framework for implementing QbD approach to formulation and process development. QbD represents a new regulatory philosophy based on deep understanding of formulations and processes using prior knowledge, experimental data, and published literature. In this thesis, QbD is described in more detail in Chapter 2.

Apart from the abovementioned regulatory guidelines, more detailed advice on specific issues relating to the development and manufacture of parenteral products can be obtained from the publications of the Parenteral Drug Association (PDA). PDA is an American organization that publishes technical reports, technical books and a bimonthly journal. Another institution closely related to sterile drug products is the International Society for Pharmaceutical Engineering (ISPE). ISPE has several guidance documents, and one of them is entirely devoted to Sterile Product Manufacturing Facilities.[8] In addition, this institution launched its Product Quality Lifecycle Implementation (PQLI) initiative[19] in June 2007 to help industry find practical approaches to the global implementation of recent quality guidelines published by International Council for Harmonisation (ICH).

References

(1) Center for Drug Evaluation and Research; U.S. Food and Drug Administration. Drugs@FDA Glossary of Terms https://www.fda.gov/Drugs/InformationOnDrugs/ucm079436.htm (accessed Feb 12, 2018).

(2) Laboratorio Reig Jofre, S. A. Reig Jofre en breve http://www.reigjofre.com/es/quienes-somos/reig-jofre-en-breve (accessed Feb 15, 2018).

(3) Broadhead, J.; Gibson, M. Parenteral Dosage Forms. In *Pharmaceutical Preformulation and Formulation*; Gibson, M., Ed.; Informa Healthcare: New York, 2009; pp 325–347.

(4) European Pharmacopoeia. Ph. Eur. 7.0. Monograph 0520 Parenteral Preparations. Council of Europe, Strasbourg, France, 2008.

(5) Agalloco, J.; Akers, J. Sterile Product Manufacturing. In *Pharmaceutical Manufacturing Hanbook: Production and Processes*; Gad, S. C., Ed.; John Wiley & Sons, Inc.: New Jersey, 2008; pp 99–135.

(6) Akers, M. J. *Sterile Drug Products: Formulation, Packaging, Manufacturing and Quality*; Swarbrick, J., Ed.; Informa Healthcare: London, UK, 2010.

(7) EudraLex The Rules Governing Medicinal Products in the European Union. Volume 4-EU Guidelines to Good Manufacturing Practice Medicinal Products for Human and Veterinary Use. Annex 1: Manufacture of Sterile Medicinal Products. European Commission, Brussels, Belgium, 2008.

(8) *Baseline Guide Vol 3: Sterile Product Manufacturing Facilities*, 2nd Ed.; International Society for Pharmaceutical Engineering, Ed.; 2011.

(9) Kieffer, R. G. The Changing Role of Quality Assurance in the Pharmaceutical Industry. *PDA J Pharm Sci Tech* **2014**, *68* (4), 313–319.

(10) ICH. Harmonised Tripartite Guideline Q9: Quality Risk Management. 2005.

(11) USP. USP 40-NF35. General Chapter <1> Injections and Implanted Drug Products (Parneterals) - Product Quality Tests. 2016.

(12) The Code of Federal Regulations Title 21-Food and Drugs Chapter 1-Food and Drug Administration Department of health and human services Subpart C-Drugs: General part 211 Current Good Manufacturing Practice for Finished Pharmaceuticals. https://www.ecfr.gov/cgi-bin/text-idx?SID=f226492c3cdc1a726e611d0393c3474c&mc=true&tpl=/ecfrbrowse/Title21/21cfr211_main_02.tpl (accessed May 29, 2018).

(13) FDA. Pharmaceutical CGMPs for the 21st Century −A Risk-Based Approach. Final Report. Department of Health and Human Services U.S Food and Drug Administration, 2004.

(14) EudraLex The Rules Governing Medicinal Products in the European Union. Volume 4-EU Guidelines to Good Manufacturing Practice Medicinal Products for Human and Veterinary Use. Draft Annex 1: Manufacture of Sterile Medicinal Products. European Commission, Brussels, Belgium, 2017.

(15) FDA. Guidance for Industry. Sterile Drug Products Produced by Aseptic Processing Current Good Manufacturing

Practice. FDA: Rockville, MD, 2004.

(16) EMA. Draft Guideline on the Sterilisation of the Medicinal Product, Active Substance, Excipient and Primary Container. European Medicines Agency. London, UK, 2016.

(17) FDA. Guidance for Industry, PAT- A Framework for Innovative Pharmaceutical Development, Manufacturing, and Quality Assurance. U.S. Department of Health and Human Services Food and Drug Administration: Rockville, MD, 2004.

(18) FDA. Guidance for Industry, Quality Systems Approach to Pharmaceutical CGMP Regulations. U.S. Department of Health and Human Services Food and Drug Administration: Rockville, MD, 2006.

(19) ISPE PQLI Guide Series. *Overview of Product Design, Development, and Realization: A Science- and Risk-Based Approach to Implementation*; 2010.

Chapter 2

Quality by Design in Pharmaceutical Manufacturing

1. Introduction

In recent years, the concept of quality in the pharmaceutical field has evolved from the idea of testing the quality to designing it. The fundamental is very simple; it consists in understanding the process variables that determines the quality of the final product from the beginning of the process development phase, instead of manufacturing following a strict and fixed process, and testing the quality of the product only at the end. This strategic thinking is based on the knowledge that "*nothing stays the same forever*" and gave birth to the well-known QbD approach.[1]

Basically, the manufacturing process should be designed to meet the desired quality attributes of the product, which guarantees therapeutic efficacy and safety. To achieve this goal, QbD states that quality should be built-in by design using a risk-based approach that emphasizes the importance of developing scientific knowledge and enhanced understanding of the sources of process variability. However, final testing must remain an essential element of quality control to verify the quality of the product.[2–4]

It is also important to highlight that QbD should be applied throughout the lifecycle of the product (new drug or an existing product), from the initial development through marketing, until product's discontinuation (Figure 2.1).

Figure 2.1. The drug product lifecycle.

In the following sections, a summary of the implementation of QbD in the pharmaceutical industry and its benefits and challenges are presented. Afterwards, the key elements of the QbD approach and the role of PAT are described and discussed.

2. Quality by design initiative in pharmaceutical industry

The concept of QbD has been successfully implemented in many industries since a long time. However, it is not since the beginning of the 21st century that QbD was introduced in the pharmaceutical industry. The ICH released several guidelines, ICH Q8 to Q12 [2,3,5–7], which provide a general framework for QbD application to drug product and drug substance development and manufacture.

QbD was put into practice in a big way with the launch of the FDA pilot program for small molecules in 2005. Nine companies participated in the program and submitted regulatory filings based on this approach. Since then, several case studies of how to apply the key elements of QbD to process development of different products, like antibodies[8], vaccines[9] or generics[10,11], have been published. As an example, in 2006, Januvia, manufactured by Merck, became the first drug approved using QbD.[12]

After the success of the first initiative, EMA and FDA launched together a pilot program for a parallel assessment of QbD applications in 2011. The program was closed in 2016 with a total of two marketing authorization applications, three variations and nine scientific advice applications.[13] Furthermore, the ISPE (Spain division) in collaboration with the Pharmaceutical Control Services of the Health Department of Generalitat de Catalunya published a case study about the application of QbD to legacy products.[14]

Much was learned from those initial filings that led the industry and regulators toward a common vision for QbD. A comparison of the traditional state and the future desired state is summarized in Table 2.1.

Table 2.1. Comparative table of the traditional vs desired QbD state in pharmaceutical processes. Adapted from ICH Q8(R2).[2]

Aspect	Traditional state	Desired QbD state
Pharmaceutical development	Empirical, sometimes random. Development research often conducted one variable at a time.	Systematic. Multivariate experiments to understand product and process. Establishment of design space. Use of PAT tools.
Manufacturing process	Fixed. Validation on three batches. Focus on reproducibility.	Adjustable within design space, supported by robust quality system and validation lifecycle approach. Focus on control strategy and robustness. Use of statistical process control (SPC) methods.
Process control	In-process testing for go/no-go decisions. Off-line analysis.	PAT tools implemented for feedback and feedforward controls. Trending analysis to support continual improvement.
Product Specification	Primary means of quality control; based on available batch data.	Part of overall quality control strategy; based on product performance with supportive data.
Control strategy	Mainly by intermediate and finished product testing and inspection.	Risk-based control strategy. Controls shifted up-stream with the possibility of real-time release testing (RTRT).
Lifecycle management	Reactive to problems and out of specifications (OOS).	Preventive action, continual improvement.

2.1. Why quality by design?

The concept of QbD has provided opportunities and challenges for both, regulatory authorities and pharmaceutical companies. Some of the major advantages are listed in Figure 2.2.

In brief, QbD provides deeper understanding of drug products and its associated processes, which, in turn, lead to more robust[a] and more efficient manufacture. This enhanced understanding also offers the potential for timely and flexible regulatory approval among other business benefits.[15]

[a] Process robustness is referred to the ability of a manufacturing process to tolerate the expected variability of raw materials, operating parameters, equipment, environmental conditions and human factors without negative impact on quality.[30]

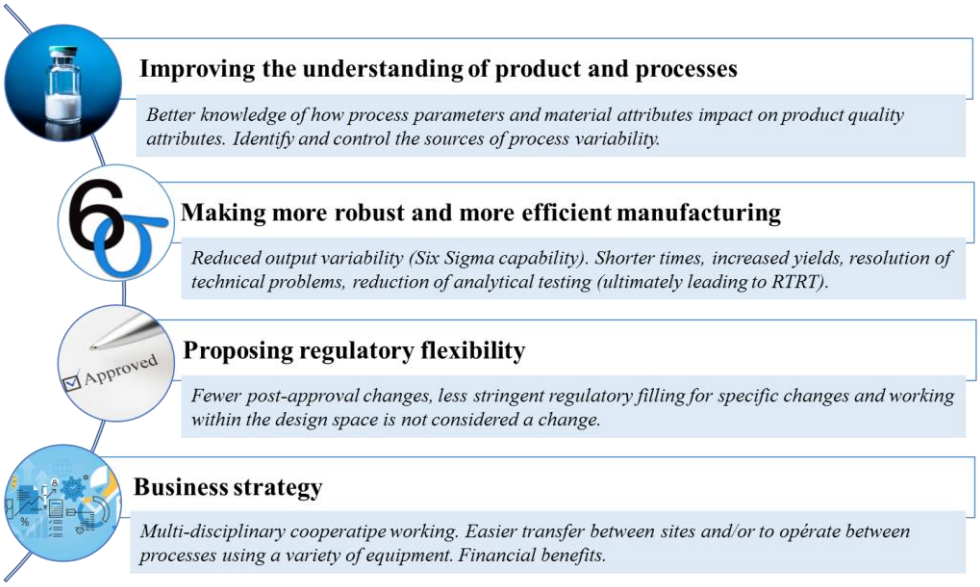

Figure 2.2. Benefits of applying QbD for the development of pharmaceutical processes.

In addition, there is also a change in the technological environment to support the use of QbD. For instance, there is increased availability of PAT tools, statistical software packages, and the development and understanding of Design of Experiment (DoE) and multivariate modelling.[1,16] However, this approach may require more resources, time, and effort initially.

According to a survey performed by the American Association of Pharmaceutical Scientists, more than two thirds of respondents agreed that the benefits of QbD included: the positive impact to the patient (78%), better knowledge management (85%) and decision making (79%). Nevertheless, more than 50% of industry professionals believed that QbD did not lead to a better return on investment.[17]

Finally, it is worth to note that, although regulatory authorities are encouraging the use of QbD, it is still not mandatory.

2.2. Quality by design applied to process validation

When developing products and processes, initial studies are usually performed at laboratory scale. However, the process should always be validated at industrial scale for commercial manufacturing purposes. The aim of the validation[b] is to demonstrate confidence that the manufacturing process delivers a drug product with the expected quality attributes in an effective and reproducible way.

The process validation concept has also evolved over time. Traditionally, the validation of pharmaceutical manufacturing processes consisted in producing three consecutive batches and testing

[b] Process Validations is defined as the collection and evaluation of data, from the process design stage throughout production, which establishes scientific evidence that a process is capable of consistently delivering quality products.[20]

that all of them comply with product specifications. Moreover, once the validation has been completed, manufacturers are not permitted to make changes.

However, concurrently with the implementation of QbD, a new process validation strategy has been introduced as an alternative strategy to the traditional approach.[18,19] It is based on continuous process verification throughout product lifecycle, linking product and process development, qualification of the commercial manufacturing process, and maintenance of the process in a state of control during routine production.[20]

In this regard, the process validation lifecycle approach can be divided in three stages:

- Stage 1: *Process design*. The commercial process at industrial scale is defined based on knowledge gained through development and scale-up activities.
- Stage 2: *Process qualification*. The designed process is evaluated to confirm that it is capable of reproducible commercial manufacturing. Evaluation of facilities design, equipment qualification and Process Performance Qualification (PPQ) are some of the activities performed at this stage.
- Stage 3: *Continued Process Verification*. Ongoing assurance is gained during routine production that the process remains in a state of control.

This approach requires a high level of knowledge from product and process development studies and an enhanced control strategy based on the implementation of PAT tools to evaluate process performance. Thus, PAT enables the introduction of this alternative to process validation approach based on QbD.

Finally, several regulatory documents have been updated introducing this new process validation concept, which reflects the interest of the authorities for its immediately application.[18–20]

3. Key elements of quality by design

A successful QbD application should be linked to a proper definition of the project objectives, multi-disciplinary cooperative working, and knowledge management.[1] Figure 2.3 displays some characteristics of a successful QbD program.

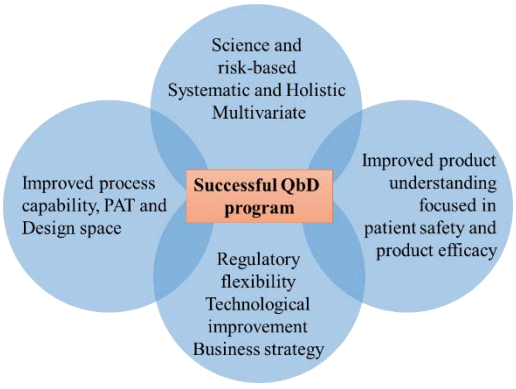

Figure 2.3. Characteristics of a successful QbD program in a pharmaceutical environment.

The key elements of the QbD approach are illustrated in the roadmap of Figure 2.4. It includes: the Quality Target Product Profile (QTPP), prior knowledge and risk assessments, Critical Quality Attributes (CQAs), Critical Material Attributes (CMAs), Critical Process Parameters (CPPs), design space, control strategy and continual improvement.[21] In fact, all these elements are used throughout the three stages of the process validation lifecycle approach.

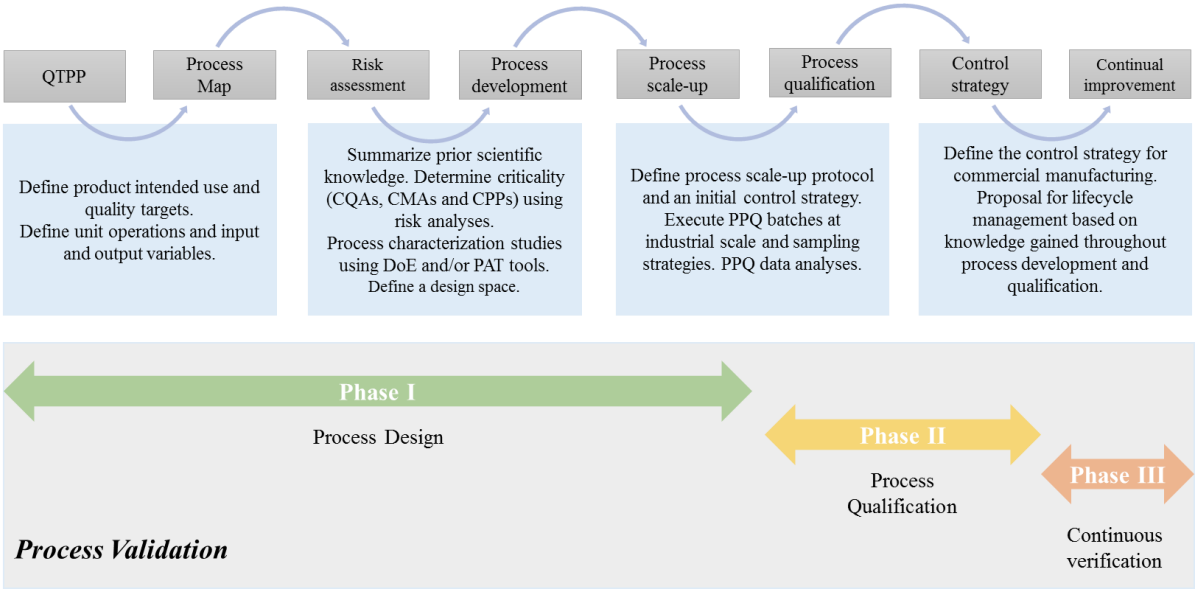

Figure 2.4. General schematic representation of the QbD approach applied throughout the process validation lifecycle of a pharmaceutical drug product.

3.1. Quality target product profile and process outline

The QbD approach begins with the establishment of the QTPP. It represents a prospective summary of the quality characteristics of a drug product that ideally will be achieved to ensure the desired quality, in terms of safety and efficacy of the product.[1,2] Hence, it is likely to be a reflective of the intended therapeutic benefits of the product relative to patient needs.

The QTPP is derived from an understanding of the mode of action of the product, patient profile, clinical indication, desired safety profile, and, where appropriate, it includes quality characteristics related to:

- Description
- Route of administration and intended use (in a clinical setting or at home)
- Dosage form and delivery system
- Dosage strength
- Container closure system
- Attributes affecting pharmacokinetic profile
- Drug product quality attributes (e.g., sterility, purity, stability)[21,22]

Finally, the QTPP is a living document that can change as more information become available. Based on the QTPP, an initial product and process outline (also named process map) is proposed based either on preliminary studies or on company experience, which should include product knowledge, manufacturing equipment, and available facilities.[23]

3.2. Criticality

Criticality is assessed over quality attributes, process parameters and material attributes to define CQAs, CPPs and CMAs, respectively.

- *Critical Quality Attributes:* ICH Q8(R2) [2] defines a CQA as a physical, chemical, biological, or microbiological property or characteristic that should be within an appropriate limit, range, or distribution to ensure the desired product quality, in terms of product safety and efficacy. CQAs of a solid oral dosage form are typically those aspects affecting product purity, strength, drug release, and stability. However, sterility, endotoxins, and particulate matter are specific CQAs for injectable products.[2]
- *Critical Material Attributes:* A CMA is defined as a physical, chemical, biological, or microbiological property or the characteristic of a raw material whose variability has an impact on CQAs. Therefore, CMAs need to be monitored and controlled to ensure the desired product quality, and acceptable ranges must be specified. CMAs are applicable to API, excipients, intermediate products and packaging components. For instance, it may include chemical and/or microbiological purity of raw materials, excipient physical properties, etc.[6,24,25]
- *Critical Process Parameters:* A CPP is as a process parameter whose variability has an impact on a CQA and, therefore, it should be monitored and controlled to ensure the process delivers a product with the desired quality.[2,26]

In summary, the relationship between CQAs, CMAs and CPPs is shown in Figure 2.5.

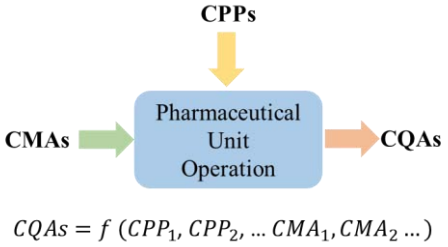

Figure 2.5. Link between CMAs, CPPs and CQAs. Adapted from reference[21].

The assignment of criticality to attributes and parameters has led to diverse interpretations. In any case, a variable that is labelled "critical" needs always to be controlled as well as monitored.

The PQLI team states that several levels of criticality may be used to describe multiple levels of risk. Hence, criticality can be ranked.[24,27] Besides, Lionberger et al.[28] provides another way to classify process parameters and materials attributes. Apart from non-critical and critical parameters, they proposed a third parameter type "unclassified" that is when the criticality is unknown because of the absence of pharmaceutical development.

Alternatively, Mitchell[29] published a three-part publication explaining critically as a continuum. The author proposed an interesting situation. It is assumed that extreme temperatures can destroy many pharmaceutical products. But, if a process inherently cannot produce such temperatures, is temperature still considered to be critical and, therefore, required to be monitored and controlled? In this sense, the author states that there is great value in understanding not only if a parameter/attribute is critical, but also how much impact the parameter/attribute has. Then, the author proposes to transform the binary yes/no decision into a continuum of criticality, ranging from high to low, depending on the impact of the parameter/attribute variability on the quality of the product.

The assessment of criticality and designation of CQAs, CMAs and CPPs is typically used to prioritise those variables that are important to characterise, and, therefore, they should be included in the process control strategy. In addition, as more knowledge is gained throughout product lifecycle, the criticality of some attributes or parameters may change and the list of CQAs and CPPs can be updated over time.[1]

Finally, the assessment of criticality as a function of the risk of impact to product quality is performed using risk assessment tools.[27]

3.3. Risk assessment tools

According to ICH Q9 [5], risk assessment consists in the identification of hazards and the analysis and evaluation of risks associated with exposure to those hazards. Prior knowledge, process understanding, and experience are used to assess and justify the criticality using risk assessment tools.

A basic principle is that the evaluation of the risk should be ultimately link to the protection of the patient. For drug product quality attributes, the level of criticality is determined by severity of harm to patient safety and efficacy.[21] However, designation of criticality for process parameters and material attributes is a function of its probability of impact on CQAs and the detectability of that impact.[27] In this sense, severity, probability and detectability are defined as:

- Severity is the measure of the possible consequences of a hazard. A measure of uncertainty is usually included when the magnitude of the impact of a CQA is not known.
- Probability is the likely occurrence that a material attribute or a process parameter has an impact on the safety, efficacy and quality of the drug product.
- Detectability is the level or ability at which an occurrence can be measured. The ability to detect when something may go wrong will often reduce the probability of an impact on quality.[5]

The measure of severity, probability and detectability is often ranked, where a high score means high severity, high probability but low detectability. There are several examples of severity, probability and detectability scales in literature.[26]

ICH Q9 [5] features several quality risk assessment tools for the assignment of criticality. The most commonly used in the pharmaceutical industry are the following:

- Ishikawa Diagram: it is a visualization and knowledge organization tool to effectively capture a brainstormed list of potential CPPs and CMAs which have influence on CQAs. It is also referred to "Fishbone Diagram" due to its shape, as observed in the example represented in Figure 2.6.

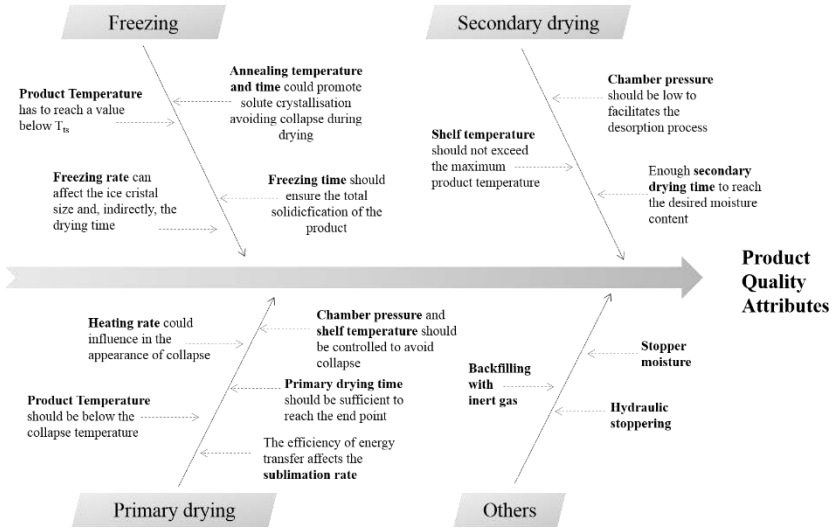

Figure 2.6. Example of Fishbone diagram for the evaluation of the freeze-drying unit operation.

The name of the basic problem of interest is entered at the end of the main bone and possible causes of the problem are drawn as sub-lines for the main bone. Ishikawa diagram is used to identify the many possible causes of potential failure and to arrive at a few key variables that contribute most significantly to the problem being examined.[25,30]

- Cause and effect matrix: it described the relationship between process inputs and outputs in a tabular form. For example, it can be used to study the impact of different unit operations of a manufacturing process (inputs) to CQAs (outputs). This matrix gives an overview of where development effort should be placed and it is commonly used as a starting point for further process evaluation.[26]

- Failure Mode and Effects Analysis (FMEA): it is the most widely used risk assessment tool in industry to identify process parameters and material attributes that could impact on CQAs.[31,32] FMEA can identify potential failure modes, estimate their effect on the desired operation of the process, establish the ability of the process to detect these failures, and identify actions to

mitigate and reduce the risks to an acceptable residual level.[30,33] Different scores are defined for severity, probability and detectability of failure and the product of the three of them is referred to Risk Priority Number (RPN):

$$RPN = Severity \times Probability \times Detectability \qquad \textit{Equation 2.1}$$

Furthermore, RPN could be ranked in low, medium and high risk. This risk ranking can also be used to prioritise the study of CPPs and CMAs during process development. Finally, this tool is widely applied in assessing change controls, complaints and failure investigations.[27]

Several examples of the application of risk assessment tools for the QbD development of different pharmaceutical formulations and dosage forms are found in literature.[34–37] Furthermore, its application for analytical method validation has also been demonstrated.[38] In this thesis, cause and effect matrix and FMEA has been used during the freeze-drying process development and qualification phases and for the evaluation of a Near infrared spectroscopy (NIRS) method.

In addition, the abovementioned risk assessment tools could be used to select the variables to include in experimental designs for the establishment of a design space (DS), which is another key element of the QbD approach.[24]

3.4. Design space

The concept of DS has been defined in ICH Q8(R2)[2] as the multidimensional combination and interaction of input variables that have been demonstrated to provide assurance of quality within an acceptable range. CPPs and CMAs are likely to be input variables (e.g., process time, temperature, pressure, excipients concentration, etc.), while CQAs are commonly used as process outputs.[26] Basically, the DS establishes the relationship between CQAs, CMAs and CPPs and defines their acceptable operating ranges.[39,40]

The DS can be applied to a single or multiple unit operations or even to the entire process.[2] As observed in Figure 2.7, beyond the DS, there is a Knowledge Space which comprises all process knowledge obtained during product development and, outside it, there is unexplored space. Normal Operating Range (NOR) is located inside the DS and defines the region around the target operating conditions that contain common operational variability. At this point, it is relevant to note that the typical Proven Acceptable Ranges[c] (PAR) do not constitute DS.[24,30] The boundaries of the DS are established experimentally and they correspond to acceptable ranges for the CQAs.

[c] A PAR for a process parameters is a characterized range for which operation within this range, while keeping other parameters constant, will result in producing a drug product meeting CQAs.[24]

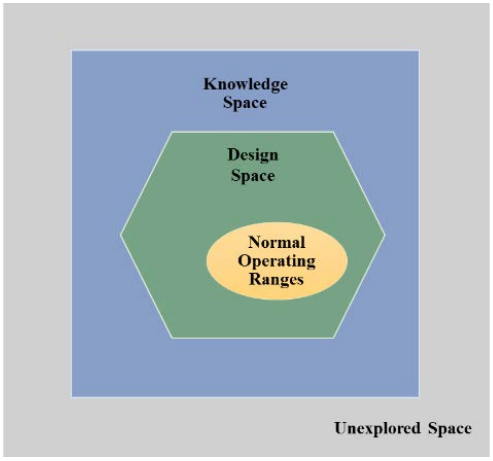

Figure 2.7. Representation of a design space.

When performing development studies, it is not necessary to find the edges of failure for the DS, as this may involve significant unnecessary experimental work and cost. Therefore, in those situations, the DS boundaries may not represent edges of failure, and the DS covers the whole experimental region. Consequently, the DS could be useful for defining broader operation ranges.[1,2]

Moreover, the DS is applicable to the three process validation stages. During process characterisation at laboratory scale, the DS should be defined, and PAT tools should be established to target optimal and robust performance. Later, during process qualification, it should be demonstrated that process can be performed at commercial scale within the already defined DS. Finally, process performance in routine manufacturing should be monitored with respect to DS using multivariate analysis and other statistical tools.[4] Some interesting examples of the application of DS in pharmaceutical manufacturing processes, like antibody drug product formulation[39], lyophilization process[41], or fermentation process[42], are found in literature.

A DS can be described by mathematical models[d]. The most common models used to describe the DS could be first principle or mechanistic and empirical models.[1,26] Lepore et al.[43] highly recommend using mechanistic models as first choice due to the inherent benefit in terms of physical significance. Otherwise, when considering interactions of multiple variables that cannot be modelled simply, empirical tests may be more appropriate.[21] As an example, several publications have developed first principles models based on heat and mass transfer equations for the freeze-drying process DS[44], while other authors had used experimental designs coupled with PAT tools to optimize the formulation and the process.[45,46] Thus, both approaches can be used for a suitable freeze-drying cycle development.

Since it must always be assumed that product and process development are multivariate, experimental plans should use a formal statistical design, called Design of Experiments. There are many possible

[d] A model is a representation of underlying complex physical or chemical phenomena.

designs and their choice depends on the experimental objective.[1] DoE is explained in more detail in Chapter 5.

In conclusion, the key milestones for building a DS are: selection of factors/variables, definition of the experimental design and execution, data analysis, model development, assessment, verification, and validation, and, finally, DS submission to regulatory authorities.[47] From a regulatory point of view, the development of DS is optional. Nevertheless, there are several benefits of building a DS, such as: high level of process understanding to support control strategies, process flexibility or justification for process validation criteria.[26]

Finally, the knowledge derived from the criticality assessment and the DS are used to develop a successful control strategy to assure the proper process performance in routine production.

3.5. Control strategy

The control strategy is also a key element of the QbD approach. It is defined as a set of planned controls, derived from current product and process understanding that assures process performance and product quality.[2] The final goal of the control strategy is to control process variability and to ensure that CQA acceptance criteria are always achieved. The control strategy can include:

- Control of input material attributes (e.g. API, excipients, packaging materials).
- Product specifications, batch release testing and drug product stability testing.
- In-process controls and RTRT (when applicable).
- Controls for unit operations that have an impact on subsequent processing or CQAs.
- A monitoring program for verifying that process remains in a state of control.[2,48]

Like criticality and design space, the control strategy should be developed using risk assessment tools based on the process ability to meet CQAs through the manufacturing process and during storage.[2] This way, unacceptable variability in a process can be reduced by a robust control strategy, based on the reduction of the probability of its occurrence and/or the increment of the ability to detect and mitigate that variability. Nevertheless, a robust control strategy does not reduce the inherent severity of the risk of failure to meet CQA acceptance criteria.[26,27]

Where a DS is proposed, the control strategy should ensure that a product of the required quality is produced consistently through operation within that DS.[1] Two general types of control strategy could be distinguished: minimal or enhanced. In a minimal control strategy, drug product quality is controlled primarily by in-process and finished product testing. However, an enhanced control strategy contains advanced process control elements, such as PAT tools, feedforward and/or feedback controls based on process models or algorithms, and more automatic actions.[2,48]

Finally, the control strategy should be reviewed and updated during the product lifecycle.

3.6. Lifecycle and knowledge management

As stated in ICH Q10 [3], the experience gained from commercial manufacturing of a drug product can be used to improve its quality. Health authorities expect that a product developed using QbD has a formalized lifecycle management plan coupled with a knowledge management program that archives and updates documents associated with product and process knowledge. The lifecycle management plan may also be included in the product registration documentation and, if so, it becomes a regulatory agreement between the health authority and the company.[33]

Actually, this plan defines the Continued Process Verification strategy (or Stage 3 of process validation lifecycle approach) focused on the monitoring and maintaining the process state of control.[49] Initially, CPPs, CMAs, and CQAs data are collected according to a predefined frequency and they are used to evaluate product quality and process robustness using SPC tools. SPC is defined as the application of statistical methods to measure and analyse the variations in a process either intra- or inter-batches. Therefore, SPC is needed for continuous quality improvement.

Standard SPC tools include trend analysis and process capability estimates for quality attributes. Typical SPC charts used for process monitoring are: control charts, bar charts, pareto charts, scatter diagrams, among others. One of the most commonly used is the control chart, also known as Shewhart charts.

A control chart is a graphical display of a product quality attribute that has been measured periodically from a process at a defined frequency. It could also be used for finished product quality attributes of different batches. In general, this chart contains a centre line that represents the mean value and the upper control limit (UCL) and lower control limit (LCL), both corresponding to $\pm k\sigma$ (where σ= standard deviation and k=3 for normally distributed data).

Control limits are plotted to investigate product and process trending, using statistically defined rules[50], in order to assess process and product stability. Figure 2.8 shows an example of a control chart for the API content of a drug product (in %) where each point corresponds to the individual result per batch.

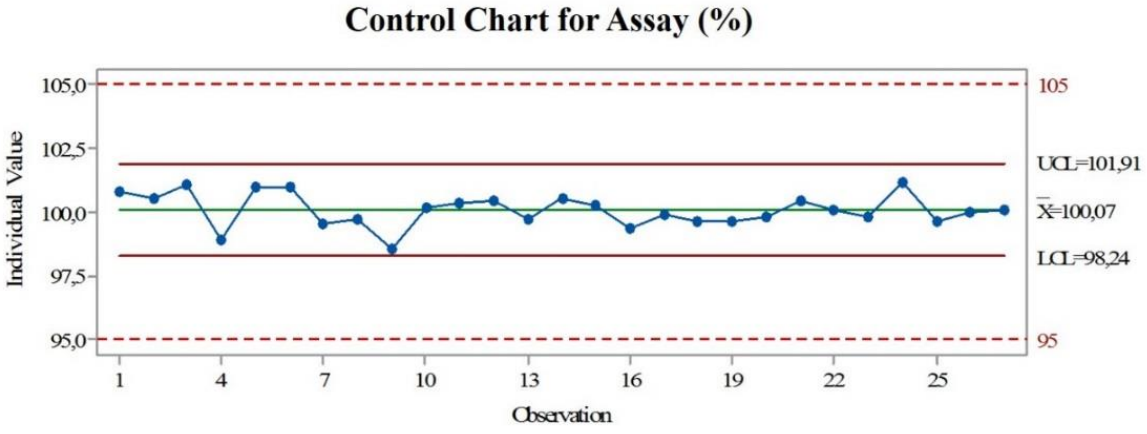

Figure 2.8. Example of a control chart for the API content of 27 batches of a pharmaceutical drug product. UCL and LCL can be set based on historical data or calculated using the current data points.

Once data normality and stability are confirmed using control charts, process capability can be assessed by the calculation of capability indices. In the pharmaceutical field, process capability consists in the evaluation of the product or process ability to meet specifications in order to show that the process remains in a statistical state of control.[30] The most commonly used capability indices in pharmaceutical processes are shown in Table 2.2.

Table 2.2. Comparative table of Process Capability and Process Performance indices.

Process capability (Cp & Cpk)	Process performance (Pp & Ppk)
Short-term or potential capability	Long-term or overall capability
Only accounts for the variation within subgroups (inherent variability due to common cause of a stable process). It indicates how well a given process could perform when all special causes have been eliminated.	Accounts for the overall variation of all data (common cause and special cause variability) It includes both the variation within subgroups and also the shift and drift between them. It indicates the actual performance of the process
$C_p = \frac{(USL - LSL)}{6\hat{\sigma}}$	$P_p = \frac{(USL - LSL)}{6s}$
$C_{pkl} = \frac{(\mu - LSL)}{3\hat{\sigma}}$ $C_{pku} = \frac{(USL - \mu)}{3\hat{\sigma}}$	$P_{pkl} = \frac{(\mu - LSL)}{3s}$ $P_{pku} = \frac{(USL - \mu)}{3s}$
$C_{pk} = \min\left(C_{pkl}, C_{pku}\right)$	$P_{pk} = \min\left(P_{pkl}, P_{pku}\right)$
Where μ = mean of all the data, $\hat{\sigma}$ = inherent variability, s= overall variability, USL and LSL = upper and lower specification limits respectively	
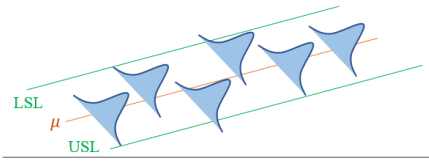	Cp/ Pp simply measures the spread of the specifications relative to the six-sigma spread in the process. Cpk/Ppk takes into account where the process mean is located relative to the specifications.

As observed in Table 2.2, formulae for capability indices are ratios of the process spread and attribute specification spread.[51,52] As an example, Figure 2.9 shows a process capability analysis of the API content data used in the control chart of Figure 2.8.

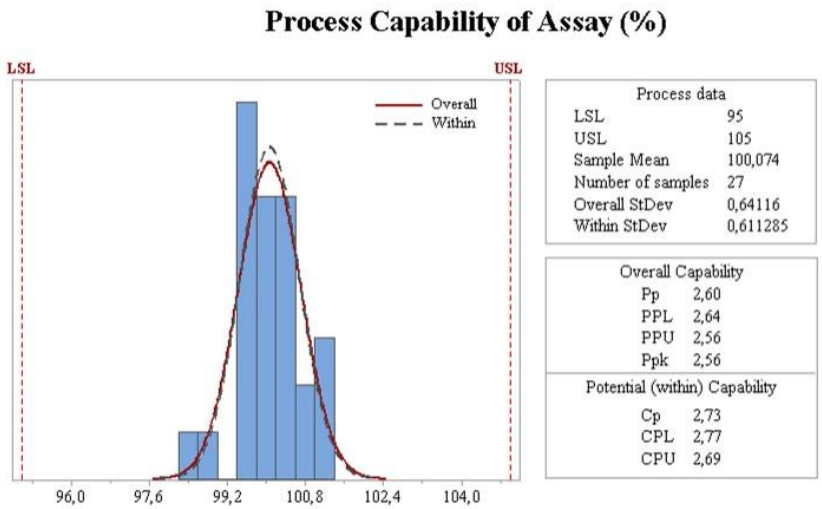

Figure 2.9. Example of a process capability report of the API content (in %) of 27 batches of a drug product.

Typically, process capability is represented using a histogram superimposed with the frequency distribution curve of the data and two reference lines corresponding to the upper and lower limit of specifications (USL and LSL respectively).[52] In the pharmaceutical sector, a process whose values of C_p/P_p and C_{pk}/P_{pk} are greater than 1.0 can be considered capable.

Furthermore, more sophisticated process monitoring programs based on multivariate analysis and batch modelling can be applied in routine pharmaceutical manufacturing as well. More information regarding SPC tools and process capability indices can be found in specific books about industrial process statistics.[52]

In summary, process monitoring plans should be designed for two main reasons. Firstly, to provide ongoing verification that product quality is appropriately controlled during routine manufacturing.[26] Secondly, to identify adverse trends and opportunities for process improvements. This continual improvement process is iterative throughout product lifecycle and process variability should be reviewed periodically, at least annually, in the Product Quality Review[e] (PQR) document.[53]

4. Process analytical technology to support quality by design

PAT is an indispensable tool for an effective implementation of QbD. PAT is intended to support innovation and efficiency in pharmaceutical development and manufacturing.[4] The goal of PAT is to enhance understanding and control of the manufacturing process to ensure acceptable and reproducible product quality, which is consistent with QbD.

PAT is defined as a system for designing, analysing and controlling manufacturing through timely measurements of critical quality and performance attributes of raw and in-process materials and processes.[54] Then, since pharmaceutical processes are multivariate and dynamic, the focus should be placed on multivariate relationships among materials attributes, process and their effects on quality. PAT framework consists of four main components:

1. Multivariate tools for design, data acquisition and analysis: the conversion of large volume of process data to knowledge and the identification of multifactorial relationships can be achieved though multivariate analysis.
2. Process analysers: which are used for the measurement of physical, chemical, and biological attributes of materials and provide real-time data about the status of the process. The process analysers can either be implemented at-line, on-line, in-line:

[e] PQR is a regular periodic quality review of all licensed medicinal products which are conducted with the objective of verifying the consistency of the existing process, the appropriateness of current specifications for both raw materials and finished drug product to highlight any trends and to identify product and process improvements.[53]

- At-line: sample is removed, isolated from and analysed in close proximity to the process stream.
- On-line: sample is diverted from the process, analysed, and may be returned to process stream or discarded after testing.
- In-line: sample is not removed from process stream. The procedure can be invasive or non-invasive.

Data collection using process analysers can be non-destructive. This represents an important reduction in sample handling and sample preparation errors. In addition, process analysers have fast or real-time response when compared to traditional methods, resulting in a reduction of process times as well.[55]

3. Process control tools: they are used to monitor and control the state of a process and make adjustments, when necessary, to maintain a desired state. Most of the time, process control relies on statistical principles, such as statistical process control tools already explained in Section 3.6 of this chapter.
4. Continuous improvement and knowledge management tools: they allow continuous learning through data collection and analysis over the lifecycle of a product.[54]

PAT can be applied in development studies, scale-up and routine production. Data collection in real time from structured experimental designs can provide increased process understanding during development. PAT also makes scale-up issues easier to deal with due to the advanced monitoring and control options.[1] Even more useful, it enables operators to make real-time adjustments in process parameters to obtain the desired product attributes at every stage of the industrial process.[54]

Available PAT tools have evolved from those that predominantly take univariate process measurements, such as pH, temperature and pressure, to those that measure biological, chemical and physical attributes. Although many forms of process analyser exist, NIRS is one of the most common in the pharmaceutical manufacturing sector.[56]

However, in pharmaceutical freeze-drying processes, NIRS and wireless product probes are available, but still not well-implemented at industrial-scale. Besides, univariate process sensors such as pressure and temperature probes are widely used to monitor and control the freeze-drying process.[40] Freeze-drying monitoring tools are explained in more detail in Chapter 3.

PAT tools should be validated to enable batch release as well as conventional analytical methods.[26] In addition, a monitoring program should be added in the control strategy for verifying the validity of process models. The monitoring program should also include requirements for model updating, when, for instance, the raw material supplier or equipment components are changed.[48]

Finally, PAT takes part of enhanced control strategies and it also supports the achievement of RTRT.[2] RTRT consists in evaluating and ensuring the quality of in-process and/or final product based on real-time process data. Initiatives from regulatory authorities, like the introduction of RTRT in the current draft version of EU GMPs guideline Annex 17 [57], highlight the advances in the application of PAT and QbD principles to pharmaceutical development and manufacturing.

5. Summary

QbD has provided opportunities for pharmaceutical companies to develop better understanding of their products and their associated manufacturing processes. This approach can provide a higher level of assurance for product quality and offer the potential of improved efficiency. In a QbD system:

- The product is designed to meet patient needs.
- The process is designed to consistently meet product CQAs.
- The impact of starting raw materials and process parameters on product quality is understood.
- Sources of process variability are identified and controlled with appropriate control strategies.
- The process is continually monitored and updated to allow for consistent quality over time.

In summary, the main steps in QbD are:

- Determine QTPP and CQAs.
- Link raw material attributes and process parameters to CQAs using risk assessment tools.
- Develop a DS to understand the relative impact of CPPs and CMAs on CQAs.
- Design and implement a control strategy for the industrial manufacturing process.
- Manage product lifecycle including continual improvement.

Moreover, PAT offers several benefits in terms of understanding and control of the manufacturing process which facilitates the development of a robust control strategy.

Over the past years, significant progress has been made to establish the industry framework for applying QbD concepts to pharmaceutical product development. Although QbD requires a significant up-front investment, it has been demonstrated that it delivers an improved and efficient process with controlled variation, reduces process risk and increases final product quality.

In this thesis, a QbD strategy for the development of two injectable freeze-dried products has been developed, implemented at laboratory and industrial scale, and successfully included in a regulatory filing at the AEMPS, spanish medicines agency.

References

(1) ISPE PQLI Guide Series. *Overview of Product Design, Development, and Realization: A Science- and Risk-Based Approach to Implementation*; 2010.

(2) ICH. Harmonised Tripartite Guideline Q8(2): Pharmaceutical Development. 2009.

(3) ICH. Harmonised Tripartite Guideline Q10: Pharmaceutical Quality System. 2008.

(4) Mhatre, R.; Rathore, A. Quality by Design: An Overview of the Basic Concepts. In *Quality by Design for Biopharmaceuticals: Principles and Case Studies*; Rathore, A. S., Mhatre, R., Eds.; John Wiley & Sons, Inc.: New Jersey, 2009; pp 1–8.

(5) ICH. Harmonised Tripartite Guideline Q9 Quality Risk Management. 2011.

(6) ICH. Harmonised Tripartite Guideline Q11: Development and Manufacture of Drug Substances (Chemical Entities and Biotechnological/Biological Entities). 2012.

(7) ICH. Harmonised Tripartite Guideline Q12: Technical and Regulatory Considerations for Pharmaceutical Product Lifecycle Management. 2017.

(8) CMC Biotech Working Group. A-Mab: a case study in bioprocess development. 2009. https://cdn.ymaws.com/www.casss.org/resource/resmgr/imported/A-Mab_Case_Study_Version_2-1.pdf (accessed Mar 28, 2018).

(9) CMC-Vaccines Working Group. A-VAX Case Study: Applying Quality by Design to Vaccines. 2012. https://www.dcvmn.org/IMG/pdf/a-vax-applying-qbd-to-vaccines_2012.pdf (accessed Mar 28, 2018).

(10) FDA. Quality by Design for ANDAs : An Example for Immediate-Release Dosage Forms. 2012. https://www.fda.gov/downloads/drugs/developmentapprovalprocess/howdrugsaredevelopedandapproved/approvalapplications/abbreviated newdrugapplicationandagenerics/ucm304305.pdf (accessed Mar 29, 2018).

(11) FDA. Quality by Design for ANDAs : An Example for Modified Release Dosage Forms. 2011. http://www.fda.gov/downloads/drugs/developmentapprovalprocess/howdrugsaredevelopedandapproved/approvalapplications/abbreviated newdrugapplicationandagenerics/ucm286595.pdf (accessed Mar 29, 2018).

(12) *Pharmaceutical Quality by Design: A Practical Approach*; Schlindwein, W. S., Gibson, M., Eds.; John Wiley & Sons Ltd.: New Jersey, 2018.

(13) Report from the EMA-FDA QbD pilot program. EMA/213746/2017. http://www.ema.europa.eu/docs/en_GB/document_library/Other/2017/04/WC500225533.pdf (accessed Mar 30, 2018).

(14) International Society for Pharmaceutical Engineering Spain. *QbD as an Improvement Methodology for Pharmaceutical Legacy Products. A Case Study.*; 2014.

(15) Kourti, T.; Davis, B. The Business Benefits of Quality by Design (QbD). *Pharm. Eng.* **2012**, *32* (4), 1–10.

(16) Potter, C. PQLI Application of Science-and Risk-Based Approaches (ICH Q8, Q9, and Q10) to Existing Products. *J Pharm Innov* **2008**, *4*, 4–23.

(17) Cook, J.; Cruañes, M. T.; Gupta, M.; Riley, S.; Crison, J. Quality-by-Design: Are We There Yet? *AAPS PharmSciTech* **2014**, *15* (1), 140–148.

(18) EMA. Guideline on Process Validation for Finished Products - Information and Data to Be Provided in Regulatory Submissions. European Medicines Agency. London, UK, 2016.

(19) EudraLex The Rules Governing Medicinal Products in the European Union. Volume 4-EU Guidelines to Good Manufacturing Practice Medicinal Products for Human and Veterinary Use. Annex 15: Qualification and Validation. European Commission, Brussels, Belgium, 2015.

(20) FDA. Guidance for Industry, Process Validation: General Principles and Practices. U.S. Department of Health and Human Services Food and Drug Administration: Silver Spring, MD, 2011.

(21) Yu, L. X.; Amidon, G.; Khan, M. A.; Hoag, S. W.; Polli, J.; Raju, G. K.; Woodcock, J. Understanding Pharmaceutical Quality by Design. *AAPS J.* **2014**, *16* (4), 771–783.

(22) Riley, B. S.; Li, X. Quality by Design and Process Analytical Technology for Sterile Products--Where Are We Now?

AAPS PharmSciTech **2011**, *12* (1), 114–118.

(23) Lambert, W. J. Considerations in Developing a Target Product Profile for Parenteral Pharmaceutical Products. *AAPS PharmSciTech* **2010**, *11* (3), 1476–1481.

(24) Garcia, T.; Cook, G.; Nosal, R. PQLI Key Topics - Criticality, Design Space, and Control Strategy. *J. Pharm. Innov.* **2008**, *3* (2), 60–68.

(25) Pramod, K.; Tahir, M. A.; Charoo, N. A.; Ansari, S. H.; Ali, J. Pharmaceutical Product Development: A Quality by Design Approach. *Int J Pharma Investig* **2016**, *6* (3), 129–138.

(26) ISPE PQLI Guide Series Part 1 - Product Realization Using Quality by Design (QbD): Concepts and Principles. In *Product Quality Lifecycle Implementation (PQLI) from Concept to Continual Improvement*; ISPE, Ed.; 2011.

(27) Nosal, R.; Schultz, T. PQLI Definition of Criticality. *J Pharm Innov* **2008**, *3*, 69–78.

(28) Lionberger, R. A.; Lee, S. L.; Lee, L.; Raw, A.; Yu, L. X. Quality by Design: Concepts for ANDAs. *AAPS J.* **2008**, *10* (2), 268–276.

(29) Mitchell, M. Determining Criticality-Process Parameters and Quality Attributes Part I: Criticality as a Continuum. *BioPharm Int.* **2013**, *12* (26), 38–47.

(30) Glodek, M.; Liebowitz, S.; McCarthy, R.; McNally, G.; Oksanen, C.; Schultz, T.; Sundararajan, M.; Vorkapich, R.; Vukovinsky, K.; Watts, C.; et al. Process Robustness – A PQRI White Paper. *Pharm. Eng.* **2006**, *26* (6), 1–11.

(31) Ahmed, R.; Baseman, H.; Ferreira, J.; Genova, T.; Harclerode, W.; Hartman, J.; Kim, S.; Londeree, N.; Long, M.; Miele, W.; et al. PDA Survey of Quality Risk Management Practices in the Pharmaceutical, Devices, & Biotechnology Industries. *PDA J. Pharm. Sci. Technol.* **2008**, *62* (1), 1–21.

(32) PDA. *Technical Report 54. Implementation of Quality Risk Management For Pharmaceutical and Biotechnology Manufacturing Operations*; Parenteral Drug Association, Inc.: Bethesda, MD, 2012.

(33) Rathore, A. S.; Winkle, H. Quality by Design for Biopharmaceuticals. *Nat. Biotechnol.* **2009**, *27* (1), 26–34.

(34) Mccurdy, V.; Ende, M. T.; Busch, F. R.; Mustakis, J.; Rose, P.; Berry, M. R. Quality by Design Using an Integrated Active Pharmaceutical Ingredient –Drug Product Approach to Development. *Pharm. Eng.* **2010**, *30* (4), 1–16.

(35) Casian, T.; Iurian, S.; Bogdan, C.; Rus, L.; Moldovan, M.; Tomuta, I. QbD for Pediatric Oral Lyophilisates Development: Risk Assessment Followed by Screening and Optimization. *Drug Dev. Ind. Pharm.* **2017**, *43* (12), 1932–1944.

(36) Claycamp, H. G.; Kona, R.; Fahmy, R.; Hoag, S. W. Quality-by-Design II: Application of Quantitative Risk Analysis to the Formulation of Ciprofloxacin Tablets. *AAPS PharmSciTech* **2016**, *17* (2), 233–244.

(37) Mishra, S. M.; Rohera, B. D. An Integrated, Quality by Design (QbD) Approach for Design, Development and Optimization of Orally Disintegrating Tablet Formulation of Carbamazepine. *Pharm. Dev. Technol.* **2016**, *22* (7), 889–903.

(38) Van Leeuwen, J. F.; Nauta, M. J.; De Kaste, D.; Odekerken-Rombouts, Y. M. C. F.; Oldenhof, M. T.; Vredenbregt, M. J.; Barends, D. M. Risk Analysis by FMEA as an Element of Analytical Validation. *J. Pharm. Biomed. Anal.* **2009**, *50*, 1085–1087.

(39) Martin-Moe, S.; Lim, F. J.; L.Wong, R.; Sreedhara, A.; Sundaram, J.; Sane, S. U. A New Roadmap for Biopharmaceutical Drug Product Development: Integrating Development, Validation, and Quality by Design. *J. Pharm. Sci.* **2011**, *100* (8), 3031–3043.

(40) Jameel, F.; Khan, M. Quality-by-Design as Applied to the Development and Manufacturing of a Lyophilized Protein Product. *American Pharmaceutical Review*. 2009.

(41) Martin-Moe, S.; Nast, C. An Overview of Quality by Design for Drug Product. In *Quality by Design for Biopharmaceutical Drug Product Development*; Al., F. J. et, Ed.; Springer Science+Business Media: New York, 2015; pp 47–59.

(42) Harms, J.; Wang, X.; Kim, T.; Yang, X.; Rathore, A. S. Defining Process Design Space for Biotech Products: Case Study of Pichia Pastoris Fermentation. *Biotechnol. Prog.* **2008**, *24* (3), 655–662.

(43) Lepore, J.; Spavins, J. PQLI Design Space. *J. Pharm. Innov.* **2008**, *3* (2), 79–87.

(44) Fissore, D.; Pisano, R.; Barresi, A. A. Advanced Approach to Build the Design Space for the Primary Drying of a

Pharmaceutical Freeze-drying Process. *J. Pharm. Sci.* **2011**, *100* (11), 4922–4933.

(45) Sundaram, J.; Shay, Y. H. M.; Hsu, C. C.; Sane, S. U. Design Space Development for Lyophilization Using DoE and Process Modeling. *BioPharm Int.* **2010**, *23* (9), 26–36.

(46) De Beer, T. R. M.; Wiggenhorn, M.; Hawe, A.; Kasper, J. C.; Almeida, A.; Quinten, T.; Friess, W.; Winter, G.; Vervaet, C.; Remon, J. P. Optimization of a Pharmaceutical Freeze-Dried Product and Its Process Using an Experimental Design Approach and Innovative Process Analyzers. *Talanta* **2010**, *83*, 1623–1633.

(47) Debevec, V.; Srčič, S.; Horvat, M.; Srcic B, S. Scientific, Statistical, Practical, and Regulatory Considerations in Design Space Development. *Drug Dev. Ind. Pharm.* **2018**, *44* (3), 349–364.

(48) Davis, B.; Lundsberg, L.; Cook, G. PQLI Control Strategy Model and Concepts. *J Pharm Innov* **2008**, *3*, 95–104.

(49) Boyer, M.; Gampfer, J.; Zamamiri, A.; Payne, R. A Roadmap for the Implementation of Continued Process Verification. *PDA J. Pharm. Sci. Technol.* **2016**, *70* (3), 282–292.

(50) Nelson, L. S. Notes on the Shewhart Control Chart. *J. Qual. Technol.* **1999**, *31* (1), 124–126.

(51) ASTM E2281-03, Standard Practice for Process and Measurement Capability Indices, ASTM International, West Conshohocken, PA, 2003, Www.astm.org.

(52) *Introduction to Statistical Quality Control*, 6th ed.; Montgomery, D. C., Ed.; John Wiley & Sons, Inc: Danvers, MA, 2012.

(53) EudraLex The Rules Governing Medicinal Products in the European Union. Volume 4-EU Guidelines to Good Manufacturing Practice Medicinal Products for Human and Veterinary Use. Chapter 1. Pharmaceutical Quality System. Brussels: European Commission, Brussels, Belgium, 2012.

(54) FDA. Guidance for Industry, PAT- A Framework for Innovative Pharmaceutical Development, Manufacturing, and Quality Assurance. U.S. Department of Health and Human Services Food and Drug Administration: Rockville, MD, 2004.

(55) Scott, B.; Wilcock, A. Process Analytical Technology in the Pharmaceutical Industry: A Toolkit for Continuous Improvement. *PDA J. Pharm. Sci. Technol.* **2006**, *60* (1), 17–53.

(56) Alcalà, M.; Blanco, M.; Bautista, M.; González, J. M. On-Line Monitoring of a Granulation Process by NIR Spectroscopy. *J. Pharm. Sci.* **2010**, *99* (1), 336–345.

(57) EudraLex The Rules Governing Medicinal Products in the European Union. Volume 4-EU Guidelines to Good Manufacturing Practice Medicinal Products for Human and Veterinary Use. Annex 17 Revision 1: Real Time Release Testing. European Commission, Brussels, Belgium, 2015.

Chapter 3

Freeze-drying of Pharmaceutical Drug Products

1. Basic principles

Many pharmaceutical products are not stable for long periods of time as liquid solutions[a]. In the presence of water, such materials either degrade through hydrolysis or undergo other chemical reactions allowed by the molecular mobility provided in liquid state. Lyophilization, also referred as freeze-drying[b], is a stabilizing process in which water is removed from a product after it is frozen and placed under vacuum, allowing the ice to change directly from solid to vapour without passing through the liquid phase.[1] A readily soluble product with low Residual Moisture Content (RMC) is obtained that guarantees long-term stability during storage. Basically, the freeze-drying process is divided in three main stages[2]:

1) Freezing: where most of water is converted into ice.
2) Primary drying: where ice is removed by sublimation.
3) Secondary drying: where the unfrozen water is removed by desorption.

The following sections provide an overview of the freeze-drying process for pharmaceutical products. The chapter starts with the key historical events that led to the development of modern freeze-drying, a general view of benefits and limitations of the process, and its widespread applications. After, the basic components of the equipment are defined as well as a detailed description of the three stages. Next, quality attributes of freeze-dried products are outlined to understand the final objectives of freeze-drying process development. Finally, some freeze-drying process monitoring tools are described, ending with some insight into process transfer and scale-up.

1.1. A little bit of history

The first evidence of freeze-drying process to preserve food came from the Incas, who stored their potatoes and other food crops on the mountain heights above Machu Picchu. The cold mountain temperatures froze the food and, under the low air pressure of the high altitudes, water inside slowly vapourized.[3] However, as part of science and technology, freeze-drying is only a matter of a century. Some key milestones in the history of freeze-drying (excluding food products) are described in Figure 3.1.

At the beginning of the 20th century, freeze-drying was established as a stabilizing process for heat labile biological substances. Earl Flosdorf, Ronald Greaves and François Henaff were responsible for the mass production of freeze-dried human plasma used extensively during World War II.[4]

[a] In this chapter, all assumptions are made regarding aqueous solutions. Although it is possible to freeze-dry from non-aqueous solvents, water is the most common solvent used.
[b] From now on, to clarify and facilitate the comprehension, the term freeze-drying will be used to define the process.

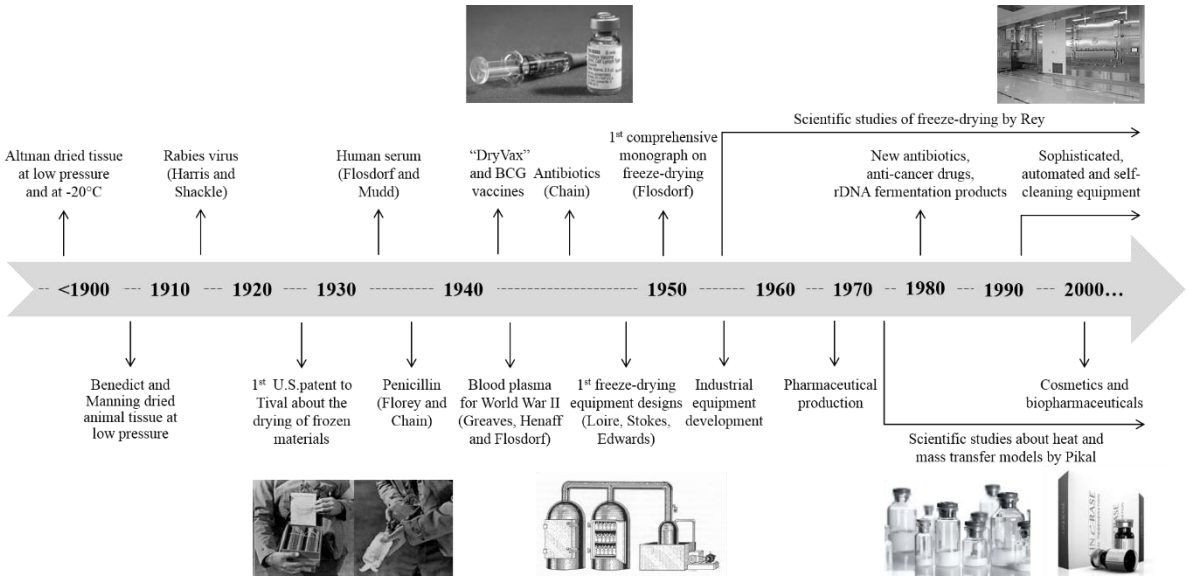

***Figure 3.1. Timeline diagram of the key milestones in the history of freeze-drying. Sourced from references*[1,5].**

Later, the freeze-drying process began to be industrialized. Loire, Stokes, Edwards and others, designed and built the first equipment for industrial purposes. Freeze-drying was commonly used for pharmaceutical production in 1970s. L.R. Rey[6], in 1976, first came up with the term lyophilization by taking into account the porous nature of the dried product and its "*liophil*" characteristic to rapidly reabsorb the solvent and restore the substance to its original state.[1] Actually, the term *lyophile* has the origin from the Greek and literally means "likes the solvent".[7]

In the 1980s, it became a mature process with large-scale applications for new antibiotics and anti-cancer drugs which required sophisticated and automated control systems. During these decades, emphasis was placed on modelling the process in terms of heat and mass transfer, the problems of collapse, the use of excipients and the development of electronic devices to monitor and control the process.[1,5] In this sense, it is worth to mention the huge contribution of M.J. Pikal†, from the University of Connecticut, in the scientific research of these topics.

Nowadays, the freeze-drying process has taken more importance in the parenteral industry because of the advent of recombinant DNA technology, proteins, peptides and other active biological compounds.[8] These products are very fragile, difficult to freeze, and sensitive to RMC. Today, considering all the above issues, freeze-drying is considered an essential tool for the pharmaceutical industry.

In September 2017, Lyophilization Technology Hub (LyoHUB) released a 10-year technology roadmap for pharmaceutical freeze drying.[9] The roadmap reflects the opinions of more than 100 industry and academic experts. According to LyoHUB roadmap, the actual worldwide market for freeze-dried foods and pharmaceuticals is approximately $16 billion per year, with increase future forecast due to the growing demand of biopharmaceuticals. Finally, the short-term priorities for the freeze-drying industry are focused on in-line monitoring tools and process mathematical models.[10]

1.2. Applications

Thanks to the advances in the last century, the freeze-drying process has application in the preservation of many different type of materials, from small molecules to whole organisms[8,11,12]:

- Healthcare and veterinary industries comprise the major area of application and includes the freeze-drying of chemical compounds, antibiotics, vaccines, hormones, biotechnology products (mainly proteins and antibodies), either as APIs or drug products.
- Cells and body tissues for surgical or medical use such as blood, bone and tendon.
- Food products like: milk, coffee, vegetables, fruits, meat or fish. In this case, freeze-drying is useful to reduce transport costs, extend their shelf life and maximize their flavour and nutritional value.
- Other applications like: preservation and recovery of museum artefacts, books, archaeological finds, floral products, algae or bacteria.

1.3. Benefits and limitations

Freeze-drying has several benefits as well as some limitations. Some of them are listed in Table 3.1.

Table 3.1. Comparative table about benefits and limitations of the freeze-drying process. Sourced from references[8,11,13].

Benefits	Limitations
Enhanced and long shelf life at warmer temperatures, often as high as room temperature.	Cost and complexity of equipment. High operating and maintenance costs.
Low temperature drying process, ideal for heat labile products (like proteins).	High energy cost due to high energy consumption.
Low RMC in the finished product.	Lengthy process.
Rapid reconstitution time due to the high specific surface area of the product (particularly important for emergency antibiotics and vaccines, which need to be administrated as soon as possible).	Sterility assurance of the freeze-dryer chamber and all connections and gases leading into the chamber.
Pharmaceutically elegant solid product that maintains its original structure and activity.	Many biological molecules are damaged by stresses during freezing and/or drying.
Drying is carried out under vacuum and vials can be sealed under vacuum or inert gas, which helps preserve products sensitive to oxygen.	Solutes with very low critical temperatures cannot be freeze-dried to obtain a pharmaceutical acceptable cake.

But, most of the times, the benefits overcome the limitations. For instance, savings due to increased product shelf life compensate for the investment in freeze drying equipment.

2. Equipment components

Freeze-drying equipment is rather complex. The main components are: a drying chamber connected to an ice condenser via a large valve, a pump vacuum system and a shelf thermoregulation system (Figure 3.2).[12] The drying chamber has a front door for loading and unloading the vials.

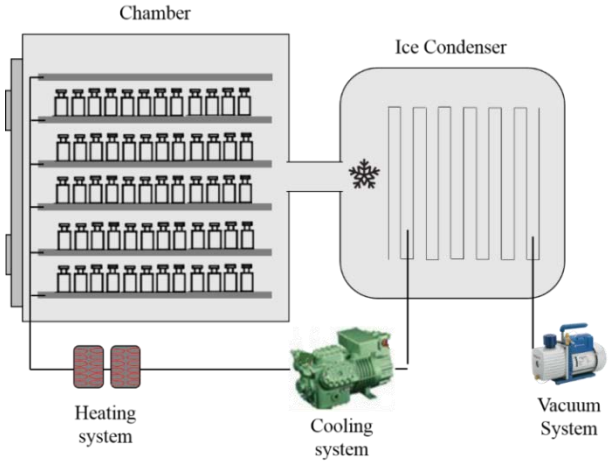

Figure 3.2. Simplified diagram showing the major components of a pharmaceutical freeze-dryer.

The drying chamber and the condenser can be exposed to low pressures by the action of vacuum pumps. The drying chamber is composed by shelves where the vials are placed, usually on trays. All shelves are of a hollow construction that permits the serpentine flow of heat-transfer fluid, typically silicone oil. Thermal fluid heating is normally done by an electrical heater and cooling by compressors. The vacuum pump compresses the non-condensable gases that pass through the condenser chamber and discharges these gases directly into the atmosphere. The condenser, operating at low temperature (up to approx. -80ºC), collects water vapour from the product and is usually located externally to the chamber. Additionally, modern freeze-dryers contain a stoppering mechanism, temperature and pressure probes and automatic monitoring and control systems[c].[1]

Depending on the production scale or processing capacity, three types of freeze-dryers can be distinguished: laboratory, pilot and production freeze-dryers. Pictures of the different types of freeze-dryers are shown in Figure 3.3. The main differences are related to the shelf area, ice condenser capacity and automatisms. Consequently, heat and mass transfer rates may vary depending on the design and performance of the freeze-dryer. Therefore, it is important to understand this variability and its impact on the dynamics of the process during its transfer from the laboratory to the industrial scale.[14,15]

[c] For the sake of simplicity, other critical devices for the production performance have not been included in the diagram: filters, valves, cleaning and/or sterilization system, among others.

Figure 3.3. Pictures of small-scale and large-scale pharmaceutical freeze-dryers.

3. Freeze-drying process overview

The total sequence of operation for a sterile freeze-drying process of a product filled in vials is: cleaning and sterilization of the chamber, loading, freezing, primary drying, secondary drying, backfill, stoppering, aeration, unloading, defrosting, cleaning, filter integrity test and leak testing.[16]

Operationally, an aqueous solution of the drug product is filled into glass vials which are loaded onto the temperature-controlled shelves of the freeze-dryer. In these vials, elastomeric stoppers are partially inserted in the neck of the vial, leaving a hollow that allows water vapour to scape. The freeze-drying cycle begins with the freezing phase. Shelves are cooled converting nearly all water into ice, and the chamber is maintained at atmospheric pressure. When freezing is complete, the cycle continues with the primary drying phase. The condenser surface is chilled by circulating a refrigerant. The chamber is evacuated by the vacuum pumps to promote sublimation of the ice crystals, and heat is transmitted through the shelves. Condenser temperature rises slightly due to initial vapour but immediately fails as ice sublimates. Product temperature falls slightly as initial sublimation removes latent heat, then it rises again towards the end of primary drying.[1,17]

The removal of ice crystals by sublimation creates an open network of pores, which allows water vapour to escape from the product through the chamber and, finally, solidifies on the wall of the condenser. Sublimation starts from the upper surface of the frozen product exposed to the vacuum. As primary drying proceeds, the interface between frozen and dried regions (i.e. the sublimation front) moves toward the bottom of the vial, leaving behind a partially dry layer of increasing thickness.[2]

During secondary drying, shelf temperature is increased to promote the desorption process. Product temperature rises until it nearly coincides with shelf temperature and chamber pressure is set at the lowest value achieved by the freeze-dryer. When the desired residual moisture is achieved, secondary drying is completed. Then, vials are stoppered under vacuum by hydraulic or pneumatic internal stoppering devices.[8,12] Alternatively, air or an inert gas (e.g. nitrogen) may be added to the chamber for

stoppering the vials under a slightly reduced pressure (this action is known as backfilling). Upon completion of the stoppering, the drying chamber is aerated, and the product can be safely removed from the freeze-dryer. Finally, the condenser is heated to remove the collected ice.[1]

As a summary, Figure 3.4 shows the evolution of the freeze-drying process in a vial.

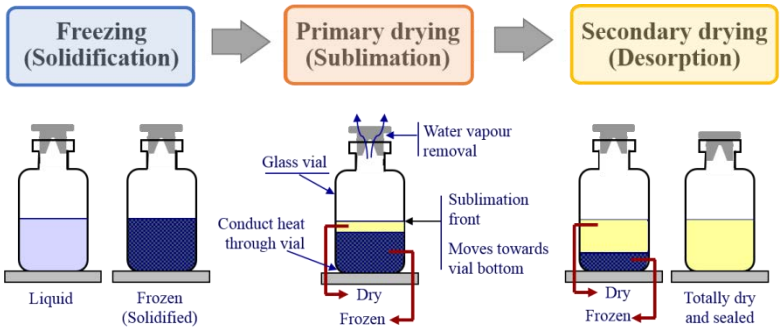

Figure 3.4. Representation of the evolution of the freeze-drying process inside a vial.

Figure 3.5 shows the appearance of the freeze-drying graph, with all temperatures and pressures monitored in a representative freeze-drying cycle.

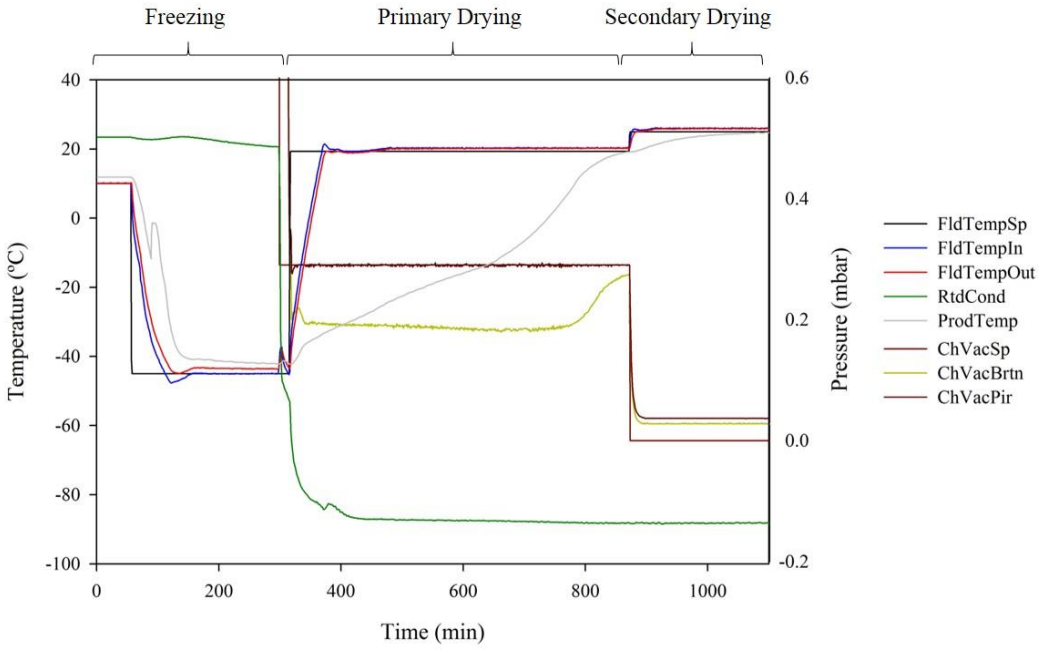

Figure 3.5. Freeze drying graph with temperature and pressure measurements indicated in different colours. Fluid temperature setpoint (FldTempSp), inlet (FldTempIn) and outlet (FldTempOut). Temperature of the condenser (RtdCond) and the product (ProdTemp). Chamber Vacuum setpoint (ChVacSp), chamber vacuum measured by Baratron (ChVacBrtn) and Pirani (ChVacPir).

Therefore, the critical controllable parameters of freeze-drying processes are: shelf temperature, chamber pressure and time. In the following sections, the physical mechanisms for each of the three stages (freezing, primary drying and secondary drying) are explained in more detail.

4. Stages of the freeze-drying process

4.1. Freezing

The principal function of the freezing[d] stage is to solidify the product allowing the separation of the solvent from the solutes. For an aqueous solution, the main physical events occurring during freezing are represented in Figure 3.6:

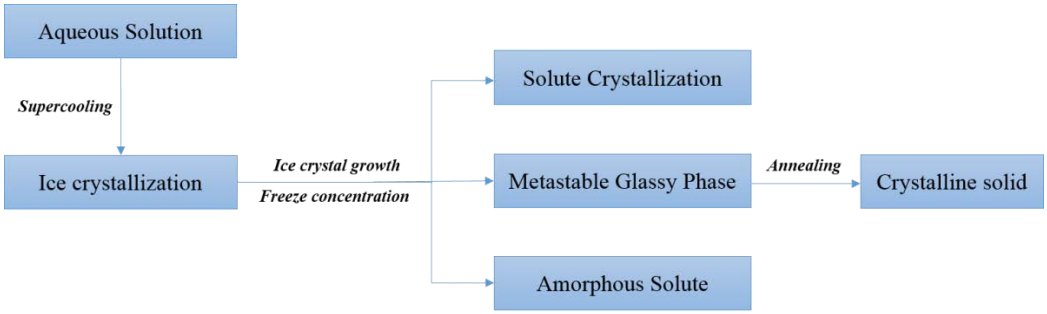

Figure 3.6. Schematic diagram of physical events occurring during freezing of an aqueous solution.

In aqueous solutions, in the absence of particles or vibration, the freezing point of water decreases below the equilibrium freezing temperature at atmospheric pressure. In that point, some nuclei appear stochastically which promote the crystallization of water.[11,17] This phenomenon is called supercooling and the degree of supercooling is defined as the difference between the equilibrium freezing point and the temperature at which ice crystals first form. It is not uncommon for parenteral solutions to exhibit 10ºC to 20ºC of supercooling.[2,18]

Due to its stochastic nature, ice nucleation may vary not only from batch to batch but also from vial to vial within the same batch. Figure 3.7 shows a representation of the temperature of the product and the principal events associated with the freezing stage.

As water crystallizes to ice, the concentration of solutes in the remaining solution increases until there comes a point at which the solutes solidify either as crystalline or amorphous. A crystalline solid is a material in which atoms and molecules are arranged in a regular, precise and highly ordered spatial array and it is characterized by its long-range order and thermodynamic stability.[1]

However, in an amorphous solid, the microscopic molecules arrangement is irregular and lacks a long-range order. In general, amorphous systems are chemically and physically unstable relative to the crystalline state, because they exhibit greater molecular mobility. In practice, many solutions produce a partially crystalline, partially amorphous matrix.[17]

[d] Although cooling and freezing are not exactly the same (shelf-cooling does not assume a change in state from liquid to solid in the formulation), both are used interchangeably in the literature to define the rate of the freezing process.[11,18]

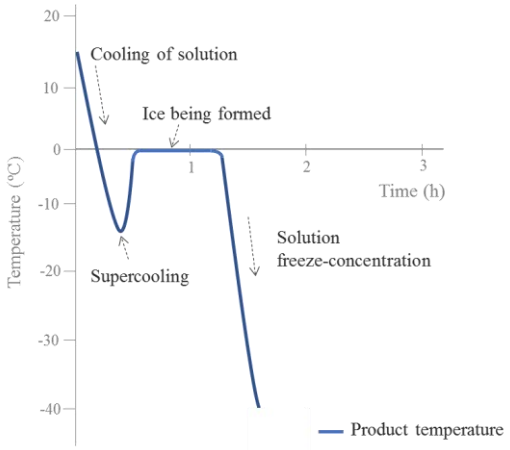

Figure 3.7. Evolution of product temperature during freezing.

When ice is completely formed, the product temperature should decrease below the critical temperatures for crystalline and amorphous materials to ensure a complete product solidification.[17]

For crystalline solutes, the eutectic temperature (T_e) is the critical temperature, and corresponds to the lowest temperature in a system in which a residual liquid phase and solid phase are in equilibrium.[11] Above the eutectic point, ice and solute concentrate persist, whereas below the eutectic point, a mixture of ice and solute crystals is formed.

In the case of amorphous solutes, the liquid increases in viscosity upon freezing sufficiently to transform into a glass state. The glass transition temperature of the maximally freeze-concentrated solution is defined as T_g'[e], and is considered the critical temperature for amorphous materials.[19,20]

Figure 3.8 showed an example of a state diagram of a binary solution of sucrose and water. As temperature is lowered, sucrose does not crystallize at T_e due to its high viscosity, so that freeze-concentration proceeds beyond T_e and goes through a glass state transition at T_g', which corresponds to ~80% sucrose and ~20% water content.

During freezing, the size of the crystals formed is strongly dependent upon the cooling rate and degree of supercooling. Table 3.2 summarizes the effects of fast (>10ºC/min) versus slow (<1ºC/min) cooling rates.[8]

Table 3.2. Impact of cooling rate and degree of supercooling in ice crystal size and primary drying duration.

Cooling rate	Degree of supercooling	Ice crystal size	Duration of primary drying
Fast	High	Small (large number of small ice crystals)	Long (smaller pores, increased resistance to mass flow)
Slow	Low	Large (small number of large ice crystals)	Short (larger pores, decreased resistance to mass flow)

[e] It is different from the glass transition temperature of the amorphous solid (denoted as T_g), which depends on the moisture content in the dried product.[18]

The higher the degree of supercooling, the smaller the ice crystals leading to a higher resistance to mass transfer and a slower drying rate. Then, ice crystals should be large to facilitate sublimation. Nevertheless, large ice crystals result in low specific surface area of the dried product which increases secondary drying times.[21,22]

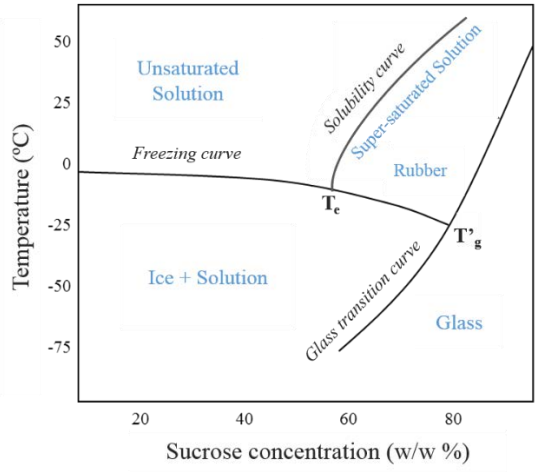

Figure 3.8. State diagram for a binary sucrose and water system. Adapted from references[18,23].

4.1.1. Annealing

Annealing refers to warming the frozen solution to a temperature above T_g', but below the onset of ice melting, and holding for several hours. At that point, the mobility of molecules increases which allows solute crystallization. Then, the product is re-cooled until it is completely frozen before starting primary drying. Moreover, annealing allows a second crystallization of ice and the phenomenon of Ostwald ripening, where large ice crystals are formed at expense of smaller ones.[21]

Forced crystallization during freezing via annealing assures that complete crystallization occurs which accelerates the sublimation and, consequently, reduce the primary drying time.[24] Searles and colleagues[25] first showed that ice nucleation temperature influences the primary drying rate, and, in a second paper[21], they demonstrated that annealing resulted in an approximate 3% increase in the primary drying rate. According to Chouvenc et al.[26], annealing accelerates the sublimation rate by increasing ice crystal sizes of the frozen matrix, thus leading to lower values of the dried layer mass transfer resistance. However, annealing does not always increase primary drying time. For instance, Lu et al.[27] found that the highly crystallized solute blocked the pathways for water vapour to scape and increase the dry layer resistance.

Annealing can prevent partial collapse of the cake and minimize ice nucleation heterogeneity within the batch.[21,24] Likewise, annealing can be used to induce crystallization of excipients (such as mannitol and glycine) that tend to crystallize upon freezing, which avoids later crystallization during drying or storage.[28]

In conclusion, the freezing stage mainly determines the morphology, size and distribution of the crystals formed, as well as the porosity of the freeze-dried product. All together influences the sublimation and desorption rates, and the final appearance of the product.[29]

4.2. Primary drying

In the primary drying phase, the ice formed during freezing is removed by a phenomenon known as sublimation. Sublimation is the phase transition of a substance directly from the solid to the gas phase without passing through the intermediate liquid phase.[8] Sublimation can be explained by a phase diagram, as the one shown in Figure 3.9.

The diagram illustrated the three phases of water at various temperatures and pressures, namely liquid phase (water), gaseous phase (vapour) and solid phase (ice). The three states are divided by solid curves: curve OC represents the equilibrium states of water and vapour, curve OB represents the equilibrium states of ice and water, curve OA represents the equilibrium states of ice and vapour. The point O at which all three phases coexist in thermodynamic equilibrium is known as the Triple point. The Triple point of water is at 0.01ºC and 6.1 mbar.

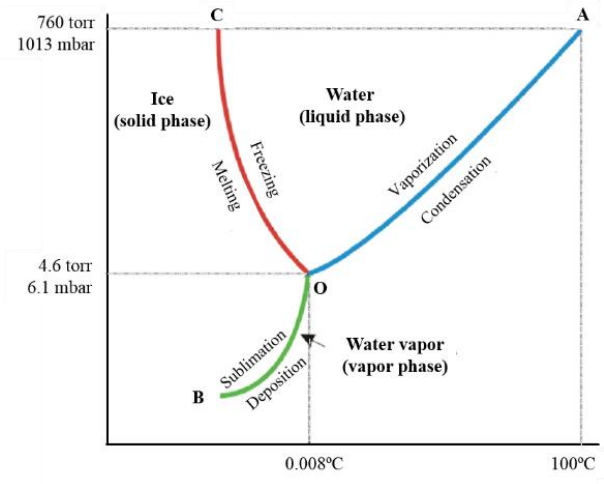

Figure 3.9. Water phase diagram.

Thus, freeze-drying is performed at temperature and pressure conditions below the triple point of water, to enable sublimation of ice.[11] Moreover, sublimation leads to evapourative cooling which will lower the product temperature. Consequently, heat energy is applied to the product to compensate for that cooling. Heat energy can be transferred to the product by a combination of:

- Radiation: mainly from the walls, upper tray and the door of the freeze-dryer.
- Conduction: by direct contact between heated shelf/container and container/solution.
- Convection: through collisions between gas molecules.

The three heat transfer mechanisms are important, but the relative importance of each mechanism depends on the vial type, and the range of shelf temperatures and chamber pressures.[12]

Figure 3.10 represents the sublimation process in a product vial placed on a shelf inside the freeze-dryer. Water vapour is removed flowing through the porous matrix of the partially dried product.[17] The direction of heat and mass transfer causes the top of the product to dry first with drying proceeding downward to the bottom of the vial. Sublimation takes place at the interface between the frozen and dry layers, known as the sublimation front, which is, therefore, the coldest region within the product.

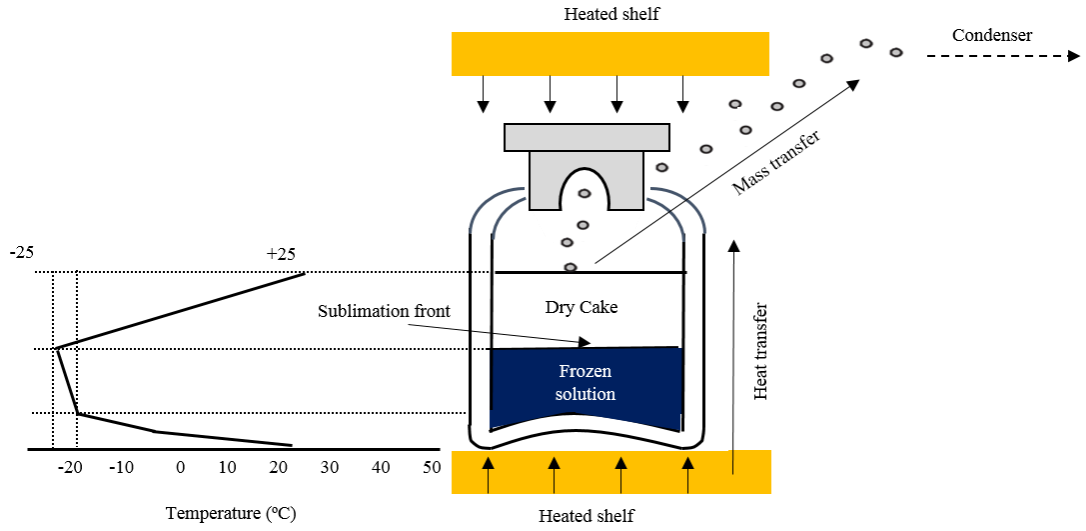

Figure 3.10. Temperature distribution inside a vial during primary drying. Shelves are heated to a temperature enough to allow sublimation. Heat and mass transfer direction are also illustrated.

Then, sublimation involves both the transfer of heat from the shelves to the product and the transfer of mass (water vapour) from the product to the ice condenser. A correct balance has to be adjusted between heat and mass transfer so that drying can proceed efficiently without inducing adverse reactions in the frozen material such as back melting, puffing, or collapse.[4]

4.2.1. Collapse and meltback

In an amorphous matrix, the solute phase exists in a glassy state during drying at temperatures below T_g'. However, above T_g', the viscosity is reduced until the glass phase begins to "soften" resulting in a loss of structural rigidity (Figure 3.11). This phenomenon is called collapse and the temperature at which it occurs is referred to collapse temperature (T_{co}). The T_{co} is often few degrees higher than the T_g'.[30,31]

Collapse can be responsible for blockage of the pores, thus increasing cake resistance to water vapour flow, resulting in slow sublimation rates. Moreover, collapse can reduce the surface area of the cake and prevent efficient secondary drying. In this case, collapsed cakes can retain a higher amount of water in the final product, the reconstitution time can increase, and they can exhibit reduced activity or

compromised stability.[11,17] However, in certain cases, collapse is not necessarily detrimental, particularly in high protein concentration formulation.[32,33]

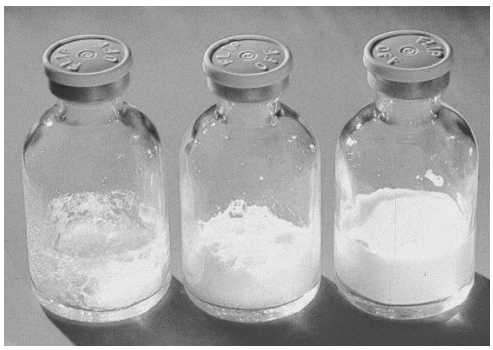

Figure 3.11. Freeze-dried vials with: total collapse (left) and partial collapse (center) and with no evidence of collapse (right). Copied from reference[34].

In crystalline materials, if T_e is exceeded during drying, the frozen solution will melt (also known as meltback) with the consequent cake shrinkage and puffing. Eutectic melting temperatures of most organic compounds are generally much higher than T_{co}, which allow maintenance of high product temperatures during primary drying, resulting in more efficient processes.[12,17]

Finally, the temperature of the sublimation front must always be kept below the maximum allowable product temperature (T_e or T_{co}) to avoid collapse. Due to the relationship between saturated vapour pressure and temperature, chamber pressure determines the product temperature at the sublimation front, and it is responsible of maintaining the product temperature at the desired values.[8,12]

4.2.2. Driving vs resistance force

An efficient freeze-drying process is one in which the primary drying rate is maximized whilst retaining product structure and activity. Hence, it is necessary to understand what drives and what resists the sublimation process to maximize the primary drying rate.

The driving force for the sublimation process is the difference between vapour pressure of ice at the sublimation front and the chamber pressure.[12] Hence if the chamber pressure exceeds the saturated vapour pressure at the sublimation interface of the product, sublimation will stop. However, heat transfer can increase the product temperature at the sublimation front (and consequently, the vapour pressure), resulting in a large impact on the vapour pressure differential. Then, both, temperature and vapour pressure differential are driving forces of the sublimation process.[11]

The resistance force is caused by resistance to the heat transfer from the shelves to the sublimation front, or by resistance to the mass transfer from the sublimation front to the condenser. Nevertheless, the greatest resistance to mass transfer is often due to the thickness of the partially dry layer.[8,17]

4.3. Secondary drying

Secondary drying is a desorption process that consists in the removal of bound water by heating the product further, at higher temperatures under reduced pressure. In contrast to primary drying, water vapour removal during secondary drying is largely by a process of diffusion.[1,17]

The effects of many variables on the kinetics of secondary drying were studied by Pikal and coworkers[35], in 1990, who affirmed that chamber pressure does not influence secondary drying rates to a significant extent. In addition, the water content decreases with time but tends to a plateau. Therefore, once the product has reached its final secondary drying temperature, there is little value in extending the drying period beyond a few hours.

On the contrary, Searles et al.[36] pointed out that lower chamber pressure values may be justified as a strategy for ensuring low partial pressure of water in the chamber which has a direct impact on the level of RMC in the freeze-dried product.

Because no ice is present, the temperature of the product does not have to be held below the T_{co} and can be as high as possible without causing degradation of the API. Therefore, the secondary drying temperature must be less than the maximum allowed temperature in solid state determined by the material nature and stress stability studies. In general, small molecule freeze-dried products can withstand secondary drying temperatures between 40ºC and 50ºC whereas secondary drying temperatures for large biomolecules cannot exceed 30ºC due to denaturation processes.

In crystalline products, the increase in temperature in the secondary drying can be carried out quickly since the product only contains a small percentage of RMC. Amorphous products may have a high RMC (>10% H_2O) at the end of the primary drying.[22] Then, if product temperature during secondary drying is higher than the glass transition of the dried solid (T_g), it is possible to induce collapse. However, due to the plasticizing effect of water, the T_g of the amorphous products increases gradually with the removal of water content during secondary drying.[11]

Preliminary experimentation should determine the temperature and time of secondary drying required to achieve the optimum RMC in the freeze-dried cake, because "*The driest product is not always the optimum"*.[17] Insufficiently dried material will often exhibit poor long-term stability. However, overdrying may equally damage sensitive biological products.[37]

Recently, and for the first time, Sahni and Pikal have published a mathematical model for the secondary drying phase which can be used as a process development tool.[38] Nevertheless, the secondary drying process is still poorly understood compared to ice sublimation.

5. Quality attributes, stability and storage of freeze-dried products

Relevant quality attributes of freeze-dried products are: cake appearance, RMC and RT[f]. The ideal freeze-dried product should have an strong and porous structure, uniform colour, without macroscopic collapse or meltback, low RMC, and sufficient porosity that permits rapid RTs.[1,13] These three attributes can be correlated with other biochemical attributes (such as purity) and long-term stability.

Besides, according to Parenteral Preparations monograph[39] of *Ph. Eur.*, other quality attributes must be analysed for batch release, such as: sterility, container closure integrity, particulate contamination, bacterial endotoxins and uniformity of content[g].

These requirements have to be met not only initially, but also throughout the shelf life of the product. The main purpose of freeze-drying is to lengthen the shelf life of products from hours/days to years, and to store that products at room temperature conditions. Nevertheless, certain freeze-dried drug products still need to be stored refrigerated or frozen. The most important factors affecting the stability of freeze-dried products are moisture, storage temperature, oxygen and, sometimes, light.

The purpose of stability is to provide evidence on the way that the quality of freeze-dried products varies with time, and to establish expiration date and recommended storage conditions.[1,13] Consequently, freeze-dried products must go through a strict stability test procedure, established in ICH Q1A[40], before they are pushed to the market.

By their nature, freeze-dried materials are hygroscopic and the exposure to moisture during storage can destabilize the product. Then, an obvious concern with the lyophilized product is the amount of moisture present in vials.

Several studies have shown that a potential cause of moisture content increment during storage period is the moisture released from the rubber stopper.[41] Packaging used for freeze-dried materials must be impermeable to atmospheric moisture and air, because oxygen is also detrimental to the stability of most freeze-dried drug products.

During storage, water can act as a reactant promoting the chemical reactions and, also, as a plasticizer reducing the T_g of amorphous solids. At storage temperatures close to or higher than T_g, the increment of molecules mobility can cause cake shrinkage and affect product stability. In this sense, storage temperature should be set below T_g and water content should be relatively low.[42,43]

[f] Reconstitution is the process that is used to restore the lyophilized product to its original formulation. The process involves the addition of a known quantity of diluent to the dried cake.

[g] Product specific quality attributes are found in pharmacopoeias monographs of API and finished products, or they are defined based on the QTPP in the initial development.

Moreover, RMC could vary in different vials of the same batch. Then, a typical question for a dossier application may be whether the manufacturer can guarantee that all vials in a batch of tens to hundreds of thousands have the same RMC.[7]

A potential cause of this intra-batch variability is the non-homogeneous heat transfer inside the freeze-dryer and the well-known vial edge effect.[12] Vials at the edge of a shelf dry faster and have lower RMC than the centre of the shelf due to atypical radiation from the chamber walls and/or door.[44] In this sense, vial-to-vial variability should be determined by extensive sampling during process qualification, ideally by mapping RMC as a function of vials position inside the freeze-dryer.

The RMC could be analysed by several techniques such as loss on drying (gravimetric method), Thermogravimetric Analysis (TGA), Karl Fischer (KF) Titration, NIRS, etc. However, the conventional method employed in the industry is KF. Alternatively, NIRS is a non-destructive technique that offers several benefits compared to KF. More information about these techniques is found in Chapter 4.

In summary, the freeze-drying process should be designed so that the product complies the abovementioned quality attributes specifications: pharmaceutically elegant cake, low RMC, minimum time of reconstitution, retention of activity and an adequate shelf life.[45]

6. Freeze-drying cycle development

The development of freeze-dried injectable pharmaceutical products has traditionally been a process of trial and error, both with respect to the composition of the formulation and the process conditions.[17] However, in recent years, it has become widely accepted that freeze-drying cycles should be developed on a more rational and scientific basis.

Since freeze-drying is a costly and time-consuming process, from an operational point of view, the process should be short, reproducible, and robust. For contextualization purposes, the duration of industrial freeze-drying processes can range from few hours for simple products to several days (even a week) for products which are more difficult to dry.

Then, an optimized process that operates within the capabilities of the equipment with appropriate safety margins should be the goal. In addition, the drying rate must be as high as possible to reduce the cycle time without affecting product quality.[46] With this regard, as the primary drying phase is the longest of all three steps, its optimization is typically the focus in the industry.[14,15]

In freeze-drying, the design of the formulation and the process are very interdependent and both, directly or indirectly, influences product quality attributes. The formulation dictates the design of the process, and the variations in the course of freeze-drying can completely change the physical states of the formulation.[22] Therefore, it is extremely important to study different formulations and characterise the freezing and drying behaviour of the formulations by different analytical techniques.

On one hand, it requires the determination of critical temperatures in the formulation, also known as formulation thermal fingerprint. On the other hand, based on the thermal fingerprint, freeze-drying cycle development requires careful determination of the following controllable parameters: shelf temperature, chamber pressure and time. While these three parameters can be modified independently, they are so intimately related that, it is not possible to modify one without affecting the others.

6.1. Formulation development

As previously stated, formulation characteristics impact on the freeze-drying performance. Successful formulations should provide sufficient stability in solution, and during freeze-drying and storage.[12,43] When excipients are needed, they fit in one of the five categories listed in Table 3.3: stabilizers, bulking agents, buffering agents, tonicity modifiers, and surfactants.[47]

***Table 3.3. Types of excipients used in freeze-dried pharmaceutical products. Sourced from references*[12,13,48].**

Excipients type	Function	Common examples
Cryoprotectants	Stabilize the product during the freezing process	Sucrose, mannitol, lactose, trehalose, polyethylene glycol, human albumin
Lyoprotectants	Stabilize the product during the drying and storage processes	
Bulking agents	Enhance the appearance of the product and provide adequate mechanical support	Mannitol and glycine
Buffers	Control and stabilize the pH of the solution	Sodium citrate, sodium phosphate, tromethamine, histidine
Tonicity Modifiers	Ensure the isotonicity of the reconstituted solution at the point of use	Sodium chloride salt and sugars
Surfactants	Reduce denaturation during freezing. Prevent protein loss due to adsorption at the surfaces of equipment and containers. Aid in refolding of structurally altered forms preventing aggregation.	Polysorbate 20 and 80

In general, collapse temperatures are much lower than eutectic melting temperatures. For instance, some formulations contain carbohydrates as cryo- and lyoprotectants, whose collapse temperatures could be below -40ºC. Such a low value would hinder or even impede the freeze-drying process. Nevertheless, some bulking agents possess high eutectic temperatures which allow maintenance of high product temperatures during primary drying resulting in a more efficient drying process.[13] Particularly, one of the formulations studied in this thesis contains mannitol, and a comprehensive review of this excipient is found in Chapter 7.

Likewise, fill depth (or cake thickness) is also a significant parameter that should be minimized to increase drying efficiency. The greater the fill depth, the greater the resistance to vapour flow and the longer the primary drying time. Ideally, a fill depth of 5 mm is recommended, never exceeding 50% of the nominal fill volume of the container.[15]

The percentage of solid content affects the product resistance during sublimation, and, therefore, the drying rate. A high solid content will decrease the porosity of the dried portion and hence raise the product resistance. However, an excessive reduction of the solid content results in a brittle and mechanically weak cake. Ideally, solid content should be around 10%w/v.

In addition, the container closure system also plays an important role in freeze-drying process design. The glass vial geometry and quality, vial diameter and rubber stopper may influence the heat conductive properties that directly impact on the freeze-drying process.[49,50]

6.2. Analytical techniques for formulation characterization

Physical characterization of formulations in frozen and freeze-dried solid states provides indispensable information for rational design of freeze-drying processes. In this sense, a thorough characterization of the formulation critical temperatures (i.e. T_g' and T_{co} for amorphous products and T_e for crystalline products) is required at the beginning.[51] Consequently, a process can be developed which ensures that the product is completely solidified during freezing and that its temperature remains below the critical temperatures during primary drying.

There are several publications that describe the techniques currently available to characterize frozen as well as final freeze-dried products.[51–53] Traditionally, differential scanning calorimetry (DSC) and freeze-drying microscopy (FDM) have been used for determining important product properties related to freeze-drying. However, currently, other techniques like low temperature X-ray powder diffraction (LT-XRPD) are of great interest to determine the microstructure of the frozen solution or freeze-dried material.

The techniques used in this thesis are further explained in the following sections:

6.2.1. Differential scanning calorimetry

DSC measures the heat flow as a function of temperature applied to a sample. The DSC instrument consists in an environmentally controlled cabinet that contains two cells, one reference cell and one sample cell. Experimentally, a small quantity of sample (typically 10-30 mg for liquid samples and 2-10 mg for solid samples) is placed in an aluminium crucible and put into the sample cell. An empty crucible is generally placed into the reference cell.

During a DSC experiment, both reference cell and sample cell are cooled and/or heated according to a selected temperature program. The difference in heat flow into the sample compared to an empty reference crucible induces a small temperature difference, which is converted to heat flow. The result of the experiment is a plot of heat flow versus temperature, known as DSC curve.[53–55] A representation of a DSC heating curve of a frozen system is illustrated in Figure 3.12.

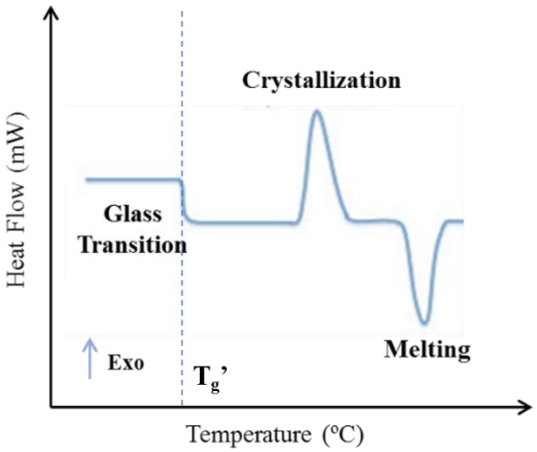

Figure 3.12. Thermal transition in frozen solutions, including eutectic melting, glass transition and crystallization.

Reference and sample curves exhibit parallel behaviour at a constant heating rate until a sample reaction occurs which yields a curve with thermal inflections. The thermodynamic structural changes that appear in the sample translate into release or absorption of heat, resulting in exothermic or endothermic transitions respectively.[17] Common physical transformations that take place by varying the temperature are: crystallization, melting and glass transitions (represented in Figure 3.12). The glass transition is represented as a step-like or a shift in the heat flow baseline. Crystallization is observed as an exothermic peak and eutectic melting as an endothermic peak.

In conclusion, DSC allows to characterise some thermal properties of formulations in frozen state, such as T_g', T_e and ice melting temperature.[18] For further information, an excellent review with several applications of DSC to characterize pharmaceutical systems in frozen state was published by Sundaramurthi and Suryanarayanan.[56]

6.2.2. Freeze-drying microscopy

FDM is used to observe structural alterations at the sublimation interface as a function of a controlled temperature program. FDM consists of an optical microscope with a specially made low-temperature freeze-drying stage and a vacuum system. It uses liquid nitrogen vapour circulated through a silver block along with a heater to control the surface temperature.[17]

FDM is carried out by placing a small quantity (around 2-4 µl) of sample solution between two glass coverslips in the freeze-drying stage. Then, sample is cooled until a determined temperature and hold there for a few minutes. Once frozen, the sample stage can be evacuated to operate at pressures representatives of freeze-drying and heated to simulate primary drying. Formation and progress of the sublimation front can be observed as well as the resulting morphology in the dried material. Moreover, real-time images, like the one represented in Figure 3.13, and videos, can be recorded in a pre-defined time interval.[55]

By using FDM a number of events occurring in a material can be determined, including: nucleation temperature, eutectic melting, collapse, the effect of annealing a sample on ice crystal structure and solute crystallization.[57] Specifically, FDM is the best technique to accurately determine the collapse temperature.[58]

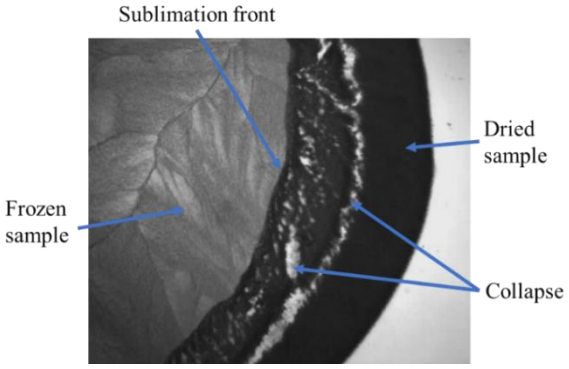

Figure 3.13. Microscopic observation of a partially freeze-dried product.

6.2.3. X-ray powder diffraction

X-ray powder diffraction (XRPD) can be used to study the crystallization processes directly in frozen systems by using a low-temperature stage attached to the X-ray diffractometer. A small quantity of solution is placed in a XRPD holder and cooled at a constant rate to the desired temperature. In addition, it is also possible to attach a vacuum pump and reproduce the primary drying phase. Then, phase changes that occur during drying can be monitored in-situ.[18,59]

The advantage of XRPD over DSC is that it provides direct evidence of crystallization and allows the identification of different polymorphs. Because polymorphs of crystalline materials have different physical properties, such as differences in melting point or solubility, XRPD can provide valuable insight into the processes underlying physical or chemical stability problems.[17,60]

6.3. Characterization of freeze-dried drug products

Additionally, the freeze-dried drug product should be characterized as well, to increase product and process knowledge. Table 3.4 summarizes the analytical techniques for the characterization of freeze-dried drug products used in this thesis[h].

[h] In this section, only characterization methods of the freeze-dried cake are included but, other analytical methods are required to evaluate the quality attributes of the drug product.

Table 3.4. Analytical methods for freeze-dried drug product characterisation.

Analytical method	Principal functions
DSC	Measures crystallinity, melting and T_g
TGA	Measures residual moisture and hydrates
XRPD	Measures crystallinity and polymorphism
NIRS	Measures residual moisture non-destructively

XRPD is the method of choice for the characterization of crystallinity in freeze-dried solids. But, for characterization of amorphous products, it is preferable to use the DSC. DSC determines the glass transition temperature (T_g) of the solid, that is the temperature at which glasses undergo a transition from a rigid state to a viscoelastic rubbery state. The T_g could vary depending on the water content in the sample (as water is removed the T_g increases) and it is used to define the product storage conditions.

TGA involves heating a sample at a defined rate in a controlled environment and measuring any change in mass. The technique is routinely used to characterize materials that exhibit mass gain or loss caused by decomposition, oxidation or dehydration. The disadvantage of TGA is that it determines mass changes but it cannot identify the nature of the species.[42] Regarding the determination of RMC specifically and non-destructively, NIRS is a great alternative option.

Once formulation and container have been decided and the solution thermal fingerprint has been determined, the next step is to design the freeze-drying process conditions.

6.4. Freeze-drying process design

In industrial practice, a freeze-drying cycle is usually specified by means of a recipe comprising values for the parameters described in Table 3.5.

Table 3.5. Freeze-drying process parameters for each stage.

Freezing	Primary drying	Secondary drying
Ramp rate	Thermal fluid temperature	Thermal fluid temperature
Thermal fluid temperature	Ramp rate	Ramp rate
Duration	Chamber pressure	Chamber pressure
	Duration	Duration

Traditionally, the freeze-drying cycle was usually determined by trial and error because of the interrelationship between process variables and product attributes. In this perspective, a correct cycle can be obtained by means of an extended experimental investigation carried out with laboratory equipment.[61]

Nowadays, according to the new QbD paradigm, the empirical approach has to be replaced by a more rational, scientific and risk-based approach. In this sense, there are two possible strategies[15,62]:

a. The recipe can be obtained in-line, by using process monitoring tools, and by manipulating the operating variables to achieve the desired goals.
b. The recipe can be designed off-line, by using mathematical models, employing highly detailed freeze-drying equations based on heat and mass transfer.

In the latter case (strategy b), mathematical models may require input data that still need to be determined experimentally or acquired from literature. Also, the success of freeze-drying process design by computer simulation depends on the accuracy of the input data used and requires a number of laboratory experiments to confirm the estimated results. Moreover, special software is usually needed to calculate some equation parameters.[63–65]

Therefore, a good alternative is the use of DoE including parameters identified by risk analysis.[66,67] After executing the DoE, the results are analysed to establish the DS. Then, DS can be used to optimize the cycle, as well as to analyse the effect of any deviation of process variables from their setpoint values.[15,46,68] For example, De Beer et al.[69] used a DoE and innovative process analysers to study the impact of two formulations variables and three process variables in product quality.

For some authors, this approach is simple, time-consuming, expensive and, sometimes, the optimal conditions cannot be found. They argue that the combination of statistical DoEs and mathematical modelling should be the preferred option to define a DS that take into account the equipment capability, process parameters and/or product physical characteristics.[70,71] In literature, several freeze-drying process DS for the primary drying phase are published.[46,72] An excellent example of primary drying DS was created by Chang and Fischer[73] and it is represented in Figure 3.14.

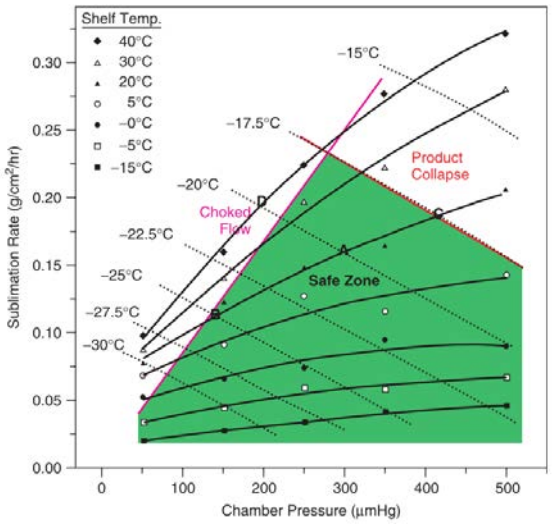

Figure 3.14. Representation of sublimation rate vs chamber pressure for different shelves temperatures (thick lines) along with product temperatures (dotted lines). Superimposed pink line represents the equipment constraints (choked flow limit). Red line defined the target product temperature. Adapted from references[71,73].

Figure 3.14 defines the set of operating conditions (shelf temperature and chamber pressure) that allows to maintain product temperature below a target value, to obtain high sublimation rates and to avoid choking flow[i]. Observations that can be made from this figure are[74]:

- Increasing chamber pressure leads to higher sublimation rate but also higher product temperature.
- Increasing shelf temperature leads to higher sublimation rate and product temperature.
- At a given product temperature, the highest sublimation rate can be found at combinations of lower chamber pressure and higher shelf temperature.

6.4.1. Helpful tips

Independently of the freeze-drying development approach, the following points have to be taken into account to obtain a robust, safe and efficient cycle[12]:

Freezing

- The freezing temperature should be below T_g' and/or T_e to guarantee a complete solidification of the product solution.
- The duration of freezing is not a critical parameter as long as a minimum stabilization time is reached to ensure that the product is completely solidified.
- The cooling rate, degree of supercooling and the effect of annealing should be evaluated depending on the formulation nature.

Primary drying

- Product temperature at the sublimation front should be lower than a critical temperature (T_e or T_{co}). This condition is essential to prevent irreversible damage to the structure of the product, such as meltback or collapse. A certain margin of 2-3ºC between the sublimation front temperature and the T_{co} must be guaranteed.[43]
- Chamber pressure should be much lower than the vapour pressure of ice at the target product temperature but yet high enough to minimize heat transfer heterogeneity in freeze drying.[75] Partial pressure of chamber vapour must be lower than the vapour pressure of ice at the sublimation front to allow for sublimation. However, if pressure is too low, the sublimation rate decreases. As a rule of thumb, chamber pressure should be no more than half and not less than quarter the vapour pressure of ice at the desire product temperature.[8,17]

[i] Drying rates can be limited by what refers to as "choked flow". The flow of water vapour between the chamber and condenser can become "choked" if the water vapour reaches the speed of sound at any point between them. Choking can lead to the chamber pressure exceeding its setpoint.[76]

- Water sublimation rate should be below a threshold, to prevent the loss of control of the pressure in the freeze-dryer chamber due to choked flow in the tube that connects the freeze-dryer chamber with the condenser.[76]

Secondary drying

- Secondary drying duration may be defined based on the achievement of a target value of RMC in the final product that maximizes product stability.
- The product temperature should be maintained below T_g of the dry product at that particular moisture content.[46]

7. Freeze-drying process monitoring and control

Once formulation and freeze-drying process have been defined, CPPs must be controlled and suitably monitored to guarantee process reproducibility and product quality.

Principally, there are three independent parameters in the freeze-drying process: shelf temperature, chamber pressure and time.[12] The classical and more advanced techniques for independent and dependent parameters measurement are explained in the following sections.

7.1. Techniques for independent parameters measurement

Temperature probes are commonly used to control the thermoregulated fluid at the inlet and outlet of the shelf. The heat transfer system provides the cooling required for freezing the product and the subsequent heat necessary to enable sublimation and desorption. It is also important to monitor and control the shelf temperature because it is the principal heat supplier and directly influences the product temperature at the sublimation front. Finally, shelf temperature uniformity across shelves inside the freeze-dryer needs to be within an acceptable range to ensure batch uniformity.[12]

Chamber pressure is measured either by thermal conductivity (Pirani) or capacitance (MKS Baratron®) gauges[77]:

- The Pirani vacuum gauge consists of a single filament which loses heat depending on the pressure of the surrounding gas. Therefore, the Pirani gauge responds to differences in thermal conductivity of individual gases present in the chamber and will read differently as the total gas composition changes over the course of the cycle.[1]
- The MKS Baratron® consists of two chambers divided by a metal diaphragm placed between two fixed electrodes. One chamber is evacuated to high vacuum to serve as a zero-reference pressure, and the other chamber is exposed to the chamber pressure. Since a change in the deflection of the diaphragm is directly proportional to the applied pressure, the capacitance manometer is able to measure the absolute pressure independent of the gas composition.[1,12]

The use of both probes in the same position of the freeze-dryer chamber will give two different measurements. Pirani vacuum gauge reads about 60% higher than capacitance manometer, as thermal conductivity of water vapour is about 60% higher than that of nitrogen.[64] In addition, the ratio between the values recorded by both pressure probes can be used as PAT tool to determine the primary drying endpoint, as explained below.

Finally, time is the third independent process parameter necessary to achieve reproducible processing conditions and a successful freeze-drying cycle.[12]

7.2. Techniques for dependent parameters measurement

Nevertheless, during freeze-drying, it is also essential to monitor other dependent variables like product temperature at the sublimation front, product resistance, residual moisture in the chamber or sublimation rate. Correct monitoring of this variables facilitates the freeze-drying process design, optimization, monitoring and control according to QbD principles.

The final aim of monitoring these variables is to define the process endpoints, sublimation and overall process endpoints, to avoid two potential scenarios[78]:

- If the secondary drying starts before the sublimation is completed, the product temperature may exceed the critical temperature, causing some vials to collapse or melt, which is an important quality issue.
- If the secondary drying is delayed several hours after the sublimation is completed or it is too long, the cycle will not be well optimized, and some freeze-drying capacity may be wasted, which is a business issue.

Currently, the following three conditions can be used to determine the endpoint of primary drying and/or secondary drying[64]:

- Increase in product temperature which indicates that heat is not consumed for sublimation.
- Gas composition change from mostly water vapour to mostly nitrogen.
- Decrease in chamber moisture.

Traditional and more sophisticated process analysers have been proposed to determine the process endpoints based on the abovementioned conditions (Table 3.6).

However, most of them interfere with the process dynamics or impair the sterile conditions, hence they are mostly used in laboratory scale equipment.[79,80] In RJ, the first forth techniques listed in Table 3.6 are currently being used. In addition, NIRS is being implemented in the company, but still as an off-line analyser.

Table 3.6. Comparative table of different process monitoring tools. Adapted from [52,64,81]. Abbreviations: Pressure Rise Test (PRT), Manometric Temperature Measurement (MTM), Pressure Rise Analysis (PRA), Dynamic Parameters Estimation (DPE) and Tunable Diode Laser Absorption Spectroscopy (TDLAS).

Process monitoring tools	Laboratory or commercial	Cost	Batch or vial	References
Sample Thief	Laboratory	€	Vial	[64]
Comparative pressure measurement	Both	€	Batch	[82]
PRT	Both	€	Batch	-
Temperature probes	Both	€	Vial	[83,84]
Electronic moisture sensor	Both	€	Batch	[83]
MTM/PRA/DPE	Both*	€€	Batch	[63,79,85,86]
TDLAS	Both*	€€€	Batch	[87,88]
Microbalance	Laboratory	€€	Vial	[89]
Residual Gas analyser	Laboratory	€€€	Batch	[82,90]
Plasma Emission Spectroscopy	Both	€€	Batch	[78]
NIRS/Raman	Laboratory	€€€	Vial	[69,91,92]

**Although not widely implemented at production scale.*

7.2.1. Sample thief

The sample thief comprises a vacuum lock attached to the freeze-dryer chamber via a valve. This valve is used to connect the lock and the chamber or isolate them from each other. The vacuum lock can be aerated or pumped down to the chamber vacuum. A rod with a pliers is used to pick up a vial from the freeze-dryer chamber. Before the extraction, vials are stoppered under vacuum by pushing a stopper closing rod to guarantee no ambient air in the headspace. Then, the lock is pumped out to equalize pressure within the chamber and the isolation valve is then opened and the vial goes down to the vacuum lock. The valve is rapidly closed to maintain the integrity of the drying chamber. Once closed, the vacuum lock is returned to atmospheric pressure via a valve and the vial can then be extracted from the bottom removable deposit. Figure 3.15 shows a sample thief and its main components.

Sampling thief is the reference standard for sublimation rate determination in primary drying, and for the establishment of time and temperature conditions for secondary drying.

For sublimation rate determination, vials are weighed before they are placed on the shelf inside the freeze-dryer chamber. Then, the sampling thief is used to pull out the samples during the drying step at the desired time intervals and samples are weighed again. The mass of water sublimed is calculated from the mass difference and the average sublimation rate is determined as the ratio between mass difference and time.[64]

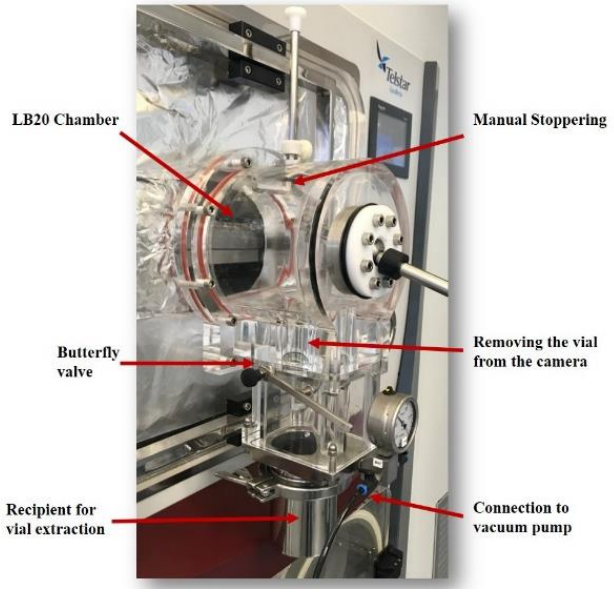

Figure 3.15. Representation of Sample Thief installed in the RJ company's pilot freeze-dryer.

For secondary drying temperature and endpoint determination, extracted vials at different time intervals are measured for RMC. Then, a desired level of RMC is established based on its correlation with drug potency, purity, and/or activity. Thus, the optimal secondary drying duration is defined based on the target level of RMC.[8]

7.2.2. Comparative pressure measurement

Comparative pressure measurement was first described by Nail and Johnson[82] in 1992. Water vapour is the dominant gas in the early phase of primary drying and nitrogen is the dominant gas at the end of primary drying. Hence, in the latter case, the pressure determined by the thermal conductivity gauge decreases in response to the decreased partial pressure of water vapour in the chamber.[52] The endpoint of sublimation is indicated when both pressure readings coincide (Figure 3.5).

It works extremely well, and it is considered a consistent PAT tool for the monitoring of freeze-drying processes. Moreover, in a study conducted by Patel et al.[93], it was concluded that comparative pressure measurement was, by far, the best choice to determine primary drying endpoint. In addition, the comparative pressure measurement is a batch technique, cheap, steam sterilisable, and easy to install without requiring any modification to the existing freeze-dryer equipment.

7.2.3. Pressure rise test

In a PRT, the chamber is isolated from the condenser during a short period of time (around 30 seconds). The principle is based on the separation of the product chamber from the ice condenser, so that water vapour from the sublimation cannot escape. This results in an increase in pressure in the chamber which can be measured. Thus, once the product is completely dry there will be little or no pressure

increment.[64,93] In this sense, at least two consecutive PRTs with comparable results should be obtained to determine the end of secondary drying.

Several algorithms[93] were proposed that use PRT data to estimate other parameters such as: product temperature at the sublimating interface, the mass transfer resistance, the sublimation rate or vial heat transfer coefficients.[94,95] These parameters are determined for the entire batch, hence they are useful for the determination of the endpoint of primary drying. Some of the published algorithms are: the manometric temperature measurement[63,86], the pressure rise analysis[85] and the dynamic parameters estimation algorithm.[96]

These algorithms have been developed with their respective software control systems, for example, the Lyodriver system for the dynamic parameters estimation algorithm (commercialized by Telstar and University of Torino). The main goal of these control systems is to minimize the cycle time by continuously adjusting the shelf temperature in order to maintain the product temperature as high as possible but below T_{co}.[79,85] Due to the increment of product temperature during the PRT at the end of primary drying, among other few limitations, this technology is not consolidated in the industrial plant yet.[92,94]

7.2.4. Product temperature probes

Thermocouples and resistance temperature detectors (RTDs) are commonly used for monitoring the mean product temperature.[85] Thermocouples measure the temperature at its end, corresponding to the temperature of the product at a precise location within the product vial. However, RTDs measure the temperature along the metal sheath surrounding the probe. This way, as observed in Figure 3.16, RTDs measures an average temperature of a greater section of the product inside the vial, considering the frozen solution, sublimation interface and dry solid.[97]

Figure 3.16. Product temperature probes: thermocouple (left) and RTD (right).

The insertion of a temperature probe is the simplest and more widespread monitoring systems adopted. Anyway, it has many disadvantages because it is a single vial technique, invasive, and it is well known

that it alters the nucleation during freezing.[46,79] The temperature probe facilitates nucleation of ice, so monitored vials generally undergo less supercooling during freezing[64], which results in larger average ice crystals size, less mass transfer resistance and faster drying.[85] Then, vials containing temperature probes could not give a true representation of the whole batch.[93]

Another source of uncertainty in product temperature is the placement of the sensor. Temperature probes are commonly placed at the bottom of the vial, but the sublimation front is constantly moving through the sample. Consequently, the temperature of the sublimation front cannot be effectively monitored using these traditional temperature probes.[46]

In addition, in production equipment with automatic vial loading and unloading, the placement of product temperature probes is no longer possible.[79] In this sense, there are wireless temperature measurement probes that are compatible with the automatic loading system and can be placed anywhere on the shelf. However, the wireless probes are still inserted into the vials.[64,84]

The end of primary drying can be determined by product temperature probes.[93] When ice sublimation front is receding from the thermocouple probe (i.e. absence of ice), the primary drying is completed in that vial, and there is an inflection in the product temperature to reach that of the shelf (Figure 3.5).

Temperature probes are of great interest in laboratory, engineering or qualification freeze-drying cycles, but, in the perspective of PAT, measurements of this type of probes are not interesting.[97] Consequently, there is a strong need for a new technology which is non-invasive and would monitor the temperature of the entire batch rather than a few selected vials.[64]

7.2.5. Other advanced monitoring techniques

Another approach is the measurement of the relative humidity in the chamber. By knowing the water vapour composition profile with time, it is possible to determine the primary drying as well as secondary drying endpoints.[64] Based on this principle, several technologies has been developed like electronic moisture sensor[83], residual gas analyser[82,90], cold plasma ionization[78] and TDLAS[87].

TDLAS is a very promising technique because it is capable to deliver a real-time measurement of the mass flow rate of water vapour without interrupting the process. Moreover, it can determine product temperature, vial heat transfer parameters, and residual water during secondary drying based on calibration curves of drying rate vs residual water developed experimentally. Although much work still needs to be done to refine the technique, it is now available as a commercial product.[87]

Furthermore, Raman or NIR spectroscopies has been used in lab-scale to noninvasively monitor a single vial during the freeze-drying process. NIRS is a more sensitive tool to monitor sublimation, whereas Raman spectroscopy is preferable for monitoring product characteristics during the freeze-drying process.[64,92] Both techniques offer unique advantage in front of the others, they provide direct

information about the freeze-dried products which is of outmost importance for the finished product quality. However, their current monitoring set up is still not applicable in production scale.[69]

Finally, De Beer et al.[91] demonstrated the benefits of using complementary techniques like NIRS, Raman, wireless product temperature probes and plasma emission spectroscopy as PAT tools. Nowadays, the more realistic application of NIRS is the RMC determination in every individual vial at the end of the freeze-drying process, to ensure that the product meets the desired RMC specification at release.[64] More information can be found in Chapter 4.

8. Process transfer and scale-up considerations

The ultimate objective in the development of every freeze-dried product is full-scale manufacture. The lifecycle of a freeze-dried product can be classified into three major stages: the first stage, freeze-dried product development, is where the formulation and packaging of the product are defined, and the freeze-drying process is developed at laboratory scale and scale-up at industrial scale. The second stage consists of the process qualification at the production level. Finally, the third phase consists of continuously maintaining the industrial routine production according to the market needs, including the possibility of transferring the product between the production facilities and/or improving the process.[98]

The scale-up and/or process transfer may require further development due to differences in freeze-dryer design and load condition from small-scale to large-scale operations.[14,15,99] For example:

- Manufacturing at industrial scale is often operated in a clean room environment with low particulate loading with respect to laboratory scale. Particles can get introduced to the bulk solution and act as nucleation sites, thus influencing the freezing and drying behaviour.
- The heating and cooling rate may vary with the equipment used as well as the distribution of the shelf surface temperature.
- Different freeze-dryers may show variations in radiative heat between shelves and chamber walls.
- Geometry and cooling performance of the condenser. Different diameter of the valve connecting the two elements, the aerodynamics of the system and the type of valve that isolates the condenser.
- Type and location of temperature and pressure monitoring devices.

These equipment variables often lead to adjustments to the cycle parameters to ensure equivalent product quality. In addition, primary drying time is commonly extended in industrial freeze-drying cycles.

In the past, various solutions were proposed to scale-up a cycle. The simplest one is based on trial and error.[100] Alternatively, scale-up of a freeze-drying cycle can be obtained by mathematical modelling.[101]

In both cases, it is recommendable to perform full-scale engineering batches with an exhaustive process monitoring and sampling plan to study whether process variability is under control.

Finally, the definition of a robust DS during product and process development at laboratory scale reduces significantly the efforts applied during scale-up to manufacturing equipment.[102] Therefore, the best approximation to accomplish the scale-up relies on a robust development based on QbD principles and the use of PAT monitoring tools.

9. Summary

The freeze-drying process is a stabilizing process divided in three stages: freezing, primary drying and secondary drying. The objective is to remove water from a frozen product by sublimation. One of the most important applications of freeze-drying process is to develop injectable drug products with long-term stability under less restrictive storage conditions.

Successful freeze-drying depends on a detailed understanding of the complex interplay between four groups of variables that influence both, the freeze-drying process performance and the properties of a freeze-dried product:

- Product parameters, such as formulation components, primary package or fill volume.
- Equipment parameters, such as equipment design, capacity, instrumentation and controls.
- Process parameters: shelf temperature, chamber pressure, ramping rates and time in the three stages.
- Product quality attributes, such as cake appearance, RMC, RT, biochemical characteristics and long-term stability.

The design of a robust freeze-drying process following QbD principles relies on the thorough understanding of the impact of the formulation and process parameters on product quality. Therefore, the determination of critical product temperatures and complete formulation characterization studies prior to freeze-drying are essential to develop an efficient freeze-drying process.

The controllable parameters of freeze-drying processes are: shelf temperature, chamber pressure and time. These parameters influence other dependent parameters, such as product temperature. Therefore, they should be adjusted to obtain a short and robust process that maintains the product temperature below a target value to avoid collapse or meltback.

Finally, several monitoring tools are available to determine process endpoints, assist during process development, support process scale-up and confirm process reproducibility in industrial manufacturing.

References

(1) Jennings, T. *Lyophilization: Introduction and Basic Principles*; Informa Healthcare: New York, 2008.

(2) Pikal, M. J. Freeze Drying. In *Enclopedia of Pharmaceutical Technology*; Swarbrick, J., Ed.; Informa Healthcare: Boca Raton, 2007; pp 1807–1833.

(3) Kessler, W. J.; Sharma, P.; Mujat, M. Advances in Instrumental Analysis Applied to the Development of Lyophilization Cycles. In *Lyophilized Biologics and Vaccines Modality-Based Approaches*; Varshney, D., Singh, M., Eds.; Springer: New York, 2015; pp 43–72.

(4) Rey, L. Glimpses into the Realm of Freeze-Drying: Classical Issues and New Ventures. In *Freeze-Drying/Lyophilization of Pharmaceutical and Biological Products*; Rey, L., May, J. C., Eds.; Informa Healthcare: London, UK, 2010; pp 1–28.

(5) Varshney, D.; Singh, M. History of Lyophilization. In *Lyophilized Biologics and Vaccines Modality-Based Approaches*; Varshney, D., Singh, M., Eds.; Springer: New York, 2015; pp 3–10.

(6) Rey LR. International Symposium on Lyophilization of Biological Products. Washington, DC; 1976.

(7) Rey, L. The Saga of Freeze-Drying. *Pharm. Technol.* **2004**, 5–8.

(8) Akers, M. J. Freeze-Dry (Lyophilization) Processing. In *Sterile Drug Products: Formulation, Packaging, Manufacturing and Quality*; Akers, M. J., Ed.; Informa Healthcare: London, UK, 2010; pp 294–312.

(9) LyoHub. Lyophilization Technology Roadmap. Available in: www.lyohub.org (accessed Apr 7, 2018).

(10) Shanley, A. Modernizing Lyophilization. *Pharm. Technol.* **2017**, *41* (12), 46–53.

(11) Adams, G. D. J.; Cook, I.; Ward, K. R. The Principles of Freeze-Drying. In *Cryopreservation and Freeze-Drying Protocols, Methods in Molecular Biology*; Wolkers, W. F., Oldenhof, H., Eds.; Springer: New York, 2015; pp 121–143.

(12) *Lyophilization of Biopharmaceuticals.*; Costantino, H., Pikal, M. J., Eds.; AAPS Press: Arlington, VA, 2005.

(13) Jameel, F.; Pikal, M. J. Design of a Formulation for Freeze Drying. In *Formulation and Process Development Strategies for Manufacturing Biopharmaceuticals*; Jameel, F., Hershenson, S., Eds.; John Wiley & Sons, Inc: New Jersey, 2010; pp 457–492.

(14) Patel, S. M.; Pikal, M. J. Emerging Freeze-Drying Process Development and Scale-up Issues. *AAPS PharmSciTech* **2011**, *12* (1), 372–378.

(15) Barresi, A. Pisano, R. Freeze Drying, Scale-up Considerations. In *Encyclopedia of Pharmaceutical Science and Technology*; Swarbrick, J., Ed.; Informa Healthcare: Boca Raton, 2012; pp 1–13.

(16) *Baseline Guide Vol 3: Sterile Product Manufacturing Facilities*, 2nd Ed.; International Society for Pharmaceutical Engineering, Ed.; 2011.

(17) Nail, S. L.; Jiang, S.; Chongprasert, S.; Knopp, S. A. Fundamentals of Freeze-Drying. In *Development and Manufacture of Protein Pharmaceuticals*; Nail, S. L., Akers, M. J., Eds.; Kluwer Academic Plenum: New York, 2002; pp 281–360.

(18) Liu, J. Physical Characterization of Pharmaceutical Formulations in Frozen and Freeze-Dried Solid States: Techniques and Applications in Freeze-Drying Development. *Pharm. Dev. Technol.* **2006**, *11* (1), 3–28.

(19) Luthra, S.; Pikal, M. J. Stabilization of Lyophilized Pharmaceuticals by Control of Molecular Mobility: Impact of Thermal History. In *Formulation and Process Development Strategies for Manufacturing Biopharmaceuticals*; Jameel, F., Hershenson, S., Eds.; John Wiley & Sons, Inc: New Jersey, 2010; pp 521–548.

(20) Pansare, S. K.; Patel, S. M. Practical Considerations for Determination of Glass Transition Temperature of a Maximally Freeze Concentrated Solution. *AAPS PharmSciTech* **2016**, *17* (4), 805–819.

(21) Searles, J. A.; Carpenter, J. F.; Randolph, T. W. Annealing to Optimize the Primary Drying Rate, Reduce Freezing-induced Drying Rate Heterogeneity, and Determine Tg′ in Pharmaceutical Lyophilization. *J. Pharm. Sci.* **2001**, *90* (7), 872–887.

(22) Jameel, F.; Searles, J. Development and Optimization of the Freeze-Drying Processes. In *Formulation and Process Development Strategies for Manufacturing Biopharmaceuticals*; Jameel, F., Hershenson, S., Eds.; John Wiley & Sons,

Inc: New Jersey, 2010; pp 763–796.

(23) Searles, J. A. Freezing and Annealing Phenomena in Lyophilization. In *Freeze Drying/Lyophilization of Pharmaceutical and Biological Products*; Rey, L., May, J. C., Eds.; Informa Healthcare: London, UK, 2010; pp 52–81.

(24) Randolph, T. W.; Searles, J. A. Freezing and Annealing Phenomena in Lyophilization: Effect upon Primary Drying Rate, Morphology, and Heterogeneity. *Am. Pharm. Rev.* **2002**, *5* (4), 40–46.

(25) Searles, J. A.; Carpenter, J. F.; Randolph, T. W. The Ice Nucleation Temperature Determines the Primary Drying Rate of Lyophilization for Samples Frozen on a Temperature-Controlled Shelf. *J. Pharm. Sci.* **2001**, *90* (7), 860–871.

(26) Chouvenc, P.; Vessot, S.; Andrieu, J. Experimental Study of the Impact of Annealing on Ice Structure and Mass Transfer Parameters during Freeze-Drying of a Pharmaceutical Formulation. *PDA J. Pharm. Sci. Technol.* **2006**, *60* (2), 95–103.

(27) Lu, X.; Pikal, M. J. Freeze-Drying of Mannitol-Trehalose-Sodium Chloride-Based Formulations: The Impact of Annealing on Dry Layer Resistance to Mass Transfer and Cake Structure. *Pharm. Dev. Technol.* **2004**, *9* (1), 85–95.

(28) Pyne, A.; Suryanarayanan, R. Phase Transitions of Glycine in Frozen Aqueous Solutions and during Freeze-Drying. *Pharm. Res.* **2001**, *18* (10), 1448–1454.

(29) Pikal, M. J.; Rambhatla, S.; Ramot, R. The Impact of the Freezing Stage in Lyophilization: Effects of the Ice Nucleation Temperature on Process Design and Product Quality. *Am. Pharm. Rev.* **2002**, *5* (3), 48–52.

(30) Meister, E.; Gieseler, H. Freeze-Dry Microscopy of Protein/Sugar Mixtures: Drying Behavior, Interpretation of Collapse Temperatures and a Comparison to Corresponding Glass Transition Data. *J. Pharm. Sci.* **2009**, *98* (9), 3072–3087.

(31) Pikal, M. J.; Shah, S. The Collapse Temperature in Freeze Drying: Dependence on Measurement Methodology and Rate of Water Removal from the Glassy Phase. *Int. J. Pharm.* **1990**, *62* (2–3), 165–186.

(32) Schersch, K.; Betz, O.; Garidel, P.; Muehlau, S.; Bassarab, S.; Winter, G. Systematic Investigation of the Effect of Lyophilizate Collapse on Pharmaceutically Relevant Proteins I: Stability after Freeze-drying. *J. Pharm. Sci.* **2010**, *99* (5), 2256–2278.

(33) Depaz, R. A.; Pansare, S.; Patel, S. M. Freeze-Drying above the Glass Transition Temperature in Amorphous Protein Formulations While Maintaining Product Quality and Improving Process Efficiency. *J. Pharm. Sci.* **2016**, *105* (1), 40–49.

(34) Patel, S. M.; Nail, S. L.; Pikal, M. J.; Geidobler, R.; Winter, G.; Hawe, A.; Davagnino, J.; Rambhatla Gupta, S. Lyophilized Drug Product Cake Appearance: What Is Acceptable? *J. Pharm. Sci.* **2017**, *106* (7), 1706–1721.

(35) Pikal, M.; Shah, S.; Roy, M.; Putman, R. The Secondary Drying Stage of Freeze Drying: Drying Kinetics as a Function of Temperature and Chamber Pressure. *Int. J. Pharm.* **1990**, *60* (3), 203–207.

(36) Searles, J. A.; Aravapalli, S.; Hodge, C. Effects of Chamber Pressure and Partial Pressure of Water Vapour on Secondary Drying in Lyophilization. *AAPS PharmSciTech* **2017**, *18* (7), 2808–2813.

(37) Jiang, S.; Nail, S. L. Effect of Process Conditions on Recovery of Protein Activity after Freezing and Freeze-Drying. *Eur. J. Pharm. Biopharm.* **1998**, *45* (3), 249–257.

(38) Sahni, E. K.; Pikal, M. J. Modeling the Secondary Drying Stage of Freeze Drying: Development and Validation of an Excel-Based Model. *J. Pharm. Sci.* **2017**, *106* (3), 779–791.

(39) European Pharmacopoeia. Ph. Eur. 7.0. Monograph 0520 Parenteral Preparations. Council of Europe, Strasbourg, France, 2008.

(40) ICH. Harmonised Tripartite Guideline Q1A(R2) Stability Testing of New Drug Substances and Products. 2003.

(41) Templeton, A. C.; Placek, J.; Xu, H.; Mahajan, R.; Hunke, W. A.; Reed, R. A. Determination of the Moisture Content of Bromobutyl Rubber Stoppers as a Function of Processing: Implications for the Stability of Lyophilized Products. *PDA J. Pharm. Sci. Technol.* **2003**, *57* (2), 75–87.

(42) Kett, V.; McMahon, D.; Ward, K. Thermoanalytical Techniques for the Investigation of the Freeze Drying Process and Freeze-Dried Products. *Curr. Pharm. Biotechnol.* **2005**, *6* (3), 239–250.

(43) Carpenter, J. F.; Chang, B. S.; Garzon-Rodriguez, W.; Randolph, T. W. Rational Design of Stable Lyophilized Protein: Theory and Practice. In *Rationale Design of Stable Protein Formulations: Theory and Practice*; Carpenter, J. F.,

Manning, M. C., Eds.; Kluwer Academic/Plenum: New York, 2002; pp 109–133.

(44) Rambhatla, S.; Pikal, M. J. Heat and Mass Transfer Scale-up Issues during Freeze-Drying, I: Atypical Radiation and the Edge Vial Effect. *AAPS PharmSciTech* **2003**, *4* (2), 1–10.

(45) Martin-Moe, S.; Nast, C. An Overview of Quality by Design for Drug Product. In *Quality by Design for Biopharmaceutical Drug Product Development*; Jameel, F., Hershenson, S., Khan, M. A., Martin-Moe, S., Eds.; Springer: New York, 2015; pp 47–59.

(46) Patel, S. M.; Jameel, F.; Sane, S. U.; Kamat, M. Lyophilization Process Design and Development Using QbD Principles. In *Quality by Design for Biopharmaceutical Drug Product Development*; Jameel, F., Hershenson, S., Khan, M. A., Martin-Moe, S., Eds.; Springer: New York, 2015; pp 303–329.

(47) Schwegman, J. J.; Hardwick, L. M.; Akers, M. J. Practical Formulation and Process Development of Freeze-Dried Products. *Pharm. Dev. Technol.* **2005**, *10* (2), 151–173.

(48) Carpenter, J.; Pikal, M. J.; Chang, B. S.; Randolph, T. W. Rational Design of Stable Lyophilized Protein Formulations: Some Practical Advice. *Pharm. Reserach* **1997**, *14* (8), 969–975.

(49) Cannon, A.; Shemeley, K. Statistical Evaluation of Vial Design Features That Influence Sublimation Rates during Primary Drying. *Pharm. Res.* **2004**, *21* (3), 536–542.

(50) Pikal, M. J.; Shah, S. Intravial Distribution of Moisture during the Secondary Drying Stage of Freeze Drying. *PDA J. Pharm. Sci. Technol.* **1997**, *51* (1), 17–24.

(51) Wang, W. Lyophilization and Development of Solid Protein Pharmaceuticals. *Int. J. Pharm.* **2000**, *203*, 1–60.

(52) Johnson, R. E.; Teagarden, D. L.; Lewis, L. M.; Gieseler, H. Analytical Accessories for Formulation and Process Development in Freeze-Drying. *Am. Pharm. Rev.* 2009, pp 54–60.

(53) Passot, S.; Tréléa, I. C.; Marin, M.; Fonseca, F. The Relevance of Thermal Properties for Improving Formulation and Cycle Development: Application to Freeze-Drying of Proteins. In *Freeze Drying/Lyophilization of Pharmaceutical and Biological Products*; Rey, L., May, J. C., Eds.; Informa Healthcare: London, UK, 2010; pp 136–166.

(54) Sun, W. Q. Calorimetric Analysis of Cryopreservation and Freeze-Drying Formulations. In *Cryopreservation and Freeze-Drying Protocols,Methods in Molecular Biology*; Wolkers, W. F., Oldenhof, H., Eds.; Springer: New York, 2015; Vol. 368, pp 163–179.

(55) Wang, D. Q. Formulation Characterization. In *Freeze-Drying/Lyophilization of Pharmaceutical and Biological Products*; Rey, L., May, J. C., Eds.; Informa Healthcare: London, UK, 2010; pp 233–253.

(56) Sundaramurthi, P.; Suryanarayanan, R. Calorimetry and Complementary Techniques to Characterize Frozen and Freeze-Dried Systems. *Adv. Drug Deliv. Rev.* **2012**, *64* (5), 384–395.

(57) Ward, K. R.; Matejtschuk, P. The Use of Microscopy, Thermal Analysis, and Impedance Measurements to Establish Critical Formulation Parameters for Freeze-Drying Cycle Development. In *Freeze Drying/Lyophilization of Pharmaceutical and Biological Products*; Rey, L., May, J. C., Eds.; Informa Healthcare: London, UK, 2010; pp 112–135.

(58) Meister, E.; Šaši, S.; Gieseler, H. Freeze-Dry Microscopy: Impact of Nucleation Temperature and Excipient Concentration on Collapse Temperature Data. *AAPS PharmSciTech* **2009**, *10* (2), 582–588.

(59) Pyne, A.; Surana, R.; Suryanarayanan, R. Crystallization of Mannitol below Tg during Freeze-Drying in Binary and Ternary Aqueous Systems. *Pharm. Res.* **2002**, *19* (6), 901–908.

(60) Raghu K. Cavatur; Raj Suryanarayanan. Characterization of Frozen Aqueous Solutions by Low Temperature X-Ray Powder Diffractometry. *Pharm. Res.* **1998**, *15* (2), 194–199.

(61) Sane, S. U.; Hsu, C. C. Strategies for Successful Lyophilization Process Scale-Up. *Am. Pharm. Rev.* **2007**, *41*, 132–136.

(62) Barresi, A. A.; Fissore, D.; Marchisio, D. L. Process Analytical Technology in Industrial. In *Freeze-Drying/Lyophilization of Pharmaceutical and Biological Products*; Rey, L., May, J. C., Eds.; Informa Healthcare: London, UK, 2010; pp 460–493.

(63) Tang, X.; Nail, S. L.; Pikal, M. J. Freeze-Drying Process Design by Manometric Temperature Measurement: Design of a Smart Freeze-Dryer. *Pharm. Res.* **2005**, *22* (4), 685–700.

(64) Patel, S. M.; Pikal, M. Process Analytical Technologies (PAT) in Freeze-Drying of Parenteral Products. *Pharm. Dev.*

Technol. **2009**, *14* (6), 567–587.

(65) Fissore, D.; Pisano, R.; Barresi, A. A. Using Mathematical Modeling and Prior Knowledge for QbD in Freeze-Drying Processes. In *Quality by Design for Biopharmaceutical Drug Product Development.*; Jameel, F., Hershenson, S., Khan, M. A., Martin-Moe, S., Eds.; Springer: New York, 2015; pp 565–593.

(66) Liu, D.; Galvanin, F.; Yu, Y. Formulation Screening and Freeze-Drying Process Optimization of Ginkgolide B Lyophilized Powder for Injection. *AAPS PharmSciTech* **2018**, *19* (2), 541–550.

(67) Sylvester, B.; Porfire, A.; Achim, M.; Rus, L.; Tomuta, I. A Step Forward towards the Development of Stable Freeze-Dried Liposomes: A Quality by Design Approach (QbD). *Drug Dev. Ind. Pharm.* **2018**, *44* (3), 385–397.

(68) Sundaram, J.; Shay, Y. H. M.; Hsu, C. C.; Sane, S. U. Design Space Development for Lyophilization Using DoE and Process Modeling. *BioPharm Int.* **2010**, *23* (9), 26–36.

(69) De Beer, T. R. M.; Wiggenhorn, M.; Hawe, A.; Kasper, J. C.; Almeida, A.; Quinten, T.; Friess, W.; Winter, G.; Vervaet, C.; Remon, J. P. Optimization of a Pharmaceutical Freeze-Dried Product and Its Process Using an Experimental Design Approach and Innovative Process Analyzers. *Talanta* **2010**, *83*, 1623–1633.

(70) Koganti, V. R.; Shalaev, E. Y.; Berry, M. R.; Osterberg, T.; Youssef, M.; Hiebert, D. N.; Kanka, F. a; Nolan, M.; Barrett, R.; Scalzo, G.; et al. Investigation of Design Space for Freeze-Drying: Use of Modeling for Primary Drying Segment of a Freeze-Drying Cycle. *AAPS PharmSciTech* **2011**, *12* (3), 854–861.

(71) Nail, S. L.; Searles, J. A. Elements of Quality by Design in Development and Scale-up of Freeze-Dried Parenterals. *BioPharm Int.* **2008**, *21* (1), 44–52.

(72) Patel, S. M.; Pikal, M. J. Lyophilization Process Design Space. *J. Pharm. Sci.* **2013**, *102* (11), 3883–3887.

(73) Chang, B. S.; Fischer, N. L. Development of an Efficient Single-Step Freeze-Drying Cycle for Protein Formulations. *Pharm. Res.* **1995**, *12* (6), 831–837.

(74) Searles, J. A. Optimizing the Throughput of Freeze-Dryers Within a Constrained Design Space. In *Freeze-Drying/Lyophilization of Pharmaceutical and Biological Products*; Rey, L., May, J. C., Eds.; Informa Healthcare: London, UK, 2010; pp 425–440.

(75) Tang, X.; Pikal, M. J. Design of Freeze-Drying Processes for Pharmaceuticals: Practical Advice. *Pharm. Res.* **2004**, *21* (2), 191–200.

(76) Patel, S. M.; Chaudhuri, S.; Pikal, M. J. Choked Flow and Importance of Mach I in Freeze-Drying Process Design. *Chem. Eng. Sci.* **2010**, *65* (21), 5716–5727.

(77) Nail, S. L.; Gatlin, L. A. Advances in Control of Production Freeze-Dryers. *J. Parenter. Sci. Technol.* **1985**, *39* (1), 16–27.

(78) Mayeresse, Y.; Veillon, R. Freeze-Drying Process Monitoring Using a Cold Plasma Ionization Device. *PDA J. Pharm. Sci. Technol.* **2007**, *61* (3), 160–174.

(79) Barresi, A. A.; Velardi, S. A.; Pisano, R.; Rasetto, V.; Vallan, A.; Galan, M. In-Line Control of the Lyophilization Process. A Gentle PAT Approach Using Software Sensors. *Int. J. Refrig.* **2009**, *32* (5), 1003–1014.

(80) Fissore, D.; Pisano, R.; Velardi, S.; Barresi, A.; Galan, M. PAT Tools for the Optimization of the Freeze-Drying Process. *Pharm. Eng.* **2009**, *29* (5), 58–70.

(81) McCoy, B. Q. W. and T. R. Advances in Process Analytical Technology in Freeze-Drying. In *Lyophilized Biologics and Vaccines Modality-Based Approaches*; Varshney, D., Singh, M., Eds.; Springer: New York, 2015; pp 157–178.

(82) Nail, S. L.; Johnson, W. Methodology for in-Process Determination of Residual Water in Freeze-Dried Products. *Dev. Biol. Stand.* **1992**, *74*, 137-50-1.

(83) Roy, M. L.; Pikal, M. J. Process Control in Freeze Drying: Determination of the End Point of Sublimation Drying by an Electronic Moisture Sensor. *J. Parenter. Sci. Technol.* **1989**, *43* (2), 60–66.

(84) Schneid, S.; Gieseler, H. Evaluation of a New Wireless Temperature Remote Interrogation System (TEMPRIS) to Measure Product Temperature during Freeze Drying. *AAPS PharmSciTech* **2008**, *9* (3), 729–739.

(85) Chouvenc, P.; Vessot, S.; Andrieu, J.; Vacus, P. Optimization of the Freeze-Drying Cycle: A New Model for Pressure Rise Analysis. *Dry. Technol.* **2004**, *22* (7), 1577–1601.

(86) Milton, N.; Pikal, M. J.; Roy, M. L.; Nail, S. L. Evaluation of Manometric Temperature Measurement as a Method of

Monitoring Product Temperature during Lyophilization. *PDA J. Pharm. Sci. Technol.* **1997**, *51* (1), 7–16.

(87) Gieseler, H.; Kessler, W. J.; Finson, M.; Davis, S. J.; Mulhall, P. A.; Bons, V.; Debo, D. J.; Pikal, M. J. Evaluation of Tunable Diode Laser Absorption Spectroscopy for In-process Water Vapour Mass Flux Measurements during Freeze Drying. *J. Pharm. Sci.* **2007**, *96* (7), 1776–1793.

(88) Schneid, S. C. Non-Invasive Product Temperature Determination during Primary Drying Using Tunable Diode Laser Absorption Spectroscopy. *J. Pharm. Sci.* **2009**, *98* (9), 3406.

(89) Roth, C.; Winter, G.; Lee, G. Continuous Measurement of Drying Rate of Crystalline and Amorphous Systems during Freeze-drying Using an in Situ Microbalance Technique. *J. Pharm. Sci.* **2001**, *90* (9), 1345–1355.

(90) Connelly, J. P.; Welch, J. V. Monitor Lyophilization with Mass Spectrometer Gas Analysis. *J Parenter Sci Technol* **1993**, *47* (2), 70–75.

(91) De Beer, T. R. M.; Wiggenhorn, M.; Veillon, R.; Debacq, C.; Mayeresse, Y.; Moreau, B.; Burggraeve, A.; Quinten, T.; Friess, W.; Winter, G.; et al. Importance of Using Complementary Process Analyzers for the Process Monitoring, Analysis, and Understanding of Freeze Drying. *Anal. Chem* **2009**, *81* (18), 7639–7649.

(92) De Beer, T. R. M.; Alleso, M.; Goethals, F.; Coppens, A.; Heyden, Y. V.; De Diego, H.; Rantanen, J.; Verpoort, F.; Vervaet, C.; Remon, J. P.; et al. Implementation of a Process Analytical Technology System in a Freeze-Drying Process Using Raman Spectroscopy for In-Line Process Monitoring. *Anal. Chem* **2007**, *79* (21), 7992–8003.

(93) Patel, S. M.; Doen, T.; Pikal, M. J. Determination of End Point of Primary Drying in Freeze-Drying Process Control. *AAPS PharmSciTech* **2010**, *11* (1), 73–84.

(94) Gieseler, H. PAT for Freeze Drying: Cycle Optimization in the Laboratory. *Eur. Pharm. Rev.* **2007**, No. 1, 62–67.

(95) Lapkin, A.; Fan, X.; Mhamdi, A.; Foerst, P.; Fissore, D. Model-Based PAT for Quality Management in Pharmaceuticals Freeze-Drying: State of the Art. *Front. Bioeng. Biotechnol* **2017**, *5* (5), 1–10.

(96) Velardi, S. A.; Rasetto, V.; Barresi, A. A. Dynamic Parameters Estimation Method: Advanced Manometric Temperature Measurement Approach for Freeze-Drying Monitoring of Pharmaceutical Solutions. *Ind. Eng. Chem. Res.* **2008**, *47* (21), 8445–8457.

(97) Jameel, F.; Kessler, W. J.; Schneid, S. Application of PAT in Real-Time Monitoring and Controlling of Lyophilization Process. In *Quality by Design for Biopharmaceutical Drug Product Development*; Jameel, F., Hershenson, S., Khan, M. A., Martin-Moe, S., Eds.; Springer: New York, 2015; pp 605–647.

(98) Sane, S. U.; Hsu, C. C. Considerations for Successful Lyophilization Process Scale-Up, Technology Transfer, and Routine Production. In *Formulation and Process Development Strategies for Manufacturing Biopharmaceuticals*; 2010; pp 797–826.

(99) Rambhatla, S.; Tchessalov, S.; Pikal, M. J. Heat and Mass Transfer Scale-up Issues during Freeze-Drying, III: Control and Characterization of Dryer Differences via Operational Qualification Tests. *AAPS PharmSciTech* **2006**, *7* (2), E39.

(100) Tsinontides, S. C.; Rajniak, P.; Pham, D.; Hunke, W. A.; Placek, J.; Reynolds, S. D. Freeze-Drying—principles and Practice for Successful Scale-up to Manufacturing. *Int. J. Pharm.* **2004**, *280*, 1–16.

(101) Pisano, R.; Fissore, D.; Barresi, A. A.; Rastelli, M. Quality by Design: Scale-up of Freeze-Drying Cycles in Pharmaceutical Industry. *AAPS PharmSciTech* **2013**, *14* (3), 1137–1149.

(102) Jo, E. Guaranteeing a Quality Scale-Up. *PMPS Formul. Ingredients Excipients* **2010**, 62–67.

Chapter 4

Near Infrared Spectroscopy

1. Introduction

1.1. A little bit of history

Back to 1800s, an astronomer, Herschel, in his famous work "*Experiments on the Refrangibility of the Invisible Rays of the Sun*"[1] demonstrated the existence of infrared (IR) radiation for the first time. He found that the heat maximum was beyond the red end of the spectrum. Nevertheless, Herschel could not believe that light and his "*radiant heat*" were related, but he was wrong, as demonstrated by Ampere in 1835.[2,3]

Later, Abney and Festing[4], in 1881, and Coblentz in 1905, collected the absorption spectra of different compounds and showed correlations between absorption bands and some chemical groups of the studied molecules. They found that each compound had a unique spectrum, and that a given chemical group presented in different molecules exhibited absorption bands grossly located at the same wavelength.[5,6]

Essentially, Coblentz gave to the analytical chemistry community a new tool to obtain structural information about compounds. Starting in the 1950s, there was a growing demand for fast, quantitative determinations of moisture, protein, and oil.[2] The development of analytical methods based on NIRS starts with Karl Norris, working in the U.S. Department of Agriculture, who began a series of experiments using NIRS for food applications.[6] In 1968, Ben-Gera and Norris published their initial work on direct spectrophotometric determination of fat and moisture in meat products.[7]

It is interesting to note that up to 1970, only about 50 papers were written concerning NIRS. However, since 1970s, the number of publications increased tremendously, particularly on the application of NIR spectroscopy in agriculture and food sectors, and more NIR spectrometers and applications for routine measurements were put on the market. Over the past 30 years, the development of NIRS methods has been strongly linked with the advance of computer technology and chemometrics.[2,6]

1.2. State of the art

Nowadays, the increasing demand for product quality and productivity improvement in industry has led to the gradual substitution of time-consuming and non-specific analytical techniques by more specific and environmentally friendly analytical tools. In this sense, NIRS has emerged as an extremely powerful tool for industrial quality control and process monitoring.[8] Its capacity to analyse samples in a fast, non-destructive and non-invasive mode, with little or no samples manipulation contribute to increase its popularity, especially as a PAT technique in the pharmaceutical industry.[9]

With this regard, NIRS has been successfully implemented as a PAT tool in the highly regulated industrial word. NIRS offers a great opportunity to provide real-time process analytical information ideally suited to process control and optimization techniques.[10]

1.3. Concepts overview

In this chapter, basic principles of NIRS will be discussed, starting by some theoretical concepts about the origin of NIR spectra, continuing with the discussion of some applications of NIRS in the pharmaceutical industry, and ending with an overview of the normative and regulatory framework.

2. Principles of near infrared spectroscopy

IR radiation comprises the region of the electromagnetic spectrum between 780 nm and 10^6 nm. Regarding the applications, the instrumentation and the spectroscopic phenomena of energy absorption by the matter, it is convenient to divide the IR spectrum in three sub-regions, named: Near Infrared (NIR), Mid Infrared (MIR) and Far Infrared (FIR).[11] A brief summary of the estimated limits and the absorption principle of the three sub-regions are shown in Table 4.1.

Table 4.1. Regions of the IR spectrum. Adapted from reference[11].

Region	Wavelength (Wavenumber)	Absorption Principle
NIR	780 nm – 2500 nm ($12800\ cm^{-1} – 4000\ cm^{-1}$)	Overtones and combination bands of the fundamental molecular vibrations.
MIR	2500 nm – 50000 nm ($4000\ cm^{-1} – 200\ cm^{-1}$)	Fundamental molecular vibrations
FIR	50000 nm – 10^6 nm ($200\ cm^{-1} – 10\ cm^{-1}$)	Molecular rotations

In this project, the studied sub-region was NIR. Its wavelength range is from 780 nm to 2500 nm and represents mainly overtones and combinations of the fundamental molecular vibrations detected in the MIR region.[12]

2.1. Theory of near infrared absorption

NIR is a type of vibrational spectroscopy, hence it is based on the absorption of radiation as a consequence of molecular vibrations, mainly stretching and bending. The absorption phenomenon is extensively explained below.

2.1.1. Molecular vibrations

The relative positions of atoms in a molecule are not fixed, they fluctuate continuously as a consequence of vibrations and rotations of the bonds in the molecule.[10] At ambient temperature, most of the molecules are in their fundamental vibrational energy levels. When these molecular vibrators absorb light of a particular frequency, they are excited to a higher energy level.[13,14]

Starting from a simple diatomic molecule, the molecular vibration can be described by a simplified model supposing a harmonic oscillator. First of all, the diatomic molecule is represented as two spherical masses "m_1" and "m_2" connected by a spring with a given force constant "*k*". Then, according to this model, an atom moves from its equilibrium position with a force proportional to the displacement (Hooke's law). Therefore, the potential energy (E) can be approximated by Equation 4.1 as a function of the displacement of the atoms (x) from the equilibrium position[13]:

$$E = \frac{1}{2}kx^2 \qquad \textit{Equation 4.1}$$

Figure 4.1 shows the symmetric behaviour of the potential energy. It can be observed that when vibration occurs, the potential energy changes continuously, approaching zero when the atoms are close to the equilibrium position, and becoming maximum when the distance between the atoms is minimal or maximal.[11]

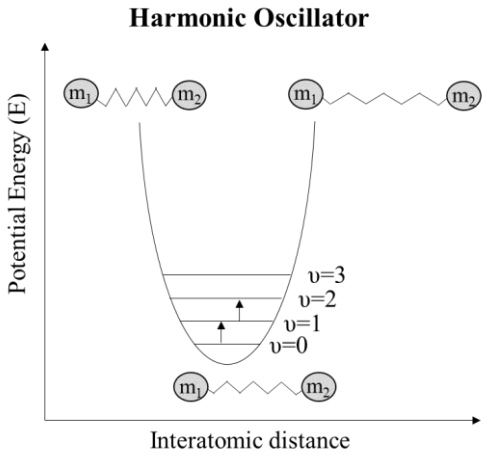

Figure 4.1. Diagram of the harmonic oscillator model. Potential energy versus interatomic distance for a diatomic molecule m_1-m_2. Adapted from references[13,15].

According to quantum mechanics, the molecular system can only have some discrete and equally spaced energy levels (E_υ) defined by the following expression[11,13]:

$$E_\upsilon = \left(\upsilon + \frac{1}{2}\right)h\nu \qquad \textit{Equation 4.2}$$

where υ is the vibrational quantum number, E_υ is the energy of the υ^{th} quantum level, h is Planck's constant, and ν is the fundamental vibrational frequency which might be approximated by:

$$\nu = \frac{1}{2\pi}\sqrt{\frac{k}{\mu}} \qquad \textit{Equation 4.3}$$

where μ is the reduced mass of the two atoms.

Hence, only a few specific energy levels are allowed. An additional restriction imposed by the harmonic model is that only 'fundamental' vibrational transitions ($\Delta\upsilon=\pm1$), are allowed.[13] These fundamental transitions are in the energy range of MIR.

2.1.2. Anharmonicity

Although a diatomic molecule is particularly useful for demonstrating the concept of vibrational energy, most real molecules contain more than two atoms and are capable of more than one type of vibration per bond. In addition, vibrations of different bonds in a polyatomic molecule cannot always be considered independent one from another.[15] In this sense, the harmonic oscillator model represents an imperfect description of the molecular vibration considering[8]:

- The repulsive forces between the vibrating atoms when pressed close together.
- The possibility of dissociation when the vibrating bond is strongly extended.

For instance, when two atoms become closer, the electrostatic repulsion between their nuclei generates a force that acts in the opposite direction of motion, which implies a faster increase in potential energy as the one predicted by the harmonic oscillator. Consequently, as atoms are not allowed to touch one another, the magnitude of the potential function approaches infinity.

On the contrary, when the atoms move away, the interatomic distance approaches the breaking distance of the bond. As a consequence, the potential energy decreases and tends asymptotically to a constant value representing complete dissociation of the molecule into atoms (Figure 4.2).

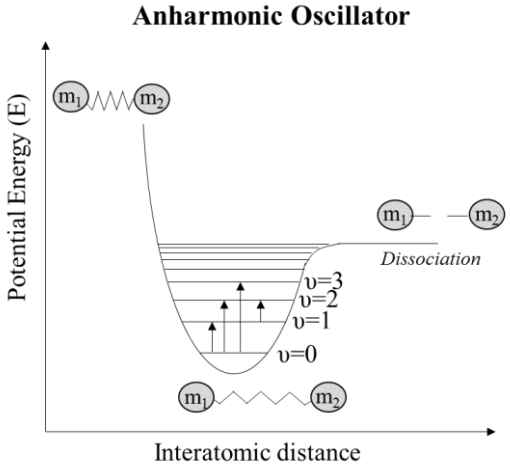

Figure 4.2. Schematic of the anharmonic oscillator model. Potential energy versus interatomic distance for a diatomic molecule m_1-m_2. Adapted from references[13,15].

Finally, the potential energy function exhibit a minimal value at the equilibrium position, which is the only position where molecules may have a harmonic behaviour.[11,16]

Then, the forces responsible for the increase in potential energy are different in the two cases, resulting in the loss of symmetry observed in the harmonic model.[10] Therefore, to explain the origin of NIR absorption, the anharmonic oscillator model should be applied.

There are two effects of the anharmonicity which have significance for NIRS. First, the gap between adjacent energy levels is no longer constant, and they are slightly closer as the quantum number increases (Figure 4.2). Second, weak absorptions can occur with $\Delta\upsilon=\pm k$ (k=2,3…), also known as overtones, which correspond to one type of bands observed in the NIR region.

In addition, combination bands appears in the NIR region, which involve a simultaneous increase of the energy levels of two or more vibrational modes from absorption of a single photon.[15] The frequencies of both are qualitatively represented in the following simplified equation:

$$\nu = n_1\nu_1 + n_2\nu_2 + \ldots \qquad \textit{Equation 4.4}$$

where *n* are integers number and *v* are the fundamental frequencies. However, in reality the calculation is more complex and includes the anharmonic effects.[8] Moreover, the frequency of overtones can be estimated from their fundamental vibrations with an anharmonicity constant χ of 0.01–0.05 by the following equation:

$$\nu_x = \Delta\upsilon\ \nu_0(1 - \Delta\upsilon\chi) \qquad \textit{Equation 4.5}$$

where ν_x is the frequency of *x* overtone and ν_0 is the frequency of fundamental vibration and υ is the vibrational quantum number.[17] As an example, Table 4.2 represents the overtones and combinational bands of the water molecule in the NIR region:

Table 4.2. Description of overtones and combinational bands for liquid water in the NIR region. Sourced from reference[18].

λ_{max} (nm)	Molar absorptivity (L/mol cm)	Band type
760	0.026	3rd overtone
970	0.046	2nd overtone
1190	1.05	combination
1450	26.0	1st overtone
1940	114.0	combination

Generally, the absorption bands corresponding to overtone or combination vibrations have much lower intensity than their fundamental analogues[8,10] and these bands tend to decrease drastically in intensity as the order of the overtone or combination increases.[15] Non-fundamental transitions are much less likely than transitions between consecutive levels and their probability decreases with an increase in the vibrational quantum number υ. As a result, the absorption bands in NIR are usually broad and not well defined.[8,17]

2.1.3. Dipole moment

Vibration is necessary but not sufficient for absorption. To absorb radiation in the IR, a molecule must undergo a net change in the dipole moment during the molecular vibration.[19] Only in these circumstances, the alternating electric field of the radiation can interact with the molecule. If the frequency of the radiation coincides exactly with the natural vibration frequency of the molecule, a net transfer of energy occurs which causes a change in the amplitude of the molecular vibration and, the consequence is the absorption of radiation.[11]

In a molecule, chemically bonded atoms that possess different electronegativities will undergo a change in the net dipole moment during normal molecular motion. The most intense bands in NIRS correspond to functional groups with heteronuclear bonds, such as C-H, N-H, O-H, S-H.[10,12] On the contrary, the dipole moment of homonuclear species such as O_2, N_2 o Cl_2, does not undergo a net change during vibration or rotation, and, therefore, this type of compounds do not absorb in the NIR.[11]

As the mass of hydrogen in C-H, N-H, and O-H bonds is so low, such vibrations tend to be very anharmonic and will tend to shift further from the integer multiples of their fundamental frequencies. The degree of anharmonicity for a molecule is further dependent on the level of hydrogen bonding, temperature, and interaction with other molecules in the sample matrix.[5] The formation of hydrogen bonds changes bond lengths and this changes the bond strength. The result of this is an apparent shift in the expected positions of absorption peaks.[20]

For this reason, NIRS, in addition to allowing the quantification of the different components of a mixture, is sensitive to intermolecular interactions, such as hydrogen bonds, which provide information on the structure of the sample. Then, it is possible to extract both chemical and physical information of NIR spectra.

2.1.4. Characteristics of the near infrared spectrum

The NIR spectrum consists in broad and overlapping bands of low intensity. These characteristics have restricted its applicability for decades because they were difficult to interpret.[2] However, the complexity of the spectra is compensated by the application of an adequate chemometric treatment (more information in Chapter 5).

In addition, the low absorptivity of the NIRS is a primary reason for the usefulness of the method for analysis of intact dosage forms. It allows to work in reflectance mode with the advantage of acquiring spectra of physically thick samples without manipulation, thus increasing the number and frequency of analysis. Moreover, the penetration depth of the radiation in diffuse reflectance measurements of solid/powder samples can be on the scale of millimetres. In this way, more material is exposed, reducing problems of heterogeneity of the sample, and the effect of possible interferences, such as contamination of surfaces and, enabling the registration of samples through transparent packaging.

2.2. Instrumentation and spectral acquisition

The basic scheme of a NIR spectrophotometer consists of: a radiation source, a wavelength selection system, a sample holder or presentation interface, and a detector, which measures the intensity of the radiation.[17] The almost universally radiation source used is the tungsten halogen lamp, although arrays of light emitting-diodes (LED) has also been employed. The sample holder could include different probes, sample compartments or cells. The most common detector used in the NIR spectral regions is made of a PbS semiconductor or, more recently InGaAs. Finally, different NIR instruments can be classified based on the wavelength selector, but, ultimately, instrument selection must be guided by the final application.[10,13,21]

Principally, there are three modes of NIR spectral acquisition: transmission, reflectance and transflectance. The main difference between the three types is the position of the sample in the instrument with respect to the detector (Figure 4.3). The appropriate mode of registration in each case is dictated by the physical properties of the sample.[17] In this thesis, the reflectance mode was used to collect the spectra of solid samples.

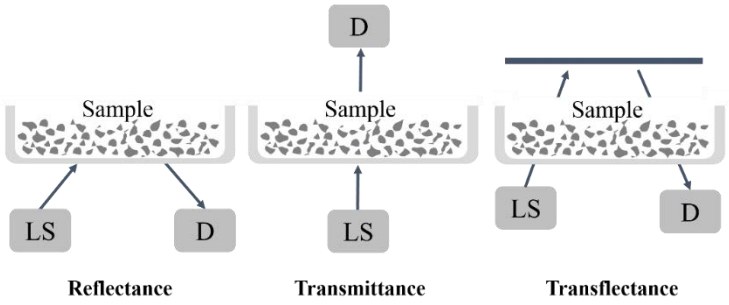

Figure 4.3. Representation of different modes of measurements employed in NIRS. LS=Light source and D=Detector. A reflector is represented in the transflectance mode.

2.2.1. Reflectance mode

This mode involves irradiation of a solid sample by a NIR light source. The incident radiation penetrates the superficial layer of particles and it can be absorbed or scattered by the particles. Then, the scattered radiation returns to the detector.[19] From the reflected radiation, two components can be distinguished: specular and diffuse radiation (Figure 4.4).

- Specular radiation, governed by the laws of Fresnel, is reflected in the same angle of incidence without penetrating the sample. Therefore, it does not contain any information about the sample. The contribution of specular reflectance is usually minimized with an appropriate position of the detectors with respect to the sample and the radiation source.

- Diffuse radiation, on the other hand, is the result of the partial absorption of the radiation by the sample and its dispersion in all directions. Then, only the incident radiation that undergoes diffuse reflectance contains information about the sample.[19]

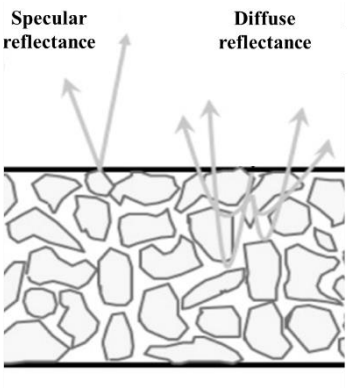

Figure 4.4. Representation of the two components of the reflected radiation. Adapted from reference[22].

Although detailed investigations of the theory of diffuse reflection have been carried out during the last century, they have not resulted in a single metric that is proportional to the analyte concentration.[23] Nevertheless, a relevant theory of diffuse reflection was derived by Kubelka-Munk (K-M).[24]

The K-M equation, applied to homogeneous mixtures of particles of infinitesimal size, states that the reflectance at any wavelength is a function of the absorption and scattering coefficients:

$$F(R_\infty) = \frac{(1-R_\infty)^2}{2R_\infty} = \frac{K}{S} \qquad \textit{Equation 4.6}$$

Where K is the absorption coefficient, S the scattering coefficient and R_∞ is the absolute reflectance of the sample infinitely thick.[25] However, the successful application of K-M transformation relies on several assumptions which constraints its routine use.

Moreover, other theories of diffuse reflection have been developed.[23] The main point of these new approaches is a better understanding of absorbance and scattering phenomena in solid samples, and the possibility of resolving K-M equation, allowing the experimental determination of K and S.[26,27] However, they arrived to practically the same final equation, so K-M equation is usually referred.

Nevertheless, from a practical point of view, the simple conversion of reflectance values to log(1/R) appears to be effective for many solid samples being analyzed by diffuse reflectance NIRS.[23] The analytical signal measured in this case is expressed in the form of apparent absorbance (A_{ap}):

$$A_{ap} = \log\frac{1}{R} = \log\frac{R_{ref}}{R_m} \qquad \textit{Equation 4.7}$$

where R_{ref} is the reference reflectance, R_m the sample reflectance, R is the reflectance of the sample relative to that of a non-absorbing reference. This relationship is not considered to adhere to Beer's law, as this law is based on non-scattering samples. Nevertheless, a linear relationship is often observed between the analyte concentration and the changes in the log(1/R) spectra in many applications.[13,21]

3. Applications of near infrared spectroscopy in the pharmaceutical field

NIRS has been used extensively in the agricultural and food industries since a long time. In addition, large bodies of work exist in the textile, polymer, petroleum, and fine chemical industries.[18] Nevertheless, NIRS application in the fields of pharmaceutical and biomedical research is more recent.[28]

As an example, NIRS has been successfully applied for in situ blood glucose measurements[29] and for cranial blood oxygenation[30,31] in the biomedical sector.

Regarding the application of NIRS in the pharmaceutical field, the earliest publications appeared in the late 1960s.[28] In 1966, Sinsheimer and Keuhnelian[32] investigated a number of pharmacologically active amine salts both in solution and in solid state and, in 1967, Oi and Inaba[33] quantified two drugs, dissolving the samples in chloroform.

At the beginning, sample extractions with organic solvents and/or samples pulverization prior to analysis were required for the analysis of components in solid dosage form. However, with advances in instrumentation, software, and sample handling procedures, rapid characterization of intact dosage forms was possible.[28]

Nowadays, NIRS has a wide and varied use in many unit operations of the manufacturing process of a drug product, from the arrival of bulk raw material to the inspection of the final product for release. This includes qualitative and quantitative analysis of both chemical and physical properties, such as: raw materials identification, determination of active ingredients, excipients and packaging materials, polymorphism, hardness, dissolution profiles, particle size, moisture, among others.

More recently, several on-line applications in process monitoring (for mixing, granulation, drying, coating, or freeze-drying unit operations) have emerged thanks to the application of PAT initiative. The early works and recent applications in pharmaceutical industry have been summarized and discussed in several book chapters[9,28,34,35] and reviews[17,36–42].

In this project, NIR spectra was collected in injectable freeze-dried drug products. In literature, there are several applications of NIRS for the off-line evaluation of freeze-dried drug products, and in-line monitoring of the freeze-drying process. These applications are deeply discussed in the following subsections.

3.1. Evaluation of freeze-dried drug products

Freeze-dried materials are challenging samples for quality control analysis because of the inability to open the container without corrupting the product.[43] Due to ability of NIRS to penetrate glass containers, it represents an excellent non-invasive technique to analyse freeze-dried products in vials.[12] Some of the most successful applications are: RMC determination, product characterization in solid-state, drug-excipient interactions and molecule conformational studies.

NIRS has been used to characterize molecular interactions of freeze-dried samples.[12] As an example, Bai et al.[44] have demonstrated that NIRS is well suited for quantify glycine crystallinity in lyophilized cakes. Compared to the reference method (XRPD), NIRS allows to reduce measurement times and sample preparation. In addition, in 2010, Grohganz and coworkers[45] investigated the effect of varying rations of mannitol and sucrose, and different RMC on mannitol crystallization in the lyophilized product by NIRS. Then, NIRS can be used to study and finally choose excipients for freeze-dried formulations.[46]

Furthermore, NIRS can be employed in the analysis of molecule conformation and stability as well.[12] Hansen et al.[47,48] demonstrated the applicability of NIRS for evaluating conformational changes of freeze-dried viral vaccine formulations with respect to the virus pre-treatment, virus volume and during an accelerated stability study. In addition, Izutsu et al.[49] made a great contribution in the investigation of protein structure and interactions by NIRS.

However, among the compounds which can be quantified by NIRS in freeze-dried pharmaceutical products, water has been the most evaluated. It is important to highlight that the measurement of water was one of the first pharmaceutical applications of NIRS. In 1986, Whitfield[50] used NIRS to determine the concentrations of moisture and lincomycin in animal feed, and became the first NIRS method accepted by the FDA in a veterinary product application. Since then, several publications demonstrated successful determinations of moisture in different solid forms, such as powders, granules or tablets.[51–55]

Due to its strong absorbance in the NIR region, water can be determined at very low concentrations. Water has three normal mode vibrations: symmetric stretch (ν_1), asymmetric stretch (ν_3) and bend (ν_2), which are represented in Figure 4.5.

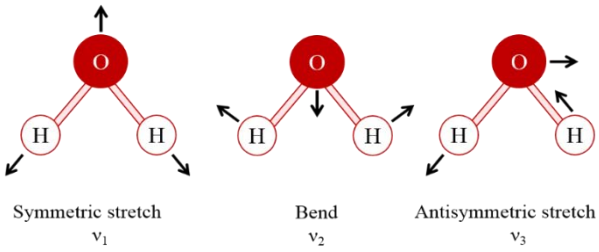

Figure 4.5. Normal mode vibrations of water.

The NIR spectrum of water exhibits five absorption maxima at 760 nm, 970 nm, 1170 nm, 1450 nm and 1940 nm (Table 4.2). Among them, 1450 nm and 1940 nm are the most intense ones and result from first overtone of the –OH stretching vibrations and combination of –OH stretching and bending vibrations, respectively[6,28] (Figure 4.6). The positions of these bands can be slightly shifted by temperature changes or hydrogen bonding between the analyte and its matrix.[56,57]

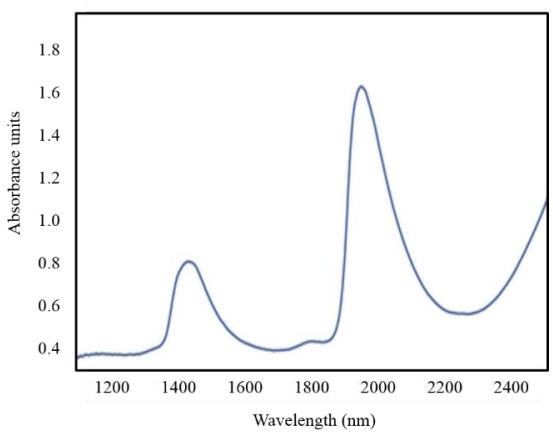

Figure 4.6. Representative NIR spectrum of water.

3.1.1. Moisture content determination in freeze-dried drug products

One of the main criteria for an acceptable freeze-dried product is to have low RMC, because moisture has an influence on its physical and the chemical stability.[58] Determination of moisture content in freeze-dried drug products is typically done by KF titration[59], loss on drying, or gas chromatography (GC).[60] However, each method has pros and cons.

Loss on drying is a wrong option if the chemicals are unstable at elevated temperatures or if other volatile species are present. GC is more expensive, standardization can be difficult, and some volatile drug substances might interfere with the measurement. Consequently, the method most widely used to determine the water content in pharmaceutical freeze-dried samples is KF titration.[61–63]

KF titration was invented by the German chemist Karl Fischer in 1935. The method relies on the quantitative redox reaction of I_2 and H_2O in the presence of an alcohol (commonly methanol), a base (commonly imidazole) and SO_2.[64] Depending on the source of I_2, two KF methods can be distinguished: volumetric (where I_2 is present in the titrant solution) and coulometric (where a Pt electrode generates I_2 when an electric current is applied). In the situations where a component reacts with the KF solvent or it does not dissolve with KF reagents, an oven accessory can be used to extract water vapor and transfer it to the titration cell.[65]

The advantages of KF over the other methods are its high accuracy, and its specificity for water, while gravimetric method will detect the loss of any volatile substance. However, KF is time consuming, destructive and uses toxic reagents. Hence, the number of samples taken for moisture analysis is limited.

Furthermore, in product stability studies, moisture data obtained from KF for one set of samples can only be correlated to other quality attributes results from different product vials. Due to the potential inter-vial variability in RMC, the validity of this correlation could be limited.[66]

Alternatively, NIRS has been demonstrated as an ideal approach for the determination of RMC on freeze-dried vials. It is non-invasive, non-destructive, fast and requires minimal or no sample preparation. Thus, the sterility of the product is conserved and the impact of ambient moisture in these highly hygroscopic samples is avoided.[12] NIRS is also safer to use because no hazardous chemicals are involved in the analysis, and little training is required for an operator.[66]

More importantly, since NIRS can determine RMC through unopened vials, it is very useful when dealing with a large number of samples, like larger-scale studies, such as long-term stability studies or freeze dryer moisture mapping. Moreover, it allows direct correlation between moisture data and stability results for the same sample vials.[67]

Nevertheless, classical methods such as KF are required as reference methods for setting up the NIR calibrations.[39] For a general overview, a summary of some publications about the off-line quantitative use of NIR for RMC determination in pharmaceutical freeze-dried products is described in Table 4.3.

At this point, it is worth to dedicate a few words about the trajectory of the application of NIRS for RMC determination in pharmaceutical freeze-dried products. Besides, great discussions are written by Roggo et al.[39] and Luypaert et al.[38].

In 1989, Kamat and DeLuca[68] first reported the NIR determination of residual moisture in intact freeze-dried sucrose using KF as the reference method. Since then, the majority of publications had used KF as reference method as well, although some authors have used GC[69], loss on drying[70] and TGA[71].

In general, several studies cited in Table 4.3 remarked the suitability of NIR method because of the reduction of sample manipulation, especially for biologic[70] and hygroscopic samples[69,72]. Others focused on the non-destructive character of the NIR method which allows to measure RMC and API concentration in the same vial, which represents a real benefit in stability studies.[67,73]

The versatility of NIRS was demonstrated by Li et al.[74], who established a NIRS method for the simultaneous analysis of moisture, API concentration and freeze-dried cake structure. Therefore, with one spectrum, three quality attributes of the product were analysed.[74]

Most published NIRS methods focus on the total amount of residual moisture, rather than water of different energetic states. However, Zhou[75] and Cao[71] were able to differentiate and quantify bound and surface water separately. More recently, other studies focused in the use of new NIR spectrometers configurations[76] and new regression methods (variants of the classical ones) which have been evaluated to improve model quality.[77] Although not quantitatively, another study has evaluate the use of NIR imaging for the qualitative analysis of the water distribution in freeze-dried samples in well plates.[78]

Table 4.3. Summary table of scientific publications about the quantitative use of NIR for RMC determination in pharmaceutical lyophilized products.

Ref.	Product	NIR Instrument	Ref. Method	Range	Algorithm	Statistical Evaluation	Use/Application
Kamat et al. 1989 [68]	Sucrose	InfraAlyzer500 + reflectance probe	KF	0.7%-4.7%	PCR	R^2=0.97 SEP=0.27%	First published rapid, non-invasive and non-destructive method for determining moisture in sealed freeze-dried vials based on NIRS.
Jones, J A et al. 1993 [79]	Not defined	NIRSystems 6500 + a HSM	KF	0.8%-4.9%	1 and 2-λ equations	r=0.95; Good precision and accuracy	Confirm the transferability of NIR methods for moisture content prediction between two sites with the same model instrument.
Last, I R and Prebble, K A, 1993 [80]	Not defined	NIRSystems 6500 + a HSM	KF	1.5%-4.9%	1 and 2-λ equations and PLS	r=0.81; Poor accuracy and precision	Study of combined vs individual NIR models for two strengths of the same product.
Zhou, X et al., 1998 [60]	FD Antibiotic LY333328	NIRSystems 6500 + a RCA	GC	0.1%-5.7%	PLS	R^2=0.99, Slope=0.988; y-intercept=0.026%; SEP=0.070%	Use a GC method as a reference to build an NIRS method to determine water in freeze-dried drug products.
Savage, M et al., 1998 [70]	FD antihaemophilic factor	NIRSystems 6500 + a RCA	Loss of drying KF	0.3%-2.5% 1%-5%	univariate 1930nm	Slope=1·00; intercept=−0·00016; r=0·980; Slope=1·00; intercept=0; r=0·978	Comparison of the predictive capacity of the NIR model obtained using LOD or KF as reference methods. The NIR model was applied to the monitoring of the moisture for virus inactivation methods for dry heat treating lyophilized products.
Zhou, X et al, 1998 [69]	Not defined	NIRSystems 6500 + a RCA	KF	0.5% - 11.4%	PLS	SEP=0.11%; R^2=0.999, Slope=1.013; y-intercept=−0.103%	Importance of a proper method of handling samples and precise and accurate reference technique, KF.
Derksen, M et al., 1998 [67]	API + 4 excipients	NIRSystem 6500 + a reflection module	KF	0.1-5.0 mg/vial	PLS	Bias <0.01 mg/vial; SE= 0.02 mg/vial; R^2= 0.98.	Correlate RMC and assay of the same vials stored for two months at 8ºC, 50ºC, and 60°C to define a suitable specification for the RMC.
Stokvold, A. et al, 2002 [73]	Not defined	FT-NIRS + a reflectance accessory	KF	0.3% -3%	PLS	SEP=0.08% (w/w) LOQ=0.24% (w/w). Complete validation.	Study the relationship between moisture, storage temperature and time.
Lin TP and Hsu CC, 2002 [66]	Five lyophilized protein	FT-NIR + an integrating sphere reflection module	KF	0.4% -5%	PLS and SMLR	R^2>0.97 bias < 0.001 RMSEC=0.114-0.168 RMSECV=0.170.200. RMSEP=0.135-0.243	5 NIR models for 5 lyophilized proteins. Determine the effect of freeze-dried cake Porosity, cake dimensions and excipient-to-protein ratio on the accuracy of those NIR models RMC predictions.
Dunko, A and Dovletoglou, A, 2002 [72]	Antifungal Caspofun-gin Acetate	PS-2 portable diode array + a reflectance probe	KF	2.6% -9.9%	PLS	r=0.9003 SEC=0.5% SEP=0.2% SECV=0.54% Good precision, accuracy and robustness	Development and validation of a NIR method for accurate and fast moisture determination for the antifungal drug substance. In addition, study the effect of measuring through glass or ACLAR® 22C liner.
Hirsch, J, 2006 [43]	Thrombin	FT-NIR	KF	0.5% -0.8%	SMLR	r=0.998; RMSEC=0.005; RMSECV=0.018	NIR analysis of critical parameters in lyophilized materials (moisture and potency).
Cao W et al, 2006 [71]	Mannitol	Diffuse reflectance NIR spectrometer + integrating sphere	TGA KF	hydrate: 0.4% -5.2% surface: 1% -3.3%	PLS	R^2 =0.9579 SEP=0.50% SEP=0.22%; R2= 0.9117	Quantitative determination of hydrate and surface water to monitor the formation and stability of mannitol hydrate during the lyophilization process.

Ref.	Product	NIR Instrument	Ref. Method	Range	Algorithm	Statistical Evaluation	Use/Application
Brülls, M et al, 2007 [81]	PVP	FT-NIR+ a reflectance probe or NIRSystems 6500 + a RCA	KF	0.5%–8.5%	Peak area determination PLS	RSEP≈5% RSEPT (%)= 4.1; RSEPC(%) = 3.3	Viability of Spectral peak area analysis in NIRS moisture assays of lyophilized samples.
Zheng Y et al, 2008 [82]	Five allergen vaccines	FT-NIR	KF	0.2%–1.5%	PLS	RMSEP= 10.20 µg H_2O/vial	Compare multi-calibration model and product-specific models for moisture determination by NIRS.
Zhang X et al. 2008 [83]	Nine beta-lactam powders for injections	Four FT-NIR + Fibreoptic probes	KF	0.5-10%	PLS	R^2=99.14; RMSEC=0.247; Bias=0.0148; RPD=10.8; Offset=0.033; S=0.992	Build universal models for drugs with diverse formulations and sources. Also, study the calibration transfer and model updating for new products emerging.
Grohganz H et al., 2009 [84]	Mixtures of mannitol–sucrose + other excipients	FT-NIR	KF	0.2% -5.6% 0.2% - 2%	PLS	RMSEE=0.42% RMSEE=0.211%	Validate a suitable NIR method for quantification of the water content in lyophilized samples with varying mannitol-sucrose ratios.
Grohganz H et al., 2010 [85]	Insulin and human growth hormone	FT-NIR + a customized motorized stage	KF	0.2%- 4.3%	PLS	S=1.00; R^2=0.98; RMSECV= 0.15%; RMSEP= 0.19%; LOD=0.04%; LOQ=0.11%	Test if a model based solely on freeze-dried mannitol–sucrose mixtures can be used to predict water contents for samples containing proteins, excipients or having a lower density of freeze-dried solids.
Li, Y et al., 2011 [74]	Potassium sodium de-hydroandrographolide succinate	FT-NIR + an integrating sphere	KF	0.7%–2.7%	BP-ANN	RMSECV = 0.2376; RMSEP=0.1471; R=0.9553	Novel method for the simultaneous analysis of moisture, active component and cake structure of lyophilized powder for injection.
Muzzio C et al, 2011 [76]	Mannitol	diffraction grating micro NIR + a fiber optic probe	KF	0.1% -8.2%	PLS	Slope = 0.992; intercept=0.0174 R^2 = 0.996; RMSEP=0.233%; RSEP = 8.21%; LOD=0.22%; LOQ=0.73%	Use of an NIR micro-spectrometer instead of a conventional NIR spectrometer, to develop a method for determination of moisture content in lyophilized mannitol.
Yip L et al, 2012 [77]	Mannitol	MPA FT-NIR	KF	0.7%-2.6%	MIPCR	MPE= 15.7–20.5%; RMSECV=0.351–0.411	Investigation of physicochemical properties of the freeze-dried product that may interfere with absorption bands related to the water content.
Clavaud M et al, 2016 [86]	2 doses of Antibody-drug conjugates	Two FT-NIRs + an integrating sphere module	KF	0.5% -4.0%	PLS	r= 0.99; Slope=0.99; y-intercept=0.02; RMSEC=0.10%; RMSEP=0.12%; SEL=0.10%; Complete validation	NIRS benefits for release, stability analyses and OOS investigation in a current GMP environment Develop a unique NIRS model with data coming from two identical devices.
Clavaud M et al., 2017 [87]	Not defined	Two FT-NIRs + an integrating sphere module	KF	0.05-4.96%	SVR	Slope=0.99 y-intercept=0.02 R^2=0.993, Bias=0.00, SEC=0.12%, SEP=0.15% linearity and accuracy	Develop a global regression model to speed up the validation time and the in-lab release analyses.

Abbreviations: HSM (Horizontal Setup Module), RCA (Rapid Content Analyzer), MPA (Multi-Purpose Analizer), SMLR (Step-wise Multiple Linear Regression), BP-ANN (Back Propagation- Artificial Neural Network), MIPCR (Main and Interactions of Individual Principal Components Regression), SVR (Support Vector Regression), FT (Fourier Transform), Limit of Detection (LOD).

Finally, two studies were published in the last two years by Clavaud and coworkers[86,87] with great emphasis in two topics:

- The validation strategy of NIR methods as basis for submission to the health authorities for release and stability activities in a current GMP environment.[86]
- Global regression models, a topic also discussed by Last and Prebble[80], Zheng[82], Zhang[83] and Grohganz[85]. The authors emphasized that this innovative approach allows to speed up the validation time and the in-lab release analysis, which represented great improvements in an industrial point of view. In addition, general multi-product models are more useful in routine quality analysis, since one model can be applied for a great number of products.[87]

During the development of NIR methods for RMC determination, it is important to properly define how calibration samples will be obtained and the spectral acquisition procedure. In the articles discussed above, several strategies were used to obtain high and low RMC in freeze-dried samples.

One way is the exposure of the vial to controlled environments with high and low relative humidity or, directly, to ambient air. Others used vials spiked with small volume of water.[67,68,71] However, in order to avoid opening the vial, it is preferred to obtain high and low RMC vials directly from the freeze-drying process.

Regarding the spectral acquisition procedure, most of the publications stated that it was performed through the bottom of the glass vial. However, Grohganz[84,85] acquired the spectra through the lateral side of the vial and Muzzi[76] and Stockvold[73] remarked the importance of vial rotation and repeated measurements for a proper spectra acquisition.

3.1.2. In-line monitoring of the freeze-drying process

NIR and Raman spectroscopies have been used to qualitatively and quantitatively monitor moisture and structure characteristics of a single vial in real-time inside the freeze-dryer chamber.[41,88,89]

De Beer et al.[88] showed that Raman spectroscopy proved to be an excellent tool for crystallization and polymorphic transformation monitoring during the freeze-drying process. In contrast, NIRS was suited for water content monitoring during freeze-drying and, thus, for the determination of the endpoint of the drying process.

Similarly, Rosas et al.[89] collected diffuse reflectance NIR spectra to identify changes in the mannitol polymorphs during the freeze-drying process. They positioned the NIR probe next to the vial (non-invasively), monitoring the sidewall of the bottom of the vial.

To solve the problem of monitoring just one vial inside the freeze-dryer, Kaupplien et al.[90,91] developed and validated a multichannel NIR instrument equipped with several probes, used to monitor different vials simultaneously at different positions.

Since now, the use of NIRS for in-line monitoring of freeze-drying processes has been successfully proved in lab-scale freeze-dryers, but the applicability in large production scale freeze-dryers is still under study.[41]

However, in the QbD framework, the possibility to predict multiple CQAs during manufacturing and, also, to control the output in order to ensure final product quality, represents a major benefit.[90]

4. Pharmaceutical regulatory framework

The development and implementation of a NIR procedure is iterative and ongoing, and is amenable to the application of lifecycle concepts and QbD principles.[92]

Currently, most pharmacopoeias have already adopted the NIR as an analytical method. NIRS is described in the *Ph. Eur.*[93] and in the USP[94]. In both, the suitability of NIR instrumentation for use in pharmaceutical analysis, focusing mainly on operational qualification and performance verification, is described.[17]

However, in the highly regulated pharmaceutical world, the most perfectly designed NIR method is of no use to the pharmaceutical world unless it has been validated and approved by regulatory authorities.[28] In this sense, EMA and FDA published guidelines about the use of NIRS by the pharmaceutical industry and the data requirements for new submissions and variations.[92,95]

Figure 4.7 displays the main steps in NIR method validation that satisfies the current GMPs. In short, three criteria must be met for a complete: validation of the software, validation of the hardware, and, after that, validation of the NIRS method.

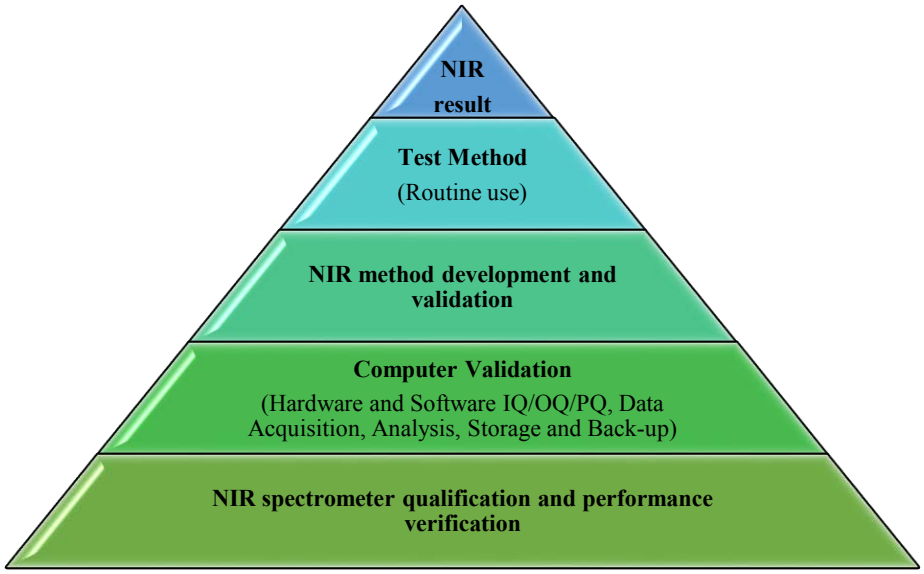

Figure 4.7. NIR method validation pyramid. Adapted from reference[28].

In this project, software and hardware validations were performed at the beginning of the PhD thesis. However, it was decided not to include it in the final thesis project, but it is stored in the company's internal document management system. As a summary, the validation master plan summarized in Table 4.4 was followed according to current regulatory guidelines.

Table 4.4. RJ's validation master plan for NIR method development and validation.

Tasks	Type of document created
NIR Instrument Qualification	Protocol and report Standard operating procedure of the routine use Standard operating procedure of performance verification
NIR software validation	Protocol and report
Reference analytical method validation	Analytical Validation Protocol Analytical Validation Report
NIRS procedure development	Task summary for Development of NIRS procedure
Risk Analysis	
Feasibility study	
Calibration	Analytical Validation Protocol Analytical Validation Report
Validation	
Regulatory proposal	Module 3 Quality, section 3.2.P.5.2 Analytical methods of the registration dossier (Common Technical Document)

5. Summary

In summary, NIRS is a type of vibrational spectroscopy that represents overtones and combinations of the fundamental molecular vibrations. The NIR spectrum is characterized by broad and overlapping bands of low intensity.

NIRS has been successfully implemented as off-line quality control and in-line process analytical tool in the pharmaceutical industry. Particularly, in the case of freeze-dried drug products, NIRS has been used to determine the RMC of a vial either off-line or in-line (inside the freeze-dryer chamber).

On one hand, the interest in NIRS has increased thanks to instrument improvements and the development of fibreoptics that allow the delocalization of the measurements for PAT purposes. On the other hand, the computer progresses, and the development of new mathematical methods for spectral data pre-treatment permitted to "*decode*" and interpret the NIR spectral information.

Actually, the validity of a NIRS method depends on its ability to detect relevant variability in the spectrum. This issue can be solved with chemometric tools. In the following chapter, multivariate calibration methods and the process of development and validation of NIR model will be further explained.

References

(1) Herschel, W. Experiments on the Refrangibility of the Invisible Rays of the Sun. *Philos. Trans. R. Soc. London* **1800**, *90*, 284–292.

(2) Hindle, P. H. Historical Development. In *Handbook of near-infrared analysis*; Burns, D. A., Ciurczak, E. W., Eds.; CRC Press: Boca Raton, 2008; pp 3–6.

(3) Miller, F. A. The History of Spectroscopy as Illustrated on Stamps. *Appl. Spectrosc.* **1983**, *37* (3), 219–225.

(4) Abney, W.; Festing, E. R. On the Influence of the Atomic Grouping in the Molecules of Organic Bodies on Their Absorption in the Infra-Red Region of the Spectrum. *Philos. Trans. R. Soc. London* **1881**, *172*, 887–918.

(5) Cogdill, R. P.; Drennen, J. K. Near-Infrared Spectroscopy. In *Spectroscopy of Pharmaceutical Solids*; Brittain, H. G., Ed.; Taylor & Francis: New York, 2006; pp 313–412.

(6) Dufour, É. Principles of Infrared Spectroscopy. In *Infrared Spectroscopy for Food Quality Analysis and Control*; Sun, D.-W., Ed.; Academic Press: USA, 2009; pp 3–27.

(7) Ben-Gera, I.; Norris, K. H. Direct Spectrophotometric Determination of Fat and Moisture in Meat Products. *J. Food Sci.* **1968**, *33* (1), 64–67.

(8) Siesler, H. W. Basic Principles of Near-Infrared Spectroscopy. In *Handbook of near-infrared analysis*; Burns, D. A., Ciurczak, E. W., Eds.; CRC Press: Boca Raton, 2008; pp 7–19.

(9) Goettler, B. S. On-Line PAT Applications of Spectroscopy in the Pharmaceutical Industry. In *Process Analytical Technology*; Bakeev, K. A., Ed.; John Wiley & Sons, Ltd: Chichester, UK, 2010; pp 439–461.

(10) Simpson, M. B. Near-Infrared Spectroscopy for Process Analytical Technology: Theory, Technology and Implementation. In *Process Analytical Technology*; Bakeev, K. A., Ed.; John Wiley & Sons, Ltd: Chichester, UK, 2010; pp 107–155.

(11) *Principios de Análisis Instrumental*, 5a ed.; Skoog, D., Holler, J., Nieman, T., Eds.; Mc Graw Hill: Madrid, 2001.

(12) Bedi, S.; Balabathula, P.; Mandal, B.; Mittal, I.; Bhattacharjee, H. NIR Applications for Lyophilization of Biopharmaceuticals. *Am. Pharm. Rev.* **2012**, 1–7.

(13) Pasquini, C. Near Infrared Spectroscopy: Fundamentals, Practical Aspects and Analytical Applications. *J. Braz. Chem. Soc* **2003**, *14* (2), 198–219.

(14) *Pharmaceutical and Medical Applications of Near-Lnfrared Spectroscopy*; Ciurczak, E. W., Drennen III, J. K., Eds.; Marcel Dekker, Inc: New York, 2002.

(15) Charles E, M. Chemical Principles of Near-Infrared Technology. In *Near-Infrared Technology in the Agriculture and Food Industries*; Williams, P., Norris, K., Eds.; The American Association of Cereal Chemists: St Paul, MN, USA, 2001; pp 19–37.

(16) Brittain, H. G. Molecular Motion and Vibrational Spectroscopy. In *Spectroscopy of pharmaceutical solids*; Brittain, H. G., Ed.; Taylor & Francis: New York, 2006; pp 205–233.

(17) Reich, G. Near-Infrared Spectroscopy and Imaging: Basic Principles and Pharmaceutical Applications. *Adv. Drug Deliv. Rev.* **2005**, *57* (8), 1109–1143.

(18) *Near Infrared Spectroscopy: Proceedings of the 11th International Conference*; Davies, A. M. C., Garrido-Varo, A., Eds.; NIR publications: Chichester, UK, 2004.

(19) Bugay, D. E.; Brittain, H. G. Infrared Absorption Spectroscopy. In *Spectroscopy of Pharmaceutical Solids*; Brittain, H. G., Ed.; Taylor & Francis: New York, 2006; pp 235–269.

(20) Davies, T. The History of near Infrared Spectroscopic Analysis: Past, Present and Future – "From Sleeping Technique to the Morning Star of Spectroscopy." *ANALUSIS Mag.* **1998**, *26* (4), 17–19.

(21) Blanco, M.; Alcal, M.; Felizardo, P. M.; Garrido, A.; Dolores, P.; Roma, R. J. Near-Infrared Spectroscopy in Laboratory and Process Analysis. In *Encyclopedia of Analytical Chemistry*; John Wiley & Sons, Ltd, 2012; pp 1–46.

(22) Laske, S.; Paudel, A.; Scheibelhofer, O.; Author Team, S.; Hoermann, T.; Khinast, J.; Kelly, A.; Rantannen, J.; Korhonen, O.; Stauffer, F.; et al. A Review of PAT Strategies in Secondary Solid Oral Dosage Manufacturing of Small Molecules. *J. Pharm. Sci.* **2017**, *106* (3), 667–712.

(23) Griffiths, P. R.; Dahm, D. J. Continuum and Discontinuum Theories of Diffuse Reflection. In *Handbook of near-infrared analysis*; Burns, D. A., Ciurczak, E. W., Eds.; CRC Press: Boca Raton, 2008; pp 22–62.

(24) Kubelka, P.; Munk, F. Ein Beitrag Zur Optik Der Farbanstriche. *Zeitschrift für Tech. Phys.* **1931**, *12*, 593–601.

(25) Torrent, J.; Barrón, V. Diffuse Reflectance Spectroscopy. In *Methods of Soil Analysis. Part 5 - Mineralogical Methods*; Ulery, A. L., Dress, R., Eds.; Soil Science Society of America: Madison, Wisconsin, USA, 2008; pp 367–385.

(26) *Interpreting Diffuse Reflectance and Transmittance: A Theoretical Introduction to Absorption Spectroscopy of Scattering Materials*; Dahm, D. J., Dahm, K. D., Eds.; NIR Publications: Chichester, UK, 2007.

(27) Burger, T.; Kuhn, J.; Caps, R.; Fricke, J. Quantitative Determination of the Scattering and Absorption Coefficients from Diffuse Reflectance and Transmittance Measurements: Application to Pharmaceutical Powders. *Appl. Spectrosc.* **1997**, *51* (3), 309–317.

(28) Ciurczak, E. W.; Igne, B. *Pharmaceutical and Medical Applications of Near-Infrared Spectroscopy*, 2nd ed.;

Ciurczak, E. W., Igne, B., Eds.; CRC Press, Taylor & Francis Group: Boca Raton, 2015.

(29) Ham, F. M.; Cohen, G. M. Determination of Concentrations of Biological Substances Using Raman Spectroscopy and Artificial Neural Network Discriminator. US005553616A, 1996.

(30) Rooks, C. R.; Thom, N. J.; Mccully, K. K.; Dishman, R. K. Effects of Incremental Exercise on Cerebral Oxygenation Measured by near-Infrared Spectroscopy: A Systematic Review. *Prog. Neurobiol.* **2010**, *92*, 134–150.

(31) Wolf, M.; Morren, G.; Haensse, D.; Karen, T.; Wolf, U.; Fauchére, J. C.; Bucher, H. U. Near Infrared Spectroscopy to Study the Brain: An Overview. *Opto-Electronics Rev.* **2008**, *16* (4), 413–419.

(32) Sinsheimer, J. E.; Keuhnelian, A. M. Near-Infrared Spectroscopy of Amine Salts. *J. Pharm. Sci.* **1966**, *55* (11), 1240–1244.

(33) Oi, N.; Inaba, E. Analyses of Drugs and Chemicals by Infrared Absorption Spectroscopy. 8. Determination of Allylisopropylacetureide and Phenacetin in Pharmaceutical Preparations by near Infrared Absorption Spectroscopy. *Yakugaku zasshi* **1967**, *87* (3), 213–215.

(34) Blanco Romía, M.; Alcalá Bernárdez, M. NIR Spectroscopy in Pharmaceutical Analysis : Off-Line and At-Line PAT Applications. In *Process Analytical Technology*; Bakeev, K. A., Ed.; John Wiley & Sons, Ltd: Chichester, UK, 2010; pp 463–491.

(35) Anderson, C. A.; Drennen, J. K.; Ciurczak, E. W. Pharmaceutical Applications of Near-Infrared Spectroscopy. In *Handbook of Near-Infrared Analysis*; Burns, D. A., Ciurczak, E. W., Eds.; CRC Press: Boca Raton, 2006; pp 585–611.

(36) MacDonald, B. F.; Prebble, K. A. Some Applications of Near-Infrared Reflectance Analysis in the Pharmaceutical Industry. *J. Pharm. Biomed. Anal.* **1993**, *11* (11/12), 1077–1085.

(37) Blanco, M.; Coello, J.; Iturriaga, H.; Maspoch, S.; De La Pezuela, C. Near-Infrared Spectroscopy in the Pharmaceutical Industry. *Analyst* **1998**, *123*, 135R–150R.

(38) Luypaert, J.; Massart, D. L.; Vander Heyden, Y. Near-Infrared Spectroscopy Applications in Pharmaceutical Analysis. *Talanta* **2007**, *72*, 865–883.

(39) Roggo, Y.; Chalus, P.; Maurer, L.; Lema-Martinez, C.; Edmond, A.; Jent, N. A Review of Near Infrared Spectroscopy and Chemometrics in Pharmaceutical Technologies. *J. Pharm. Biomed. Anal.* **2007**, *44*, 683–700.

(40) Jamrógiewicz, M. Application of the Near-Infrared Spectroscopy in the Pharmaceutical Technology. *J. Pharm. Biomed. Anal.* **2012**, *66*, 1–10.

(41) De Beer, T.; Burggraeve, A.; Fonteyne, M.; Saerens, L.; Remon, J. P.; Vervaet, C. Near Infrared and Raman Spectroscopy for the in-Process Monitoring of Pharmaceutical Production Processes. *Int. J. Pharm.* **2011**, *417*, 32–47.

(42) Erxleben, A. Application of Vibrational Spectroscopy to Study Solid-State Transformations of Pharmaceuticals. *Curr. Pharm. Des.* **2016**, *22* (32), 4883–4911.

(43) Hirsch, J. Near-Infrared Analysis of Critical Parameters in Lyophilized Materials. *BioPharm Int.* **2006**, *19* (2), 32–36.

(44) Bai, S. J.; Rani, M.; Suryanarayanan, R.; Carpenter, J. F.; Nayar, R.; Manning, M. C. Quantification of Glycine Crystallinity by near-Infrared (NIR) Spectroscopy. *J. Pharm. Sci.* **2004**, *93* (10), 2439–2447.

(45) Grohganz, H.; Fonteyne, M.; Skibsted, E.; Falck, T.; Palmqvist, B.; Rantanen, J. Classification of Lyophilised Mixtures Using Multivariate Analysis of NIR Spectra. *Eur. J. Pharm. Biopharm.* **2010**, *74* (2), 406–412.

(46) Izutsu, K.; Hiyama, Y.; Yomota, C.; Kawanishi, T. Near-Infrared Analysis of Hydrogen-Bonding in Glass- and Rubber-State Amorphous Saccharide Solids. *AAPS PharmSciTech* **2009**, *10* (2), 524–529.

(47) Hansen, L.; Beer, T. De; Pieters, S.; Heyden, Y. Vander; Vervaet, C.; Remon, J. P.; Montenez, J. P.; Daoussi, R. Near-Infrared Spectroscopic Evaluation of Lyophilized Viral Vaccine Formulations. *Biotechnol. Prog.* **2013**, *29* (6), 1573–1586.

(48) Hansen, L.; Renterghem, J. Van; Daoussi, R.; Vervaet, C.; Paul, J.; De Beer, T. Spectroscopic Evaluation of a Freeze-Dried Vaccine during an Accelerated Stability Study. *Eur. J. Pharm. Biopharm.* **2016**, *104*, 89–100.

(49) Izutsu K, Fujimaki Y, Kuwabara A, Hiyama Y, Yomota C, A. N. Near-Infrared Analysis of Protein Secondary Structure in Aqueous Solutions and Freeze-Dried Solids. *J. Pharm. Sci.* **2006**, *95* (4), 781–789.

(50) Whitfield, R. G. Near-Infrared Reflectance Analysis of Pharmaceutical Products. *Pharm. Manuf* **1986**, *3* (4), 31–40.

(51) Dreassi, E.; Ceramelli, G.; Cortia, P.; Perrucciob, P. L.; Lonardic, S. Application of Near-Infrared Reflectance Spectrometry to the Analytical Control of Pharmaceuticals: Ranitidine Hydrochloride Tablet Production. *Analyst* **1996**, *121*, 219–222.

(52) Blanco, M.; Coello, J.; Iturriaga, H.; Maspoch, S.; Rovira, E. Determination of Water in Ferrous Lactate by near Infrared Reflectance Spectroscopy with a Fibre-Optic Probe. *J. Pharm. Biomed. Anal.* **1997**, *16*, 255–262.

(53) Mantanus, J.; Ziémons, E.; Lebrun, P.; Rozet, E.; Klinkenberg, R.; Streel, B.; Evrard, B.; Hubert, P. Moisture Content Determination of Pharmaceutical Pellets by near Infrared Spectroscopy: Method Development and Validation. *Anal. Chim. Acta* **2009**, *642*, 186–192.

(54) Corredor, C. C.; Bu, D.; Both, D. Comparison of near Infrared and Microwave Resonance Sensors for at-Line Moisture Determination in Powders and Tablets. *Anal. Chim. Acta* **2011**, *696*, 84–93.

(55) Bär, D.; Debus, H.; Brzenczek, S.; Fischer, W.; Imming, P. Determining Particle Size and Water Content by near-

Infrared Spectroscopy in the Granulation of Naproxen Sodium. *J. Pharm. Biomed. Anal.* **2018**, *151*, 209–218.

(56) Delwiche, S. R.; Norris, K. H.; Pitt, R. E. Temperature Sensitivity of Near-Infrared Scattering Transmittance Spectra of Water-Adsorbed Starch and Cellulose. *Appl. Spectrosc.* **1992**, *46* (5), 782–789.

(57) Chavan, R. B.; Nallamothu Bhargavi; Lodagekar, A.; Shastri, N. R. Near Infrared Spectroscopy: A Tool for Solid State Characterization. *Drug Discov. Today* **2017**, *22* (12), 1835–1843.

(58) Terakita, A.; Matsunaga, H.; Handa, T. The Influence of Water on the Stability of Lyophilized Formulations with Inositol and Mannitol as Excipients. *Chem. Pharm. Bull. (Tokyo).* **2009**, *57* (5), 459–463.

(59) Fischer, K. A New Method for the Analytical Determination of the Water Content of Liquids and Solids. *Angew Chem* **1935**, *48*, 394–396.

(60) Zhou, X.; Hines, P. A.; White, K. C.; Borer, M. W. Gas Chromatography as a Reference Method for Moisture Determination by Near-Infrared Spectroscopy. *Anal. Chem.* **1998**, *70* (2), 390–394.

(61) European Pharmacopoeia. Ph. Eur. 8.0. Chapter 2.5.32. Water: Micro Determination. Council of Europe, Strasbourg, France, 2014.

(62) European Pharmacopoeia. Ph. Eur. 8.0. Chapter 2.5.12. Water: Semi-Micro Determination. Council of Europe, Strasbourg, France, 2014.

(63) USP. USP40-NF35. General Chapter <921> Water Determination. 2016.

(64) May, J. C. Regulatory Control of Freeze-Dried Products: Importance and Evaluation of Residual Moisture. In *Freeze Drying/Lyophilization of Pharmaceutical and Biological Products*; Rey, L., May, J. C., Eds.; Informa Healthcare: London, UK, 2004.

(65) Leon Zhou, Jerome M. Socha, Frederick G. Vogt, Sarah Chen, A. S. K. A Systematic Method Development Strategy for Water Determinations in Drug Substance Using Karl Fischer Titrations. *Am. Pharm. Rev.* **2010**, *13*, 74–84.

(66) Lin TP and Hsu CC. Determination of Residual Moisture in Lyophilized Protein Pharmaceuticals Using a Rapid and Non-Invasive Method: Near Infrared Spectroscopy. *PDA J Pharm Sci Technol* **2002**, *56*, 196–205.

(67) Derksen, M. W. J.; van de Oetelaar, P. J. M.; Maris, F. A. The Use of near-Infrared Spectroscopy in the Efficient Prediction of a Specification for the Residual Moisture Content of a Freeze-Dried Product. *J. Pharm. Biomed. Anal.* **1998**, *17*, 473–480.

(68) Kamat, M. S.; Lodder, R. A.; DeLuca, P. P. Near-Infrared Spectroscopic Determination of Residual Moisture in Lyophilized Sucrose Through Intact Glass Vials. *Pharm. Res.* **1989**, *6* (11), 961–965.

(69) Zhou, X.; Hines, P.; Borer, M. W. Moisture Determination in Hygroscopic Drug Substances by near Infrared Spectroscopy. *J. Pharm. Biomed. Anal.* **1998**, *17*, 219–225.

(70) Savage, M.; Torres, J.; Franks, L.; Masecar, B.; Hotta, J. Determination of Adequate Moisture Content for Efficient Dry-Heat Viral Inactivation in Lyophilized Factor VIII by Loss on Drying and by Near Infrared Spectroscopy. *Biologicals* **1998**, *26*, 119–124.

(71) Cao, W.; Mao, C.; Chen, W.; Lin, H.; Krishnan, S.; Cauchon, N. Differentiation and Quantitative Determination of Surface and Hydrate Water in Lyophilized Mannitol Using NIR Spectroscopy. *J. Pharm. Sci.* **2006**, *95* (9), 2077–2086.

(72) Dunko, A.; Dovletoglou, A. Moisture Assay of an Antifungal by near-Infrared Diffuse Reflectance Spectroscopy. *J. Pharm. Biomed. Anal.* **2002**, *28*, 145–154.

(73) Stokvold, A.; Dyrstad, K.; Libnau, F. O. Sensitive NIRS Measurement of Increased Moisture in Stored Hygroscopic Freeze Dried Product. *J. Pharm. Biomed. Anal.* **2002**, *28*, 867–873.

(74) Li, Y.; Fan, Q.; Liu, S.; Wang, L. Simultaneous Analysis of Moisture, Active Component and Cake Structure of Lyophilized Powder for Injection with Diffuse Reflectance FT-NIR Chemometrics. *J. Pharm. Biomed. Anal.* **2011**, *55*, 216–219.

(75) Zhou, G. X.; Ge, Z.; Dorwart, J.; Izzo, B.; Kukura, J.; Bicker, G.; Wyvratt, J. Determination and Differentiation of Surface and Bound Water in Drug Substances by near Infrared Spectroscopy. *J. Pharm. Sci.* **2003**, *92* (5), 1058–1065.

(76) Muzzio, C. R.; Dini, N. G.; Simionato, L. D. Determination of Moisture Content in Lyophilized Mannitol through Intact Glass Vials Using NIR Micro-Spectrometers. *Brazilian J. Pharm. Sci.* **2011**, *47* (2), 289–297.

(77) Lam Yip, W.; Gausemel, I.; Arne Sande, S.; Dyrstad, K. Strategies for Multivariate Modeling of Moisture Content in Freeze-Dried Mannitol-Containing Products by near-Infrared Spectroscopy. *J. Pharm. Biomed. Anal.* **2012**, *70*, 202–211.

(78) Trnka, H.; Palou, A.; Panouillot, P. E.; Kauppinen, A.; Toiviainen, M.; Grohganz, H.; Alcalà, M.; Juuti, M.; Ketolainen, J.; Rantanen, J. Near-Infrared Imaging for High-Throughput Screening of Moisture Induced Changes in Freeze-Dried Formulations. *J. Pharm. Sci.* **2014**, *103* (9), 2839–2846.

(79) Jones, J. A.; Last, I. R.; MacDonald, B. F.; Prebble, K. A. Development and Transferability of near-Infrared Methods for Determination of Moisture in a Freeze-Dried Injection Product. *J. Pharm. Biomed. Anal.* **1993**, *11* (11/12), 1227–1231.

(80) Last, I. R.; Prebble, K. A. Suitability of near-Infrared Methods for the Determination of Moisture in a Freeze-Dried Injection Product Containing Different Amounts of the Active Ingredient. *J. Pharm. Biomed. Anal.* **1993**, *11* (11/12), 1071–1076.

(81) Brülls, M.; Folestad, S.; Sparén, A.; Rasmuson, A.; Salomonsson, J. Applying Spectral Peak Area Analysis in near-

Infrared Spectroscopy Moisture Assays. *J. Pharm. Biomed. Anal.* **2007**, *44*, 127–136.

(82) Zheng, Y.; Lai, X.; Wrang Bruun, S.; Ipsen, H.; Larsen, J. N.; Løwenstein, H.; Søndergaard, I.; Jacobsen, S. Determination of Moisture Content of Lyophilized Allergen Vaccines by NIR Spectroscopy. *J. Pharm. Biomed. Anal.* **2008**, *46*, 592–596.

(83) Zhang, X.-B.; Feng, Y.-C.; Hu, C.-Q. Feasibility and Extension of Universal Quantitative Models for Moisture Content Determination in Beta-Lactam Powder Injections by near-Infrared Spectroscopy. *Anal. Chim. Acta* **2008**, *630*, 131–140.

(84) Grohganz, H.; Fonteyne, M.; Skibsted, E.; Falck, T.; Palmqvist, B.; Rantanen, J. Role of Excipients in the Quantification of Water in Lyophilised Mixtures Using NIR Spectroscopy. *J. Pharm. Biomed. Anal.* **2009**, *49*, 901–907.

(85) Grohganz, H.; Gildemyn, D.; Skibsted, E.; Flink, J. M.; Rantanen, J. Towards a Robust Water Content Determination of Freeze-Dried Samples by near-Infrared Spectroscopy. *Anal. Chim. Acta* **2010**, *676*, 34–40.

(86) Clavaud, M.; Roggo, Y.; Dégardin, K.; Sacré, P.-Y.; Hubert, P.; Ziemons, E. Moisture Content Determination in an Antibody-Drug Conjugate Freeze-Dried Medicine by near-Infrared Spectroscopy: A Case Study for Release Testing. *J. Pharm. Biomed. Anal.* **2016**, *131*, 380–390.

(87) Clavaud, M.; Roggo, Y.; Dégardin, K.; Sacré, P.; Hubert, P.; Ziemons, E. Global Regression Model for Moisture Content Determination Using near-Infrared Spectroscopy. *Eur. J. Pharm. Biopharm.* **2017**, *119*, 343–352.

(88) De Beer, T. R. M.; Vercruysse, P.; Burggraeve, A.; Quinten, T.; Ouyang, J.; Zhang, X.; Vervaet, C.; Remon, J. P.; Baeyens, W. R. . In-Line and Real-Time Process Monitoring of a Freeze Drying Process Using Raman and NIR Spectroscopy as Complementary Process Analytical Technology (PAT) Tools. *J. Pharm. Sci.* **2009**, *98* (9), 3430–3446.

(89) Rosas, J. G.; Hans, de W.; Thomas, D. B.; Chris, V.; JeanPaul, R.; Wouter L.J, H.; Henderik W., F.; Marcelo, B. NIR Spectroscopy for the in-Line Monitoring of a Multicomponent Formulation during the Entire Freeze-Drying Process. *J. Pharm. Biomed. Anal.* **2014**, *97*, 39–46.

(90) Kauppinen, A.; Toiviainen, M.; Korhonen, O.; Aaltonen, J.; Järvinen, K.; Paaso, J.; Juuti, M.; Ketolainen, J. In-Line Multipoint Near-Infrared Spectroscopy for Moisture Content Quantification during Freeze-Drying. *Anal. Chem.* **2013**, *85* (4), 2377–2384.

(91) Kauppinen, A.; Toiviainen, M.; Lehtonen, M.; Järvinen, K.; Paaso, J.; Juuti, M.; Ketolainen, J. Validation of a Multipoint near-Infrared Spectroscopy Method for in-Line Moisture Content Analysis during Freeze-Drying. *J. Pharm. Biomed. Anal.* **2014**, *95*, 229–237.

(92) EMA. Guideline on the Use of Near Infrared Spectroscopy (NIRS) by the Pharmaceutical Industry and the Data Requirements for New Submissions and Variations. European Medicines Agency; London, UK, 2014.

(93) European Pharmacopoeia. Ph. Eur. 8.0. Chapter 2.2.40. Near-Infraed Spectrophotometry. Council of Europe, Strasbourg, France, 2014.

(94) USP. USP 40-NF35. Monograph <1119> Near- Infrared Spectroscopy Introduction. 2016.

(95) FDA. Guidance for Industry, Development and Submission of Near Infrared Analytical Procedures Guidance for Industry. U.S. Department of Health and Human Services Food and Drug Administration: Silver Spring, MD, 2015.

Chapter 5

Chemometrics

1. Introduction

According to *Ph. Eur.* General Chapter 5.21 on Chemometric methods applied to analytical data[1], chemometrics is defined as: *"The chemical discipline that uses mathematical and statistical methods to design or select optimal measurement procedures and experiments and, to provide maximum chemical information by analysing chemical data"*.

Chemometric methods consist mainly of multivariate data analysis that result in empirical mathematical models that are subsequently used for the indirect prediction of properties of interest. Hence, the validation of these mathematical models, focusing in the predictive ability, is a fundamental stage and should never be overlooked.[1]

Applications of chemometrics can be used for qualitative or quantitative analysis, which are mainly focused in three purposes: exploratory, classification and regression analysis[2]:

- Exploratory Data Analysis attempts to find the hidden structure in large and complex data sets to gain a qualitative sense of the significant patterns in the data variance. The main methods are cluster analysis and Principal Component Analysis (PCA).
- Classification is the separation of a group of objects into one or more classes based on distinctive features in the objects with the aim to identify new or existing classes. Classification methods can be divided into unsupervised and supervised methods. In the pharmaceutical industry, classification can be used for raw material identification or selection of candidates for drug discovery.[3]
- Regression analysis is the process of developing a model from the available data that estimates the relationships among variables to predict a desired response.

In fact, the three areas have extraordinary applications when using NIR data. Actually, chemometric methods have revolutionized NIR allowing its use in PAT and QbD initiatives.[1] Chemometrics allows to extract relevant information from the NIR spectrum, which is apparently complex with a large number of variables (wavelengths) highly correlated.

Chemometrics gives a broader knowledge of the problem, using fast and robust statistical software to reduce costs and analysis time. It can also be used for process monitoring applications linked to the modelling of batch process data and multivariate statistical process control tools.[4,5]

In this thesis, chemometrics has been applied in two experimental works. On one hand, it was used to develop empirical non-destructive quantitative NIR models for the determination of RMC in pharmaceutical freeze-dried products. On the other hand, it was also used for the DoE and modelling for the freeze-drying process design at laboratory scale.

In this sense, this chapter is divided in two sections. Firstly, the principles of the DoE, with special focus in the optimization methods, will be discussed. Secondly, multivariate calibration methods and the different stages for the generation of a quantitative NIR model will be explained.

2. Design of experiments

DoE is a related subject to multivariate analysis, and its main application is the development of rational designs that require minimal number of experiments to extract the maximal relevant information.[6] It is a systematic and rigorous approach to determine the multidimensional relationship between input factors (i.e. process parameters) and responses (i.e. quality attributes).[7]

A classically applied univariate procedure is the one-variable-at-a-time (OVAT) approach, where only one variable at a time is varied and optimized. The OVAT procedure, however, has some disadvantages: interactions between factors are not taken into account, many experiments are needed when the number of factors increases, only a small part of the experimental domain is examined, and it is difficult to find the optimal conditions.[8]

On the other hand, with DoE, several factors can be studied simultaneously at different levels in a predefined number of experiments, which represents a solution to the disadvantages of the OVAT approach. In practical terms, DoE is used for a number of different purposes, including[6]:

- Development or enhancement of new/existing processes, analytical methods and products.
- Optimization of an existing manufacturing process, analytical methods and products quality.
- Screening of important factors.
- Robustness testing of products and processes.

Regarding the applications and the experimental problem, different designs can be used based on three main experimental objectives[5,6,8]:

- Screening: it is used to identify the most influential factors, and to determine the ranges in which these factors should be investigated. Typically, two levels for each factor are defined. It allows to study a large number of factors in a small number of experiments.
- Optimization: it is used to define which combination of important factors will result in optimal operating conditions. It can also predict the response values for all possible combinations of factors within the defined experimental region. It requires more experiments per factor compared to the experiments for screening and factors are examined at least at three levels to estimate variability and to detect potential curvature. The optimal conditions are usually derived from response surfaces build with the design results.
- Robustness testing: it is used to determine the sensitivity of a product or manufacturing process to small changes in the factor settings.

Prior to conducting any experiments, it is important to specify the number of factors and their ranges, the number of responses and the experimental objective. Then, the experimental design can be created and chosen over a variety of potential design families.

For screening purposes, full-factorial designs and fractional factorial designs are traditionally employed, whereas composite designs are more useful for optimization. These are typical examples, but other design families are also defined for both applications. For instance, three-level full factorial designs, Box-Behnken designs, Doehlert designs or Optimal designs can be used alternatively to composite designs to deal with a lot of factors in fewer runs for optimization purposes. Figure 5.1 shows a schematic distribution of the experimental conditions in some common designs.

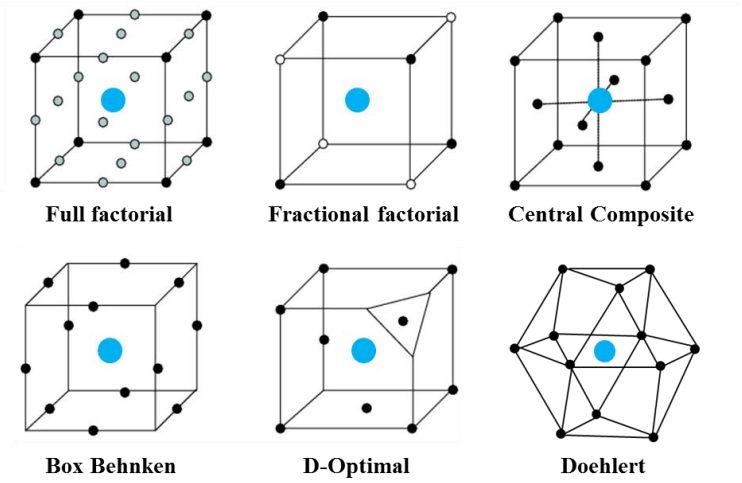

Figure 5.1. Schematic representation of some typical experimental designs. Blue dots represent the centre point where some replicate experiments are performed.

In addition, there are two important considerations when doing DoE: experiments randomization and replicates. In order to eliminate time-dependent effects, experimental runs should be randomized. Moreover, replicate runs are crucial for estimating the underlying variability of the study. It is a common practice to include replicate centre points to assess the repeatability of the instrument response and the sample preparation method.[9]

Usually, when planning DoE, the most important factors are first identified using screening designs. Then, using those factors in an optimization design, the experimental region is defined that presumably contains the optimal point. After the experiments are carried out, results of each experiment are collected and investigated using regression analysis. A polynomial model relating the changes in factors to changes in responses is obtained. Therefore, causal[a] relationship are best established through the use of DoE.[5]

[a] A causal relationship implies that a change in one variable, a factor, caused another variable, a response, to increase or decrease.[5]

It should be noted that a model is an approximation of the reality, which is never 100% perfect. In screening designs, simple linear or interaction polynomial models are sufficient whereas quadratic or more complex polynomial models are needed for optimization.[6]

The fit of the model to the data can be evaluated statistically applying either Analysis of Variance (ANOVA), a residual analysis, or an external validation using a test set. Model evaluation should be conducted to identify significant factors and eliminate the non-significant ones (if desired), and to analyse how they combine in influencing the responses.[6,8]

Afterwards, the model can be interpreted with different graphical representations.[8] As an example, in optimization designs, the obtained model can be visualized by drawing 2D contour plots or 3D response surface plots.

3. Multivariate calibration methods

The ideal situation for quantitative analysis is one in which the sample is analysed with a high precision instrument, which produces a specific signal that is linearly related to the concentration of the analyte. In chemical analysis, such ideal situations are not likely. There is always a certain noise in the measurement, data are affected by chemical and physical interferences, and the instrument does not always respond linearly to changes in the concentration of the analyte. However, certain problems of interference and non-linearity can be solved satisfactorily with multivariable calibration.[10]

In fact, quantitative data analysis mainly consists of calibration, which is the process that establishes the mathematical relationship between a property of interest and the variables measured by an instrument. This mathematical expression is known as the calibration equation or model.[10,11] In the case of NIRS, concentrations or properties are the dependent data, "y", and absorbance spectra the independent data, "x".[1]

Constructing a multivariate calibration model with good predictive ability is a complex, time-consuming process, that requires knowledge not only of the samples, but also of the different types of calibration methods.[11]

3.1. Classification

Calibration methods can be classified in different ways depending on the following characteristics[10,11]:

- *Linear/Non-linear*: linear methods are those that relate the dependent variables with linear functions of the independent variables. When the functions are not of this type, the methods are non-linear.

- *Direct/Indirect*: direct methods are those that the calibration parameters are known directly from the signal of each of the analytes individually. When the calibration parameters are known from the analytical signals of mixtures of the components, the calibration is indirect.
- *Classical/Inverse*: in classical calibration, as stated in Beer–Lambert's law, the independent variable is the concentration and the dependent variable is the analytical signal. In inverse calibration, the concentration is the dependent variable and the analytical signal is the independent variable, allowing an easier mathematical calculation of the concentration.
- *Rigid/Flexible*: rigid methods use a pre-set number of terms in the regression equation, whereas flexible methods use the optimum number established by the method itself.
- *Full-spectrum/variable-compression*: full-spectrum methods use analytical information contained in a large, unrestricted number of variables. In contrast, variable-compression methods reduce an initially large number of variables to a much smaller one without losing relevant analytical information.

The most common calibration methods for spectroscopic data are: Multiple Linear Regression (MLR) which can be further divided into Classical Least Square (CLS) and Inverse Least Square (ILS) regression. Principal Component Regression (PCR) and Partial Least Squares (PLS) regression.

CLS is defined as a rigid method compatible with direct and indirect calibration. On the other hand, ILS is flexible and only accepts indirect calibration. PCR and PLS are both flexible, full-spectrum, variable-compression method compatible with inverse and indirect calibration. A shared characteristic of all abovementioned calibration methods is that they are linear, that is, the final calibration model will be described as follows:

$$y = b_0 + \sum_{k=1}^{K} b_k x_k \qquad \textit{Equation 5.1}$$

where b_0 and b_k are the parameters to determine.

Nevertheless, other methods are applicable to non-linear systems. For instance, artificial neural networks can be applied to both linear and non-linear systems. Essentially, they can be defined as an iterative system of calculation, which tries to reproduce, in a simple way, the system of connections that exists between neurons.[10–12]

In the following sections, MLR, PCR and PLS methods will be explained in more detail.

3.2. Multiple linear regression

The MLR technique is an effective calibration approach when the analytical signal is linearly related to the concentration, spectral noise is low, and the analyte does not interact with other sample components.[13]

MLR involves using more than one variable in order to predict the concentration of an analyte. But, the number of variables used cannot exceed that of the samples, and variables cannot be highly correlated.[9,11]

It consists in finding regression equations in the form:

$$y_i = b_0 + b_1 x_{i1} + b_2 x_{i2} + b_3 x_{i3} + \cdots + b_q x_{iq} = b_0 + \sum b_q x_{iq} + \varepsilon_i \qquad \textit{Equation 5.2}$$

where each value of the dependent variable y_i is expressed as a combination of polynomial terms $b_q x_{iq}$ where q is the number of independent variables x, and b the regression coefficients. Finally, ε corresponds to the random error. Equation 5.2 can be expressed in matrix form[9,11]:

$$\boldsymbol{y = Xb + \varepsilon} \qquad \textit{Equation 5.3}$$

The values of matrix **X** are estimated by minimizing the summation of the squares of the errors using Least Square Regression (LSR).[11] The objective is to find the vector of regression coefficients ***b*** that best minimises the error term **ε**.[1]

Then, depending on the meaning of x and y, two types of MLR methods are distinguished: CLS and ILS.

Note: From now on, the calculations of multivariate calibration methods will be explained in spectroscopic terms.

3.2.1. Classical least squares

In CLS, y is the absorbance and x the concentration of each individual component. So, CLS assumes that the model error come from the spectroscopic data rather than the concentrations. It also assumes fulfilment of Beer's law by individual component of a mixture throughout the working range and additivity of individual absorbances in the mixture.[10,11]

In this case, the spectrum for any sample is a linear combination of the pure components spectra. The matrix of the pure spectra for the mixture analytes can be calculated directly or indirectly[9,11]:

- Direct: It is obtained by recording the spectra for the pure components in the sample. Therefore, it is assumed that the components contributing to the analytical signal are known, and no interaction between analytes or with the sample matrix should exist.
- Indirect: It is calculated by using mixtures of all the components, using calibration standards of known concentration for the analytes present in the mixture.

Application of CLS requires prior knowledge of the total number of analytes present in the samples, which is very difficult in real life. Therefore, the applicability of CLS for NIRS calibration is limited.[9,11]

3.2.2. Inverse least squares

In ILS, *y* represents the concentration and is expressed as a function of the absorbance, *x,* at different wavelengths. So, it assumes that the error of the model is present in the concentration matrix.

ILS uses the inverse form of Beer's law, and the calibration with ILS is always of the indirect type using samples where the concentration (or other property of interest) has previously been determined by using a reference method.[11]

Mathematically, following the MLR equation, the concentration y_i of an analyte in a sample is expressed as a function of the absorbance intensities x_i at K wavelengths of *M* samples:

$$y_i = b_0 + b_1 x_1 + \cdots + b_{K-1} x_{K-1} + \varepsilon_i \qquad \textit{Equation 5.4}$$

where ε_i is the random error in the measurement. This equation can be expressed in matrix form:

$$\boldsymbol{y} = \boldsymbol{X}\boldsymbol{b} + \boldsymbol{e} \qquad \textit{Equation 5.5}$$

where vector $\boldsymbol{y}$ contains concentrations values, matrix $\boldsymbol{X}$ the spectroscopic data selected for calibration, $\boldsymbol{e}$ is the vector of the random residuals of the concentrations and, $\boldsymbol{b}$ is the unknown vector of regressors.[10,11] Then, the regressors $\widehat{\boldsymbol{b}}$ can be calculated by LSR following Equation 5.6:

$$\widehat{\boldsymbol{b}} = \left(\boldsymbol{X}^T\boldsymbol{X}\right)^{-1}\boldsymbol{X}^T\boldsymbol{y} \qquad \textit{Equation 5.6}$$

Finally, based on vector $\widehat{\boldsymbol{b}}$, the concentration of the analyte for new samples, $\hat{\boldsymbol{y}}$, can be estimated from the sample spectra, $\boldsymbol{X}$, as follows:

$$\hat{\boldsymbol{y}} = \boldsymbol{X}\widehat{\boldsymbol{b}} \qquad \textit{Equation 5.7}$$

In conclusion, ILS has the advantage over CLS that prior knowledge of all components present in the sample is not required to quantify the concentration of the target analytes. For this reason, the ILS method has been widely used as a calibration method for quantitative analyses in NIRS. However, those components not included in the quantitation process should be present in all samples and are implicitly modelled.[11]

The greatest disadvantages of ILS are that it requires using a number of samples exceeding that of variables, the selection of the target variables is not an easy task, and, sometimes, the use of too many variables lead to overfitting problems.

To overcome these issues, variable-compression methods are commonly used because they are more robust, there is no need for careful selection of the target wavelengths and they allow individual analytes in mixtures to be quantified without the need to know the other components.[9–11] The most widely used methods of this category in analytical chemistry for multivariable calibration are: PCR and PLS regression.

3.3. Calibration methods based on variable reduction

PCR and PLS regression use the information contained in the whole spectrum and "compress" it into a small number of variables without losing relevant information. Then, the regression is performed over these new variables and not over the original ones. This avoids the need to select variables. Thus, the whole spectrum can be used, which facilitates the detection of outliers.

These methods also use an orthogonal space for the regression, thereby avoiding problems derived from collinearity between variables. Since both methods are based on PCA, , its mathematical basis will also be explained below although it is not a calibration method.[10,11]

3.3.1. Principal component analysis

To understand how PCA works, one must remember that: large systematic variation in a variable, is attributed to information.[2] This method starts from a data matrix where each row corresponds to the spectrum of a sample, and the columns are the k wavelengths of the spectrum. The spectrum of a sample collected at k wavelengths can be described mathematically as a vector of k coefficients. This vector can be represented by a point in the k-dimension space. Then, for M samples, M points can be represented in the space of K dimensions.[10]

The principle of PCA is to find the directions in the data space that describe the largest variation of the data set. This can be interpreted as finding the linear combinations of the initial variables (wavelengths) that contribute most to make the samples different from each other. These directions are called principal components (PCs) and represent the new coordinate system.

PCs are commonly calculated in a sequential manner via an iterative least-squares process, followed by subtraction of the contribution of each component. This way, the first PC described the greatest source of variation within the data set and the remaining variance is captured by the other PCs sequentially. Then, each subsequent PC contains, in order, less information than the previous one. Therefore, last PCs will be correlated mostly with noise and they can be omitted, resulting in a reduction of the number of variables while keeping the relevant information of the original spectra.[1,14]

In addition, PCs are orthogonal to each other, so they are completely uncorrelated. At the end of this process, the complex table of original data is replaced by a table with fewer dimensions, but still fitting the original data. Hence, PCA is considered a data reduction technique.[1,11,12]

The whole process is shown graphically in Figure 5.2.

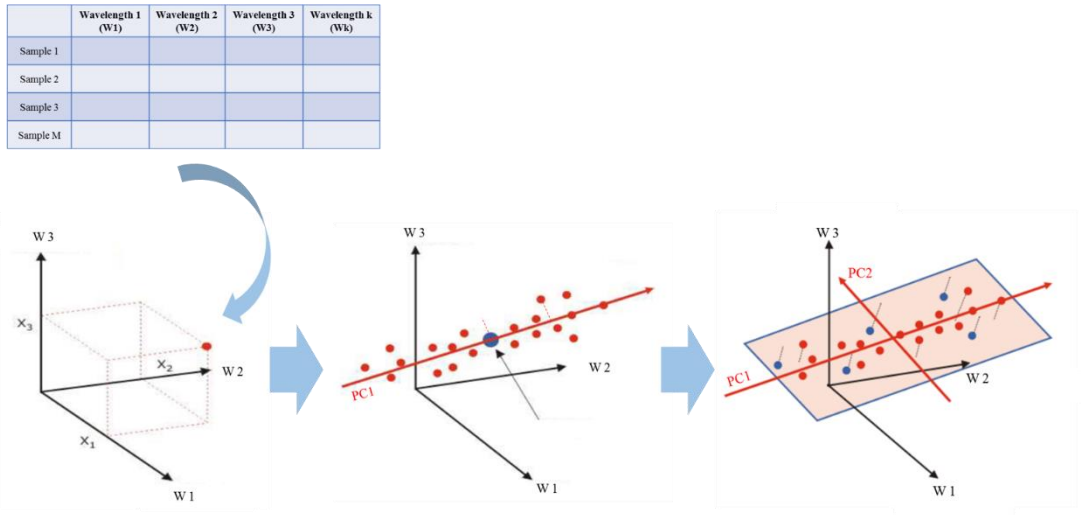

Figure 5.2. Representation of the process for establishing the PCs in PCA. Sourced from reference [2].

In PCA, every original variable has a loading on each PC, which reflects how much the individual variable contributes to that PC. In geometrical terms, a loading is the cosine of the angle between the original variable and the current PC. The loading describes the magnitude (large or small) and the manner (positive or negative) in which the measured variables contribute to the scores.[5]

The projection of the samples in the PCs are the scores.[11] Then, the distance between samples in the scores plot is a measure of similarity/dissimilarity, where similar samples group together.[1]

Mathematically, the PCA model is constructed from the expression:

$$\boldsymbol{X} = \boldsymbol{T}\boldsymbol{P}^{\boldsymbol{T}} + \boldsymbol{E} = \sum_{\boldsymbol{a}=\boldsymbol{1}}^{\boldsymbol{A}} \boldsymbol{t_a p_a^T} + \boldsymbol{E} \qquad \textit{Equation 5.8}$$

where matrix $\boldsymbol{X}$ (KxN) of spectral data is decomposed in the product of two matrices, scores matrix $\boldsymbol{T}$ (NxA) and loadings matrix $\boldsymbol{P}$ (KxA) plus a matrix $\boldsymbol{E}$ (KxN) of residuals. Also, $\mathbf{t_a}$ and $\mathbf{p_a}$ are the vector of scores and the vector of loadings of the a^{th} PC (with a = 1, 2, …A PCs) respectively. Then, multiplying the scores by the loadings of the first A PCs allows the original matrix to be converted into the new matrix $\boldsymbol{X}$ (considering a certain error, $\boldsymbol{E}$).

Different algorithms can be used to obtain matrices $\boldsymbol{T}$ and $\boldsymbol{P}$. The Unscrambler software, which was used in the present thesis, uses Nonlinear Iterative Partial Least Squares (NIPALS) or singular value decomposition. The NIPALS algorithm calculates one principal component at a time and it handles missing values well, whereas the singular value decomposition calculates all of the PCs in one calculation, but does not handle missing values.[15]

PCA is a useful tool for exploratory data analysis. PCA can reveal sample and variable interrelationships, leading to the interpretation of certain sample groupings, sample patterns, detect outliers, etc. It is used in multivariate statistical process control as well. PCA also forms the basis for some classification techniques and regression methods, such as PCR.[1,9]

3.3.2. Principal component regression

Briefly, PCR involves a PCA of the matrix $\boldsymbol{X}$, followed by least squares regression between the scores of the samples and the reference values of the parameter to be modelled. In this case, the scores are used rather than the original variables (wavelengths). Therefore, it represents an improvement over ILS because the score matrix contains the same information as the original matrix, but random noise is removed.[10,11]

As a general concept, PCR and PLS can be used for determining several analytes in a sample, but, because of the calibration complexity, only one analyte is usually determined. However, when analyte concentrations are correlated, it is preferable to determine them simultaneously.

Mathematically, the first step is the decomposition of the matrix $\boldsymbol{X}$ in its PCs as indicated previously in PCA (Section 3.3.1). Once the optimal number of PCs for describing the matrix $\boldsymbol{X}$ has been chosen, the matrix of scores $\boldsymbol{T}$ is represented as follows:

$$\boldsymbol{T} = \boldsymbol{XP} \qquad \textit{Equation 5.9}$$

where $\boldsymbol{P}$ is the loading matrix and $\boldsymbol{X}$ the original data matrix. Matrix $\boldsymbol{Y}$ can be obtained by regressing $\boldsymbol{Y}$ against $\boldsymbol{T}$:

$$\boldsymbol{Y} = \boldsymbol{TB} + \boldsymbol{E} \qquad \textit{Equation 5.10}$$

where $\boldsymbol{B}$ is the matrix of regressors, and it is found by least squares in a way analogous to that used in ILS, knowing the values of $\boldsymbol{Y}$ in the calibration and using the scores matrix $\boldsymbol{T}$:

$$\widehat{\boldsymbol{B}} = \left(\boldsymbol{T}^{\boldsymbol{T}}\boldsymbol{T}\right)^{-1}\boldsymbol{T}^{\boldsymbol{T}}\boldsymbol{Y} \qquad \textit{Equation 5.11}$$

Once the correct model has been established, new set of samples can be predicted from its spectra. The scores of these new samples are calculated by means of the matrix of loadings with A optimal PCs (following the Equation 5.9). Finally, the regressor matrix $\widehat{\boldsymbol{B}}$, together with the scores of these new samples, $\boldsymbol{T}^*$, are used to calculate the corresponding $\widehat{\boldsymbol{Y}}$ [11]:

$$\widehat{\boldsymbol{Y}} = \boldsymbol{T}^*\widehat{\boldsymbol{B}} \qquad \textit{Equation 5.12}$$

The principal weakness of PCR is that it decomposes $\boldsymbol{X}$ and $\boldsymbol{Y}$ matrices independently. Consequently, this approach may take into account variations in **X**-data that are not necessarily relevant for an optimal regression with **Y**-data.[1] This issue is solved using PLS regression.

3.3.3. Partial least squares regression

PLS regression is the most popular algorithm for constructing predictive models when the factors are many, and highly collinear.[1]

PLS compresses data in such a way that the most variance in both matrices, $\boldsymbol{X}$ and $\boldsymbol{Y}$, is explained obtaining new variables called latent variables or factors. Then, compared to PCR, the first PLS factors contain the information that is most relevant for the prediction of the y-values of unknown samples. This way, PLS reduces the potential impact of large and irrelevant variations in $\boldsymbol{X}$ during calibration.[1,10,11]

In PLS, each factor is obtained by maximizing the covariance between $\boldsymbol{Y}$ and every possible linear function of $\boldsymbol{X}$.[11] PLS factors are computed using a sequential algorithm. The first PLS factor is the direction that explains the larger amount of variance in $\boldsymbol{X}$ which is directly related with variance in $\boldsymbol{Y}$. Then, the second PLS factor is orthogonal to the first and has maximal residual covariance. After that, the calculation of the subsequent factors is performed with the same procedure.[14,16]

Mathematically, each matrix, **X** and **Y**, is resolved into a combination of A factors (where A<K, being K the number of original variables of the matrix **X**), following Equation 5.8 and 5.13 [11]:

$$\boldsymbol{X} = \boldsymbol{T}\boldsymbol{P}^{\boldsymbol{T}} + \boldsymbol{E} = \sum_{\boldsymbol{a}=\boldsymbol{1}}^{\boldsymbol{A}} \boldsymbol{t}_{\boldsymbol{a}}\boldsymbol{p}_{\boldsymbol{a}}^{\boldsymbol{T}} + \boldsymbol{E} \qquad \textit{Equation 5.8}$$

$$\boldsymbol{Y} = \boldsymbol{U}\boldsymbol{Q}^{\boldsymbol{T}} + \boldsymbol{E} = \sum_{\boldsymbol{a}=\boldsymbol{1}}^{\boldsymbol{A}} \boldsymbol{u}_{\boldsymbol{a}}\boldsymbol{q}_{\boldsymbol{a}}^{\boldsymbol{T}} + \boldsymbol{F} \qquad \textit{Equation 5.13}$$

where, for M samples, A factors, K original variables and P analytes, matrices $\boldsymbol{T}$ and $\boldsymbol{U}$ of MxA dimensions are the scores matrices for blocks $\boldsymbol{X}$ and $\boldsymbol{Y}$, respectively; matrices $\boldsymbol{P}^{\boldsymbol{T}}$ (AxK) and $\boldsymbol{Q}^{\boldsymbol{T}}$ (AxP) are the loadings matrices for blocks $\boldsymbol{X}$ and $\boldsymbol{Y}$, respectively; and $\boldsymbol{E}$ and $\boldsymbol{F}$ are the residuals matrices for blocks $\boldsymbol{X}$ and $\boldsymbol{Y}$, respectively.[11]

While $\boldsymbol{Y}$ -matrix is decomposed into the loadings and scores matrices, the decomposition of $\boldsymbol{X}$-matrix produces not only the loadings and scores matrices,but also a loading weights matrix $\boldsymbol{W}$ which represents the relationship between $\boldsymbol{X}$ and $\boldsymbol{Y}$.[1]

In fact, matrix $\boldsymbol{W}$ gives information about how the X-variables combine to form the scores **t**. In addition, matrix $\boldsymbol{W}$ is used, together with loading matrices $\boldsymbol{P}$ and $\boldsymbol{Q}$ (of $\boldsymbol{X}$ and $\boldsymbol{Y}$ respectively) to estimate the matrix of regression coefficients $\widehat{\boldsymbol{B}}$ [11]:

$$\widehat{\boldsymbol{B}} = \boldsymbol{W}\left(\boldsymbol{P}^{\boldsymbol{T}}\boldsymbol{W}\right)^{-\boldsymbol{1}}\boldsymbol{Q}^{\boldsymbol{T}} \qquad \textit{Equation 5.14}$$

Once the calibration model is established, it is possible to predict the concentration of a new set of samples. Thus, if the spectrum of a sample is given by the vector $\boldsymbol{x_i}$, the concentrations of the analytes $\boldsymbol{y_i}$ can be determined by the following expression:

$$\hat{y}_i = x_i^T \hat{B} \qquad \textit{Equation 5.15}$$

where the matrix of regressors $\hat{\boldsymbol{B}}$ allows for prediction without the need to decompose its spectrum into scores and loadings matrices.[10]

As stated above, PLS can be used to determine one or several analytes simultaneously. These procedures are usually differentiated by PLS1 and PLS2, respectively.

4. Stages of the calibration process

The mathematical basis of the most common calibration methods has been explained in the above sections. This section focuses on the whole process of developing a calibration model for routine use in the pharmaceutical industry. Particularly, this section will be explained following the example of the development of a calibration model using NIR data for the quantitative determination of a property of interest (such as concentration of an analyte), which is contemplated in specific guidelines of the EMA[17] and the FDA[18]. Then, according to these guidelines, the construction of NIRS model is a step-like process represented in Figure 5.3.

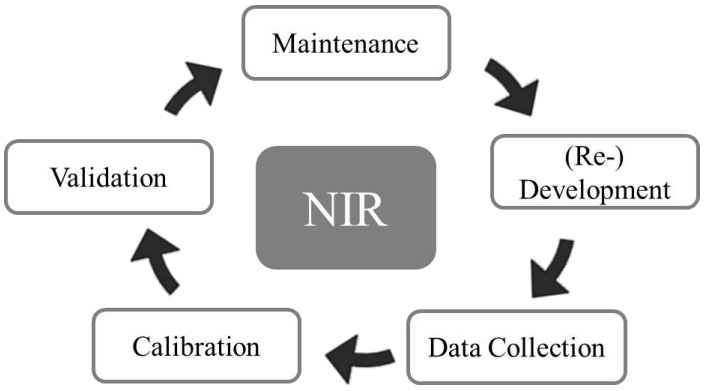

Figure 5.3. NIRS model lifecycle. Sourced from reference [17].

Briefly, the process of obtaining a robust NIRS model starts with the specification of the property of interest (or analyte) with the corresponding concentration range(s). The next step consists in the selection of a representative set of calibration samples followed by the measurement of the spectra, and the determination of the property to be predicted using a reference method.

Then, the spectral data are pre-treated to remove the variation that is detrimental to model performance, thus enhancing the chemical signal, and improving model predictions and interpretability. After that, the calibration model is constructed, and properly validated. When the predictive ability of the model is

satisfactory, the model is applied to predict unknown samples. Finally, an adequate maintenance plan should be designed to guarantee the correct performance of the model over time.[5,11] In the following subsections, each phase of the generation of a NIRS model depicted in Figure 5.3 is explained in detail.

4.1. Development

According to EMA guideline[17], the development phase includes; the definition of the scope of NIRS procedure and the description of NIRS method. It is also recommended to study the feasibility of using NIRS for the intended purpose, which could include a study of the elements affecting the spectral response, the effects of sample handling and preparation, investigations into specificity and matrix interference, and the verification of instrument performance, among others.

An appropriate form to initiate a feasibility study is to undertake a comprehensive assessment, according to the principles given in ICH Q9 [19], of those risks that may adversely affect the performance of the NIRS procedure in delivering valid results. For instance, the environment in which measurement takes place; optical quality of the glassware, sample optical properties, temperature, thickness, polymorphism, the age of the samples, particle size, time of measurement, among others. The final aim is to get as much knowledge as possible about the NIRS instrument, the NIRS method and the samples under study, to obtain a model that fits the intended purpose.[17]

4.2. Data selection and collection

This phase includes the preparation of samples, the selection of calibration and validation sets, the spectral acquisition of the samples, and the analysis by the reference method.[17]

Samples are usually split into three subsets[11,17]:

1) A calibration set for constructing the calibration model.
2) A calibration test set for internal validation and optimization of the model. However, when few samples are available, cross-validation techniques may be applied instead, by using statistical resampling techniques within the calibration set of samples.
3) An independent validation set for external validation of the model. It challenges the calibration model to obtain information on its predictive ability.

4.2.1. Selection of samples for each subset

There are few basic requirements for the selection of the calibration set of samples: samples in which the property to be determined is known, they should contain all possible sources of physical and chemical variability present in the samples to be subsequently predicted, in both spectra and property of interest. They should be representative of the production process and, if feasible, exhibit values of the property of interest uniformly spanning its potential range of variation.[11,17,18]

When needed, development and pilot scale batches can be used to expand the narrow range of production samples. Such samples should be prepared using the same commercial manufacturing procedure, i.e. same composition, process and raw material quality attributes.[13,18]

However, constructing calibration sets containing all potential sources of variability in the samples to be predicted is usually difficult. This topic has been extensively discussed in the literature. If feasible, it is recommended to include production samples in the calibration set. Besides, the inter-batch variability should be considered as well. For this reason, it is recommendable to add different batches in all sample sets. Nevertheless, when it is not possible, other strategies has been developed to introduce the variability of production samples in the calibration set.

Blanco et al.[20] developed a methodology for preparing calibration samples in the laboratory incorporating the intrinsic variability of the production process. This method allows to obtain more simple models of acceptable predictive ability to be constructed without the need for production samples. Furthermore, Blanco et al.[21] and Cárdenas et al.[22] developed another strategy to incorporate all sources of variability in production samples into the calibration set. The strategy consisted in the calculation of a virtual spectrum called *process spectrum*. Then, this spectrum is mathematically added to a calibration set prepared in the laboratory to account for production samples variability.

One simple method for selecting samples for calibration is based on the spectral variability observed in a scatter plot from a PCA applied to the whole samples set.[23] Those samples located in the extremes and the middle of the score maps should be included in the calibration set. In addition, it should be checked that those samples uniformly cover the range spanned by the quantity to be determined. This method is effective when the first two or three PCs contain a high proportion of the total variance. Nevertheless, a great number of alternative chemometric algorithms are also available for selecting calibration samples in an efficient manner.[11]

Regarding the calibration test set, it should cover but not exceed the range of variations in the calibration set, in order to present a meaningful challenge to the calibration. The calibration test set samples may be used to optimize the calibration model and progress towards the prediction of an independent validation set for external validation of the model.[5,24] The external independent test set may be composed by one or more external batches of the same population of samples used for calibration. It is recommended that the size of the independent test set should be in the order of 20-40 per cent of the samples used for the calibration model.[1]

4.2.2. Reference methods and spectra acquisition

First of all, spectra of all samples sets are collected. Spectra acquisition is done first when the reference method is destructive. Replicate measurements are recommended to account for the variability in the sample preparation procedure and sample heterogeneity.

Then, those samples are analysed by the reference analytical method, to correlate the spectral information with the response determined by the reference method. Therefore, the reference method should be validated properly and the Standard Error of the Laboratory (SEL) should be known.[17] It is important to remark that accurate reference results are required to obtain an accurate model.

4.3. Calibration

Following acquisition of spectra and reference data measurement, the calibration model should be developed. This phase includes: data pre-treatment, NIR model construction and assessment.

4.3.1. Spectral pre-treatments

In reflectance measurements, the diffuse reflection component is due to absorption and scattering processes. Scattering is the principal cause of undesired system variations in spectra. Scattering depends fundamentally in the particle size, shape and distribution. It has a multiplicative effect in the sample spectra, and other additives effects like baseline shifts and non-linearities.[25,26]

Along with random noise, which could be produced by imperfections of analytical instruments, they can account for much of the undesired variation among samples, which could be detrimental for the model when the objective is to quantitatively determine a component.[27]

This problem could be reduced by applying spectral pre-treatments before model construction. The objective is to remove this unwanted variation without excluding or altering chemically relevant variation. Actually, mathematical pre-treatments are designed to compensate for these non-linear relationships, and, thus, to improve the linear relationship between the spectral signals and analyte concentrations.[28]

Commonly used pre-processing methods for spectral data include scatter correction methods, for example, first- and second-order derivatives, Multiplicative Signal Correction (MSC), and Standard Normal Variate (SNV) transformation. These methods do not require a response variable in the pre-processing step, which is a prerequisite when, for example, Orthogonal Signal Correction (OSC) methods are applied.[29]

The pre-treatments can also be classified in those applied to individual spectra (derivative spectra, SNV, MSC) and those applied to all selected samples (mean-centring, autoscaling).

The selection of the pre-treatment is mostly driven by parameters such as type of data, instrument or sample, the purpose of the model and user experience. The best choice should be chosen in an empirical manner, using a trial-and error approach, which is a major disadvantage.[11]

Derivatives and SNV, the two most used pre-treatments in this thesis, are explained below.

Derivatives

The first derivative spectrum is the slope of the tangential straight line at each point of the original spectrum. However, the second derivative spectrum is a measure of the curvature at each point on the original spectrum.[23]

Derivatives can serve for a dual purpose: to remove constant offset and slope variations in spectra, and to improve the resolution of overlapped spectral features.[9] The first derivative allows the removal of constant terms at all wavelengths (baseline offsets). The second derivative eliminates the terms that vary linearly with the wavelength (slope variations).[11,28]

A problem with derivatives is that it may reduce the signal and increase the noise, thus producing very noisy spectra (more prominently when the degree of the derivative increases). Hence, higher order derivatives are not recommended. Realizing this risk Savitzky-Golay (SG) proposed an improvement based on a smoothing approach.[5,28]

The SG algorithm[30], usually involves smoothing data by fitting a polynomial expression to the data within a moving window. This entails previously defining the number of points to be included in the window, and the order of the polynomial function, and that of the derivative to be obtained. As a consequence of this procedure, some points at each end of the spectra will be lost.[9,11]

Normally, using 7–11 points for smoothing and a second-degree polynomial for the fitting procedure is sufficient for typical high-resolution spectral data.[28]

SNV

The basic equation for SNV correction was introduced by Barnes et al. in 1989 [31]. It is applied to minimize baseline offsets and multiplicative scattering effects[28,29], giving very similar results with MSC.[32] Basically, SNV consists in autoscaling each spectrum. First, the spectrum to be corrected (x_i) is centered by subtracting the mean value of the absorbance of the spectrum ($\bar{x}_i$) from the absorbance values obtained at each wavelength j. Subsequently, the centered spectrum is scaled by dividing it by the standard deviation (s_i) of the absorbance values.

$$x_i^{SNV} = \frac{x_{ij} - \bar{x}_i}{s_i} \qquad \textbf{\textit{Equation 5.16}}$$

SNV corrected spectra have an average value of zero and a variance equal to one. A common scale for all spectra is obtained, which facilitates the comparison of spectral differences.[9,10]

Furthermore, it is common practice to combine derivatives with SNV in spectroscopic data. Fearn[33] showed that the order of the combination matters. The author demonstrated that doing the SNV first, less of the scattering effect is removed. Finally, Figure 5.4 shows an example of the application of derivatives and SNV pre-processing techniques on a set of NIR absorbance spectra.

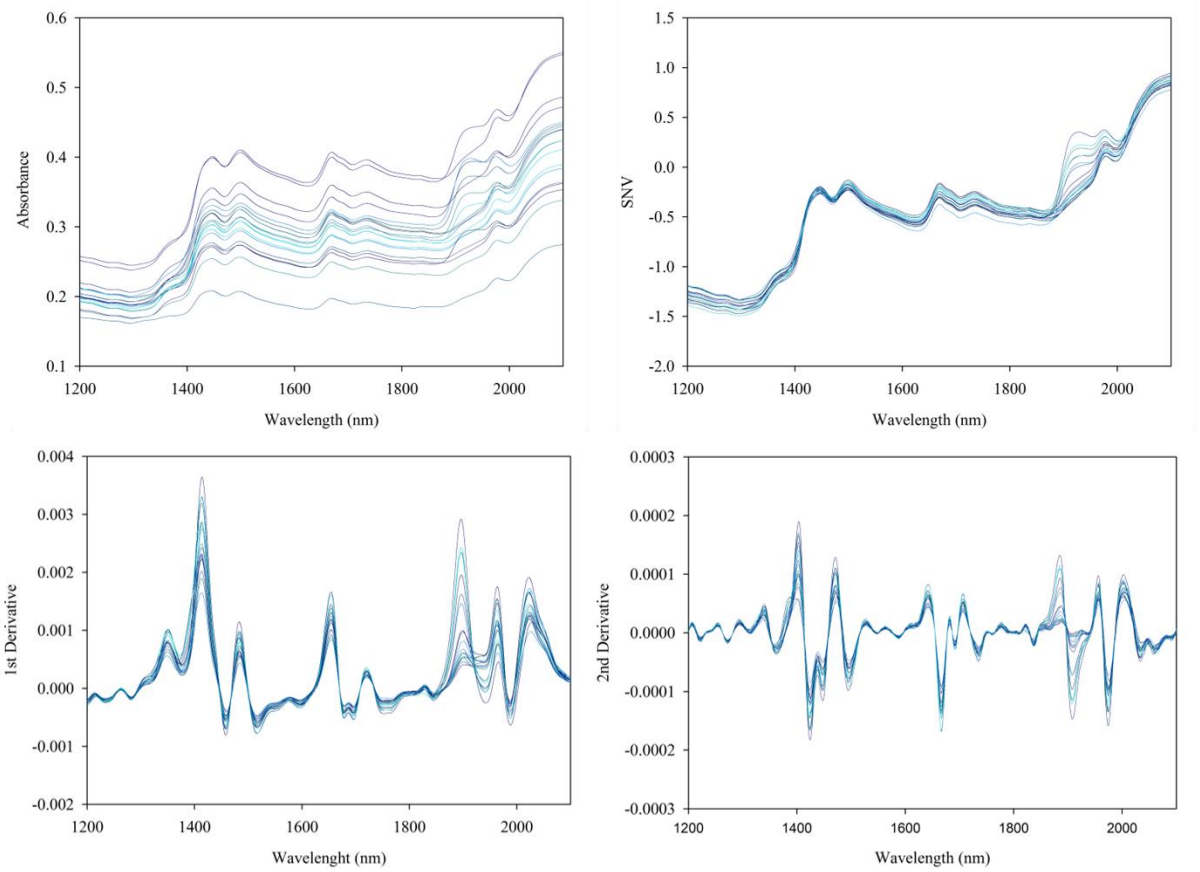

Figure 5.4. Examples of common pretreatments on a set of NIR reflectance spectra (n=18). The figure displays: raw spectra (upper left), SNV corrected spectra (upper right), SG 1st derivative preprocessing (lower left) and spectra after 2nd derivative preprocessing (lower right). Derivatives were performed using a window width of 11 points and the polynomial order was 2.

4.3.2. Selection and evaluation the calibration model

After the pre-treatment(s) of choice has been applied, the next step is the construction of the calibration model. As stated above, a variety of mathematical algorithms are available for constructing models, and a wide range of statistical techniques exist for their assessment and optimization.

Two examples of such statistical expressions are the Standard Error of Calibration (SEC) and the coefficient of determination (R^2).[1,11] It is important to emphasize that they are calculated with the calibration sample set and, thus, they do not provide any information about the predictive ability of the model.

SEC has the same units as the dependent variables and reflects the degree of modelling error, i.e. the goodness of fit of the calibration regression equation. Its general expression is:

$$SEC = \sqrt{\frac{\sum_{i=1}^{m}\left(y_{cal,i} - y_{teo,i}\right)^2}{m-k}} \qquad \textit{Equation 5.17}$$

where m is the number of samples used in the calibration, k the number of PCs/factors, including the independent term that are used in the model equation; y_{cal} and y_{teo} are, respectively, the calculated and theoretical concentrations for each of the samples.

The R^2 is a measure of how much of the original variation in the data is described by the model. The R^2 is calculated by the ratio between explained sum of squares and the total sum of squares. It is a dimensionless measure and it can have values between 0 and 1. As the value of R^2 increases, the X-data becomes an increasingly more accurate predictor of the reference values.[1] With regards to the regression analysis, a slope, bias and intercept not statistically different from 1, 0 and 0 respectively, are expected in good calibration models as well.

To assess the predictive ability of the model, a measure of the uncertainty of future predictions, the Predicted Residual Error of Sum of Squares (PRESS) or its mean value (MSE) are commonly used. However, some authors use the square root of MSE, which is called the Root Mean Square Error (RMSE) or the Relative Square Error (RSE).

$$PRESS = \sum_{i=1}^{n} (\hat{y}_i - y_i)^2 \qquad \textit{Equation 5.18}$$

$$MSE = \frac{\sum_{i=1}^{n} (\hat{y}_i - y_i)^2}{n} \qquad \textit{Equation 5.19}$$

$$RMSE = \sqrt{\frac{\sum_{i=1}^{n} (\hat{y}_i - y_i)^2}{n}} \qquad \textit{Equation 5.20}$$

$$RSE = \sqrt{\frac{\sum_{i=1}^{n} (\hat{y}_i - y_i)^2}{\sum_{i=1}^{n} (y_i^2)}} \qquad \textit{Equation 5.21}$$

where n is the number of samples, y_i is the i_{th} concentration and the $\hat{y}_i$ estimated concentration. The evaluation of the predictive ability of the model can be performed with a set of samples different from the calibration set or using cross-validation techniques. Therefore, depending on the sample set, the above statistics can be defined as:

- MSECV/RMSECV/RSECV: in cross-validation.
- MSEP/RMSEP/RSEP: in calibration test set or external validation set.

Cross-validation is used when the number of samples available is relatively small. This procedure involves sequentially removing samples from the data set, calculating a model with the remaining samples, and applying that model to the samples set aside to obtain a prediction. Finally, this prediction provides an indication on how robust the model is to predict new samples. When only one sample is left

out to construct the model, the process is known as full cross-validation or leave-one-out. However, when the calibration set is split into several blocks or segments, the process is called segmented cross-validation. There are theoretical and practical results indicating that, if the model changes considerably when 10% of the objects is taken out it means the model is not stable.[16]

4.3.3. Selection of the spectral range and number of factors

Selection of the spectral range is usually performed by trial-and-error until an adequate predictive ability is achieved. Nevertheless, several algorithms are also described in the literature.[11]

The selection of the number of factors is a compromise between simplicity, robustness and goodness of fit of the model.[1] Selecting too few factors will inadequately explain variability in the calibration data set, which will lead to underfitting of the model and, hence, to large prediction errors. However, too many factors will cause overfitting and instability in the resulting calibration, increased noise, and large errors as well.[11,18]

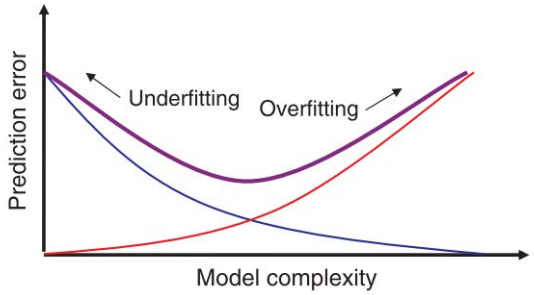

Figure 5.5. Description of model complexity vs predictive error. Relative to model complexity, bias (blue), variance (red) and trade off (violet). Adapted from reference[23].

The optimal number of factors can be selected in various ways. The simplest way is to represent the explained variance as a function of the number of PCs/factors and choose the minimum number for which a significant improvement is not found.[2]

Another simple way involves plotting RMSECV/P or PRESS against the number of factors and choosing the one corresponding to the minimum of the curve. This way, it is assumed that the error decreases with increasing the number of factors up to a point where further factors contribute mainly to noise, and RMSECV/P or PRESS rise by effect of overfitting.[10,11,16]

Because of the relative small number of samples used for calibration, it has been recommended not to use the absolute minimum but the number of factors in which PRESS or RMSECV/P is not significantly different from the minimum value.[10,11] To do this, an F test is applied with a significance level $\alpha = 0.25$ (criterion of Haaland and Thomas[34]).

4.3.4. Outliers

An outlier can be defined as any observation not fitting the model. Outliers could be samples that do not belong to the population, or they can be obtained by instrument malfunction, reference method failure or transcription error.[23] In general, three different types of outliers can be distinguished when developing a multivariate calibration model[9,11]:

- X-sample outliers or spectral outlier: samples for which the spectra depart markedly from those for the others.
- Y-sample outliers or prediction outlier: samples for which the model provides a target value considerably different from the actual value.
- X-variable outliers: based on the behaviour of a single x variable relative to the other x variables. Spectral variables that behave markedly differently from the others.

Outliers can be detected by using a number of available methods.[23] For example, PCA method can be used to detect X-sample and Y-variable outliers. More specifically, the Hotelling T^2 statistic can be used to assess objects that are 'extreme' within the model space. Besides, PLS or PCR can be effective for detecting Y-sample outliers, through the use of the y residuals.[9]

It should be noted that the word "outlier" is not synonymous with "incorrect".[9] For example, it does not necessarily indicate an OOS result of the batch. However, one should always ascertain whether an outlier is the result of an actual phenomenon or an artefact that appeared while constructing the calibration model.[17] In fact, identifying and suppressing outliers is of utmost importance since their presence can adversely affect the robustness and predictive ability of the resulting model.[11]

4.4. Validation

Once the calibration model has been developed, its ability to predict unknown samples not used to construct the model should be assessed.[1]

Model validation can be typically done by internal validation (or cross-validation), described in Section 4.3.2, or by external validation. In the latter case, the model is used to generate predictions for a new independent data set not used during model development. In the external validation, the predicted y-values are then compared to the reference y-values, resulting in a prediction residual that can be used to compute PRESS/SEP/MSEP/RMSEP/RSEP (statistics defined in Section 4.3.2).

According to EMA NIR guideline[17], validation must comply with data requirements for Module 3.2.P.5.3. of the CTD and the guidance given in ICH Q2(R1)[35]. Hence, the following parameters should be determined for quantitative models: specificity, linearity, range, accuracy, precision and robustness. It is also recommendable to calculate the detection and quantitation limit. Table 5.1 describes each of these parameters using the ICH terminology.

Table 5.1. ICH Q2(R1) definitions of the validation parameters for quantitate methods.

Parameter	ICH Q2(R1) Definition
Specificity	The ability to assess unequivocally the analyte in the presence of components which may be expected to be present.
Linearity	The ability to obtain test results which are directly proportional to the concentration of analyte in the sample within a given range.
Range	The interval between the upper and lower concentration of analyte in the sample (including these concentrations), for which it has been demonstrated that the analytical procedure has a suitable level of precision, accuracy and linearity.
Accuracy	Expresses the closeness of agreement between the value which is accepted either as a conventional true value, or an accepted reference value and the value found.
Precision	Expresses the closeness of agreement between a series of measurements obtained from multiple sampling of the same homogeneous sample under the prescribed conditions. Precision may be considered at three levels: repeatability, intermediate precision and reproducibility. Repeatability expresses the precision under the same operating conditions (same measurement procedure, same operators, same measuring system) and the same laboratory over a short interval of time. Intermediate precision expresses the precision within-laboratories variations: different days, different analysts, different equipment, etc. Reproducibility expresses the precision between laboratories.
Detection limit	The lowest amount of analyte in a sample which can be detected but not necessarily quantitated as an exact value.
Quantitation limit	The lowest amount of analyte in a sample which can be quantitatively determined with suitable precision and accuracy.
Robustness	A measure of the analytical method capacity to remain unaffected by small, but deliberate variations in method parameters and provides an indication of its reliability during normal usage.

Different approaches to validate NIR quantitative models are available in the literature. Nevertheless, the applied validation principles are not different from conventional analytical methods.

First, the published Guidelines for the Development and Validation of NIR Spectroscopic Methods in the Pharmaceutical Industry[36], written by the NIR group of the UK Pharmaceutical Analytical Sciences Group, cover the specific NIR requirements whilst remaining complementary to ICH Q2(R1)[35].

In addition, there are a great number of papers about validation analysis as well. Important research on this topic was performed at the end of the 90s by the Applied Chemometrics Group, from the Universitat Autònoma de Barcelona, who reported on the development and validation of NIR methods for the analysis of pharmaceutical preparations.[37,38] Later, Moffat et al.[39] presented an excellent paper on how best to meet the ICH guidelines on validation. Furthermore, in 2012, De Bleye[40] published a comprehensive overview of the methodologies applied to assess the validity of quantitative NIRS methods for pharmaceutical applications.

4.5. Routine analyses

Finally, the validated NIR model should be used for routine analyses, to predict the property of interest in new samples. New samples will be predicted by interpolation within the model limits, as no accurate prediction can be ensured by extrapolation.[11]

4.6. Maintenance of chemometric models

Chemometric methods should be reassessed regularly to demonstrate a consistent level of acceptable performance over a long period of use.[1] A possible assessment is analysing some samples with the reference method from time to time in order to check whether it continues to produce accurate and precise results. In addition, recalibration of the model is required if model range needs to be expanded.

Likewise, the instrument should be monitored over time to detect any alteration in its response or performance. Instrument performance can be evaluated before its use (daily verification check) and throughout a defined period of time following an ongoing monitoring plan, as stated in the *Ph. Eur.* 2.2.40 Chapter on NIRS[41]. Nevertheless, the extent of the maintenance required, including the choice of the necessary parameters, should be based on risk analysis, considering the analytical method used and the chemometric model.

In addition to this periodical task, an assessment should be carried out for critical parameters when changes are made to application conditions of the chemometric model (process, sample sources, measurement conditions, analytical equipment, software, etc.).[1,11] Extensions outside of the approved scope of the NIRS procedure are subject to variation application. For quantitative analysis, extensions of the scope of NIRS procedures include for example, changes of ranges and/or specification limits. Variation applications for such changes require evidence of recalibration and validation of the NIRS model.[17]

5. Conclusions

Chemometrics is an interdisciplinary field that involves multivariate statistics, mathematical modelling, computer science, and analytical chemistry. This chapter is divided in two areas in which chemometrics are applied: DoE and multivariate calibration models.

DoE is a systematic approach that aims to maximise the amount of information extracted from a set of experimental runs while minimizing the number of runs required in achieving that goal. This approach allows experimenters to study simultaneously the impact of several factors in the product quality, and to fully explore relationships between factors in the experimental design space.

Three calibrations methods for the development of quantitative models have been described in this chapter: MLR, PCR and PLS. The most important problems arising in calibration are: non-selectivity,

collinearity, non-linearity, calibration data selection and outlier detection. By using multivariate calibration, LSR algorithms, pre-treatments and statistical tests it is possible to overcome all those problems.

In addition, NIR spectrum not only includes chemical information of the sample components. Therefore, the use of mathematical pre-treatments and multivariate calibration techniques is needed to extract the relevant chemical/physical information and obtain suitable quantitative models.

Essentially, the procedure for quantification using multivariate calibration involves the following steps: (a) selecting a representative sample set; (b) acquiring the analytical signals and obtaining the reference values; (c) mathematical processing of the signals; (d) selecting the model that relates the property to be determined and the signals; (e) detection and elimination of outliers and (f) validating the model. A complete validation of the model is necessary to assure its quality before routine application.[11]

Finally, it is important to keep in mind that a regression model is only as good as the quality of the data used.

References

(1) European Pharmacopoeia. Ph. Eur. 8.7. Chapter 5.21. Chemometric Methods Applied to Analytical Data. Council of Europe, Strasbourg, France, 2016.

(2) CAMO Process AS. The Unscrambler: Tutorials. CAMO Process AS 2006.

(3) Miró Vera, A. Y.; Alcalà Bernàrdez, M. Near-Infrared Spectroscopy in Identification of Pharmaceutical Raw Materials. *Encycl. Anal. Chem.* **2017**, 1–19.

(4) Westad, F.; Gidskehaug, L.; Swarbrick, B.; Flåten, G. R. Assumption Free Modeling and Monitoring of Batch Processes. *Chemom. Intell. Lab. Syst.* **2015**, *149*, 66–72.

(5) Eriksson, L.; Byrne, T.; Johansson, E.; Trygg, J.; Vikström, C. *Multi- and Megavariate Data Analysis Basic Principles and Applications*, 3rd ed.; MKS Umetric AB: Malmö, Sweden, 2013.

(6) Eriksson, L.; Johansson, E.; Kettaneh-Wold, N.; Wikström, C.; Wold, S. *Design of Experiments: Principles and Applications*, 3rd ed.; MKS Umetrics AB: Umea, Sweden, 2008.

(7) Altan, S.; Bergum, J.; Pfahler, L.; Senderak, E.; Sethuraman, S.; Vukovinsky, K. E. Statistical Considerations in Design Space Development. Part I of III. *Pharm. Technol.* **2010**, 62–66.

(8) Dejaegher, B.; Heyden, Y. Vander. Experimental Designs and Their Recent Advances in Set-Up, Data Interpretation, and Analytical Applications. *J. Pharm. Biomed. Anal.* **2011**, *56*, 141–158.

(9) Miller, C. E. Chemometrics in Process Analytical (PAT). In *Process Analytical Technology*; Bakeev, K. A., Ed.; John Wiley & Sons, Ltd: Chichester, UK, 2010; pp 353–438.

(10) Maspoch, S.; Coello, J. Calibración Multivariable. In *Temas Avanzados de Quimiometría*; Blanco, M., Cerdà, V., Eds.; Universitat de les Illes Balears: Palma, Illes Balears, 2007; pp 239–286.

(11) Blanco, M.; Alcalà, M. Multivariate Calibration for Quantitative Analysis. In *Infrared Spectroscopy for Food Quality Analysis and Control*; Sun, D.-W., Ed.; Academic Press: USA, 2009; pp 51–82.

(12) Miller, J. N.; Miller, J. C. *Statistics and Chemometrics for Analytical Chemistry*, 6th ed.; Pearson Education Limited: Harlow, England, 2010.

(13) Blanco, M.; Coello, J.; Iturriaga, H.; Maspoch, S.; De La Pezuela, C. Near-Infrared Spectroscopy in the Pharmaceutical Industry. *Analyst* **1998**, *123*, 135R–150R.

(14) Ferreira, A. P.; Tobyn, M. Multivariate Analysis in the Pharmaceutical Industry: Enabling Process Understanding and Improvement in the PAT and QbD Era. *Pharm. Dev. Technol.* **2015**, *20* (5), 513–527.

(15) Esbensen, K. H.; Geladi, P. Principal Component Analysis: Concept, Geometrical Interpretation, Mathematical Background, Algorithms, History, Practice. *Compr. Chemom.* **2010**, *2*, 211–226.

(16) *Chemometrics in Food Chemistry*; Federico, M., Ed.; Elsevier: Osford, UK, 2013.

(17) EMA. Guideline on the Use of Near Infrared Spectroscopy (NIRS) by the Pharmaceutical Industry and the Data Requirements for New Submissions and Variations. European Medicines Agency; London, UK, 2014.

(18) FDA. Guidance for Industry, Development and Submission of Near Infrared Analytical Procedures Guidance for Industry. U.S. Department of Health and Human Services Food and Drug Administration: Silver Spring, MD, 2015.

(19) ICH. Harmonised Tripartite Guideline Q9 Quality Risk Management. 2011.

(20) Blanco, M. ; Bautista, M. ; Alcalà, M. Preparing Calibration Sets for Use in Pharmaceutical Analysis by NIR Spectroscopy. *J. Pharm. Sci.* **2008**, *97* (3), 1236–1245.

(21) Blanco, M.; Peguero, A. Analysis of Pharmaceuticals by NIR Spectroscopy without a Reference Method. *Trends Anal. Chem.* **2010**, *29* (10), 2010.

(22) Càrdenas, V.; Blanco, M.; Alcalà, M. Strategies for Selecting the Calibration Set in Pharmaceutical Near Infrared Spectroscopy Analysis. A Comparative Study. *J Pharm Innov* **2014**, *9*, 272–281.

(23) Næs, T.; Isaksson, T.; Fearn, T.; Davies, T. *A User-Friendly Guide to Multivariate Calibration and Classification*; NIR publications: Chichester, UK, 2002.

(24) Workman, J. J. NIR Spectroscopy Calibration Basics. In *Handbook of Near-Infrared Analysis*; Burns, D. A., Ciurczak, E. W., Eds.; CRC Press: Boca Raton, 2008; pp 123–150.

(25) Rinnan, Å.; Berg, F. van den; Engelsen, S. B. Review of the Most Common Pre-Processing Techniques for near-Infrared Spectra. *Trends Anal. Chem.* **2009**, *28* (10), 1201–1222.

(26) Bedi, S.; Balabathula, P.; Mandal, B.; Mittal, I.; Bhattacharjee, H. NIR Applications for Lyophilization of Biopharmaceuticals. *Am. Pharm. Rev.* **2012**, 1–7.

(27) Trygg, J.; Gabrielsson, J.; Lundstedt, T. Background Estimation, Denoising, and Preprocessing. *Compr. Chemom.* **2010**, *2*, 1–8.

(28) Rinnan, Å.; Nørgaard, L.; Berg, F. van den; Thygesen, J.; Bro, R.; Engelsen, S. B. Data Pre-Processing. In *Infrared Spectroscopy for Food Quality Analysis and Control*; Sun, D.-W., Ed.; Academic Press: USA, 2009; pp 29–50.

(29) Jonsson, H.; Gabrielsson, J. Evaluation of Preprocessing Methods. *Compr. Chemom.* **2010**, *2*, 199–206.

(30) Savitzky, A.; Golay, M. J. E. Smoothing and Differentiation of Data by Simplified Least Squares Procedures. *Anal. Chem.* **1964**, *36* (8), 1627–1639.

(31) Barnes, R. J.; Dhanoa, M. S.; Lister, S. J. Standard Normal Variate Transformation and De-Trending of Near-Infrared Diffuse Reflectance Spectra. *Appl. Spectrosc.* **1989**, *43* (5), 772–777.

(32) Fearn, T.; Riccioli, C.; Garrido-Varo, A.; Guerrero-Ginel, J. E. On the Geometry of SNV and MSC. *Chemom. Intell. Lab. Syst.* **2009**, *96*, 22–26.

(33) Fearn, T. The Interaction between Standard Normal Variate and Derivatives. *NIR news* **2008**, *19* (7), 16.

(34) Haaland, D. M.; Thomas, E. V. Partial Least-Squares Methods for Spectral Analyses. 1. Relation to Other Quantitative Calibration Methods and the Extraction of Qualitative Information. *Anal. Chem.* **1988**, *60* (11), 1193–1202.

(35) ICH. Harmonised Tripartite Guideline Q2(R1) Validation of Analytical Procedures: Text and Methodology. 2009.

(36) Broad, N.; Graham, P.; Hailey, P.; Hardy, A.; Holland, S.; Hughes, S.; Lee, D.; Prebble, K.; Salton, N.; Warren, P. Guidelines for the Development and Validation of Near-Infrared Spectroscopic Methods in the Pharmaceutical Industry. In *Handbook of Vibrational Spectroscopy*; Chalmers, J. M., Griffiths, P. R., Eds.; John Wiley & Sons Ltd: Chichester, UK, 2002.

(37) Blanco, M.; Coello, J.; Eustaquio, A.; Itturriaga, H.; Maspoch, S. Development and Validation of Methods for the Determination of Miokamycin in Various Pharmaceutical Preparations by Use of near Infrared Reflectance Spectroscopy. *Analyst* **1999**, *124*, 1089–1092.

(38) Blanco, M.; Coello, J.; Eustaquio, A.; Iturriaga, H.; Maspoch, S. Development and Validation of a Method for the Analysis of a Pharmaceutical Preparation by Near-Infrared Diffuse Reflectance Spectroscopy. *J. Pharm. Sci.* **1999**, *88* (5), 551–556.

(39) Moffat, A. C.; Trafford, A. D.; Jee, R. D.; Graham, P. Meeting the International Conference on Harmonisation's Guidelines on Validation of Analytical Procedures: Quantification as Exemplified by a near-Infrared Reflectance Assay of Paracetamol in Intact Tablets. *Analyst* **2000**, *125*, 1341–1351.

(40) De Bleye, C.; Chavez, P.-F.; Mantanus, J.; Marini, R.; Hubert, P.; Rozet, E.; Ziemons, E. Critical Review of near-Infrared Spectroscopic Methods Validations in Pharmaceutical Applications. *J. Pharm. Biomed. Anal.* **2012**, *69*, 125–132.

(41) European Pharmacopoeia. Ph. Eur. 8.0. Chapter 2.2.40. Near-Infrared Spectroscopy. Council of Europe, Strasbourg, France, 2014.

MATERIALS AND METHODS

Chapter 6

Samples, Instrumentation and Analytical Methods

This chapter describes samples, instruments and equipment, analytical methods and software used throughout the development of this PhD thesis.

1. Samples

Two freeze-dried drug products were used during the PhD project: Injectable Freeze-dried Product A and B, named IFDA and IFDB respectively for confidential reasons.

IFDA drug product was used as a model product for two experimental purposes: for freeze-drying cycle development and qualification using a QbD approach, and for the development and validation of quantitative NIRS models for prediction of RMC. However, for IFDB drug product, the purpose was restricted to the development of a freeze-drying cycle at laboratory scale using a QbD approach.

The following subsections describe the characteristics of both products in more detail.

1.1. Injectable freeze-dried product A

This generic pharmaceutical preparation is presented in two strengths, named IFDA 500 mg and IFDA 1 g, in the pharmaceutical form of powder for solution for infusion. It consisted solely of an API with residual amounts of water, no excipients were included in the formulation. It is a generic existing product, already commercialized by RJ.

Physically, the product consisted in a vial that contains the freeze-dried powder to be reconstituted before use (Figure 6.1). The freeze-dried formulation was packed in moulded glass vials (SGD pharma, Germany) of 10 ml capacity for IFDA 500 mg and 20 ml capacity for IFDA 1 g. In both cases, vials were closed with 20 mm grey rubber stoppers (West Pharmaceutical Services, France) and sealed with aluminium capsules with flip-off (West Pharmaceutical Services, Germany). Both strengths differed in terms of volume (6 ml in IFDA 500 mg and 12 ml in IFDA 1 g), body diameter size of the glass vial and total amount of API. However, both strengths have the same concentration (w/v), therefore the same process conditions are used and the only difference is the fill volume.

IFDA vials from laboratory and production batches were used. Laboratory batches were prepared for two reasons: to expand the narrow RMC range of production samples for the development of NIRS calibration models and to execute the experimental runs of the DoE for freeze-drying cycle development.

Laboratory batches were obtained using vials filled with solution manufactured in the production plant or with solution prepared in the laboratory following exactly the same industrial manufacturing procedure. In both cases, vials were freeze-dried using the laboratory freeze-dryer.

The preparation of IFDA bulk solution (either at production plant or at the laboratory) consisted in the following steps: a volume of WFI corresponding to approximately 80-90% of the total batch volume were placed in a vessel. The vessel was equipped with N_2 bubbler, pH meter, thermometer, stirrer and oximeter. Water was cooled at a temperature ≤ 15ºC and degassed with N_2 bubbling until the level of O_2 was ≤ 0.10 ppm. API was added carefully, and constant stirring was applied until complete dissolution. Then, the pH was checked (2.5 – 4.5) and WFI was added up to the desired final volume. During all this process, residual O_2 level and solution temperature were continuously monitored. After that, the solution was filtered (filter pore size 0.2 µm). Filtered solution was collected into a clean vessel and, later, vials were filled with the corresponding volume, for each strength. A weight control was performed at the beginning, middle and end of the filling process. Simultaneously, rubber stoppers were partially inserted into the filled vials. Finally, vials were placed into trays and were loaded on the freeze-dryer shelves.

1.2. Injectable freeze-dried product B

This medicinal product is presented in the IFDB 600 mg strength, and in the pharmaceutical form of powder for solution for injection or infusion. The formulation consisted in 600 mg of API, 600 mg of mannitol and residual amounts of water. In this case, mannitol (Roquette Frères, Lestrem, France) was used as excipient. It is a product under development by the Research & Development (R&D) department of RJ.

The freeze-dried formulation was packed in moulded glass vials of 50 ml capacity (SGD, S.S., France). Vials were closed with 20 mm grey rubber stoppers (West Pharmaceutical Services, France) and sealed with aluminium capsules with flip-off (West Pharmaceutical Services, Germany).

In this case, only laboratory samples were used. IFDB solution was prepared following a laboratory manufacturing batch record and IFDB vials were freeze-dried in the laboratory freeze-dryer.

The preparation of IFDB bulk solution consisted in placing a volume of WFI, corresponding to approximately 75% of the total batch volume, in a vessel. The vessel was equipped with a thermometer and a stirrer. WFI was cooled at a temperature ≤15ºC. Then, mannitol and API (in this order) were added and the solution was maintained under constant stirring until complete dissolution. After, WFI was added up to a volume of 90-95% of the total batch volume. Then, once complete dissolution was observed, pH was adjusted to 6.5 with NaOH 1N. After that, WFI was added up to the desired final volume and pH was checked again (5.5-7.5). Next, solution was filtered (filter pore size 0.2 µm) and collected into a clean vessel. Then, vials were filled with 12 ml solution and pre-stoppered with rubber stoppers. Finally, vials were placed into trays and were loaded on the freeze-dryer shelves.

Figure 6.1. Pictures of two vials of IFDA 1 g drug product (blue caps), IFDA 500 mg drug product (white caps), and IFDB 600 mg drug product (green caps).

2. Equipment, instruments and methods

2.1. Freeze-drying

At laboratory-scale, a Lyobeta20 freeze-dryer (Telstar, Spain) with a sample thief installed on the front door of the freeze-drying chamber was used. The sample thief was used to obtain vials with different RMC at pre-determined time intervals during the primary and secondary drying phases of the freeze-drying cycle. At production-scale, two freeze-dryers were used, Edwards Freeze-dryer 1 and 2 (IMA Life, Italy). Figure 6.2 shows a representation of both types of freeze-dryers.

Figure 6.2. Representation of a Lyobeta20 freeze-dryer (left) and industrial freeze-dryer (right). Lyobeta20 freeze-dryer is a model example which does not contain the sample thief in the front door.

Table 6.1 describes and compares the main characteristics of the three freeze-dryers.

Table 6.1. Comparative table of the main characteristics of the laboratory and industrial freeze-drying equipment.

Parameters	**Lyobeta20**	**Edwards 1**	**Edwards 2**
Number of shelves	3+1	10	14
Total shelves area	0.45 m^2	25.58 m^2	26 m^2
Condenser maximum capacity	30 kg	600 kg	525 kg
Condenser maximum temperature	-80ºC	-75ºC	-75ºC

Parameters	Lyobeta20	Edwards 1	Edwards 2
Shelves temperature range	-60ºC - +80ºC	-75ºC - +80ºC	-55ºC - +80ºC
Pressure monitoring probes	Capacitance (Baratron, MKS Instruments, USA) and a thermal conductivity gauge (Pirani, MKS Instruments, USA)		
Product temperature probes	Thermocouple	Pt100	Pt100

The maximum cooling and heating rate of the three freeze-dryers was 1ºC/min but they performed at approx. 0.5ºC/min (based on the latest qualification). All freeze-dryers were equipped with a stoppering and PC control systems.

2.2. Near infrared spectroscopy

Spectral data were collected using a LabSpe5000 VIS/NIR Benchtop Spectrometer (ASD Inc®, Colorado, USA), coupled with the High Intensity Muglight sampling device that included tungsten quartz halogen light source (spot size: 12 mm). Spectra were acquired in reflectance mode throughout the wavelength range of 350–2500 nm in 1 nm increments. LabSpec5000 is configured with three separate holographic diffraction gratings with three separate detectors: Visible/Near-Infrared (350-1000 nm) 512 element silicon array, Short-Wavelength Infrared 1 (1000-1800 nm) and Short-Wavelength Infrared 2 (1800-2500 nm) InGaAs photodiode. The spectral resolution is 3 nm at 700 nm and 10 nm at 1400 nm and 2100 nm. 32 scans were recorded for each spectrum which were sufficient to obtain a good signal-to-noise ratio. Spectra were recorded with 100 ms per scan. NIR spectrometer was qualified and maintained under cGMP environment. A daily NIRS check was performed before spectral acquisitions according to *Ph. Eur.* 2.2.40.

Figure 6.3. Spectrometer LabSpec5000 with ASD Muglight accessory.

The spectra acquisition procedure consisted in placing the bottom of the glass vial in the Muglight accessory above the small sample holder and taking the scan after the standard baseline. The sample was rotated slightly (thorough the vertical axis) among measurements, for good coverage of the variation in spectra from one portion to the other of the freeze-dried cake. Therefore, three spectra replicates were taken for each vial. All sample vials were warmed at room temperature at least one hour before spectra acquisition.

2.3. Karl Fischer titration

Residual moisture levels in IFDA and IFDB drug products were determined with volumetric Karl Fischer (KF) titration using a 852 Karl Fischer Titrator (Metrohm, Switzerland). Vials were weighed using the analytical balance XSE-205-DU (Mettler Toledo, Location). In volumetric titration, Aquagent solvent (Scharlab SL, Spain) and Hydranal Formamide dry (Scharlab SL, Spain), in a proportion of 3:1 for IFDA and 1:1 for IFDB respectively, were used as the KF medium in the titration cell. Aquagent Titrant 5 (Scharlab SL, Spain) was added to the burette. Titration endpoint was indicated voltametrically by polarising a double platinum electrode.

The percentage of water was automatically calculated using the following formula:

$$\%\,Water = \frac{V \times f \times 100}{P} \qquad \textit{Equation 6.1}$$

Where:

- V: volume of Karl Fischer Titrant 5 consumed (ml)
- f: Karl Fischer Titrant 5 factor (g/ml)
- P: mass of sample added to the KF cell (g)

Sample preparation:

- IFDA: the vial with product was shaken gently until the freeze-dried cake was pulverized. Then, the capsule was removed and the whole vial with powdered product was weighed and then added to the KF cell. Consequently, only one replicate was obtained for each vial. The mass of product corresponds to the difference between the initial weight prior KF determination and the final weight after powder was added to the cell.
- IFDB: the difference with respect to IFDA is that the powder was not included directly to the titration cell. First, 500 mg of pulverized product were weighed in a glass weighing funnel and, then, it was added the cell.

Analysis were carried out in duplicate and according to *Ph. Eur.* 2.5.12. In addition, both KF methods were validated. A summary of the validation results of the KF method for IFDA drug product is included in the experimental Chapter 8. Standards used for method validation were Hydranal Water Standard 5.0 (VWR International Eurolab S.L., Spain) and Hydranal Water Standard 10.0 (VWR International Eurolab S.L., Spain).

2.4. X-ray powder diffraction

XRPD was performed at X-ray Diffraction Service (UAB, Cerdanyola del Vallès). A powder X'Pert X-ray diffractometer (PANalytical, The Netherlands) equipped with a PIXcel^{1D} detector was used, coupled with a variable temperature stage (TTK 450; Anton Paar, Austria). Cu Kα radiation (λ=1.5419 Å) was used at 45 kV and 40 mA. X-ray patterns of solid samples were measured over an angular range of 3.0-40.0° 2θ and step size of 0.0263°. X-ray patterns of frozen samples were measured over an angular range of 3.0-23-0° 2θ and step size of 0.0263. The angular range, step size and net time per step of the diffraction patterns are described in the corresponding sections. Some XRPD patterns were obtained using a Nickel beta-filter of 0.020 mm thickness to reduce the intensity of spurious signals. Results are presented as peak positions at 2θ and X-ray counts (intensity) in the form of x-y plot.

Sample preparation and measurement procedures depend on the nature of the sample:

- *Powder:* the freeze-dried cake was gently broken up and grinded to a fine powder and back mounted in a standard flat aluminium sample holder (Figure 6.4.A). The XRPD pattern of powders (API or freeze-dried drug product) was obtained at room temperature.
- *Solution:* approximately 100 µl of solution were placed into the open, rectangular aluminium sample holder placed inside the temperature chamber (Figure 6.4.B). The chamber was evacuated at reduced pressure before freezing in order to avoid the formation of an ice layer on the holder. Solutions were subjected to a controlled temperature program. The XRPD patterns were obtained under isothermal conditions at the selected temperatures. Specific details are provided in the Results section.

For the identification of crystalline phases, the experimental powder pattern was searched against the Powder Diffraction File, a database produced by the International Centre for Diffraction Data (www.icdd.com).

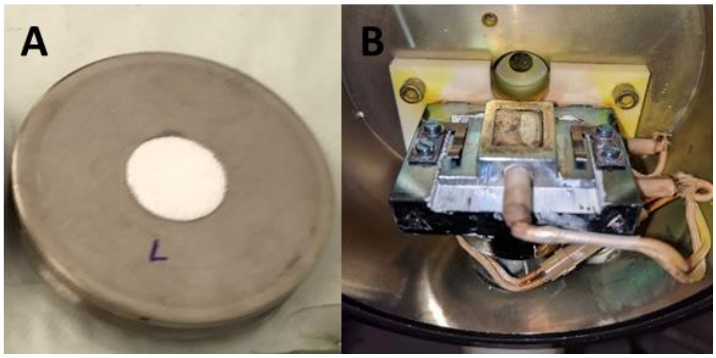

Figure 6.4. XRPD Sample holder for powders (A) and for solutions (B).

2.5. Differential scanning calorimetry

DSC was performed at the Thermal Analysis and Calorimetry Service of IQAC-CSIC (Barcelona, Spain). DSC studies of solutions were performed using a DSC 821e (Mettler-Toledo, Spain) equipped with a liquid N_2 cooling accessory for low temperatures. For the analysis of powders, a DSC 823 (Mettler Toledo, Spain) was used. DSC instruments were calibrated using indium as standard.

In practice, approximately 30 mg of the sample solution or 2-3 mg of powder were placed in aluminium pans, which were sealed immediately. In powders, depending on the analysis requirements, perforated seal may be used. An empty pan was used as a reference.

Experimental conditions, such as temperature ranges, cooling and heating rates (ºC/min), are provided in the results section of the corresponding experiment. Nitrogen was used as the purge gas, at a rate of 50 ml/min.

All glass transition temperatures were reported as the onset temperature of the heat capacity step associated to the glass transition. The enthalpy of the exothermic or endothermic peaks was calculated by integration of the area under the peak.

2.6. Thermogravimetry analysis

TGA was performed by a thermogravimetric Analyzer TGA/SDTA 851e (Mettler Toledo, Spain) at the Thermal Analysis and Calorimetry Service of IQAC-CSIC (Barcelona, Spain). TGA instrument was calibrated using indium and aluminium as standards. About 4 mg of freeze-dried powder was put in an open pan. Experimental conditions, such as temperature ranges and heating rate (ºC/min), are provided in the Results section of the corresponding experimental chapter.

2.7. Freeze-drying microscopy

FDM was performed at the CoEL in RJ, Sant Joan Despí, Barcelona. An Olympus BX51 (Olympus Iberia S.A.U., Spain) microscope with a 10x objective, equipped with a Linkam FDCS 196 Freeze Drying Stage and a liquid nitrogen cooling system, controlled by Lynkam temperature controller TMS 94 and liquid nitrogen pump (Linkam Scientific Instruments, Surrey, UK) was used. The FDCS 196 stage was evacuated by a Trivac® rotary vacuum pump and controlled by an Oerlikon Leybold single-Channel vacuum gauge controller. Pressure was measured using a Pirani gauge (Linkam Scientific Instruments, Surrey, UK) attached to the FDCS 196 stage. The process is monitored by a PixeLINK camera mounted on top of the microscope, that takes pictures every 2 s of the changes that occur within the product (freezing, sublimation, collapse and fusion), registering time and temperature as well. Figure 6.5 shows a representation of the instruments installed in CoEL facilities.

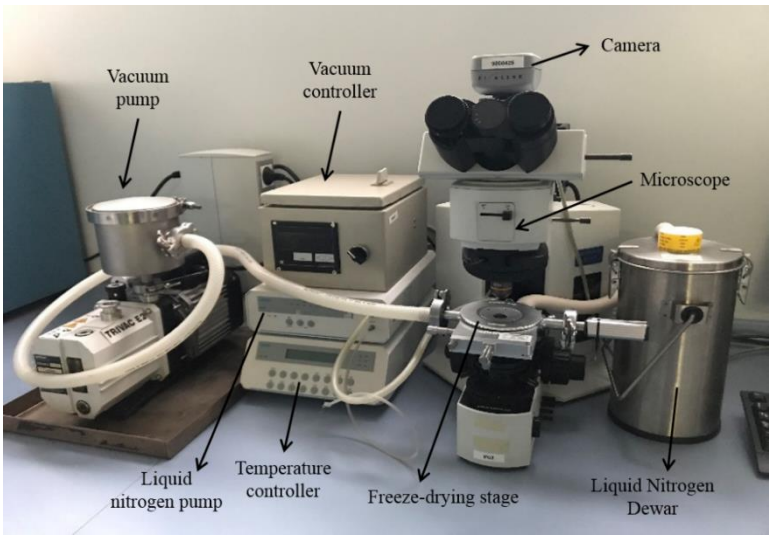

Figure 6.5. Freeze-drying Microscope located at CoEL department of RJ.

A droplet of the solution (normally 2 µl) was placed onto a quartz coverslip (lying on the silver block oven of the stage) and covered with second glass coverslip, causing the solution to spread evenly. A metallic spacer was placed between the cover slips to maintain the sample thickness almost constant between each experiment. Silicone grease was used between the silver block and the glass cover slide to improve heat transfer from the heat source to the sample. A schematic representation of the sample presentation procedure is shown in Figure 6.6.

All samples were cooled from room temperature to -50°C. Then, the system was placed under vacuum at about 0.100 mbar and the sample was kept at this temperature to attain equilibrium for 3 min. After that, frozen sample was heated up to 20ºC at 5ºC/min until collapse was observed. Cooling rates and annealing conditions were manually controlled with regards to the specific experimental requirements.

Pictures were analysed to determine the nucleation temperature and collapse temperature. The nucleation temperature was determined using the first recorded picture illustrating a frozen structure of the product. The collapse temperature was defined as the temperature at which first gaps and fissures were visible adjacent to the sublimation interface.

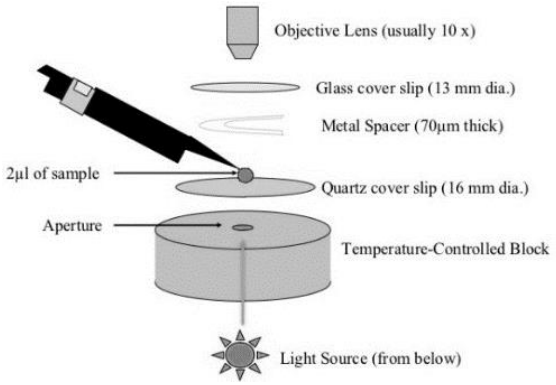

Figure 6.6. Sample preparation for freeze-drying microscopy analysis using Linkam FDCS 196 Freeze Drying Stage.

2.8. Physicochemical and microbiological analysis

The following analytical methods were used to analyse the quality of the freeze-dried products according to its quality attributes specifications. These methods are grouped separately because all of them were performed by the QC and R&D department of RJ.

General methods for IFDA and IFDB

Appearance

The appearance of the freeze-dried product cake was inspected visually for its structural integrity and pharmaceutical elegancy. The vial content was examined against a white background and the following parameters are determined: colour, degree of shrinkage, and level of uniformity. It is considered a qualitative, relatively subjective method, which provides information solely on the macroscopic structure.

Reconstitution time

Each vial was reconstituted with 50 ml WFI and it was shaken until complete dissolution. The result was expressed as measured time since the WFI was added until it was visually checked that the freeze-dried powder was completely dissolved without particles or air bubbles.

Other general methods[a]

According to *Ph. Eur.* 0520 Parenteral preparations (injections type): particulate contamination (*Ph. Eur.* 2.9.19), sterility (*Ph. Eur.* 2.6.1), Uniformity of dosage units (*Ph. Eur.* 2.9.40), Uniformity of content (*Ph. Eur.* 2.9.6) and Bacterial endotoxins (*Ph. Eur.* 2.6.14).

Specific methods

Assay and impurities

In both products, drug purity (assay and impurities) was assayed by a validated High Performance Liquid Chromatography (HPLC) method according to *Ph. Eur.* 2.2.29. An Alliance 2695 HPLC system (Waters, Massachusetts, USA) with a 2998 Photodiode Array Detector (Waters, Massachusetts, USA) and an autosampler injection device was used. Chromatograms were processed with Empower software (Waters, Massachusetts, USA).

HPLC method for IFDA

The buffer solution was prepared with 0.2% v/v triethylamina and 99.8% v/v MilliQ and pH was adjusted to 3.2 with orthophosphoric acid. The mobile phase A consisted of 92% v/v of buffer solution, mixed with 1% v/v tetrahydrofuran and 7% v/v acetonitrile. The mobile phase B

[a] These methods were used only to analyze the scale-up and manufacturing process performance qualification batches of IFDA freeze-dried product at industrial-scale. They were not applied to analyze laboratory scale-samples.

consisted of 70% v/v of buffer solution mixed with 1% v/v tetrahydrofuran and 29% v/v acetonitrile.

A series of standard and test solutions of API and impurities were independently prepared.

- 0.5 mg/ml API standard solution in water R (*Ph. Eur.*).
- API test solution: Four vials of IFDA freeze-dried product were reconstituted with water and the content was poured into a 200 ml volumetric flask. Then, 2 mg/ml, 0.08 mg/ml and 0.002 mg/ml API test solution in mobile phase A were prepared.
- 0.25 mg/ml for each Impurity stock solution in mobile phase A.
- Solution for impurities identification: 2 ml of each Impurity stock solution and 0.25 ml of 2 mg/ml test solution were added to a 20 ml volumetric flask and dissolved with mobile phase A up to complete volume.

A gradient was carried out with mobile phases A and B. Initially, 100% mobile phase A was eluted. After 13 min, a gradient increasing 11% the mobile phase B concentration v/v per minute was established. Finally, 100% mobile phase B were used the last 4 min of elution.

Analyses were performed using a Hypersil ODS C18 analytical column (Thermo Fisher Scientific, Massachusetts, USA) of 4.6 mm ID x 25 cm and 5 µm of particle size. A run time of 40 min was used with 1.0 ml/min flow rate, an injection volume of 20 µl and a detection wavelength of 280 nm at room temperature.

The percentage content of API and each impurity was calculated by determining the area of the corresponding peak as a percentage of the total area.

HPLC method for IFDB

The buffer solution was prepared with 6.8% of KH_2PO_4 and 93.2% of water Milli-Q, and adjusted to pH to 2.35 with concentrated H_3PO_4. Mobile phase consisted of buffer solution and acetonitrile.

A series of standard and test solutions of API and impurities were independently prepared:

- 0.1 mg/ml API standard solutions in Milli-Q water.
- 0.002 mg/ml Impurities standard solutions in Milli-Q water.
- 1.98 mg/ml Test solution in Milli-Q water.

A gradient was carried out with buffer solution and acetonitrile.

Table 6.2. Elution gradient for the HPLC assay and impurities methods.

Assay			Impurities		
Time (min)	**Buffer (%)**	**Acetonitrile (%)**	**Time (min)**	**Buffer (%)**	**Acetonitrile (%)**
0	87	13	0	87	13
5.0	87	13	5	87	13
22.0	80	20	22	80	20
33.0	60	40	33	60	40
36.0	87	13	40	60	40
38.0	87	13	43	87	13
			45	87	13

A Novapack C18 analytical column (Waters, Massachusetts, USA) of 15 cm, ID 3.9 mm and 4 µm particle size was used for separation. Analysis were performed using a 0.8 ml/min flow rate, an injection volume of 20 µl and 220 nm as the detection wavelength at room temperature. A run time of 38 min (for API method) and 45 min (for impurities method) was used. Column temperature was set at 30ºC and autosampler temperature was set at 10ºC.

The percentage content of API was calculated by dividing the area of API peak in sample test solution by mean area of total injections related to main peak in API standard. Similarly, the percentage content of each impurity was calculated by dividing the area of each impurity obtained in test solution by the mean area of API peak in the Impurity standard solution. According to the method validation, limit of quantitation (LOQ) is 0.05% and LOD is 0.005%.

IFDA microbiological assay

The potency of an antibiotic is estimated by comparing the inhibition of growth of sensitive micro-organisms produced by known concentrations of the antibiotic and a reference substance. The assay was carried out by diffusion method. It was performed in the Microbiology department of RJ according to *Ph. Eur.* 2.7.2.

3. Software and statistical computation

Instrument control and data acquisition

- Lyosuitelab2 (Telstar, Spain) was used to set and monitor the freeze-drying process in the Lyobeta20 laboratory scale freeze-dryer.
- SAMIS-win software (Metrofísica S.L., Spain) was used to set and control the freeze-drying process in the industrial scale freeze-dryers (Edwards 1 and Edwards 2).
- IndicoPro™ software (ASD Inc®, Colorado, USA) was used for spectra acquisition. It was validated according to FDA 21 CFR requirements.

- Tiamo™ (Metrohm, Switzerland) is the control software and database for Karl Fischer titration analysis.
- X'Pert Powder excels (PANalytical, Netherlands) was used for X-ray data acquisition. Data Viewer software (PANalytical, Netherlands) was used to preview, scale, and compare X-ray data before performing the final analysis using High Score Plus software (PANalytical, Netherlands).
- STAR^e Thermal Analysis software (Mettler Toledo, Spain) was used for acquisition and evaluation of thermal analysis data (DSC and TGA).
- Linksys 32 software (Linkam Scientific Instruments, Surrey, UK) was used to define and control the temperature program, and to take and display pictures in FDM analysis.

Statistical sofware

- Unscrambler® X version 10.3 (CAMOs Software AS, Oslo, Norway) was used for preprocessing and multivariate analysis of spectroscopic data.
- MODDE 11 (Umetrics, Umeå, Sweden) for the creation and analysis of the design of experiments.
- Matlab R2014a was used to calculate the multivariate limits of detection.
- JMP software (SAS, Cary, USA) was used to build the 3D representation of the industrial freeze-dryers moisture mapping.
- Minitab 17 Software (Minitab Ltd, Coventry, UK) was used for statistical process control studies and the analysis of RMC predictions from the freeze-dryers moisture mapping and stability studies.
- Excel 2010 (Microsoft office professional) was used for general statistical computation.

RESULTS AND DISCUSSION

Chapter 7

Freeze-drying cycle development and qualification

Part 1. Definition of the experimental strategy

1. Introduction

The application of QbD in the pharmaceutical industry has provided an opportunity for a harmonized pharmaceutical quality system which can yield safer and more efficacious drug products.[1]

The premise of QbD is that product and process performance characteristics should be scientifically designed using a comprehensive assessment of the risk of failing to achieve the desired quality attributes.[2] The ICH Q8 [3], Q9 [4] and Q10 [5] guidelines describe general principles and tools for the implementation of QbD in the pharmaceutical industry.

In general terms, a QbD study comprises the following steps: (a) define the QTPP, (b) determination of CQAs, (c) risk assessment to identify CPPs and CMAs, (d) study the impact of CPPs on CQAs, (e) establish a design space, and (f) design and implement a control strategy to ensure continuous improvement.

In the present project, a case study has been developed to apply a QbD approach for the manufacturing process design of two freeze-dried parenteral products, IFDA and IFDB. A key feature of this project is that it combines prior knowledge, experimental data, and a formalized risk assessment tools. Prior knowledge from published literature is particularly important in freeze-drying, since the physical chemistry of the process, materials characterization, heat and mass transfer operations, and process monitoring and control have been extensively studied within the past 50 years.[6,7]

Freeze-drying is used to ensure long-term stability and increased shelf life of drug products, by preserving them in a more stable dry state. This process can be divided into three stages: freezing, primary drying, and secondary drying.

The objective of the freezing process is to immobilize the product in the solid state and fix the structure of the porous dried material. Moreover, the morphology of the frozen cake may strongly affect the time required to complete the drying process, as well as the properties of the final freeze-dried products.

Primary drying serves to remove ice by sublimation under vacuum. During primary drying, the sublimation front progresses downwards until it reaches the bottom of the vial, leaving a dried product behind. In order to avoid collapse or meltback, the product temperature at the sublimation front should be below the critical temperatures for crystalline and amorphous solutes. At the completion of primary drying, the product contains some residual moisture (up to 10%, in some cases) that will be removed during secondary drying by desorption at relatively elevated temperature, to finally achieve the desired RMC.

However, the freeze-drying process can generate stress, affecting the quality attributes of the final product. Therefore, the freeze-drying process design should guarantee the quality of the final product,

that is, it should be safe, efficacious, and stable. In this sense, the product should look pharmaceutically elegant without collapse, with low RMC, short RT, retention of activity and adequate shelf life.

Nevertheless, the manufacturing of this type of products not only consists of this unit operation. The whole manufacturing process for an injectable freeze-dried drug product include several unit operations: compounding, filtration, filling, freeze-drying and capping (which are explained in more detail in Chapter 1). All this unit operations were studied in parallel, but, in this thesis, more emphasis was placed in the freeze-drying unit operation.

This experimental chapter is divided in different chapters. In the present chapter, the selection of the model drugs and the scope of the project for each product are explained. After that, the QTPP, CQAs and CMAs are defined. Then, before focusing in the freeze-drying unit operation, a cause and effect matrix of the whole manufacturing process and a simplified process map are shown to provide a general view of the project. Finally, a risk assessment of the freeze-drying process is provided with the aim to identify the CPPs and define the experimental strategy for the design of the freeze-drying process for each product.

1.1. Selection of the model drugs

Two freeze-dried drug products were chosen (products characteristics are explained in Chapter 6):

- IFDA is a legacy product, already commercialized by RJ. It consisted solely of an API with residual amounts of water, no excipients were included in the formulation. The API is thermo-labile, sensitive to oxygen and hygroscopic. It is freely soluble in water. The solid structure of the freeze-dried product is amorphous. This formulation exists in two strengths: IFDA 500 mg and IFDA 1 g. Since both are legacy products, a lot of historical data and prior knowledge about the manufacturing process was available. However, no risk assessment was done initially to design the manufacturing process.
- IFDB is a product under development by the R&D department of RJ. Therefore, no historical data and prior-knowledge was available at the beginning of the project. The formulation consisted in 600 mg of API, 600 mg of mannitol and residual amounts of water. The API is a crystalline powder, thermo-labile, hygroscopic and freely soluble in water.

In 2015, the company planned to increase the batch size of the IFDA product to match the full capacity of a bigger freeze dryer. As a result, a requalification of the manufacturing process was needed. Taking the advantage of this opportunity, a comprehensive review and evaluation of the definition, design and characterization of the current commercial manufacturing process was performed, to present a QbD based variation of the current dossier.

Then, IFDA drug product was used for freeze-drying cycle development and qualification at industrial scale. However, for IFDB drug product, the purpose was restricted to the development of a freeze-drying cycle at laboratory scale using a QbD approach.

2. Quality target product profile

First of all, the QTPP was defined for each product based on the clinical and pharmacokinetic characteristics, summary of product characteristics, pharmaceutical development, as well as the *Ph. Eur.* Monographs for APIs and mannitol. As an example, Table 7.1 shows the QTPP of IFDA drug product.

Table 7.1. QTPP of IFDA drug product.

Product attribute	**Target**
Therapeutic classification	Antibiotic
Route of administration	Intravenous
Dosage strength	500 mg/vial and 1 g/vial
Excipients	Water in residual amounts after freeze-drying. Nitrogen for the backfilling in the freeze-dried vials.
Pharmaceutical dosage form	Sterile freeze-dried powder for solution for injection.
Recommended Posology	2 g/day (500 mg every 6 h or 1 g every 12 h).
Container-closure system	IFDA 500 mg: 10 ml moulded type II glass vial mouth 20 mm, closed with a grey chlorobutyl rubber stopper and a flip-off cap. IFDA 1 g: 20 ml moulded type II glass vial mouth 20 mm, closed with a grey chlorobutyl rubber stopper and a flip-off cap.
Special storage conditions	Protected from light, room temperature (25ºC).
Shelf life	3 years
Appearance	White or almost white porous freeze-dried cake.
Identification	Positive for IFDA
Uniformity of mass	Meets compendial requirements (*Ph. Eur.* 2.9.5).
Uniformity of dosage units	Meets compendial requirements (*Ph. Eur.* 2.9.40).
Reconstitution time	≤ 1 min
Residual Moisture Content	≤ 5%
API content	≥ 93.0%
Related compounds	Any individual known impurity ≤ 4.0% Any individual unknown impurity ≤ 2.0% Total impurities ≤ 7.0%
Particles	Meets compendial requirements (*Ph. Eur.* 2.9.19).
Microbiological assay	Estimated potency between 95.0 % – 115.0 %.
Sterility	Meets compendial requirements (*Ph. Eur.* 2.6.1).
Bacterial endotoxins	Meets compendial requirements (*Ph. Eur.* 2.6.14).

3. Critical quality attributes

Secondly, CQAs were defined based on prior knowledge, QTPP and current specifications of the products. Criticality was ranked based on the severity of harm to the patient (safety and efficacy). The descriptor terms used to rank quality attributes are shown in Table 7.2. As an example, a list of CQAs and the corresponding justifications for IFDA drug product are shown in Table 7.3.

Table 7.2. Ranking of quality attributes – descriptor terms.

Score	Description
10	Established or expected direct impact on safety or efficacy
7	Unknown or expected indirect impact on safety or efficacy
5	Unlikely to impact product safety or efficacy
1	No impact on product safety or efficacy

Table 7.3. Risk score for CQAs of IFDA drug product.

Quality attribute	Score	Justification
Appearance	7	A wrong appearance may be due to collapse, which may cause product degradation influencing the efficacy and safety of the freeze-dried product. Collapsed cakes would be indicative of potentially elevated RMC levels and long RTs, and, both, could adversely affect stability of the freeze-dried product. However, appearance is less relevant as long as all other quality attributes complied with specifications.
Reconstitution time	5	An increase of the time needed to reconstitute the vial may be due to problems during freeze-drying cycle, such as collapse, which may impact on the efficacy of the drug product. At the same time, there may also be an increase in the number of (sub)visible particles due to longer than usual RT or incomplete reconstitution, being a safety risk. However, RT is generally less critical as long as dissolution is complete.
Residual Moisture Content	7	Higher values of water than expected may be due to collapse during freeze-drying, or not enough drying time during primary and secondary drying phases. Therefore, if RMC is higher than the specification, degradation may take place during shelf life compromising the stability of the drug product. Hence, RMC can have an indirect effect on drug purity or potency.
Purity	10	High concentration of related compounds can lead to a decrease in efficacy and safety problems, if any of the compounds is toxic. API degradation due to manufacturing related problems can be expected, which may lead to a decrease or loss of product efficacy. Anything directly related with recovery of the original activity would be the maximum score.
Microbiological assay (Estimated potency)	10	A microbiological assay out of the specification range can lead to a lack of efficacy (low dose) or side effects (overdose). Anything directly related with recovery of the original activity would be the maximum score.
Uniformity of mass	10	These are CQAs for all injectable products and are described in general chapters of *Ph. Eur.*
Uniformity of dosage units	10	
Sterility	10	These are CQAs for all injectable products and are described in general chapters of *Ph. Eur.* In addition, container/closure integrity (hermeticity) would presumably result in compromised asepsis.
Endotoxins	10	
Extraneous particulate contamination	10	
Hermeticity	10	

For lab-scale studies of the freeze-drying process, uniformity of mass and uniformity of dosage units were not analysed since they principally reflect the variability of the filling machine. In addition, extraneous particulate contamination, sterility, endotoxins and hermeticity were not analysed in non-sterile conditions. As a result, the CQAs evaluated to investigate the impact of freeze-drying process parameters on product quality were:

- Appearance
- RT
- RMC
- Purity: API assay and impurities
- Microbiological assay (estimated potency)

4. Critical material attributes

The input materials for IFDA and IFDB drug products are: APIs, mannitol (only for IFDB), WFI, nitrogen, vials, stoppers and caps. With regards to quality attributes, API, mannitol (*Ph. Eur.* 0559), WFI (*Ph. Eur.* 0169), nitrogen (*Ph. Eur.* 1247), glass containers (*Ph. Eur.* 3.2.1.) and rubber stoppers (*Ph. Eur.* 3.2.9.) have acceptance criteria defined in *Ph. Eur.*, and they are analysed by RJ or by the supplier.

Nevertheless, the criticality of all materials attributes was assessed in collaboration with the corresponding departments in the company to define a quality plan for each material attributes before manufacturing both products at industrial scale. After that, all CMAs were considered to have a low impact on CQAs, because the variability was controlled by analytical testing (either performed by RJ or the supplier) and fixed quantitative or qualitative acceptance criteria were defined in each material quality plan based on *Ph. Eur.*

Besides, from the point of view of the freeze-drying process, it is important to determine quality attributes of the solution, which are considered either CMAs or intermediate CQAs. These quality attributes constitute the thermal fingerprint of the product in solution, and they are determined by the thermal characterization of the solution (results are found in Part 2 of this experimental chapter).

5. Initial risk analysis

A formalized risk analysis is an essential feature of QbD. Once CQAs and CMAs were defined, the potential impact of each unit operation on the final product CQAs was thoroughly analysed applying a cause-and-effect matrix approach.

Previous experience with the manufacturing of the same product, and other sterile freeze-dried products, was used to determine the existence of risk. The following pre-requisites of the manufacturing process of sterile freeze-dried products, which are of regulatory compliance, were assumed in the risk analysis:

- Aseptic processing was ensured by appropriate equipment and facilities qualification and instruments calibration.
- Filtration system was validated to guarantee the sterility of the solution. The validation consisted in the following tests: bacterial viability and bacterial challenge tests, adsorption, compatibility, extractables and product wet integrity tests.
- Before manufacturing, cleanliness was checked in all manufacturing areas, equipment and tools.
- Adequate cleaning and sterilization procedures were in place, and media-fill tests were successfully executed.
- Environmental monitoring was done as per cGMP requirements (particles count and microbiological tests of air, rooms, surfaces and operators).
- Environmental conditions during process (room temperature, humidity) were continuously monitored and controlled with pre-established setpoints.
- Both solutions were stable 24 h at room temperature. For that reason, it was not considered as having an impact on CQAs, if the 24 h of the holding time were not exceeded.

Table 7.4 and Table 7.5 how examples of the risk analysis and the corresponding justification for the manufacturing process of IFDA drug product.

Table 7.4. Cause-and-effect matrix for the unit operations of the manufacturing process of IFDA drug product. Green= no risk of impact and red= risk of impact. Numbers refer to the sequential order in Table 7.5.

Unit operations / **CQAs**	*Compounding*	*Filtration*	*Solution collection*	*Filling*	*Freeze-drying*	*Capping*
Visual appearance	1		8	10	14	16
Reconstitution time					14	
Residual moisture content					14	16
Purity	1	3,4	8	10	14	
Potency (microbiological assay)	1	4		10,11	14	
Extraneous Particulate Contamination		5		12	14	
Sterility		6				16
Endotoxins	2	7	9	13	15	
Hermeticity						16

Table 7.5. Justifications for the initial risk assessment of the manufacturing process described in Table 7.4.

Unit operation	#	CQAs	Justification
Compounding	1	Appearance	If the solution manufacturing conditions (temperature, relative humidity, light) are not correctly established and controlled during powder addition and dissolution, the product may be degraded. In addition, there is a potential impact on the quality of the product when the holding time is exceeded.
		Purity	
		Potency	
	2	Endotoxins	Endotoxins can come from drug substance, WFI, environment or equipment.
Filtration	3	Purity	Purity could be affected by the release of leachables from the filters.
	4	Potency and Purity	Purity and potency could be affected if there is adsorption of the drug substance to the filters.
	5	Extraneous Particulate Contamination	The filters retain particles bigger than 0.22 µm. Then, visible and subvisible particles of the solution do not pass through the filters. However, filters may shed particles that are mostly composed of the material they are made of.
	6	Sterility	Sterility is affected if the filter membrane is damaged or there is a leak in the filtration system.
	7	Endotoxins	Endotoxins can come from the filtration system.
Solution collection	8	Appearance	Uncontrolled conditions of temperature, air removal or nitrogen bubbling during solution preservation before filling could impact on the appearance of the finished product. In addition, there is a potential impact on the quality of the product when the holding time is exceeded.
		Purity	
		Potency	
	9	Endotoxins	Endotoxins can come from equipment and environment.
Filling	10	Appearance	API is sensitive to oxygen. Uncontrolled and long exposition to air could induce oxidation of the solution and could impact on these CQAs if the holding time is exceeded.
		Purity	
		Potency	
	11	Potency	Unadjusted fill volume could impact on the potency of the finished product.
	12	Particle	The primary packaging materials and needles of the filling machine can contain visible and subvisible particles that can be transferred to the solution during the filling process.
	13	Endotoxins	Endotoxins can come from stoppers, equipment and environment.
Freeze-drying	14	Appearance	Product not completely solidified during freezing, bad drying (sublimation incomplete, collapse) or incorrect water desorption might impact on CQAs like appearance, RT, residual moisture, purity and potency. Incomplete vials stoppering (some vials slightly opened or leaks) might cause the entry of air (oxygen and moisture) in the headspace of the vial, which could impact the appearance, RMC and particulate contamination.
		Reconstitution time	
		Residual moisture content	
		Purity	
		Potency	
		Particles	
	15	Endotoxins	Endotoxins can come from equipment and environment.
Capping	16	Appearance	If there are leaks, the RMC could increase, and oxygen could enter to the headspace. Even though the product is in a solid state, the impact of the oxygen to the appearance of the cake is not completely resolved. In addition, if there are leaks, or capsules are distorted, the hermeticity could be compromised and, thus, the sterility of the product.
		Residual water	
		Sterility	
		Hermiticity	

5.1. Process map

According to the results of the initial risk analysis of the IFDA manufacturing process, a process map was drawn to relate the unit operations with their process parameters and quality attributes of their input and output materials (Figure 7.1). This process map was useful to establish in-process controls and the sampling plan for IFDA process characterization and qualification strategies. In fact, quality attributes of the output materials of each unit operation should be tested to verify the correct performance of each unit operation.

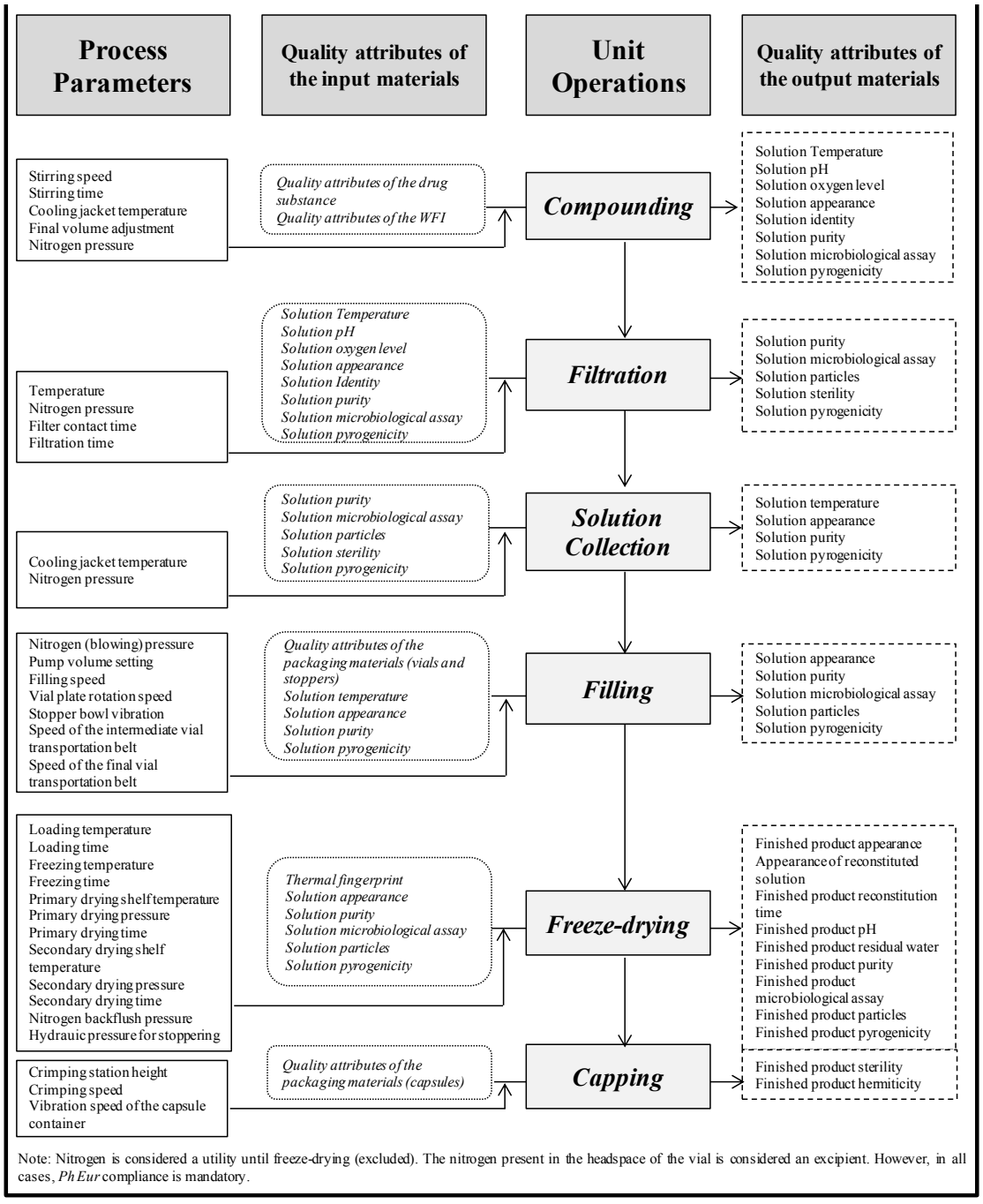

Figure 7.1. Manufacturing process map of IFDA 500 mg and 1 g drug products.

Finally, for each unit operation, a risk analysis was conducted to identify potential process parameters that could impact the identified intermediate CQAs and, ultimately, drug product CQAs. This step was done with the support of the engineering, production and QA departments. Nevertheless, as the focus of the thesis is in the development of freeze-drying process, only the risk analysis of the freeze-drying process is shown.

6. Risk analysis of the freeze-drying process

Before going to the format risk analysis, an evaluation of formulation and container closure system characteristics that could affect the freeze-drying process performance was performed. The most relevant characteristics were: total solid content, vial size and fill volume and presence of excipients in the formulation.

In both products, total solid concentrations were set between 2-10% (w/v) to obtain an efficient drying with an elegant product appearance. Fill volume and vial size were established considering that the height of the solution did not result in high resistance to mass transfer and long drying times, and that the required reconstitution volume could be added into the vial.

In addition, for IFDB drug product, mannitol was used as bulking agent. Therefore, complete crystallization is important for the appearance and stability of the product. Investigation about mannitol crystallization and its impact on the drug product quality should be performed to develop the freeze-drying process. All these considerations were established during the formulation development studies before the design of the freeze-drying process.

After that, a formal risk analysis was conducted to identify the critical parameters of the freeze-drying process. Process parameters are essentially the measurable operating parameters for the unit operations involved in the manufacturing process. According to ICH Q8(R2)[3], a CPP is a process parameter whose variability has an impact on a CQA, and therefore should be monitored or controlled to ensure that the process yields a product with the desired quality.

Risk analysis was based on the scientific literature (first principles of freeze-drying processes[8]) and the knowledge gained by the experience of the company in the development of similar freeze-drying processes. Prior knowledge, in this study, came from published literature and internal company technical reports (development and manufacturing reports, annual product reviews, deviations, batch release data, stability data, product complaints, etc.). In addition, prior knowledge from API forced degradation and pre-formulation studies, such as stability in liquid formulation, were used as well.

The risk analysis procedure consisted in assessing the impact of each parameter of the freeze-drying process on process efficiency and product safety and/or efficacy. Process efficacy was defined as the completion of the freeze-drying cycle when all process parameters are within acceptable range without

affecting any product quality attributes. For the study of the freeze-drying process, the following CQAs will be considered: appearance of the freeze-dried cake, RMC, and RT, purity[a] (assay and impurities). A priority number was set for each CQA, which corresponded to the score of each CQA in the risk analysis. Scores were put below each attribute in the first row of the risk analysis. (Table 7.9). In addition, a priority number of 7 was set for process efficiency.

Then, for each freeze-drying process parameter, a final score was put based on its ability to impact CQAs and process efficiency. Table 7.6 and Table 7.7 summarized the scores ranking in each case:

Table 7.6. Process parameter score based on ability to impact product quality attributes.

Description	Score
Established impact on product safety and/or efficacy	10
Expected impact on product safety and/or efficacy	7
Do not know for sure the impact on product safety and/or efficacy	5
No impact on product safety and/or efficacy	1

Table 7.7. Process parameter score based on ability to impact process efficiency.

Description	Score
Strong relationship	10
Expect relationship	7
Do not know for sure	5
No relationship	1

The final score for each parameter was calculated by multiplying their scores for the scores of each CQA and process efficiency and getting the total sum. According with the final score, risk levels were classified in three categories (Table 7.8).

Table 7.8. Final risk score.

Scores	Overall risk level	Justification
1-120	Low	Potential impact on CQAs was identified and controls are currently in place. A fixed value or range(s) were already defined for the parameter in the current manufacturing process, yielding with a product of the required quality.
1-240	Medium	Potential impact on CQAs identified. Experimental studies have to be conducted to analyse whether variability has an impact on CQAs and define levels or ranges. In addition, a monitoring/control system needs to be introduced or improved.
241-360	High	

Only those with medium and high risk were used for further study of each stage of the freeze-drying process.

[a] In this case, it was assumed that impact on purity represented a direct effect on the drug product activity.

Table 7.9. Risk analysis of the freeze-drying process development. Abbreviatures: RMC (Residual moisture content), RT (Reconstitution time), PE (Process Efficiency), T_{shelf} (Shelf Temperature), P_c (Chamber Pressure).

Stages	Function	Process Parameters	Justification	Impact on CQAs and process performance					Risk level	Mitigation action(s) and experimental strategy
				Purity	RMC	RT	Appearance	PE		
				10	7	5	7	7		
Soak	Temperature uniformity among vials prior to freezing	T_{shelf}	Temperature should be below the temperature at which the degradation occurs. Currently, soak temperature and time are 10ºC and 1 h respectively. The associated risk is low given that both solution are stable up to 24 h at 10ºC (IFDB) and room temperature (IFDA). It is considered sufficient to let the whole system equilibrate (including the last loaded vials) for one hour as per current practice.	1	1	1	1	1	36	No mitigation necessary. Data available from development stability studies to define the acceptable temperature range and duration.
		Time		1	1	1	1	1	36	
Freezing	Yield with a product that is completely solidified prior to drying. Freezing of water into ice to produce a rigid frozen Solute structure where solute concentrates among ice crystals	Cooling rate	The cooling rate influences the morphology of the ice crystals and, thus, the drying characteristics and drying time. Cooling rate could also affect the ability of crystalline products to crystallize during freezing. With an annealing step, this effect is expected to diminish or even disappear. The cooling rate depends on the freeze-dryer and its performance (checked by an annual requalification). It may be considered constant for a given freeze-dryer. The maximum cooling rate for lab and industrial scale freeze-dryer is 1ºC/min.	5	5	5	7	10	229	For IFDA, which is an amorphous product, cooling rate will be set to the maximum value and will be maintained constant in all experimental and industrial freeze-drying cycles. For IFDB, where mannitol is present, a study to identify if cooling rate has any effect on mannitol crystallization, product attributes and process efficiency should be performed.
		T_{shelf}	If T_{shelf} during freezing is higher than product critical temperatures (T_e/T_c), the product will not be completely solidified before drying. Progress into primary drying before complete freezing can result in loss of cake structure which could further affect product stability. However, as a rule of thumb, during cycle development, T_{shelf} will be set below product critical temperature with a safety margin of at least 10ºC.	1	1	1	1	1	36	No mitigation necessary.
		Freezing time	A short freezing time may result in incomplete solidification among vials. For this reason, additional freezing time will be added once the product temperature reaches the T_{shelf}.	1	1	1	1	10	99	No mitigation required as long as freezing time is maintained constant in all freeze-drying cycles.

Stages	Function	Process Parameters	Justification	Impact on CQAs and process performance					Risk level	Mitigation action(s) and experimental strategy
				Purity	RMC	RT	Appearance	PE		
				10	7	5	7	7		
		Ramp rate for annealing	No effect expected as annealing will remove any heterogeneity introduced due to ramp rate.	1	1	1	1	10	99	For IFDB, a study to justify the suitability of the annealing step should be performed. If so, the optimal annealing temperature and time that minimize drying time should be investigated.
		Annealing temperature	An annealing step could be introduced to minimize drying heterogeneity due to differences in ice nucleation temperature and to allow solute crystallization if desired (only in the case of IFDB that contains mannitol). Annealing may have the added benefit of increasing primary drying rate. Annealing temperature should be above T_g' but not too high to avoid ice/product melting.[9]	5	5	5	5	7	194	
		Annealing time	Should be long enough to achieve ice crystal growth. Too short may result in no added advantage of annealing step.	5	5	5	5	10	215	
Primary drying	Eliminate frozen water by sublimation	Ramp rate to Primary Drying T_{shelf}	High ramp rates can cause rapid ice sublimation leading to overload on condenser and loss of pressure control. However, the maximum allowable shelf ramp rate defined by the equipment is 1ºC/min, which would be less in product temperature.	5	5	5	5	10	215	The effect of maximum shelf ramp rate on P_c deviations and product temperature should be evaluated in first cycles. It no impact is found; this ramp rate should be maintained constant.
		T_{shelf}	High T_{shelf} could increase product temperature at the sublimation front above critical temperatures (T_e/T_c), driving to collapse, shrinkage or meltback. However, low temperature results in long drying time. Damage occurred during primary drying cannot be repaired.	7	7	7	10	10	324	Perform a study to define T_{shelf} and P_c ranges, investigating the influence of these parameters on the quality of the finished product. If possible, create a design space and define the operational region.
		P_c	High pressure could lead to product collapse/meltback; if too low, it could result in long drying time and it could also be difficult to control at industrial scale.	7	7	7	10	10	324	
		Time	If sublimation were incomplete because not enough primary drying time is given, collapse/melting could appear in secondary drying.	5	7	7	7	10	253	Use PAT tools (ratio between Pirani and Baratron gauges) to determine the end of primary drying. Primary drying time could be studied as a response of the study of the impact of primary drying temperature and pressure on the quality of the finished product to evaluate drying efficiency.

Stages	Function	Process Parameters	Justification	Impact on CQAs and process performance					Risk level	Mitigation action(s) and experimental strategy
				Purity	RMC	RT	Appearance	PE		
				10	7	5	7	7		
		Condenser temperature	If the condenser temperature is high, the mass transfer is not promoted, the drying is not efficient, and it could cause loss of control of the P_c and collapse/meltback of the product. It is not possible to put a setpoint value, thus it cannot be controlled. However, in laboratory and industrial freeze-dryers, condenser temperature is always <-60ºC, in normal situations. In addition, redundant compressors are installed, and a preventive maintenance and PLC control is in place to guarantee the temperature of the condenser.	1	1	1	1	7	78	No mitigation necessary.
Secondary drying	Eliminate residual moisture by desorption. Remove adsorbed water from the dried solute in order to achieve RMC needed for stability	Ramp rate to Secondary Drying T_{shelf}	High shelf ramp rates may result in collapse if product temperature exceeds T_g (due to the plasticizing effect of water, T_g values are lowered if high quantity of adsorbed water is still present in the dried product at the end of primary drying).	7	7	7	7	10	273	Perform a study to identify optimal shelf ramp rate for secondary drying that would not result in product collapse. It is important for IFDA, but also for IFDB if some mannitol remains amorphous after drying.
		T_{shelf}	Too low T_{shelf} may result in long secondary drying to obtain the desired RMC or could prevent water desorption. Too high T_{shelf} may result in product degradation.	7	7	5	5	10	249	A study to identify optimal T_{shelf} is needed.
		P_c	During secondary drying, the product temperature is close to the T_{shelf} and the partial pressure of water is much lower than the P_c. As a result, the effect of P_c is inconsequential.[10]	1	1	1	1	1	36	P_c is set as the lowest achievable value.
		Time	Insufficient drying could lead to high residual moisture levels. Too long time at high temperature could also affect stability by increasing degradation products.	7	7	5	5	10	249	A study to determine the optimal secondary drying time is needed.

Based on the overall risk level, the CPPs (with medium or high-risk level) that were further evaluated were:

- Freezing: cooling rate, T_{shelf}, annealing temperature and time.
- Primary drying: T_{shelf}, P_c and time.
- Secondary drying: ramp rate, T_{shelf} and time.

This risk analysis was useful to define the experimental strategy.

7. Experimental strategy

As a result of the risk analysis, the experimental plan included the following actions:

1. Characterization of the solution thermal fingerprint by DSC and FDM to determine the maximum allowable product temperature during primary drying.
2. Characterization of the physical state of the IFDB product in frozen state. In addition, the impact of annealing in mannitol crystallization, freeze-drying process efficiency and/or quality attributes of the freeze-dried solid was studied for IFDB drug product.
3. Definition of the T_{shelf} and P_c during primary drying. Understand the relationship between these variables and product quality through DoE experiments at lab scale to define a design space, if possible. As indicated in the risk analysis, the primary drying duration was considered a response of the DoE, since it is very important from the economic point of view.
4. Investigation of the kinetics of secondary drying (temperature and time) using a sample thief. This is particularly important for IFDA (which is an amorphous product).
5. Freeze-drying process scale-up and qualification at commercial scale.
6. Stability studies to relate freeze-drying process design with quality attributes throughout shelf life.

Based on the results of the above process characterization studies, acceptable ranges for the freeze-drying process parameters were established for both products, IFDA and IFDB.

Finally, the results of the study are divided in three parts:

- Part 2: Solution and freezing stage characterization.
- Part 3: Primary and secondary drying characterization.
- Part 4: Industrial scale-up, qualification and stability.

Part 2. Characterisation of the thermal behaviour of IFDA and IFDB solutions

1. Introduction

Solution thermal fingerprinting is essential to develop and optimise freeze-drying processes. Liquid formulations can be characterized by thermal analytical techniques, XRPD as well as FDM. These techniques are used to determine critical temperatures, such as T_e or T_{co} for crystalline and amorphous materials respectively, which define the maximum allowable product temperature during primary drying.[11] Moreover, they are useful for the determination of the physical state of the drug in the frozen system.

In this sense, it is important to consider the influence of formulation composition on the ability of the API or excipient(s) to crystallize, either during the freezing process itself or during an annealing step. In fact, freezing is the stage that most affects the crystallinity of the final freeze-dried product.[12]

IFDA drug product does not contain any excipient, and the freeze-dried powder is an amorphous solid. Consequently, its characterization was quite simple, based on traditional techniques like DSC and FDM. However, a more exhaustive study of the frozen product was performed for IFDB solution due to the presence of mannitol.

Mannitol is a bulking agent often used in freeze-dried drug products. It tends to crystallize to provide a rigid structure to the resulting cake.[13] Because of its high T_e (approx. -1.5ºC), it enables primary drying at high temperatures resulting in an efficient drying. However, in protein formulations, mannitol is present as a lyoprotectant and it should remain amorphous to guarantee protein stability during storage.[14,15]

When mannitol is used as bulking agent, complete crystallization is important for the appearance and stability of the product. For this reason, an annealing step is often incorporated in the freeze-drying process. Some published reports stated that the physical form of mannitol and its crystallization are influenced by different parameters, such as: mannitol concentration, API concentration, cooling rate, buffer concentration, annealing or drying conditions, among others.[16,17]

Three anhydrous polymorphs (α, β, and δ-mannitol) and an hemihydrate form of mannitol have been observed in freeze-dried formulations.[17] Variation in crystal form is normally of little concern from a freeze-drying perspective; however, the hydrate form of mannitol, if present, could have a negative impact on the storage stability of the drug product.[18]

Mannitol hemihydrate (MHH) was first observed by Yu et al.[19] in 1999, and was believed to be a product formed only at low temperatures. Some years later, Larsen HML et al.[20] showed that the most prominent factors enhancing the formation of MHH were high protein concentration, low mannitol content, and annealing at −20ºC.

The composition of the hemihydrate is two molecules of mannitol held by a water molecule. It is a metastable form that converts to anhydrous polymorphs of mannitol upon heating and exposure to moisture. For instance, Johnson et al.[21] reported that MHH may be converted to the anhydrous form by conducting secondary drying at 40ºC or higher. However, De Beer et al.[22] found that secondary drying at 40ºC was not able to transform all MHH to anhydrous forms.

Additionally, MHH may transform to anhydrous mannitol during storage with release of water.[23] Then, released water can have significant impact on the stability of the product by reducing the T_g, and potentially accelerating hydrolysis reactions.[24]

In conclusion, it is important to investigate the effect of mannitol crystallization in IFDB formulation during freeze-drying, and in the finished freeze-dried product. In short, the objectives of the study were:

- Characterization of IFDA solution thermal fingerprint by DSC and FDM.
- Characterization of IFDB solution thermal fingerprint by DSC and FDM. In addition, the effect of cooling rate, presence of API[b], annealing temperature and annealing duration on mannitol crystallization during freezing was studied by DSC, LT-XRPD and FDM. Moreover, the effect of annealing was also studied in freeze-dried products using XRPD, DSC and TGA. Quality attributes of freeze-dried products obtained from freeze-drying cycles, with and without annealing in the freezing stage, were analysed to ascertain the impact of annealing on the overall product quality. Finally, process efficiency was also determined to further justify the selection of the final freezing conditions.

2. Material and methods

2.1. Samples

An IFDA solution manufactured at industrial scale and different IFDB solutions prepared at laboratory scale (as explained in Chapter 6) were used. In addition, for the study of IFDB solution, API and Mannitol solutions were separately prepared as well. Considering the low sensitivity of the analytical techniques, IFDB solutions at different concentrations were prepared. For LT-XRPD analyses the solutions studied were: 15% Mannitol, 15% API and the IFDB formulation (mixture of API and mannitol) at a total concentration of 10% (current), 20% and 30%. For DSC analyses, 5% mannitol solution, 5% API solution and the current IFDB formulation (mixture of 5 % API and 5% mannitol) were used. Freeze-drying cycles with and without annealing were performed using the current IFDB product formulation. For each cycle, 500 ml of solution were manufactured, resulting in 35 vials.

[b] From now on, API Will be used to refer to IFDB API molecule.

2.2. Differential scanning calorimetry

Approximately 30 mg of solution were placed in an aluminium pan, and it was crimped. For IFDA, a standard temperature program was used: temperature was lowered from 20°C to -60°C at 10°C/min and held for 1 min to ensure thermal equilibrium. Then, temperature was raised at 5ºC/min to 25°C. For IFDB, samples were frozen at a controlled rate (1ºC/min or 10ºC/min) to -55ºC and held for 1 min to ensure temperature equilibrium. Then, samples were heated at 5ºC/min to 25ºC. When an annealing step was introduced, the frozen solutions were annealed at either -15ºC or -28ºC for periods of 10 min and 60 min using the same cooling and heating rates.

In the case of freeze-dried powders, approximately 3 mg of powder were placed into a perforated aluminium pan, and heated from 0ºC to 200ºC, at 10ºC/min, under a stream of nitrogen.

2.3. Freeze-drying microscopy

Samples were frozen at 10ºC/min from 20ºC to -50°C and then heated up to 20ºC at 5ºC/min after vacuum was applied to the system. For IFDB formulation solutions, an annealing step at -15ºC and -28ºC, during 10 min and 60 min (for both temperatures) was added during the freezing step. T_{co} was determined as the temperature at which the sublimation front became fragile with pores.

2.4. Thermogravimetry

This technique was used only to analyse IFDB drug product. About 4 mg of freeze-dried product was heated in an open pan from 25ºC to 250ºC, under nitrogen purge, at 10ºC/min.

2.5. Low-temperature X-ray powder diffraction

This technique was only applied to study IFDB solution. As observed in Figure 7.2, liquid solution was placed in a rectangular holder (1 mm depth) and it was cooled at 1ºC/min or 10ºC/min until -50ºC. At this temperature, a frozen solution was clearly observed.

XRPD patterns were measured in the range from 3º to 23º 2θ (which comprises the first peak of hexagonal ice 22.5º 2θ, taken as reference). Then, as hexagonal water peaks appeared above 22º 2θ, no interferences of ice on the XRPD pattern of the cryo-concentrate solute were expected

Freeze-dried samples were measured in the range from 3º to 40º 2θ. Identification of mannitol polymorphs was carried out by comparing the diffraction pattern of the sample with the International Centre for Diffraction Data in Powder Diffraction Files (PDF).[25] Some XRPD measurements were performed with a nickel filter to reduce the background radiation (artefacts).

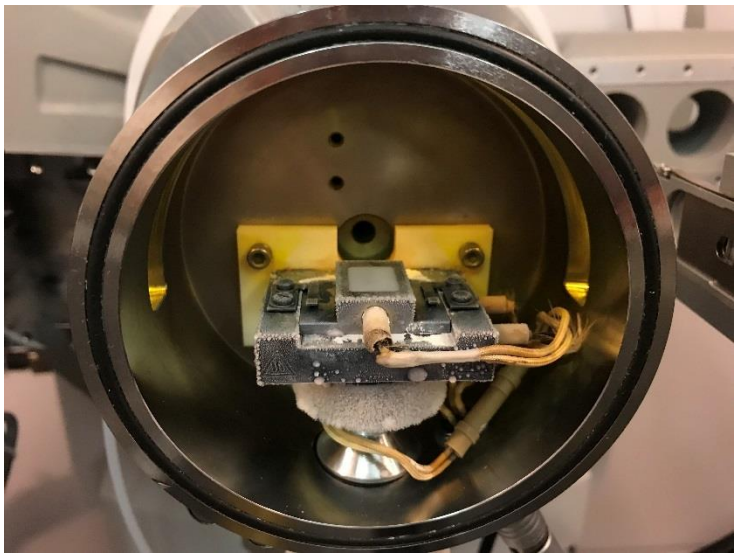

Figure 7.2. Real picture of frozen sample at -50ºC inside the LT-XRPD chamber.

2.6. Freeze-drying process

IFDB formulation solutions were freeze-dried using a laboratory freeze-dryer (see Chapter 6 for further details of the equipment). Vials were placed on trays and loaded onto the freeze-dryer at a temperature of 10ºC and remained for 1 h. Two conservative freeze-drying cycles were run: Lyo-cycle 1 without annealing and Lyo-cycle 2 with annealing. Freeze-drying cycle conditions were defined based on the results of the solution characterization studies.

In Lyo-cycle 1 (without annealing), vials were cooled at maximum ramp rate to a final temperature of -50ºC for 4 h. At the completion of the freezing, the chamber was evacuated and maintained below $1.33x10^{-2}$ mbar and the T_{shelf} was raised to -5ºC until both vacuum gauges (Pirani and MKS Baratron) converge, resulting in a ratio Pirani/Baratron=1.2. Secondary drying was carried out at 25ºC for 4 h at the lowest achievable pressure of the system. Same primary and secondary drying conditions were used in Lyo-cycle 2. However, an annealing step was added in the freezing stage at -28ºC for 4 h, followed by 2 additional hours of re-cooling at -40ºC. In both cases, vials were stoppered under vacuum with elastomeric stoppers, crimped with aluminium capsules and stored in the refrigerator at 2-8ºC.

The responses analysed in both cycles were: sublimation rate (g/vial), cake appearance, XRPD pattern, thermal profile (powder DSC and TGA), API assay, impurities, RMC and RT. The analysis of assay and impurities were performed by the R&D department of the company. See Chapter 6 for more details about the analytical methods.

Sublimation rate was measured by the difference between the weight of a filled vial before freeze-drying and the weight of the same vial extracted during the primary drying phase (when an inflection of the product temperature was observed). After that, the weight lost was divided by the primary drying time and expressed in g/h. Three vials were used to measure the sublimation rate.

3. Results and discussion

3.1. Thermal profile of IFDA solution

Figure 7.3 displays cooling and heating curves of the DSC analysis of IFDA solution. The DSC cooling curve showed a big exotherm corresponding to ice formation. As no other thermal events were appreciated when cooling until -60ºC, the endset temperature of the ice formation event, -24.43ºC, was considered the total solidification temperature (T_{ts}). Moreover, although the solid product was amorphous, the DSC heating curve of the IFDA solution did not show any T_g' in the range from -60°C to 0ºC. Only the ice-melting endotherm, with onset temperature at -1.13ºC, was clearly observed.

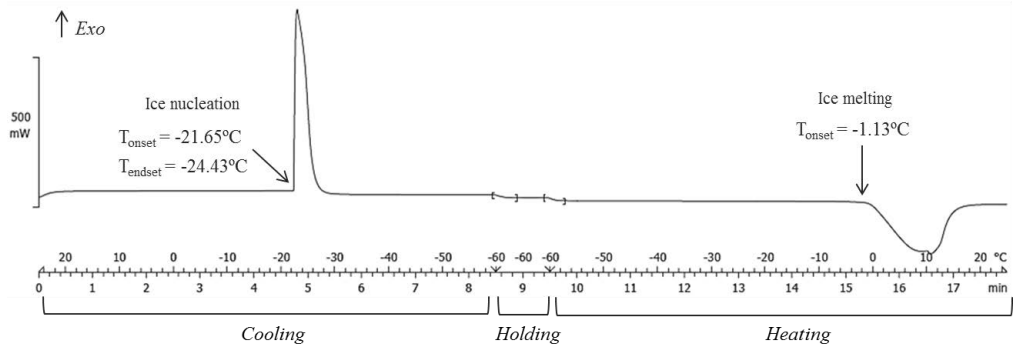

Figure 7.3. DSC curve of the IFDA solution showing two events, ice nucleation and ice melting. No T_g' was observed.

In FDM analysis, ice nucleation was observed at -23ºC. The sublimation front appeared at -50ºC when vacuum was introduced, but it began to move forward at approx. -39ºC. Some dry product fragmentation was evident as sublimation front progressed. Finally, ice melting was observed at -1ºC without signs of collapse (Figure 7.4). The ice nucleation and ice melting temperatures agree with the results observed by DSC.

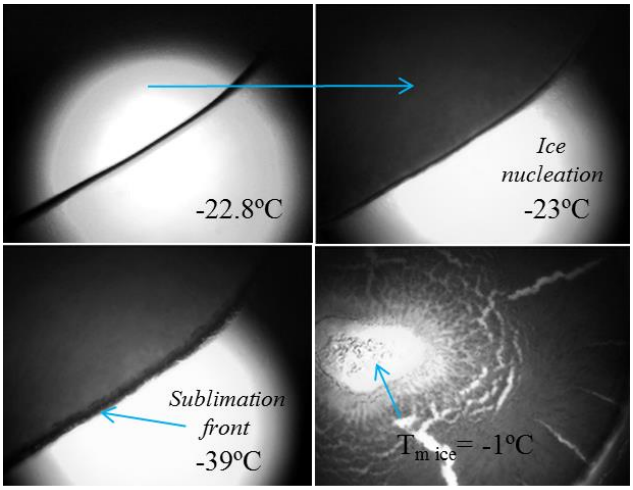

Figure 7.4. Pictures of the FDM analysis of the IFDA solution where ice nucleation, formation of the sublimation front and ice melting are indicated with blue arrows.

In conclusion, no critical temperature was found in IFDA solution. The thermal profile of IFDA solution is shown in Table 7.10**.**

Table 7.10. IFDA solution thermal fingerprint.

Abbreviation	Definition	Technique	Value
T_{ts}	Total solidification temperature	DSC	-24.43ºC
T_n ice	Ice nucleation temperature	FDM	-23ºC
T_g'	Glass transition temperature of the freeze-concentrate	DSC	Absent
T_{co}	Collapse temperature	FDM	Absent
T_m ice	Ice melting temperature	DSC	-1.13ºC

3.2. Characterization of IFDB raw materials

Raw materials were characterized by XRPD before conducting solution characterization studies. The obtained XRPD patterns are shown in Figure 7.5. The XRPD pattern of API revealed a crystalline powder, and it shows four intense peaks below 20º 2θ. Nevertheless, no reference pattern was found in the International Centre for Diffraction Data database.

Seemingly, the XRPD pattern of mannitol shows a crystalline phase that matched that of the β-polymorph (PDF Card #00-022-1797). The same polymorphic phase was previously reported in the literature as well.[26]

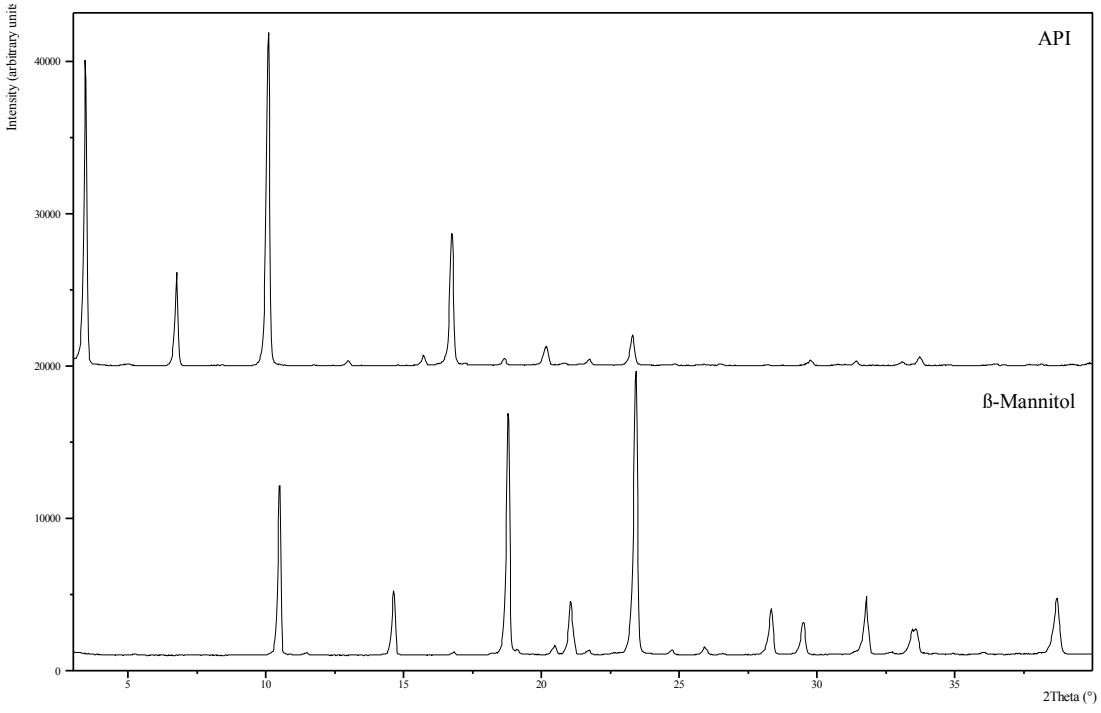

Figure 7.5. XRPD pattern of API and mannitol raw materials.

Figure 7.6 shows the representative XRPD patterns of mannitol polymorphs along with the obtained XRPD pattern of mannitol raw material. While β-peak was clearly observed in the diffractogram of mannitol raw material, the characteristic α-peak, δ-peaks and MHH were absent (indicated by black dots in Figure 7.6**)**.

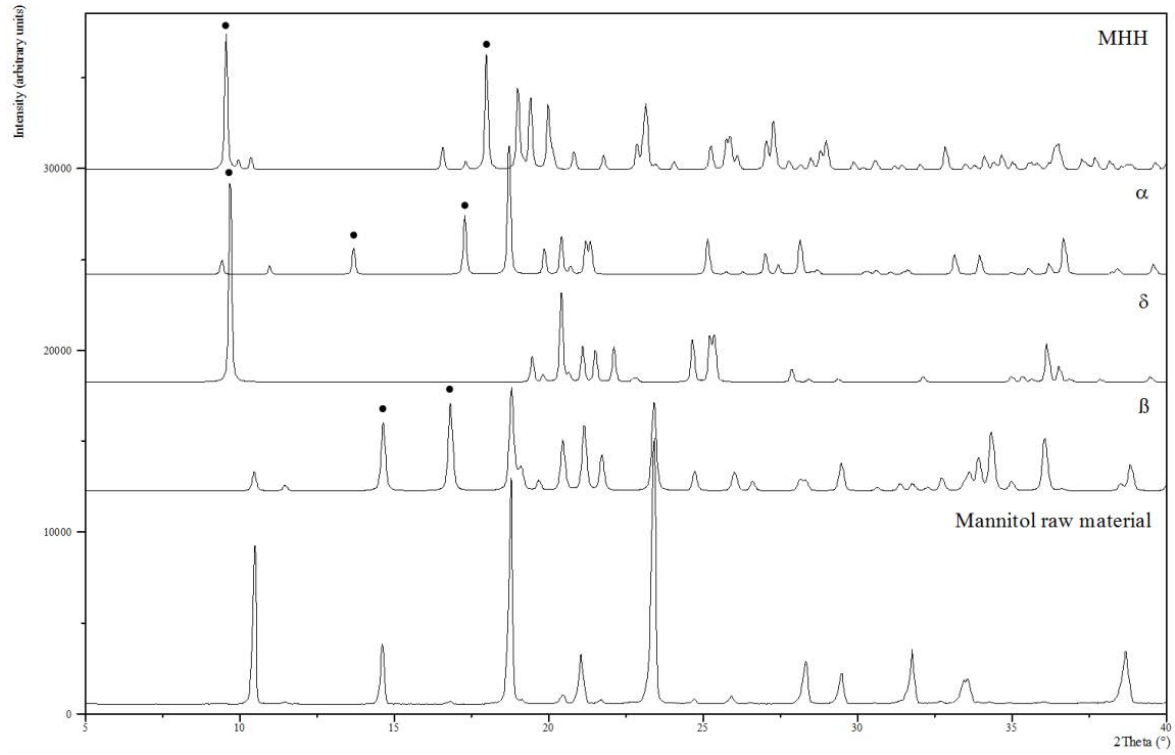

Figure 7.6. XRPD pattern of mannitol raw material, α-mannitol (card #022-1793), β-mannitol (card #022-1797), δ-mannitol (card #022-1794) and MHH (calculated pattern). Most characteristic peaks are indicated by black dots.

Table 7.11 shows the peaks used for identification of each mannitol polymorph.

Table 7.11. Mannitol XRPD Peak Assignments. Adapted from reference [27]**.**

Mannitol Phase	Main peaks [°2θ]	Intensity (%)	Peaks used for identification [°2θ]
α-mannitol	9.4	10	
	13.6	20	13.6
	17.2	45	17.2
	18.7	100	
β-mannitol	10.5	18	
	14.6	65	14.6
	16.8	85	16.8
	18.8	100	23.4
	23.4	90	
δ-mannitol	9.7	100	9.7
	20.4	50	No peak at 17.9
MHH	9.6	80	9.6
	17.9	100	17.9

3.3. Effect of cooling rate and API on IFDB freezing characteristics

In general, mannitol crystallization may be inhibited by rapidly cooling mannitol solutions whereas mannitol has been shown to crystallize when frozen at low cooling rate.[26,28] Nevertheless, some authors had shown mannitol crystallization under fast cooling.[16,29] If mannitol partially crystallize during freezing, it may result in additional crystallization during drying at higher temperatures.

When mannitol crystallizes out during freezing, different polymorphic structures have been described in the literature. For instance, Cannon and Trappler[29] reported that slow cooling rate (0.5ºC/min) caused a mixture of δ- (predominant) and α-forms of mannitol. However, Kim et al.[16] reported that slow cooling (0.2ºC/min) of 10% mannitol solutions produced a mixture of α and β polymorphs.

Besides, the presence of API or other excipients like lyoprotectants, buffer salts or proteins can also promote or inhibit mannitol crystallization. For instance, sucrose and trehalose[16], glycine[26], human serum albumin[30], potassium phosphate buffer salt[28] or different proteins[31,32] could inhibit mannitol crystallization depending on their concentrations.

In most of the abovementioned studies, LT-XRPD was used to identify phases that crystallize during freezing. It has been proven to be a powerful tool since phase transitions and crystallinity could be accurately determined.[28]

The maximum rate of shelf-ramp cycles in laboratory and industrial freeze-dryers is 1ºC/min. So, at the beginning, this value was thought to be the highest cooling rate. However, cooling rates < 1ºC/min were difficult to reach with the analytical techniques used in this study. For this reason, 1ºC/min was used as low cooling rate and 10ºC/min was arbitrary established as high cooling rate.

In the following subsections, DSC, LT-XRPD and FDM analytical results are shown, interpreted and compared.

3.3.1. Differential scanning calorimetry

IFDB solutions (mixture of 5% API + 5% mannitol) were analyzed at low and high cooling rates. The resulted DSC heating curves demonstrated that, irrespective of the cooling rate, the same thermal events were observed with a temperature shift of 1-2ºC (Table 7.7). Two glass transitions ($T_g'_1$ and $T_g'_2$), immediately followed by an exothermic event, were observed. After that, the ice melting endotherm was observed with onset at approx. -4ºC in both DSC curves. As defined by Kett[33,34], T_g' values are influenced by the scanning rate, so the observed thermal events were only evaluated qualitatively.

Then, solutions of each component individually (5% mannitol solution and a 5% API solution) were analysed by DSC to identify the thermal events observed in Figure 7.7.

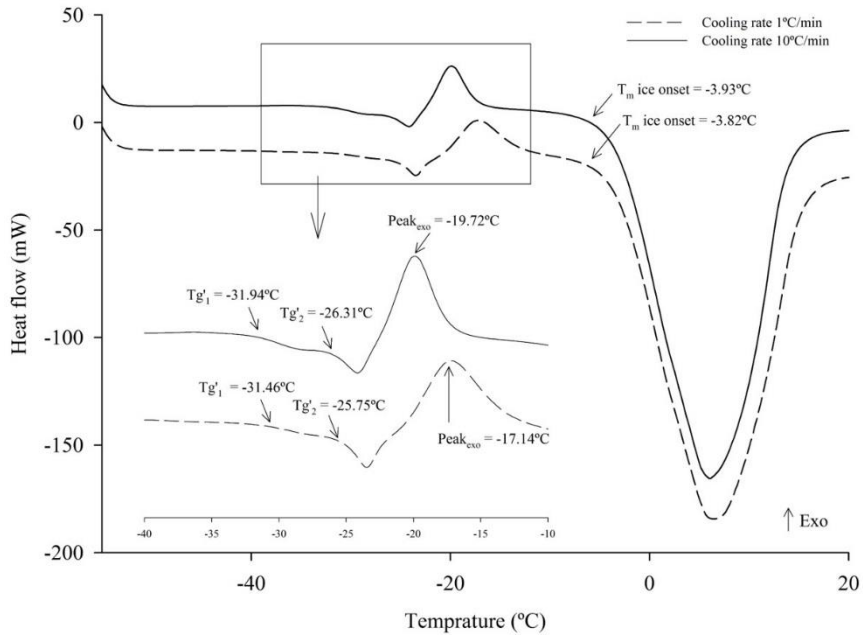

Figure 7.7. DSC heating profile of the frozen IFDB formulation (5%API+5%mannitol) cooled at -1ºC/min (dotted line) and at -10ºC/min (solid line).

The DSC curve of 5% mannitol solution was characterized by two glass transitions: a first glass transition ($T_g'_1$) of the amorphous cryo-concentrate with onset at -30.34ºC and a second glass transition ($T_g'_2$) with onset at -25.52ºC (Figure 7.8). In fact, the $T_g'_2$ could be interpreted as an endotherm, but Cavatur et al.[28] defined this event as a glass transition studying its reversibility using modulated DSC. Unlike first-order exothermic and endothermic events, glass transitions are reversible, so they are observed again after re-cooling and re-heating.

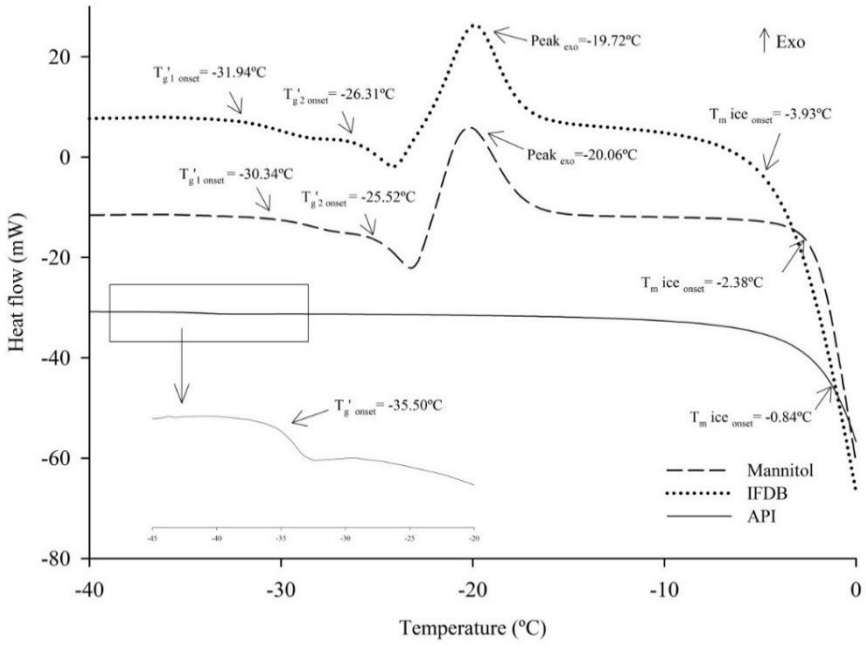

Figure 7.8. DSC heating curves of IFDB solution, mannitol 5% solution and API 5% solution cooled and heated at 10ºC/min.

Then, DSC indicated partial crystallization of mannitol during cooling and, because of the remaining amorphous mannitol fraction, two T_gs were detected. An exotherm peak at -20.06ºC was also observed and it was attributed to the crystallization of mannitol. Finally, an overlapped mannitol and ice melting endotherm (onset -2.38ºC) was observed. Actually, the observed thermal events in IFDB solution are the same as the ones observed in 5% mannitol solutions (Figure 7.8). In addition, the DSC heating curve of 5% API solution revealed a T_g' at -35.5ºC and no exothermic events were observed. This suggests that once the solution was frozen, the product remained amorphous.

In summary, DSC results suggest that a certain amount of amorphous mannitol is obtained together with an amorphous API cryo-concentrate at both cooling rates. The occurrence of the crystallization exotherm indicated that, using both cooling rates, there was partial crystallization of mannitol during heating. In addition, it was concluded that the thermal behaviour of mannitol seemed to be unaffected by the presence of API.

Table 7.12 summarized the overall results of the DSC analyses shown in Figure 7.7 and Figure 7.8.

Table 7.12. Summary of the thermal events observed in the DSC heating curves.

Sample	Cooling rate	$T_g'_1$ onset	$T_g'_2$ onset	Exotherm peak	Endotherm onset
10% IFDB solution (31.59 mg)	-10ºC/min	-31.94ºC	-26.31ºC	-19.72ºC	-3.93ºC
10% IFDB solution (34.82 mg)	-1ºC/min	-31.46ºC	-25.75ºC	-17.14ºC	-3.82ºC
5% mannitol solution (31.47 mg)	-10ºC/min	-30.34ºC	-25.52ºC	-20.06ºC	-2.38ºC
5% API solution (28.73 mg)	-10ºC/min	-35.50ºC	-	-	-0.84°C

3.3.2. Low temperature X-ray powder diffraction

Additionally, LT-XRPD was used to complement DSC results. Individual solutions of mannitol and API were also analysed by LT-XRPD at high and low cooling rates.

Figure 7.9 shows the LT-XRPD patterns of API solutions at two concentrations (15% and 30%) cooled at 1ºC/min. Only 22.5º 2θ peak corresponding to hexagonal ice along with spurious peaks of ice (artefacts) were observed because no filters were used in these XRPD measurements.

In addition, a slight baseline shift starting around 15º 2θ was observed, which was more prominent in the solution with the highest concentration. This baseline shift is typical of the diffraction patterns of amorphous materials where X-rays are scattered in many directions leading to a wide curvature of the baseline signal instead of high intensity narrower peaks. Therefore, the LT-XRPD results suggested that API seems to remain in an amorphous state in the frozen solution, which coincides with DSC results.

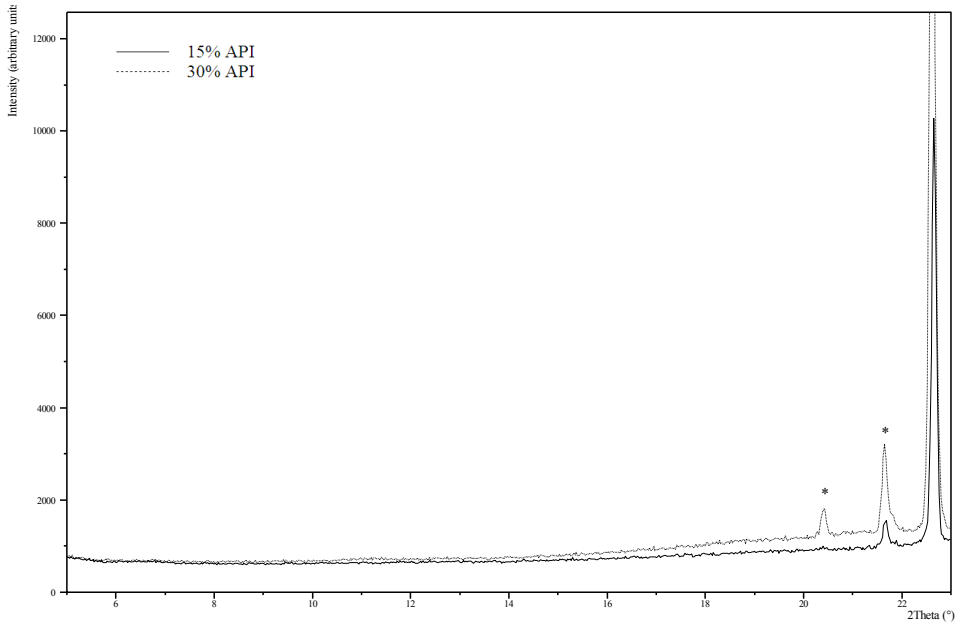

Figure 7.9. Overlapped LT-XRPD patterns of frozen IFDB solution at two concentrations: 15% and 30%.

In a same way, an aqueous solution of 15% mannitol was cooled at 10ºC/min or 1ºC/min from room temperature to -50ºC and LT-XRPD patterns were measured at this temperature. Crystallization of mannitol was observed in the frozen solution cooled at 1ºC/min (Figure 7.10). However, when cooling at 10ºC/min, no peaks were detected, which suggested that mannitol crystallization was inhibited.

The observed pattern matches with that of MHH along with ice (Figure 7.10). None of the anhydrous mannitol phases were observed. These finding are in agreement with previous published results.[23,28,32]

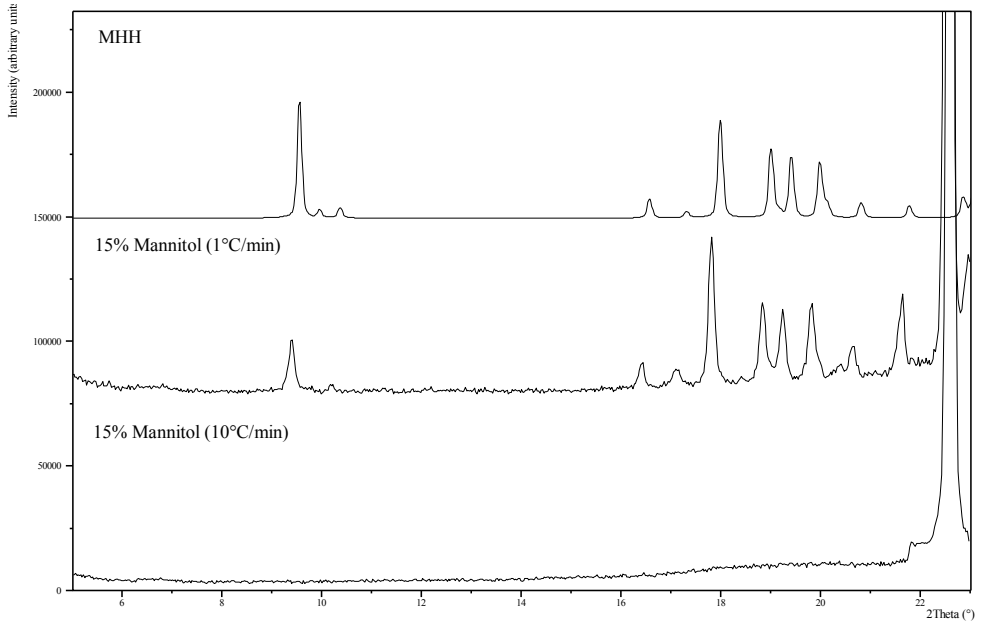

Figure 7.10. LT-XRPD patterns of frozen 15% mannitol solution cooled at 1ºC/min and 10ºC/min. The reference pattern of MHH is also displayed that matched with the pattern of 15% mannitol solution cooled at 1ºC/min.

Finally, three different mixtures of IFDB solutions (5+5%; 10+10% and 15+15%, API and mannitol respectively) were also analysed following the same procedure. Only the frozen solution of the highest concentration cooled at 1ºC/min showed some peaks in the XRPD pattern. As observed in Figure 7.11, the pattern of frozen 15+15% IFDB solution matches with reference patterns of α-mannitol and MHH.

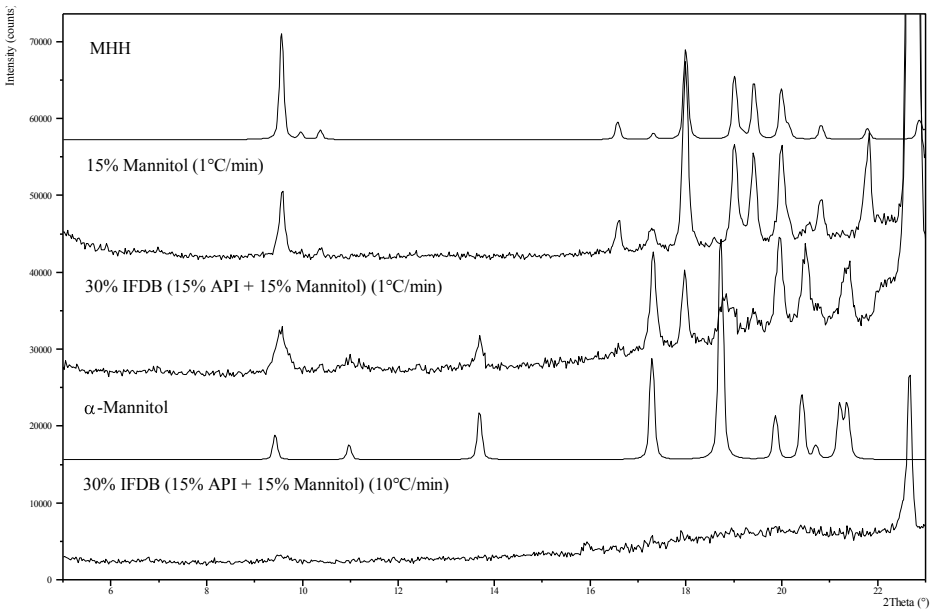

Figure 7.11. LT-XRPD patterns of frozen 15-15% IFDB solution and 15%mannitol solution cooled at 1ºC/min to -50ºC. Reference patterns of MHH and α-mannitol are also represented.

In addition, the same LT-XRPD pattern, corresponding to a mixture of MHH and α-mannitol, was observed upon freezing until -30ºC at -1ºC/min. Furthermore, using the same ramp, the temperature was decreased to -50ºC and the same pattern was observed. Figure 7.12 shows the overlapped diffraction patterns at -30ºC and -50ºC.

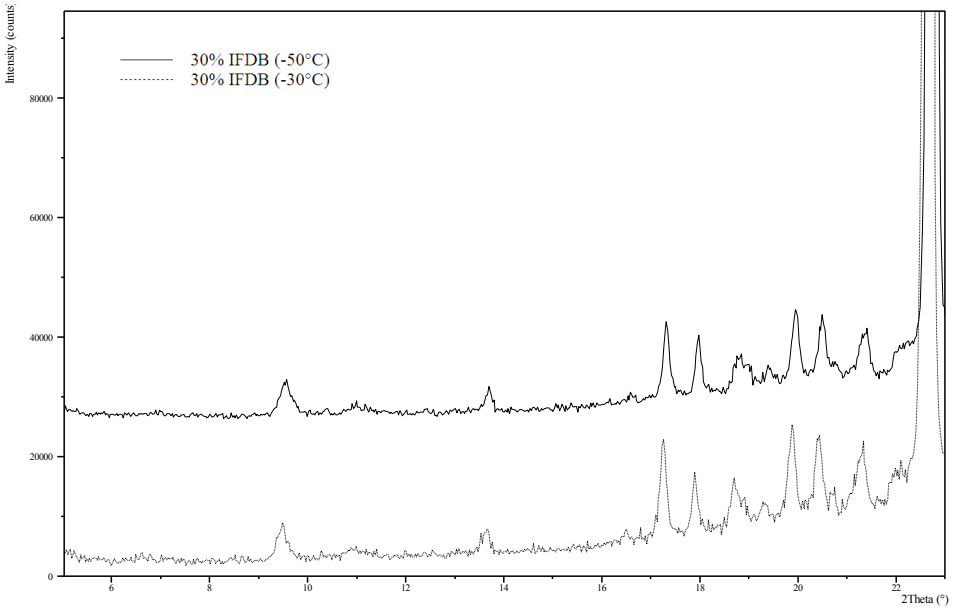

Figure 7.12. LT-XRPD patterns of 30% IFDB solution cooled at 1ºC/min to -30ºC and -50ºC.

The result is consistent with the hypothesis that, when mannitol is formulated with API, it crystallizes in a mixture of MHH and α-mannitol at either -30ºC or -50ºC, but in pure solution, it crystallizes mainly in the MHH form.

3.3.3. Freeze-drying microscopy

FDM was used as a complementary technique to investigate whether T_g's observed in DSC analyses of IFDB solutions can cause collapse during sublimation. Theoretically, collapse will occur when the product temperature during sublimation exceeds the T_g', or T_e (the last one when solute crystallized). The experimental conditions along with the results are summarized in Table 7.13.

Table 7.13. Summary of FDM experimental conditions and results.

Cooling rate	Freezing temp	Heating rate	Ice Nucleation Temp	T_{co} onset	DSC $T_g'_1$ onset
10ºC/min	-50ºC	5ºC/min	-19.6ºC	-33.7ºC	-31.94ºC
1ºC/min	-50ºC	5ºC/min	-20.9ºC	-32.5ºC	-31.46ºC

In FDM, formation of the dry layer was observed when vacuum was applied and T_{co}s were determined when the first structural changes (visible holes and cracks) appeared in the dried structure adjacent to the sublimation front (Figure 7.13). FDM measurements showed the onset of collapse at −33.7°C (when cooled at -10ºC/min) and at -32.5ºC (when cooled at -1ºC/min). Considering a conservative freeze-drying process design, the product temperature at the ice sublimation interface must remain below −32.5°C during primary drying to mitigate the risk of collapse.

As observed in Table 7.13, onset T_{co} at both cooling rates were very similar to T_g's observed in DSC analysis of the same solutions (differing by less than 2ºC).

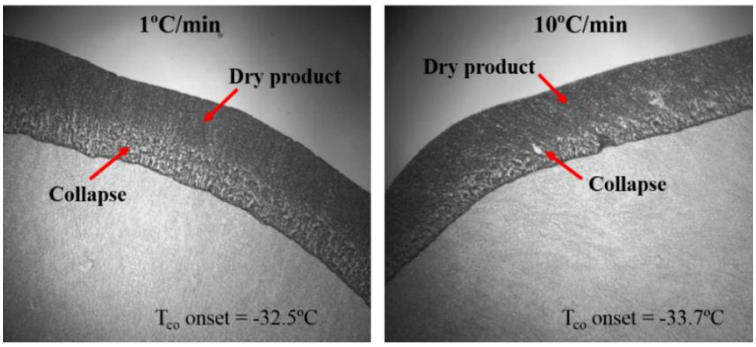

Figure 7.13. FDM pictures of IFDB frozen solutions showing the onset of collapse near the sublimation front.

In summary, in DSC and LT-XRPD analyses, mannitol was able to crystallize when cooled at 1ºC/min even in the presence of API. No crystallization was observed by LT-XRPD at high cooling rate in any of the studied solutions. DSC revealed that some fraction of mannitol may crystallize during heating in 5% mannitol solutions and IFDB solutions. However, API remains amorphous in the frozen state. In turn, the T_{co}s observed in FDM correlated with $T_g'_1$ observed in DSC.

3.4. Effect of annealing in the crystallization of IFDB components

An annealing step is commonly included in the freeze-drying process to promote a complete crystallization during freezing. In annealing, the product is held isothermally at a temperature above the T_g' providing enough energy to promote crystallization. This way, the uncontrolled crystallization of mannitol during drying is avoided.

Beatti et al.[35] investigated the annealing behaviour of mannitol solutions at -30ºC using Raman microscopy. They could demonstrate that the mannitol was crystallized rapidly (<1 min) and that both the β and δ forms appeared upon annealing, with no significant preference for either form initially. However, the β form dominated after the annealing step. Other publications have shown that the annealing step at low temperatures, below the T_g', promoted the formation of MHH, which was converted into the anhydrous polymorphs upon storage.[17,23,26,27]

Therefore, the annealing temperature could have an impact in the crystallization phase (i.e. MHH formation). Moreover, annealing time should be sufficiently long to ensure complete crystallization of mannitol.

In this study, annealing temperature range was set based on DSC analyses. The lower annealing temperature was -28ºC, which is 4ºC above the first T_g' onset at -32ºC. The higher annealing temperature was -15ºC, which is above the exothermal event determined at around -19ºC.

The experimental range for annealing time was set based on previous experience and a published study[26] which demonstrated that the difference between 10 min and 60 min was sufficient to observe variations experimentally in small sample amounts. However, the annealing time in the freeze-drying process will have to be scale-up from minutes to hours depending on the batch size.

Finally, IFDB solutions were used to study the effect of annealing temperature (-15ºC and -28ºC) and annealing time (10 min and 60 min) by DSC, LT-XRPD and FDM.

3.4.1. Differential scanning calorimetry

Table 7.14 summarizes the results of the DSC analyses of IFDB solutions when an annealing step was introduced during freezing.

Table 7.14. Thermal events observed in the DSC heating curves after annealing at different conditions.

Method	T_g' onset	ice T_m onset
Annealing -28ºC 60 min	-34.64°C	-2.79°C
Annealing -28ºC 10 min	-35.34ºC	-3.63°C
Annealing -15ºC 60 min	-35.81°C	-3.12°C
Annealing -15ºC 10 min	-35.35°C	-3.08°C

A common feature of all DSC thermograms of annealed formulations was that only a T_g' with onset at approx. -35°C was observed. This temperature is very similar to the T_g' of API alone (-35.5ºC, Table 7.12). In addition, as shown in Figure 7.14, the extent of the T_g was very similar in all the experimental conditions, meaning that approximately the same amount of amorphous structure is present in the samples.[36] Therefore, regardless of the annealing temperature and time, the quantity of amorphous product was similar.

Furthermore, in annealed samples, the DSC heating curve did not exhibit any exothermic event, suggesting the completion of mannitol crystallization during annealing (Figure 7.14). Consequently, minimal thermal treatment was needed to cause the crystallization exotherm to disappear, leaving only a weak T_g' at approx. -35ºC, and the ice melting endotherm.

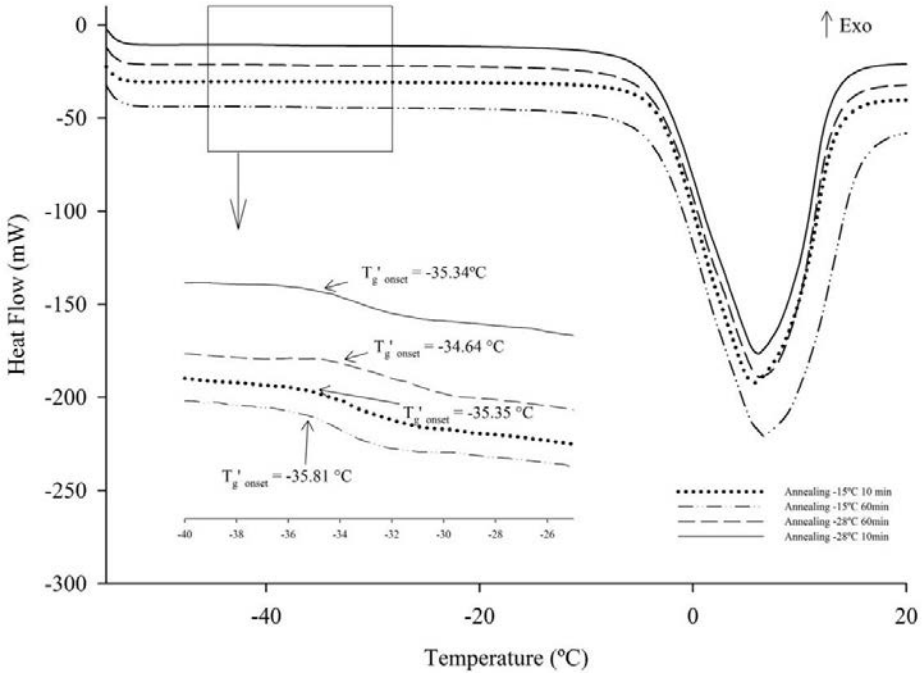

Figure 7.14. DSC heating curves of annealed IFDB solution at different temperatures (-28ºC and -15ºC) and times (10 min and 60 min). T_g' onset is indicated for each annealing condition in the zoomed image.

Then, as observed in Figure 7.15, the values of T_g' of annealed IFDB solutions were very close to the T_g' of 5% API solution (approx. -35ºC and -35.5ºC, respectively) and slightly lower than the $T_g'_1$ onset of the unannealed IFDB solutions (-32ºC/-33ºC).

Hence, the implementation of an annealing step revealed a glass transition whose T_g' onset was comparable to the one observed in unannealed API solutions (Figure 7.15).

In conclusion, the T_g' observed in annealed IFDB solutions was due to the presence of amorphous API, while mannitol seemed to be completely crystallized during freezing.

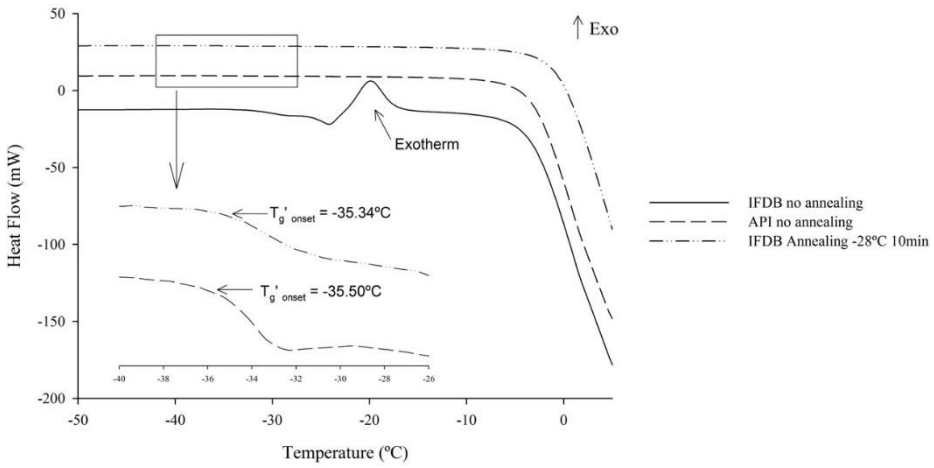

Figure 7.15. DSC heating curves of IFDB solutions annealed at -28ºC during 10 min with unannealed IFDB solution and unannealed API solution. T_g' onset values of unannealed API solution and annealed IFDB solution are indicated.

3.4.2. Low-temperature X-ray powder diffraction

In addition, annealing temperature and time were studied by LT-XRPD using a more concentrated IFDB solution (15% API + 15% mannitol). Solutions were cooled to -50ºC at a cooling rate of 1ºC/min, and, then, heated at the same rate until the desired annealing temperature (-28ºC or -15ºC). Then, a XRPD pattern was measured every 15 min until 1 h under isothermal conditions. In total, 4 XRPD patterns were measured in each annealing condition.

After heating the samples to the two annealing temperatures peaks of crystalline mannitol were detected immediately in the first LT-XRPD pattern. The same peak position and intensity was observed in the four consecutive XRPD patterns for each annealing temperature (Figure 7.16).

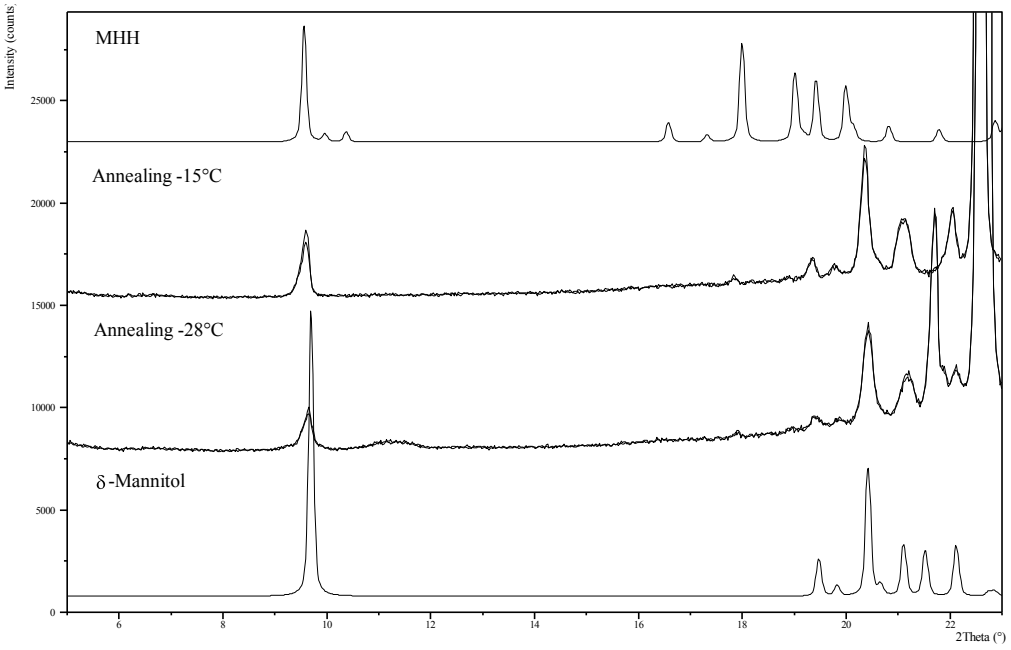

Figure 7.16. LT-XRPD patterns of 30% IFDB frozen solution annealed at -28ºC and -15ºC and the reference patterns of MHH and δ-mannitol phases. Complete overlapping of the four XRPD patters at each annealing temperature is observed.

It indicates there was no further crystallization when the solutions where annealed either for 10 min or 60 min. Peaks identification revealed that only mannitol crystallized in the studied annealing conditions. The observed phases were a mixture of MHH and δ-mannitol (Figure 7.16). Although by LT-XRPD it is not possible to confirm complete mannitol crystallization, by using DSC it was possible to conclude that mannitol completely crystallized during annealing.

3.4.3. Freeze-drying microscopy

The same IFDB solutions used for DSC analysis were subjected to FDM analysis at different annealing temperatures, but at a constant annealing time[c] (10 min). Figure 7.17 shows the FDM pictures just before and after collapse was observed.

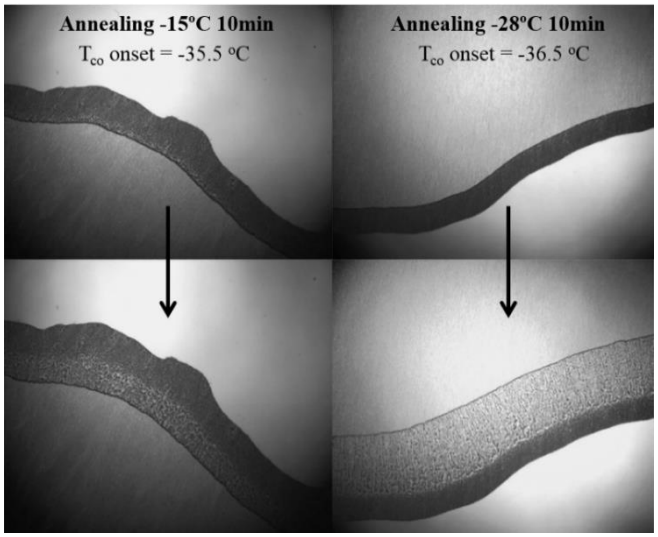

Figure 7.17. FDM pictures of IFDB solution annealed either at -15ºC or at -28ºC, showing the initial presence of collapse near the sublimation front in the first-row pictures and, evidence of collapse in the second-row pictures.

Table 7.15 described the T_{co}s for each annealing temperature, both close to -36ºC. Moreover, T_{co}s coincide with T_g's determined by DSC, which confirms that this thermal event can cause collapse during freeze-drying if product temperature reaches or exceeds T_{co}.

Table 7.15. T_{co} determined in different annealing conditions compared to the T_g' of the same IFDB solutions.

Conditions	Ice nucleation temperature	Onset T_{co}	DSC $T_g'_1$ onset
Annealing -15ºC 10 min	-19.1ºC	-35.5ºC	-35.35ºC
Annealing -28ºC 10 min	-22.9ºC	-36.5ºC	-35.34ºC

Furthermore, once characterization studies of frozen solutions were completed, the impact of annealing in the freeze-dried product quality and product performance was assessed. Based on results of the annealing studies with DSC, FDM and LT-XRPD, no significant differences were observed between -

[c] Because no differences have been observed as a function of the annealing time by DSC and LT-XRPD.

15ºC and -28ºC. Then, to optimize time and energy, -28ºC was chosen as the annealing temperature for the following Lyo-cycle experiments.

3.4.4. Freeze-drying cycles with and without annealing

Two Lyo-cycles were defined: Lyo-cycle 1 (without annealing) and Lyo-cycle 2 (with annealing at -28ºC for 4 h). Both cycles progressed correctly with no incidences.

With regards to primary drying efficiency, it was not incremented with the addition of annealing in the freezing phase (Table 7.16). The freezing duration is higher in Lyo-cycle 2 due to the addition of 6 h in the annealing step (4 h at isothermal conditions at -28ºC and 2 more hours of re-cooling).

Table 7.16. Summary of the duration of the freeze-drying phases in both Lyo-cycles.

Freeze-drying cycles	Freezing duration	Primary Drying duration (Pirani/Baratron=1.2)	Averaged sublimation rate* (n=3)
Lyo-cycle 1 (no annealing)	4 h	35 h 45 min	0.31 g/h ± 0.01
Lyo-cycle 2 (annealing)	10 h	36 h 57 min	0.31 g/h ± 0.01

* average ± standard deviation

In addition, the sublimated mass flux was 0.31 g/h in each of the three vials extracted during primary drying in both cycles. It should be noted that, when using a constant T_{shelf}, the sublimation rate decreases as primary drying proceeds, due to the increase in dry layer resistance. Thus, the calculated average sublimation rate is lower than the sublimation rate expected early in primary drying. It is expressed as an average sublimation rate per vial.

In conclusion, annealing at -28ºC for 4 h did not increase drying efficiency. Similarly, Lue et al.[37] found out that annealing did not minimize the drying duration in mannitol-containing formulations. The authors explained that this fact might be attributable to a pathway blockage by the crystalline material. Then, water vapour could not be escape in an efficient way. On the contrary, Searles et al.[9], demonstrated that annealing above T_g' increases primary drying rate due to increased ice crystal sizes, simplified amorphous structures, and larger and more numerous holes on the cake surface of annealed samples.

Annealed and unannealed IFDB freeze-dried products were also analysed by XRPD in duplicate. The XRPD patterns are represented in Figure 7.18. A crystalline powder was obtained in both conditions and all peak positions overlapped completely.

X-ray patterns of API raw material and reference patterns of mannitol polymorphs were matched with the patterns obtained in both freeze-dried products to identify the phases. It was clear that δ-mannitol was present (characteristic peak at 9.6º 2θ) as observed in Table 7.19. The other anhydrous polymorphic forms (α and β) and MHH form were not observed. In the same way, Liao et al.[17] found that the primary drying seemed to favour the formation of δ-mannitol. Thus, even if MHH was formed during primary drying, it may be unstable at high primary drying temperature and may be transformed to δ-mannitol.

The crystalline form of API raw material was also present in both freeze-dried products, evidenced by the peak at 3º 2θ.

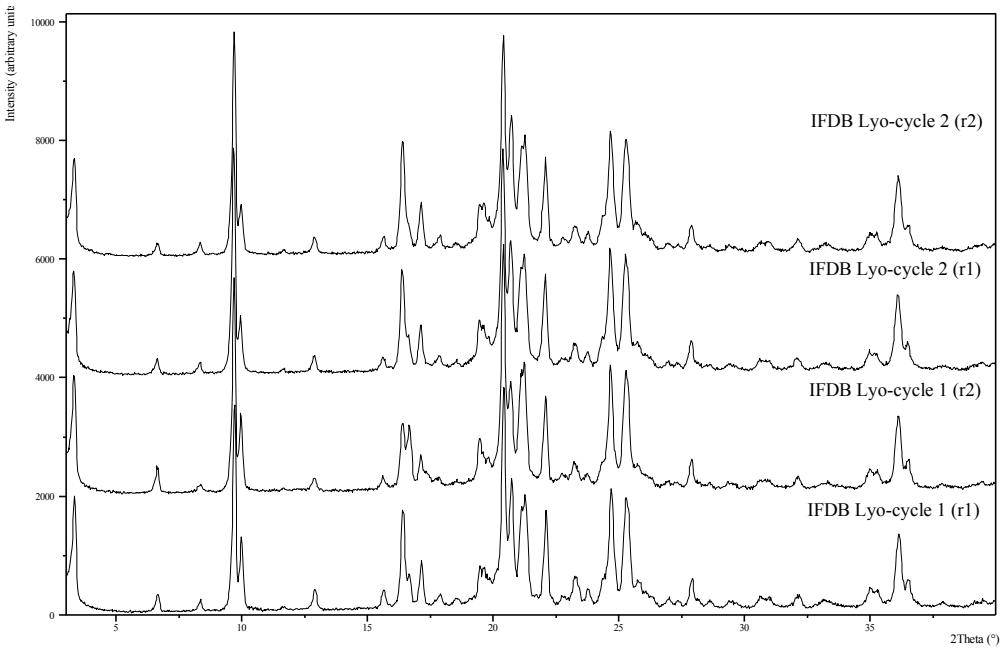

Figure 7.18. Duplicate XRPD patterns of freeze-dried powder from Lyo-cycle 1 and 2.

It can be concluded that, when the frozen solution was heated during primary and secondary drying, API crystallization was promoted. However, some peaks were still unidentified (black dots in Figure 7.19), suggesting that there could be other polymorphisms or co-crystals in the final product.

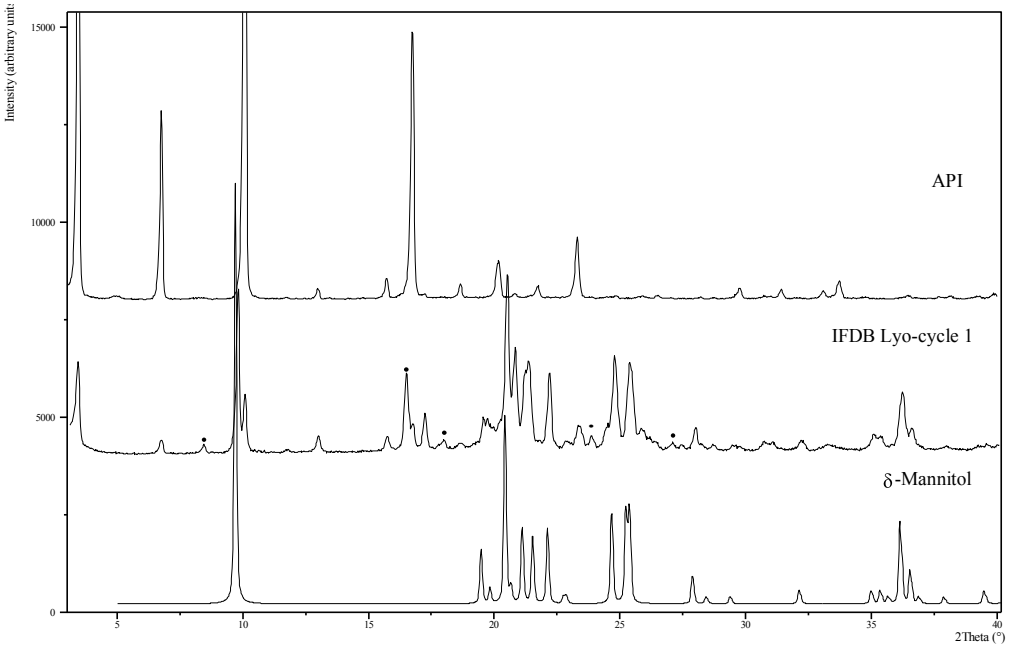

Figure 7.19. XRPD patterns of δ-mannitol, API raw material and freeze-dried powder from Lyo-cycle 1. Black dots are placed in unknown peaks.

After that, DSC was performed to observe the melting temperatures of the crystals observed by XRPD and investigate whether other transitions occurred. The DSC conducted in perforated pans of annealed and unannealed freeze-dried products showed a broad endotherm at temperatures around 30ºC, two sharp endotherms at around 120ºC and 160ºC and a broader endotherm at 140ºC (Figure 7.20). No T_g was observed which indicated that there were no amorphous components or, if present, in a very low amount.

The melting point of mannitol has been established at ~165ºC [38] while the melting point of the API is 123-127ºC[d] (value obtained by the API characterization data from the supplier). Then, it was hypothesised that the sharps endotherms observed in the DSC were caused by melting of the API and mannitol, respectively. Some temperature shifts can be observed because the formulation is a mixture, and the values of the melting points of the pure components might be affected, so the direct comparison with theoretical values could not be performed.

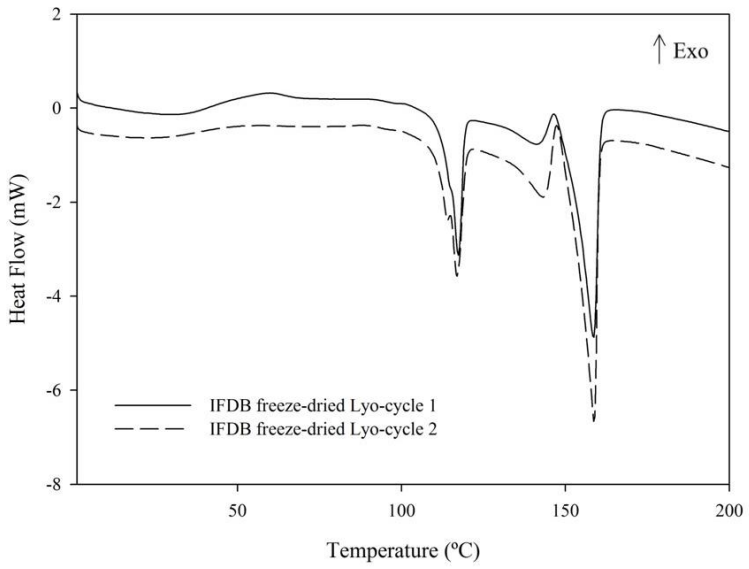

Figure 7.20. Overlapped curves of perforated and sealed DSCs of freeze-dried powders.

In addition, the broad endotherm at temperatures around 30ºC could be related to loss of sorbed water. To further investigate this effect, a TGA of the freeze-dried powder from Lyo-cycle 1 (unannealed) was performed. The analysis showed a step-like weight loss near 37ºC (1.33% weight loss). In addition, a slight progressive weight loss was also observed until onset of decomposition at 192ºC (Figure 7.21). The first step-like weight-loss was predominantly attributable to the loss of sorbed water and could explain the broad endotherm observed in the DSC.

[d] It was not possible to freeze-dry an aqueous solution of only API using the same freeze-drying cycle conditions of the entire formulation. The cake collapsed, and it was not possible to perform a DSC analysis of the freeze-dried powder of the API alone to identify the melting point.

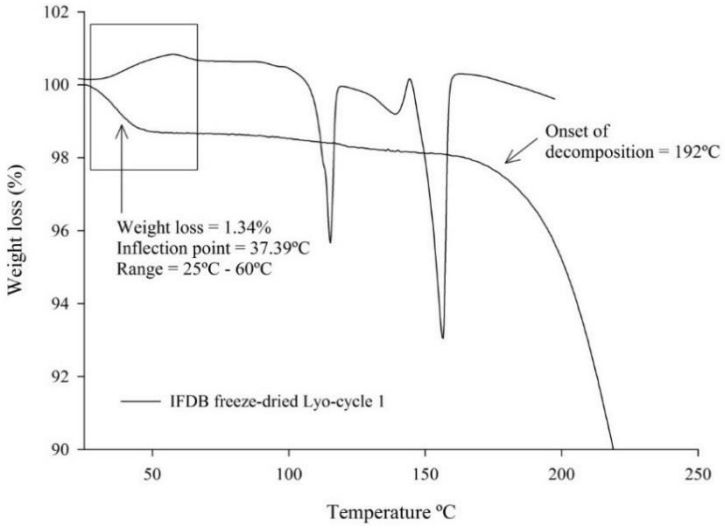

Figure 7.21. Overlapped TGA and DSC curves of unannealed IFDB freeze-dried powder.

Finally, some CQAs were analysed to investigate if the introduction of annealing had an impact on the quality of the drug product. Visual examination of both freeze-dried products did not show any sign of collapse or shrinkage immediately after the process. Both annealed and unannealed freeze-dried products presented a uniform and compact cake, without signs of collapse, as observed in Figure 7.22.

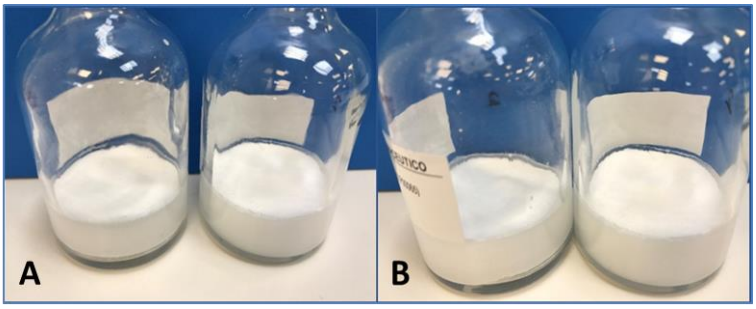

Figure 7.22. Pictures of freeze-dried vials from Lyo-cycle 1 (A) and Lyo-cycle 2(B).

Results of RMC, RT and HPLC assay are shown in Table 7.17. All analytical results complied with current specifications of the freeze-dried product.

RMC results were very homogeneous, around 0.80% in both conditions. Such low RMC value was expected because the freeze-dried product was predominantly crystalline and, during the primary drying, almost all water was already removed.

Table 7.17. CQAs results from Lyo-cycle 1 and 2.

CQAs	**Lyo-cycle 1**	**Lyo-cycle 2**
RMC (n=2)	0.80%	0.79%
RT (n=2)	67 s	82 s
Assay	100.90%	99.60%

The RT was slightly longer in annealed samples compared to unannealed ones. It was not possible to find out an explanation to that fact, since both products have the same crystalline phases (as per XRPD), same RMC and no collapse was observed. Similarly, Webb et al.[39] also reported that annealing caused longer RTs in a formulation of interferon-γ. However, there are few reports in the literature about this, and other authors found contradictory results. For instance, Searles et al.[9] reported that RTs were decreased by annealing, and they suggested that it is due to the increased pore sizes observed in annealed samples. The difference in the assay results was within the analytical error as estimated during the corresponding method validation by the parameter precision. Results of 100%±1% were considered equal.

Finally, the impurities results are represented in Table 7.18. I-1, M-1 and unknown impurities increased in the freeze-dried product compared to their respective levels in the solution prior to freeze-dry, regardless of the introduction of annealing. Very similar percentages of total impurities were obtained in both Lyo-cycles.

Table 7.18. Impurities results of API, solutions and freeze-dried samples from Lyo-cycle 1 and 2.

Parameters	**Lyo-cycle 1**		**Lyo-cycle 2**		**Specification**
	Solution	**FD product**	**Solution**	**FD product**	
I-1 Impurity	0.16%	0.22%	0.15%	0.19%	≤0.30%
M-1 Impurity	<LOQ	0.06%	0.08%	0.10%	≤0.10%
Unknown Impurities	<LOQ	0.05%	<LOQ	0.05%	≤0.10%
Total Impurities	0.16%	0.33%	0.23%	0.34%	≤0.5%

Note: LOQ for any impurity was 0.05%

Finally, it was concluded that there was no need to include the annealing step in the freezing phase, as it did not improve neither product quality nor process efficiency.

3.5. Thermal profile of IFDB solution

IFDB solution thermal fingerprint is described in Table 7.19, based on DSC and FDM analyses.

Table 7.19. IFDB solution thermal profile.

Abbreviation	**Definition**	**Technique**	**Without annealing**	**With annealing**
T_n ice	Ice nucleation temperature	FDM	-20.9ºC	-22.9ºC
T_g'	Glass transition temperature of the freeze-concentrate	DSC	-31.5ºC	-35.3ºC
T_{co}	Collapse temperature	FDM	-32.5ºC	-36.5ºC
T_m ice	Ice melting temperature	DSC	-4ºC	-4ºC

4. Conclusions

In IFDA solutions, no critical temperature was found by either DSC or FDM. Therefore, no special restrictions were determined for the freeze-drying cycle design. However, a more comprehensive study was performed for the determination of the IFDB thermal fingerprint and the study of the physical state of the frozen system.

The X-ray characterization of IFDB raw materials revealed that both API and mannitol are crystalline powders. IFDB freeze-dried products were also crystalline. The crystalline form of API raw material was observed in the drug product, and the predominant phase of Mannitol was δ-mannitol. Nevertheless, in the freeze-dried product, some XRPD peaks were still unidentified, which might mean that there could be other polymorphisms or co-crystals.

Regarding the structure of API in an aqueous solution with Mannitol, it seemed to remain amorphous in the frozen state but crystallizes upon heating. Hence, API could crystallize during the primary and secondary drying phases of the freeze-drying process.

However, mannitol seemed to crystallize at low cooling rates and upon annealing, with and without API. The effect of cooling rate studied by low temperature X-ray powder diffraction in IFDB solutions showed that, at low cooling rates (1ºC/min), mannitol crystallized mainly in the MHH and α-form, regardless of the freezing temperature (-30ºC or -50ºC). No crystallization was observed at 10ºC/min.

In DSC, the thermal behaviour of mannitol seemed to be unaffected by the presence of API irrespective of the cooling rate. There was partial crystallization of mannitol and certain amount of amorphous mannitol and amorphous API. The observed $T_g'_1$ in 10% API and mannitol solutions resulted in collapse, as observed by FDM.

The effect of annealing during the freezing phase was studied by DSC, FDM and LT-XRPD. In DSC heating curves, no crystallization event was observed after annealing, irrespective of the annealing temperature and time. In addition, only one T_g' was detected in annealed solutions which may correspond to API in its amorphous state.

In FDM, no significant differences in T_{co} among solutions annealed at -28ºC or -15ºC during 10 min were observed. In LT-XRPD, annealing of an API and mannitol 10% solution at either -28ºC or -15ºC resulted in a rapid crystallization of mannitol. The same peak intensities were observed after 10 min or 60 min of annealing. The identification of the peaks revealed that δ-mannitol was likely to be formed. As no significant differences were observed between the studied annealing temperatures, -28ºC was used to study the impact of annealing in the quality of freeze-dried products and freeze-drying process performance.

Neither drying efficiency (in terms of primary drying duration) nor the average sublimation rate were incremented with the addition of annealing in the freezing phase. No collapse was observed in any case.

According to powder XRPD results, both freeze-dried products were crystalline, and all peak positions overlapped completely. The δ-mannitol form was identified, like in previous LT-XRPD annealing studies, along with the crystalline form of API raw material.

DSC analyses of both freeze-dried powders revealed the same thermal events. Two sharp endotherms, at around 120ºC and 160ºC, corresponded to the melting of crystalline phases of API and anhydrous mannitol, respectively. Using the information gathered by TGA, the broad endotherm around 20-30ºC was predominantly attributable to the loss of sorbed water.

Additionally, all CQAs of the annealed and unannealed freeze-dried products complied with the proposed specifications. All CQAs were comparable between freeze-drying cycles except for the RT, which was slightly longer in annealed samples compared to unannealed ones.

Therefore, based on the overall quality results, there is no reason to introduce an annealing step in the freeze-drying cycle. The freezing temperature was set at -50ºC because it must be set below the T_g' (determined by DSC at -31.5ºC without annealing) considering a safety margin. These data support the conclusion that there is no effect of ramp rate during shelf cooling, and no effect of annealing.

Part 3. Freeze-drying process design at laboratory scale for IFDA and IFDB formulations

1. Introduction

Based on the previous risk analysis, presented in Table 7.9 of this chapter, medium and high-risk parameters for each stage of the freeze-drying process were:

- Freezing: cooling rate, T_{shelf}, annealing temperature and time.
- Primary drying: T_{shelf}, P_c and time.
- Secondary drying: ramp rate, T_{shelf} and time.

First, conservative freeze-drying cycles[e] were designed for each formulation, IFDA and IFDB. These freeze-drying cycles were considered "standard" processes as their final aim was to obtain a drug product with suitable freeze-dried cake appearance. For IFDA formulation, the commercial freeze-drying process was used as standard (Table 7.20) because there was enough evidence of its suitability at industrial scale.

Table 7.20. Standard freeze-drying cycle for IFDA formulation. Maximum temperature ramp rates were used between stages of the process.

Parameters	Freezing*	Primary Drying	Secondary Drying
T_{shelf} (ºC)	-40	20	40
P_c (mbar)	Atmospheric	$4.2x10^{-1}$	Minimum achievable value
Duration (h)	Min. 4.5	Min. 30.5	Min. 5
Total duration (h)		Min. 41 **	

* Loading temperature at 10ºC for 1 h before freezing.
** Durations of each freeze-drying process stage may be reduced at laboratory scale.

Nevertheless, the standard cycle for IFDB formulation was designed based on its thermal profile obtained in Part 1 of this chapter. Data and general guidelines were also used for the selection of freeze-drying cycle conditions.[40,41]

IFDB formulation has a T_g' of -31.5ºC as measured by DSC. According to general guidelines, T_{shelf} during freezing should be set below this value, considering at least 10ºC of safety margin to guarantee a complete solidification.[8] Hence, the freezing temperature was set to -50ºC. In addition, as demonstrated in Part 2, there was no need to add an annealing step during freezing. Freezing duration should ensure that product temperature reached T_{shelf}, considering some extra time to guarantee temperature equilibrium among vials. For this reason, freezing duration was established in the first freeze-drying cycle.

Moreover, IFDB formulation has a T_{co} of -32.5ºC as measured by FDM. Hence, product temperature during primary drying should not exceed this value to avoid collapse and P_c should be lower than the

[e] Freeze-drying cycle and freeze-drying process are used indistinctly.

vapour pressure of ice at the T_{co}. According to the saturated vapour pressure table, the corresponding vapour pressure of ice at -32.5ºC is 4.7 $x10^{-1}$ mbar. Consequently, P_c was set at 2.2 $x10^{-1}$ mbar. In addition, as a rule of thumb, a T_{shelf} approximately 30°C higher than the formulation T_{co} was established.[42,43] Secondary drying temperature was initially defined based on stability studies of the API [43], which demonstrated that API was stable at 40ºC for 24 h.

Finally, setpoints parameters for the standard freeze-drying cycle of IFDB formulation are shown in Table 7.21.

Table 7.21. Standard freeze-drying cycle for IFDB formulation. Maximum temperature ramp rates were used between stages of the process.

Parameters	Freezing*	Primary Drying	Secondary Drying
T_{shelf} (ºC)	-50	0	35
P_c (mbar)	Atmospheric	$2.2x10^{-1}$	Minimum achievable value

Note: Loading temperature at 10ºC for 1 h before freezing. The duration of all stages was established during the experimental study, as will be explained later.

Nevertheless, both standard freeze-drying cycles consisted in recipes with conservative and fixed parameters that may result in long drying times. Hence, process optimization was required to obtain more flexible and efficient processes for both formulations.

In this sense, freeze-drying process optimization should be focused on the primary drying phase because it is the longest stage of the process, it is the most time-consuming part of the process and it is generally associated with the highest risk to product quality. However, it should be considered that primary drying time needs to be long enough such that all of the ice has sublimed before starting the secondary drying phase to avoid product collapse.

Tang and Pikal stated that product temperature is the most relevant variable for primary drying time optimization.[40] Sublimation rate increases dramatically as the product temperature increases. In fact, Pikal[44] showed that 1ºC increase in product temperature during a freeze-drying cycle cut up to 13% of the primary drying time.

The product temperature highly depends on the T_{shelf} and the P_c applied during primary drying, and the same product temperature[f] can be achieved by different combinations of process conditions. Therefore, it is important to investigate the role and importance of each variable, or the combination of both variables, in reducing primary drying time while ensuring the quality of the product.

According to the principles of freeze-drying, higher P_c decreases the driving force for the transport of water vapour-from the product sublimation front to the chamber. Likewise, high P_c increases the heat

[f] It should be very clear, that the temperature of the product inside the vial, is not the T_{shelf} due to the kinetics of the transfer of heat from the shelf to the product and to the cooling produced by the sublimation of the ice.

transfer rate by increasing the thermal conductance which results in an increase in the temperature of the product and the sublimation rate.

Additionally, the temperature at which a product is freeze-dried must be balanced between the temperature that maintains its frozen integrity, and the one that maximizes the product temperature without exceeding T_e or T_{co}. Moreover, an increase in T_{shelf} increases the vapour pressure of the sublimation front, accelerating the sublimation process.[7]

However, different scientific studies provide opposite results on the effect of T_{shelf} and P_c on sublimation rate. Some pointed out that lower pressure decreases the resistance to mass transfer, thus accelerating the sublimation rate.[43,45,46] Other studies have shown that a moderate increase in P_c often increase the drying rate due to more effective heat transfer, leading to a higher product temperature.[47,48]

According to Trappler[49], T_{shelf} influences product temperature and has the greatest impact on sublimation rate. P_c has an important effect on product temperature, and to a lesser degree on drying rates, due to influence on heat transfer.

It should be noted, however, that the P_c should not exceed the saturation vapour pressure of water over ice at the product temperature, otherwise there will be no driving force. Additionally, increasing the T_{shelf} and the pressure will increase the sublimation rate, but it will also increase the risk of collapse or meltback by overheating the product. Therefore, a balanced degree of vacuum and T_{shelf} in the drying chamber is needed to achieve the desired drying rate.[50]

In this study, a DoE approach was used to ascertain the role of each factor in both formulations. Several studies have employed a DoE approach to investigate and optimize the freeze-drying process.[51–53] For example, De Beer et al. used a DoE with 19 runs to study the impact of three formulation variables and two process variables on the quality of a freeze-dried product and process performance.[53]

Finally, secondary drying duration and temperature should be optimized as well, principally based on the desired RMC in the final product. RMC would be expected to be important if a substantial portion of the drug is amorphous as a freeze-dried solid because of its capacity to interact with water. In addition, amorphous products could collapse during secondary drying if T_g is exceeded. Moreover, T_g is affected by the level of residual water in the dried cake.[54] Hence, it is recommended to determine the T_g of the dried product at the end of primary drying to justify secondary drying temperature.

Finally, the objectives were:

- To optimize the freeze-drying process to obtain a cycle that maximizes the sublimation rate while preserving the quality of the product.
- To investigate the effect of secondary drying temperature and time on product quality.

2. Materials and methods

2.1. Samples

IFDA 1 g solutions[g] were taken from industrial manufacturing batches, while IFDB 600 mg solutions were prepared at laboratory scale (as explained in Chapter 6). The batch size was 100 vials for each freeze-drying cycle of the secondary drying study and 30 vials for each freeze-drying cycle of the primary drying study. Batch size remained constant since it may have a direct influence on the drying duration.

2.2. Freeze-drying process

A laboratory freeze dryer LyoBeta 20 was used (equipment characteristics are explained in Chapter 6). 14 freeze-drying cycles were performed for IFDA formulation: three cycles for the secondary drying study and 11 cycles for the primary drying study (9 were experimental runs of the DoE study + 2 verification cycles at laboratory scale). For IFDB, 12 freeze-drying cycles were performed (the same as IFDA, but excluding the verification cycles).

Each freeze-drying cycle was monitored by product thermocouple probes and by comparative pressure measurement using a MKS Baratron® and a Pirani vacuum gauges inside the freeze-dryer chamber. Each thermocouple was introduced through a stopper and positioned in the bottom-centre of the vial, to achieve representative temperature monitoring. Pirani gauge measures the thermal conductivity of the gas present in the freeze-dryer chamber while Baratron measures absolute pressure, irrespective of gas composition. At the time that the composition of the gas in the chamber changes from water vapour to nitrogen, sublimation is complete and pressure values registered by Pirani are approximated to the pressure values obtained by Baratron.

Therefore, the following criteria was used to determine the endpoint of primary drying: when the product stabilised at a temperature close to the T_{shelf}, and when pressure measured by Pirani and Baratron, reached comparable values. During sublimation, the ratio between the values measured by the two probes is usually within 1.5-1.7. Hence, convergence of both probes was evidenced when the ratio begins to be lower than 1.5. For this reason, Pirani/Baratron = 1.2 was chosen as a criterion to define the duration of the drying of each experiment.

Nevertheless, for IFDA, it was observed that 1.2 was never accomplished in the industrial freeze-drying cycles. In those cycles, pressure values converged until approx. 1.3 and, maintaining the same ration until a point at which both started to decrease. Hence, it was decided to use Pirani/Baratron = 1.3 for the

[g] All experiments were performed with IFDA 1 g drug product because it was considered the worst case. Nevertheless, final conditions were verified with the lower dose, IFDA 500 mg, before going to industrial scale.

endpoint determination of the primary drying phase of IFDA freeze-drying processes and Pirani/Baratron = 1.2 for IFDB.

2.3. Variables and responses

For each formulation, primary drying and secondary drying stages were studied independently. Variables and responses of each study are summarized in Table 7.22.

Table 7.22. Variables and responses of primary and secondary drying experimental studies.

Phase	Variables	Responses
Primary drying	T_{shelf} P_c	Cake Appearance RT RMC Primary drying duration
Secondary drying	T_{shelf} Duration	RMC Assay Impurities Microbiological potency*

*Only for IFDA formulation.

A complete analysis of the quality of the product for each study would have resulted in many analytical tests which would have been lengthy and not practical. Therefore, it was decided to design a reduced analytical strategy.

For the study of primary drying stage, only CQAs directly related to the appearance of collapse (appearance of the freeze-dried cake, RMC and RT) and primary drying duration were analysed. Product temperature was monitored by thermocouples but, as explained in Chapter 3, it does not determine the temperature of the sublimation front, and the position inside the vial is not highly reproducible. Therefore, thermocouples were only used as monitoring tools.

DSC method was also used to thermally characterize both freeze-dried drug products. The results of the DSC were used to justify the suitability of the maximum ramp rate and the secondary drying temperature range for each product. Then, the secondary drying study was based on the evaluation of RMC at different drying temperatures and times. Nevertheless, assay, impurities, and microbiological potency were also analysed to confirm product quality in the studied conditions.

Finally, Table 7.23 describes the specifications of the quality attributes analysed for both formulations.

Table 7.23. Quality specifications for IFDA and IFDB drug products.

IFDA drug product		**IFDB drug product**	
Attribute	**Specification**	**Attribute**	**Specification**
Appearance	White to almost white powder	*Appearance*	White to almost white powder
RMC	≤ 5.0%	*RMC*	≤ 2.0%
RT	< 60 s	*RT*	< 120 s
Assay	≥ 93%	*Assay*	95.0 – 105.0%
Greatest individual known impurity	≤ 4.0%	*I-1 Impurity*	≤ 0.20%
Unknown impurities	≤ 1.5%	*M-1 Impurity*	≤ 0.15%
Total Impurities	≤ 7.0%	*Unknown impurities*	≤ 0.10%
Microbiological potency	95.0%-110.0%	*Total Impurities*	≤ 0.5%

2.4. Experimental strategy

Temperature and duration of secondary drying stage were studied with three cycles at three different secondary drying temperatures and times for each drug product (Table 7.24). Freezing and primary drying conditions of the standard cycles were kept constant. An interval of ±10°C from the setpoint of the standard cycle was established to define secondary drying temperature range. Moreover, the shortest secondary drying time was established base on product temperature (when it reaches that of shelf).

Vials were pulled at different intervals during secondary drying (30 vials per extraction time) using a sample thief to analyse the quality attributes described in Table 7.24. It should be noted that RMC was determined by KF in IFDB (as the NIRS method is currently under development[h]) whereas for IFDA it was determined by NIRS (model development and validation results are explained in Chapter 8).

Table 7.24. Schema of the secondary drying study for both drug products. SD=secondary drying

SD temp \ **SD time**		IFDA	3 h	6 h	16 h
		IFDB	4 h	8 h	12 h
IFDA	IFDB	Appearance			
50ºC	25ºC	RMC			
40ºC	NP*	Assay			
30ºC	45ºC	Impurities			
		Microbiological Potency**			

*Central point was not analysed in first instance (only if differences between 25ºC and 45ºC were evident) due to limited availability of API for the entire study. **Only for IFDA drug product.

[h] The quantitative NIR model for RMC prediction in IFDA freeze-dried vials was developed once the secondary drying had been performed. Hence, samples of the secondary drying study were measured by KF.

Primary drying stage was studied with a two-factor DoE with four responses (Table 7.22). Freezing conditions of the standard freeze-drying cycles were kept constant. In addition, the conditions of the secondary drying stage were established in the previous study and maintained constant as well.

To study the linear and quadratic relationship, and the effect of interactions between variables, a minimum of three levels for each variable were needed. Different designs types were evaluated, and the minimum number of experiments required to define the model equation are shown in Table 7.25.

Table 7.25. Comparison of optimization experimental designs with 2 factors. Centre replicates are not included in the total number of experiments.

Design	Nº of runs	Factor levels
Full factorial	9	3
Central Composite circumscribed / inscribed	8	5
Face-centered central composite	8	3
Doehlert	7	3 and 5
D-optimal	9[i]	5

Considering the cost and energy necessary for a single experiment, it was necessary to minimize the amount of experiments, while choosing the most informative combination of factors. For this reason, a Doehlert design was chosen with a total of nine experiments for each drug product considering three replicates in the central point of the design to study the model reproducibility.

Doehlert design is constructed from regular hyper-triangles (simplexes) with uniform space-filling properties and an equal spaced distribution of points lying on concentric spherical shells.[55] The basic hexagon has six points lying on a circumference around the centre point (Figure 7.23).

With *k* variables, the total number of experiments is $k^2 + k + n$, where *n* is the number of replicates at the centre point. It allows to estimate the coefficients of a model containing linear terms, interactions and quadratic terms without any confounding effect.

Experiment	Variable 1	Variable 2
1	-0.5	0.866
2	-1	0
3	-0.5	-0.866
4	0.5	-0.866
5	1	0
6	0.5	0.866
7,etc	0	0

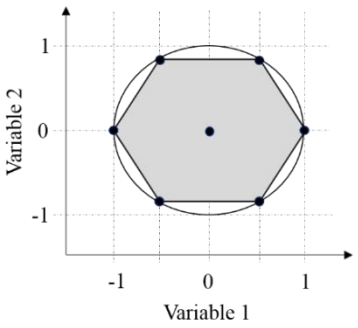

Figure 7.23. Structure of the Doehlert design for two variables or factors.

[i] The selection of the best D-optimal design was based in the G-efficency criterion *(> 60%)*.

Doehlert design has some interesting characteristics[56,57]:

- The number of experiments required is less than that of central composite designs.
- The number of levels is not the same for all variables. With two variables, the first one is studied at five levels, while the second one at three.
- They are extendable in different directions and new factors can be added to an existing design, preserving some of the runs already carried out.
- Despite being spherical, Doehlert designs are neither orthogonal nor rotatable.

For the primary drying study, T_{shelf} and P_c were investigated at different levels in both formulations. For IFDA formulation, P_c was studied at five levels while for IFDB it was studied at three levels. Standard cycle setpoints were taken as central values of the ranges. The number of experiments was reduced to 9 runs for each drug product.

The range for each variable was established in such a way that they were rather large to study the effects of these variables on the quality of freeze-dried product (Table 7.26). For IFDB, the extreme value of the range corresponds to the vapour pressure of ice at -35ºC (T_{co}) which was approx. 0.320 mbar.

Table 7.26. T_{shelf} and P_c ranges for each drug product in the primary drying study.

Parameters	**IFDA**			**IFDB**		
	-	0	+	-	0	+
T_{shelf} (ºC)	0	20	40	-10	0	10
P_c (mbar)	0.200	0.400	0.600	0.120	0.220	0.320

2.5. Statistical analysis

MODDE 11 software (Umetrics, Umeå, Sweden) was used for DoE analysis. Models were fitted with MLR considering linear and quadratic terms. Then, the model was improved by removing non-significant model terms. Goodness of fit was evaluated by R^2 and goodness of prediction by Q^2, which represents the fraction of the variation of the response that can be predicted by the model. In this study, as a general rule, R^2 >0.8 indicates that a high percent variation of the response is explained by the model. Q^2 > 0.5 indicates that the model has good predictive ability and will have small prediction errors.[58]

Moreover, the statistical significance of the regression model was checked by ANOVA test. The confidence level was chosen to be 95%, therefore a model with a p-values <0.05 was considered significant.

Microsoft Office Excel and Minitab® 15 (Minitab Inc., Coventry, UK) were also used for graphical representation and statistical calculations.

3. Results and discussion

3.1. Secondary drying study

At first, T_g was measured by DSC in vials extracted during the freeze-drying process at the end of primary drying, and when the product temperature reached the secondary drying T_{shelf} (40ºC for IFDA and 35ºC for IFDB). In the DSC curves for IFDA, a broad endotherm in the temperature range from 100ºC to 200ºC was observed (Figure 7.24), which was likely due to the high residual RMC of the vials at the end of primary drying stage. Then, this broad endotherm may hide the T_g of the amorphous dry product. Despite several trials, it was not possible to determine a T_g using DSC.

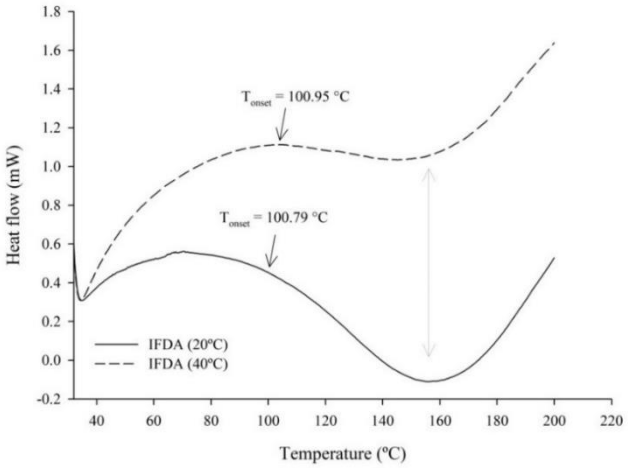

Figure 7.24. DSC of IFDA freeze-dried powder pulled from the freeze-drying cycle at the end of primary drying (IFDA 20ºC) and during secondary drying when the product temperature reached the T_{shelf} (IFDA 40ºC).

On the other hand, no T_g was observed in IFDB DSC curves which was expected because it is a crystalline freeze-dried powder (Figure 7.25). Moreover, the onset of the first thermal event was observed at temperatures >100ºC.

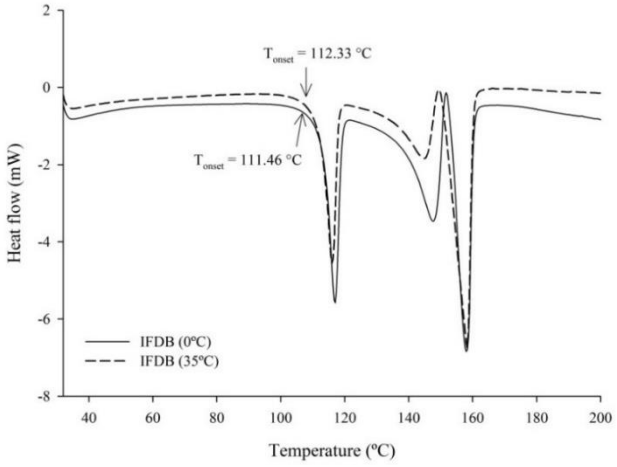

Figure 7.25. DSC of IFDB freeze-dried powder pulled from the freeze-drying cycle at the end of primary drying (IFDB 0ºC) and during secondary drying when the product temperature reached the T_{shelf} (IFDB 35ºC).

As in both cases the first thermal event appeared >50ºC, both secondary drying temperature ranges were adequate. Thus, the maximum ramp rate was also justified, as no relevant changes in the DSC curves were observed at the beginning and at the end of the secondary drying ramp.

After that, the impact of T_{shelf} and secondary drying time on CQAs for both drug products was investigated. The main objective was to choose secondary drying setpoints principally based on the RMC level. Nevertheless, changes in other CQAs were also evaluated to verify product quality.

For IFDA formulation, three freeze-drying cycles were performed at different secondary drying temperatures (50ºC, 40ºC and 30ºC) keeping the freezing and primary drying stages constant. In the three cycles, samples were extracted after 3 h, 6 h and 16 h of secondary drying. As a large historical data was available for this product, results of these three cycles were compared with the results of 37 industrial batches of the last year (mean, standard deviation, minimum and maximum value). Table 7.27 shows the obtained results.

As observed in Table 7.27, all quality attributes results met IFDA 1 g drug product specifications. In addition, they are within the range of the results from 37 industrial batches, except for RMC at 50ºC after 16 h of secondary drying which is drier than any industrial batch.

Table 7.27. CQAs results of the secondary drying study for IFDA. SD=secondary drying.

Batches	**SD temp**	**Residual moisture content (%)**			**Microbiological potency (%)**			**Assay (%)**		
		3 h	6 h	16 h	3 h	6 h	16 h	3 h	6 h	16 h
SD_Cycle1	50ºC	0.69	0.60	0.40	99.0	98.2	98.1	95.7	95.6	95.3
SD_Cycle2	40ºC	0.83	0.59	0.59	98.9	97.7	98.8	95.8	95.5	95.6
SD_Cycle3	30ºC	0.82	0.57	0.74	99.0	98.2	97.5	95.8	95.6	95.5
		Mean	**std**	**Range**	**Mean**	**std**	**Range**	**Mean**	**std**	**Range**
Industrial (n=37)	40ºC	1.21%	0.48%	0.5%-2.6%	99.7%	1.9%	97.3%-107.5%	95.1%	0.58%	93.7%-96.0%
Specification		≤5.0%			95%-110%			≥93%		
Batches	**SD temp**	**Greatest individual known impurity** (%)			**Individual unknown impurities** (%)			**Total impurities** (%)		
		3 h	6 h	16 h	3 h	6 h	16 h	3 h	6 h	16 h
SD_Cycle1	50ºC	1.68	1.66	1.69	0.68	0.66	0.77	4.30	4.41	4.67
SD_Cycle2	40ºC	1.67	1.71	1.66	0.65	0.82	0.87	4.24	4.48	4.43
SD_Cycle3	30ºC	1.64	1.66	1.65	0.78	0.81	0.80	4.25	4.36	4.53
		Mean	**std**	**Range**	**Mean**	**std**	**Range**	**Mean**	**std**	**Range**
Industrial (n=37)	40ºC	1.99%	0.30%	1.25%-2.49%	0.51%	0.30%	0.10%-1.24%	4.87%	0.58%	4.00%-6.40%
Specification		≤4.0%			≤1.5%			≤7.0%		

After 6 h of secondary drying, all RMC results were very similar and, only at 50ºC, samples were able to desorb more water after 16 h of secondary drying. Figure 7.26 shows the results graphically as a

function of secondary drying temperature and time. As expected, at 50ºC, RMC dropped faster when compared to the other two temperatures Nevertheless, all RMC results were ≤ 1% which is a typical target level of RMC in freeze-drying cycles development.

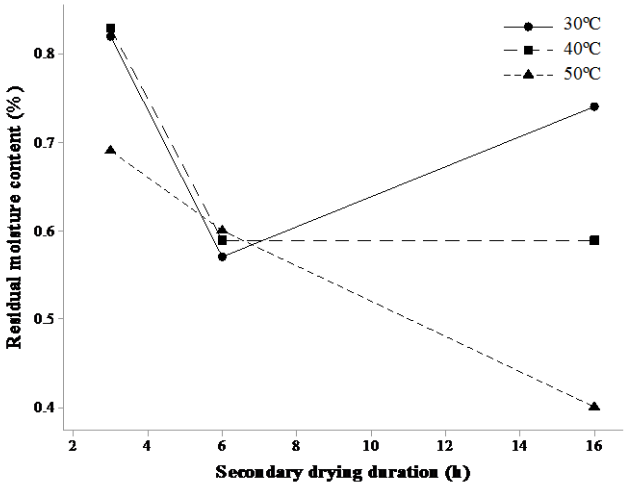

Figure 7.26. RMC results as a function of time at three secondary drying temperatures for IFDA.

In all cases cake appearance was acceptable, no collapse was observed. Microbiological potency varied from 99% to 97.5%, which was considered a minor change considering the greater variability of biological methods. Assay remained above 95% and it seems to be unaffected by secondary drying temperature. Nevertheless, a slight reduction in microbiological potency and HPLC assay, and a slight increment in impurity results were observed throughout secondary drying time.

As observed in Figure 7.27, the increment in total impurities is more significant at 50ºC, and the highest percentage of total impurities at 40ºC is observed after 6 h of secondary drying. However, compared with the specification value (7.0%), this tendency was considered irrelevant.

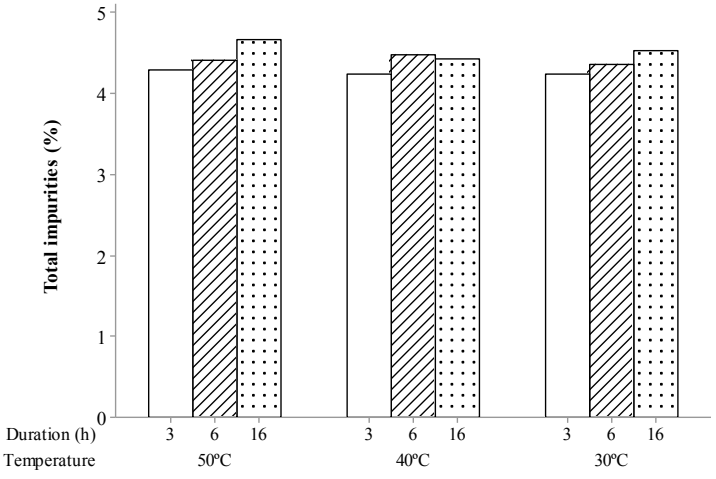

Figure 7.27. Total impurities results as a function of time at three secondary drying temperatures.

In conclusion, based on the RMC levels, 6 h of secondary drying seemed to be the optimum. But, considering the results of the rest of CQAs evaluated and the objective of optimizing drying efficiency, 3 h of secondary drying were chosen for the freeze-drying cycle setpoint. After 3 h, RMC was <1% and the decrease in potency and assay was minimized. The levels of individual and total impurities were also minimized. Moreover, the temperature was maintained at 40°C, to guarantee a safety margin, even though at 50°C the quality of the finished product was correct. However, it has been shown that secondary drying is robust between 30ºC and 50ºC and from 3 h to 16 h.

For IFDB formulation, only the extremes of the secondary drying temperature range (25ºC and 45ºC) were studied after 4 h, 8 h and 12 h of secondary drying. Results are shown in Table 7.28.

Table 7.28. CQAs results of the secondary drying study for IFDB. SD=secondary drying.

Batches	**SD temp**	**Residual Moisture Content (%)**			**Assay (%)**			**Total impurities (%)**		
		4 h	8 h	12 h	4 h	8 h	12 h	4 h	8 h	12 h
SD_Cycle1	45ºC	0.91	0.82	0.75	103.2	-	102.9	0.34	0.35	0.36
SD_Cycle3	25ºC	0.80	0.78	0.73	100.90	-	102.20	0.33	0.32	0.33
Specification		≤2.0%			95.0%-105.0%			≤0.5%		
Batches	**SD temp**	**I-1 impurity** (%)			**M-1 Impurity** (%)			**Unknown impurities** (%)		
		4 h	8 h	12 h	4 h	8 h	12 h	4 h	8 h	12 h
SD_Cycle1	45ºC	0.20	0.21	0.22	0.09	0.09	0.09	0.05	0.05	0.05
SD_Cycle3	25ºC	0.22	0.21	0.22	0.06	0.06	0.06	0.05	0.05	0.05
Specification		≤0.30%			≤0.15%			≤0.10%		

The RMC results decreased slightly at longer secondary drying times with no significant difference with regards to secondary drying temperature (Figure 7.28). However, with 4 h of secondary drying it was enough to obtain RMC < 1% in both cycles.

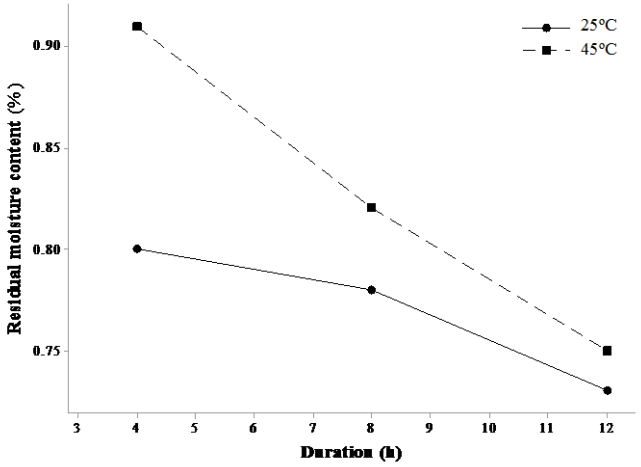

Figure 7.28. RMC results as a function of time at three secondary drying temperatures for IFDB.

All the evaluated CQAs complied with specifications. Similar results were obtained in all CQAs regardless of the secondary drying temperature except for the increment in M-1 impurity. Although M-1 results are within specification, there seemed to be a correlation between temperature and the level of Impurity M-1, which did not depend on time. As a result, 4 h and 35ºC were selected for the freeze-dying cycle of IFDB.

In both formulations it was demonstrated that the shortest secondary drying time and the midpoint temperature of the range were suitable conditions for freeze-drying cycle design balancing the process efficiency with product quality.

3.2. Primary drying study

Once the conditions for the secondary drying phase were established, the DoE for the primary drying was executed for both formulations.

Table 7.29 shows the parameters of the primary drying used in each cycle of the DoE and the results of the responses. During DoE data analysis, the abbreviations used for temperature and pressure were T and P respectively.

Table 7.29. Worksheet of the DoE for the primary drying study of IFDA drug product.

Exp	T (ºC)	P (mbar)	Primary drying time (h)	Appearance	RT (s) (n=2)	RT (s) (std)	RMC (%) (n=5)	RMC (%) (std)
SP E1	20	0.600	17.92	Complies	36.5	0.7	0.52	0.13
SP E2	40	0.500	14.42	Complies	34.5	0.7	0.32	0.06
SP E3	40	0.300	15.50	Complies	39.5	3.5	0.24	0.02
SP E4	0	0.500	28.75	Complies	37.0	4.2	0.85	0.19
SP E5	0	0.300	30.75	Complies	32.5	0.7	0.52	0.05
SP E6	20	0.200	21.92	Complies	31.0	1.4	0.33	0.02
SP C1	20	0.420	18.33	Complies	36.0	2.8	0.33	0.03
SP C2	20	0.420	19.58	Complies	34.0	1.4	0.39	0.02
SP C3	20	0.420	19.67	Complies	35.0	1.4	0.35	0.04

Table 7.30. Worksheet of the DoE for the primary drying study of IFDB drug product.

Exp	T (ºC)	P (mbar)	Primary drying time (h)	Appearance	RT (s) (n=2)	RT (s) (std)	RMC (%) (n=5)	RMC (%) (std)
SP E1	10	0.220	21.17	Complies	71.0	1.4	1.06	0.03
SP E2	5	0.307	21.17	Complies	69.0	1.4	1.20	0.09
SP E3	-10	0.220	39.17	Complies	68.5	0.7	1.30	0.08
SP E4	-5	0.133	34.75	Complies	57.0	4.2	1.33	0.08
SP E5	5	0.133	26.92	Complies	60.0	0.0	1.29	0.07
SP E6	-5	0.307	30.00	Complies	77.0	4.2	1.19	0.08
SP C1	0	0.220	27.90	Complies	69.5	2.1	1.21	0.10
SP C2	0	0.220	27.17	Complies	63.5	4.9	1.29	0.13
SP C3	0	0.220	27.00	Complies	72.0	1.4	1.19	0.08

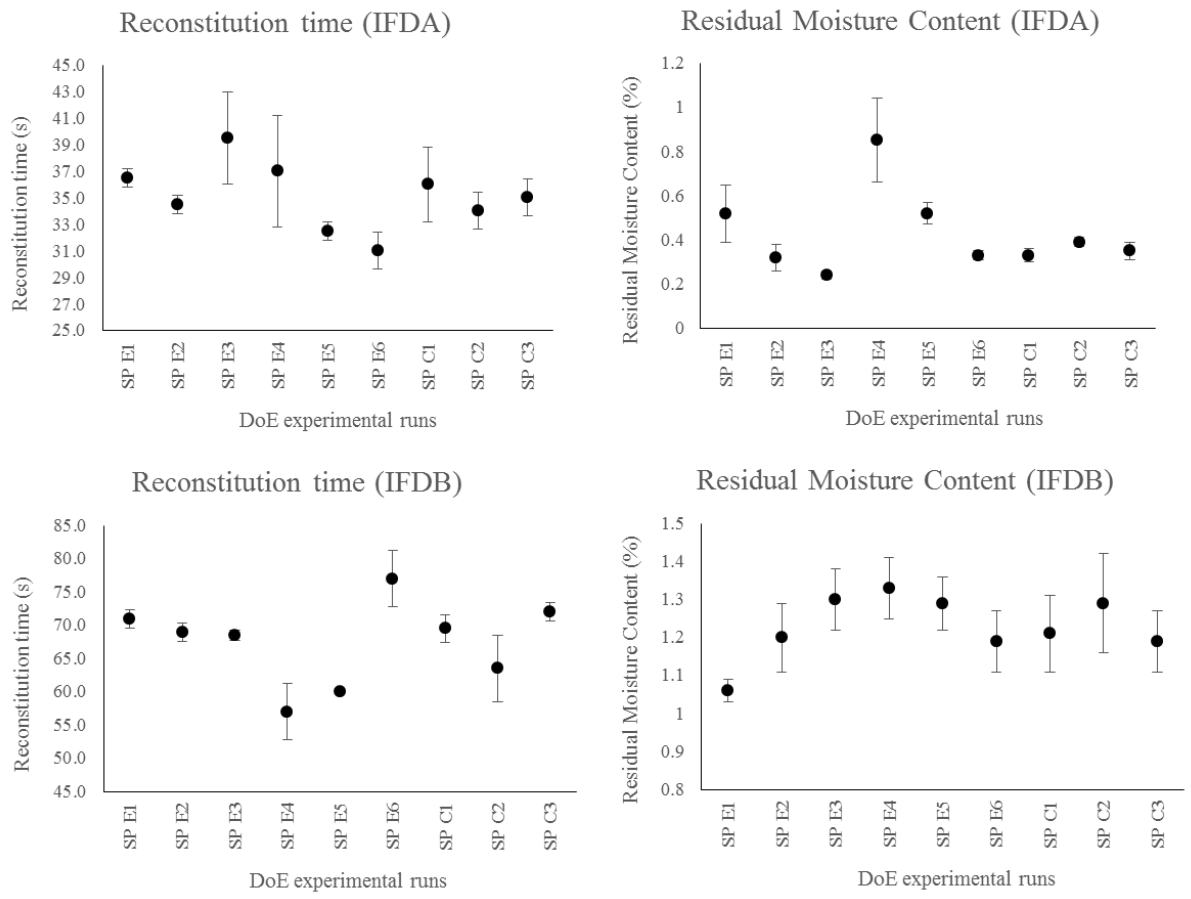

Figure 7.29. Representation of RT and RMC results of the experimental runs for each drug product study. Error bars represented ±1 std.

Responses showed small variations within the examined experimental space compared to the specification value as can be seen in Figure 7.29. All the experiments, in both designs, yielded white to off-white powders after freeze-drying. As observed in Figure 7.30, freeze-dried vials presented a porous and whitish powder with no visible shrinkage or macroscopic collapse of the cake structure.

Moreover, the results shown in Table 7.29 and Table 7.30 indicated that RT and RMC in both freeze-dried products were within product release specifications (Table 7.23).

RMC in IFDA drug product was predicted using a NIR model. However, for IFDB drug product, RMC was determined by KF. Replicates variability was greater in KF analysis of IFDB drug product compared to NIR analysis of IFDA drug product. Nevertheless, the observed variability was more homogeneous among batches. For IFDA, batches SP E1 and SP E4 showed greater variability compared to the other batches of the same product. In fact, one of the five replicates used to calculate the average RMC in SP E4 was an outlier (1.04%). Then, it was removed, and the RMC average decreased to 0.77% with a standard deviation of 0.12% (n=4). Finally, the latter result was used as a response of the MLR model.

Finally, primary drying time showed relevant variability among experimental runs.

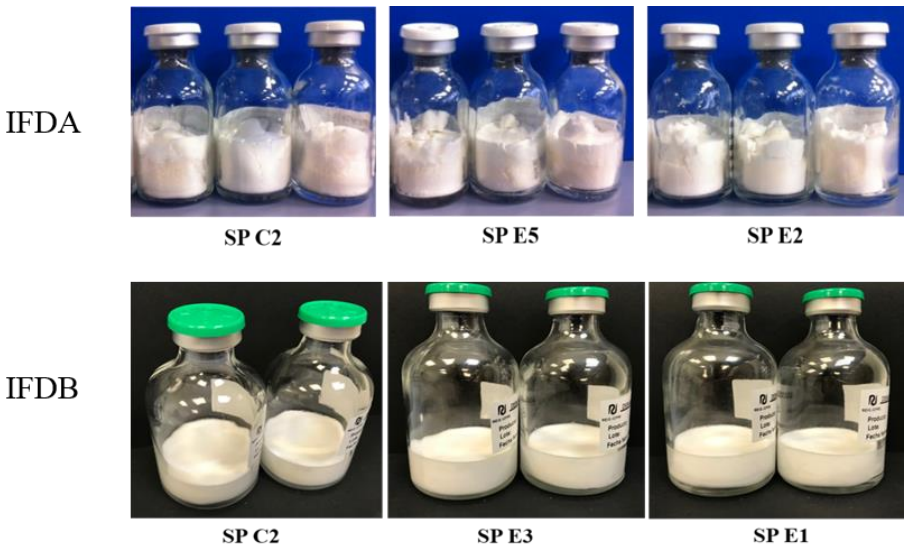

Figure 7.30. Pictures of IFDA and IFDB freeze-dried vials of three DoE runs.

After a general data examination, MLR models were fitted for each quantitative response.

3.2.1. Reconstitution time

The model for RT in IFDA drug product did not show any significant coefficient. In addition, ANOVA regression was not significant even after sequentially removing non-significant terms of the model. Hence, no significant relationship was found between T_{shelf} and pressure with RT for this drug product. A possible cause could be the narrow range of this response obtained in the experimental runs, from 31 s to 39.5 s. In routine analysis, a difference of 10 s in RT is not considered a relevant variation given the inherent variability of the analytical method.

Nevertheless, for IFDB, pressure showed a significant relation with RT (p=0.007). No lack of fit was detected (p=0.689) and reproducibility was high. Hence, a straight line was obtained with regression coefficients described in Table 7.31.

Table 7.31. Regression coefficients for the model of the RT in IFDB drug product.

Reconstitution time (s)	**Coefficient**	**std**	**P-value**	**Confidence interval (±)**
Constant	67.50	1.3	0.000	3.01
P	8.33	2.2	0.007	5.19
N = 9	**DF = 7**		**R^2** = 0.673	**Q^2** = 0.401

However, R^2 was 0.673 and Q^2 was 0.401, both below the desired threshold (0.8 and 0.5 respectively). Predicted vs observed plot showed how different RTs observed in the experimental designed has similar predictions (Figure 7.31).

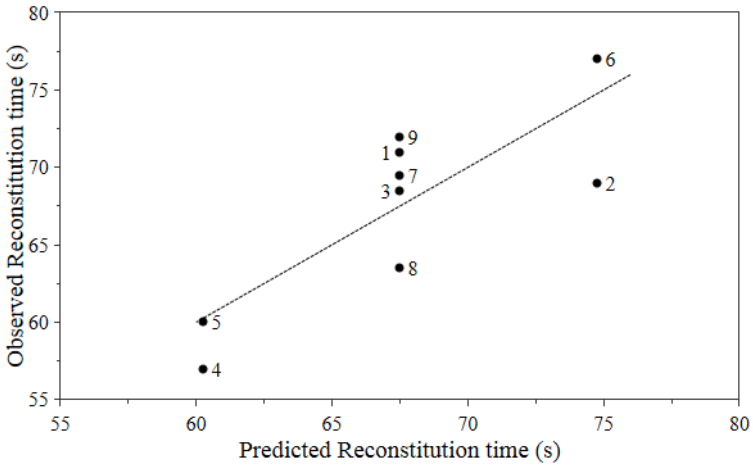

Figure 7.31. Observed vs predicted plot for IFDB reconstitution time.

Finally, although the model was statistically significant ($p<0.05$), the predictive ability of the model was poor. Therefore, only the significant positive correlation between pressure and RT was considered for selection of primary drying conditions.

3.2.2. Residual moisture content

It was only possible to obtain a significant model for RMC in IFDA drug product. The variability of RMC results in all experimental runs of IFDB drug product was very low, of the same magnitude observed in centre-points replicates. This such a low variability could be explained by the crystalline structure of the freeze-dried powder. If the drug crystallizes under the chosen processing conditions, then the drug would be expected to be dry shortly after the end of primary drying, and the desorption process would be of secondary importance. However, as IFDA freeze-dried product is amorphous in the solid state, more water is expected to interact with the molecule that is not removed during primary drying. Then, by applying the same secondary drying conditions, those differences could be easily revealed. A summary of the regression statistics of the model for RMC of IFDA 1 g drug product are described in Figure 7.31.

Table 7.32. Regression coefficients for the model of the RMC for IFDA drug product.

Residual Moisture Content (%)	**Coefficient**	**std**	**P-value**	**Confidence interval (±)**
Constant	0.41	0.03	3.78×10^{-6}	0.06
P	0.11	0.05	0.047	0.11
T	-0.18	0.04	0.003	0.09
N = 9	**DF** = 6		**R^2** = 0.825	**Q^2** = 0.595

Residuals were normally distributed and unrelated to the run order and predicted value. No lack of fit was detected ($p= 0.100$) and the regression was significant ($p=0.005$). The model fit ($R^2=0.825$) and the prediction power ($Q^2=0.595$) were reasonably good.

The regression coefficients of the two significant factors, P_c and T_{shelf}, expressed as parameter estimates, and their statistical significance, are also presented in Table 7.32 and Figure 7.32. Non-significant factors (interaction and quadratic terms) were removed. In addition, the correlation between observed and predicted RMC results is shown in Figure 7.32.

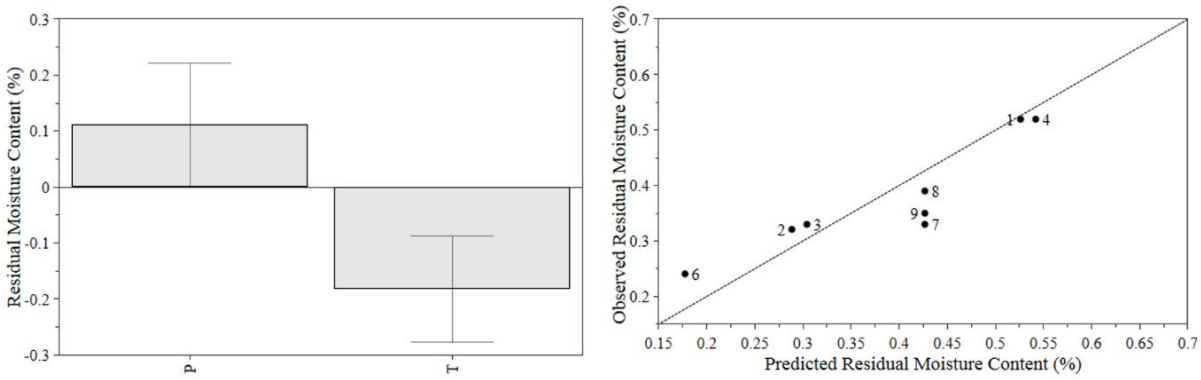

Figure 7.32. Regression coefficients plot (right) and predicted vs observed plot (left) of the RMC model for IFDA.

The effect of the two significant factors is represented in Figure 7.33. An increase in temperature resulted in lower RMC values, whereas an increase in pressure resulted in higher RMC values.

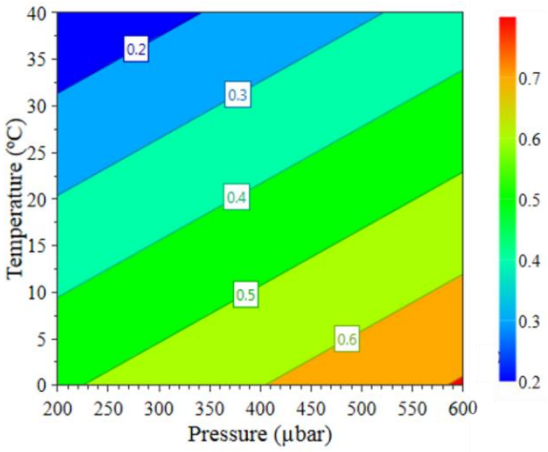

Figure 7.33. Contour plot of the RMC model for IFDA drug product.

3.2.3. Primary drying time

In this case, it was possible to model the primary drying time as a function of temperature and pressure in both formulations. In first instance, it was verified that variability of repeated experiments was much less than the overall variability. Hence, model reproducibility was high. Residuals followed a normal distribution and were randomly distributed as a function of run order.

Moreover, the observed primary drying times and those predicted by the model were very similar in all the experiments, lying very close to the line of slope=1 (Figure 7.34). Additionally, the validity of the model in predicting the selected response was determined by ANOVA. The regression model was significant (p=0.009 for IFDA and p=0.000 for IFDB) and no lack of fit was detected (p=0.744 and

p=0.574 for IFDA and IFDB respectively). Model fit was excellent (R^2=0.99) in both models, thus more than 99% of the variance in the response was explained by each model. Both models also had a high predictive ability (Q^2 > 0.98 in both cases).

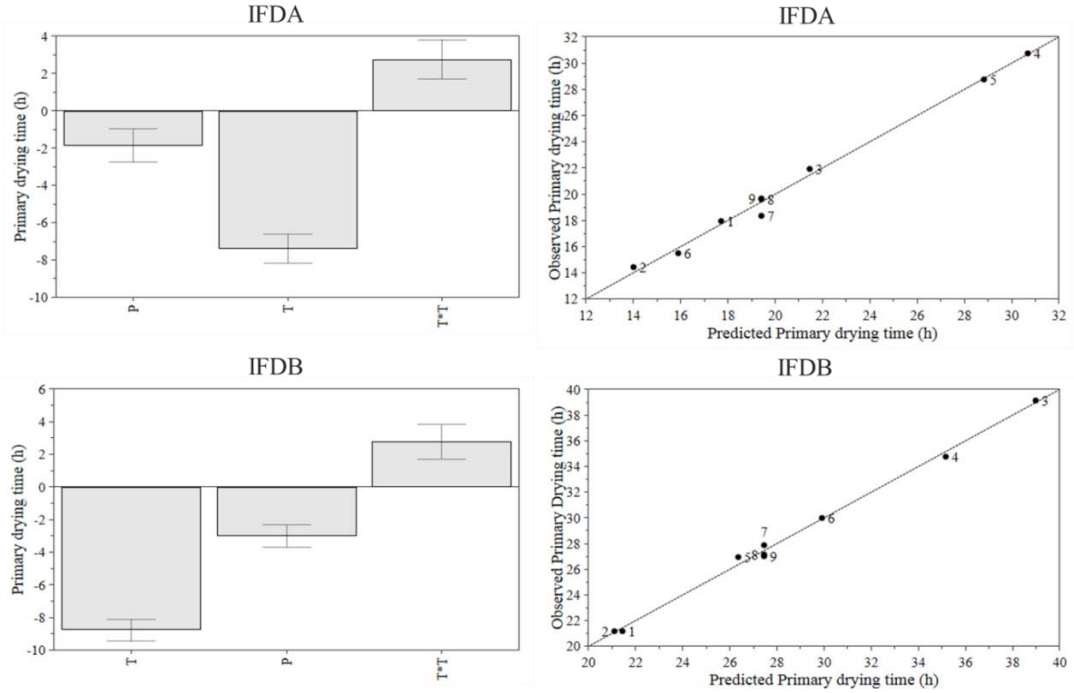

Figure 7.34. Regression coefficients plots (right) and scatter plots of the relationship between observed and predicted response values (left) for both formulations. Error bars indicates the 95% confidence interval.

In both formulations, factors P*P and P*T were not significant (p>0.05). However, the coefficients of variables T, P and T*T were significant, and its values are shown in Table 7.33.

Table 7.33. Coefficients and statistical regression parameters.

	Model terms	**Coefficient**	**std**	**P-value**	**Confidence interval (±)**
IFDA	*Constant*	19.60	0.27	$9.59x10^{-9}$	0.70
	P	-1.87	0.35	$3.03x10^{-3}$	0.89
	T	-7.39	0.30	$2.12x10^{-6}$	0.78
	*T*T*	2.76	0.41	$1.05\ x10^{-3}$	1.04
	N = 9	**DF** = 5		**$R^{2=}$** 0.993	**$Q^{2=}$** 0.980
	Model terms	**Coefficient**	**std**	**P-value**	**Confidence interval (±)**
IFDB	*Constant*	27.44	0.21	$4.46\ x10^{-10}$	0.53
	T	-8.78	0.27	$4.73\ x10^{-7}$	0.68
	P	-3.02	0.26	$8.97\ x10^{-5}$	0.68
	*T*T*	2.77	0.41	$1.08\ x10^{-3}$	1.06
	N = 9	**DF** = 5		**R^{2}**= 0.996	**Q^{2}**= 0.982

In both models, the most influent factor for the modelling of primary drying time was T_{shelf}. This result agrees with other published studies. For example, Xiang et al.[59] also observed that T_{shelf} had the greatest impact on the sublimation rate in their experiments. They found that high temperature resulted in high sublimation rate, regardless of the P_c (30 µbar to 1 mbar).

Figure 7.35 shows a representation of the primary drying time as a function of T_{shelf} and chamber pressure. Some curvature was observed in the contour plot because the quadratic factor T*T was significant in the models of both products. As observed in Figure 7.35, for both products, the shortest primary drying time was obtained using the highest temperature and pressure values.

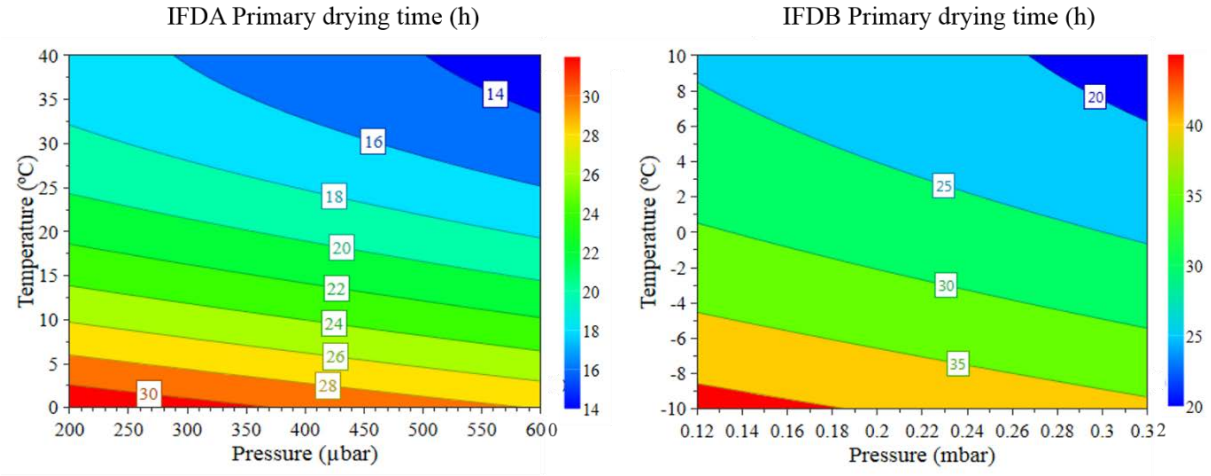

Figure 7.35. Contours of primary drying time as a function of T_{shelf} and P_c during primary drying. Thick line represents the isoline for highest acceptable primary drying time.

This is consistent with the principles of heat and mass transfer of the freeze-drying process. In primary drying stage, T_{shelf} should be high enough to accelerate sublimation without comprising sample quality, combined with a high P_c designed to optimize heat conduction by convection. So, there is no advantage of evacuating the chamber to a substantially reduced pressure.

3.2.4. Determination of optimal primary drying conditions

The obtained models allowed to predict the optimal conditions of the primary drying process that minimize drying time, RT and RMC in the final product. MODDE'S optimizer was used for this purpose. Only significant models were used to select the optimal process conditions.

For the estimation of the optimum, the drying time was weighed by a factor double than the other variables. According to the optimizer, the optimal cycle for IFDA formulation should be performed at 40ºC and 0.600 mbar. These setpoints correspond to the highest limits of the temperature and pressure ranges. Normally, the operating conditions are set within parameters ranges, considering that small fluctuations of the parameters should not fall outside the experimental region studied.

Hence, after adding a safety margin, the following set-points were selected: 35ºC and 0.450 mbar. Model predictions are shown in Table 7.34.

Table 7.34. Model predictions for primary drying time and RMC of IFDA drug product. (CI 95% of the prediction).

Pressure (mbar)	Temperature (ºC)	Primary drying time (h)	Residual Moisture Content (%)
0.600	40	13.09 (11.67, 14.51)	0.34 (0.19, 0.50)
0.450	35	15.13 (14.32, 15.95)	0.31 (0.21, 0.40)

For IFDB, with the objective of minimizing primary drying time as well as RT, the selected optimal conditions were 10ºC and 0.320 mbar. Again, considering a safety margin, the following setpoints were selected: 5ºC and 0.280 mbar. Model predictions are shown in Table 7.35.

Table 7.35. Model predictions for primary drying time and RT of IFDB drug product.

Pressure (mbar)	Temperature (ºC)	Primary drying time (h)	Reconstitution time (s)
0.320	10	18.42 (17.16 , 19.67)	75.83 (69.83 , 81.84)
0.280	5	21.93 (21.26 , 22.60)	72.50 (68.17 , 76.83)

As observed in Table 7.34 and Table 7.35, model predictions for primary drying time have a small confidence interval, suggesting that robust models were obtained. In addition, the differences in the quality attributes were very small between the optimal conditions and the proposed ones, but the primary drying time was extended 2 h and 3 h for IFDA and IFDB respectively. Nevertheless, considering the industrial batch size and industrial freeze dryer characteristics, primary drying time could vary.

For instance, applying a scale correction (multiplying the obtained duration by 1.3, coefficient based on the company experience with other products), the total cycle would last approx. 28.2 h for IFDA and 37.5 h for IFDB. In both cases, the freeze-drying cycles at industrial scale will have a duration of less than 2 days.

Additionally, it was necessary to prove that the mathematical model predictions conform to reality. Two freeze-drying cycles (named SP V1 and SP V2) with the selected parameters were performed at lab-scale to verify that the observed values of primary drying time and RMC were consistent with the ones predicted by the model. This verification was performed only for IFDA drug product.

The appearance of the freeze-dried cake complied with the specification. The primary drying time obtained in the verification cycles PD V1 and PD V2 using the same laboratory freeze-dryer and the same batch size (30 vials), were 15.58 h and 14.58 h respectively. Both results laid within the confidence interval predicted by the model MLR in such conditions of temperature and pressure. In addition, the obtained RMC values were 0.32% (std=0.04%) and 0.21% (std=0.01%) for PD V1 and PD V2 respectively. In both cases, the predicted RMC values were within the 95% confidence interval of the model prediction (0.21%, 0.40%).

Finally, the proposed setpoints for industrial freeze-drying cycles for each drug product are indicated in Table 7.36.

Table 7.36. Proposed freeze-drying cycles for industrial batches of IFDA and IFDB drug products.

IFDA				
Parameters	Soak	Freezing	Primary Drying	Secondary Drying
T_{shelf} *(ºC)*	10	-40	35	40
P_c *(mbar)*	Atmospheric	Atmospheric	$4.5x10^{-1}$	Minimum achievable value
Duration (h)	1	4.5	Pirani/Baratron≤ 1.3	3
IFDB				
Parameters	Soak	Freezing	Primary Drying	Secondary Drying
T_{shelf} *(ºC)*	10	-50	5	35
P_c *(mbar)*	Atmospheric	Atmospheric	$2.8x10^{-1}$	Minimum achievable value
Duration (h)	1	4	Pirani/Baratron≤ 1.2	4

In the next step, the developed freeze-drying process for IFDA 1 g drug product was further confirmed during scale-up and qualification activities (Part 4 of this chapter).

4. Conclusions

It has been demonstrated that a better understanding of formulation characteristics allows to develop a standard freeze-drying cycle with scientific basis.

Regarding the secondary drying study, CQAs analysis of the freeze-dried product with different secondary drying temperatures and durations complied with the specifications in all extraction times. There were no great differences in RMC results over the studied ranges of temperature and durations. Therefore, the selected secondary drying conditions were 40ºC and 3 h for IFDA and 35ºC and 4 h for IFDB.

For the primary drying study, a Doehlert design was executed with two factors (T_{shelf} and pressure) and four responses (primary drying time, appearance, RMC and RT) for each product. Statistical significant models were obtained for RMC and primary drying time in IFDA drug product and RT, and primary drying time for IFDB. The best fit and predictive ability was observed in the primary drying time models, in which temperature factor was the predominant to predict the duration of the primary drying stage. Then, it can be concluded that, while P_c creates the conditions for allowing sublimation to occur, heat input is really the driving force behind the whole process.

In addition, with two additional lab-scale batches. it was verified that the mathematical model predictions matched the experimental evidences. Based on the obtained models for each product, optimal primary drying conditions were selected that minimise the duration of primary drying, while

preserving the quality of the product. Considering 30% of extra time in industrial scale, both cycles will take less than 2 days.

Finally, the design space can be defined as the whole experimental region of the DoE for the primary drying, because all the studied process parameters combinations yielded acceptable product quality in both drug products.

Part 4. Freeze-drying process scale-up and qualification for IFDA drug product

1. Introduction

In the previous experimental section (Part 3), the freeze-drying process of IFDA formulation was designed at laboratory scale. The studied CQAs complied with product quality specifications within the proposed ranges of primary and secondary drying parameters. Then, setpoints were chosen to obtain a freeze-drying recipe suitable for industrial scale qualification batches.

The first step before going through freeze-drying process qualification was the process scale-up. This first batches at industrial scale are commonly named engineering batches. The main objective of the freeze-drying process scale-up was to verify that the process can be executed reproducibly at industrial scale, and yields a product of acceptable quality, consistent with the drug product manufactured at laboratory scale.[60]

Engineering batches can also be used to demonstrate that the process on production scale is robust. Then, the freeze-drying cycle can be set at the upper limits of the process parameters ranges. The more aggressive processes applied lead to greater susceptibility of the product to potential process deviations and inhomogeneities within the batch.[61] Therefore, the engineering batches are used to test the worst-case conditions.

One of the key challenges in scale-up is a thorough understanding of the performance attributes of different freeze-drying equipments.[62] The sublimation rate during primary drying is an important parameter, which needs to be maintained below the maximum allowable sublimation rate for a given freeze-dryer, to avoid dryer overload, which could be caused by condenser overload, refrigeration system overload, or choked flow[j].[63,64] Running under conditions that are excessively aggressive may, for example, result in loss of P_c control, and, perhaps, it may lead to loss of the entire batch.[60]

Once the freeze-drying process has been successfully scale-up to production scale, it can be qualified with full-scale batches under GMP conditions.[47,65] PPQ is the Stage 2 of the process validation lifecycle approach[66], and it consists in the verification that the process operates in a state of statistical control. Therefore, sampling and additional testing during this stage should be more extensive than in routine production, to demonstrate statistical confidence within and between batches of the same product.

There are different methodologies for determining the number of samples and PPQ batches required to satisfy Stage 2 of process validation lifecycle approach.[67–69] In this study, the statistical strategy proposed by Wiles[68] was used to qualify the freeze-drying unit operation of the manufacturing process of IFDA 1 g freeze-dried product. Wiles proposed a combination of risk assessment and capability

[j] Choke point is the maximum sublimation rate that can be supported while maintaining the set point of chamber pressure. The phenomenon of choked flow is associated with the dynamics of the gas flow in the tube that connects the chamber with the condenser.[62] This phenomenon restricts the maximum sublimation speed.[75]

statistics to define the monitoring and testing strategy required to show that a process is operating in a qualified state.

Finally, PPQ batches must undergo a stability[k] program based on ICH Q1A(R2)[70]. This guideline defines the stability data package for a new drug product that is sufficient for a registration application within Europe, Japan, and the United States. Additionally, the engineering batches, and other laboratory batches manufactured at extreme conditions, can be placed on real-time and accelerated stability studies to assess their degradation rate compared to the target freeze-drying cycle.[47]

The purpose of stability testing is to provide evidence on the way that the quality of a drug product varies with time under the influence of a variety of environmental factors, such as temperature, humidity, and light, and to establish a shelf life for the drug product, and recommended storage conditions.[70]

In this study, the scale-up and qualification of the freeze-drying process for IFDA 1 g drug product is presented. The scale-up batch was performed with the most aggressive conditions of the primary drying design space obtained in Part 2 of this chapter (40ºC and 500 µbar, black dot in Figure 7.36), while maintaining the same freezing and secondary drying conditions of the proposed freeze-drying cycle for PPQ batches (green dot, Figure 7.36). Industrial freeze-dryers performance under such aggressive conditions were previously tested using a full-size batch of IFDA 1 g vials filled with water for injections.

Additionally, a laboratory scale batch with parameters set at outer limits of the design space (45ºC and 600 µbar) was executed to expand the studied region and try to find the edge of failure (red dot in Figure 7.36).

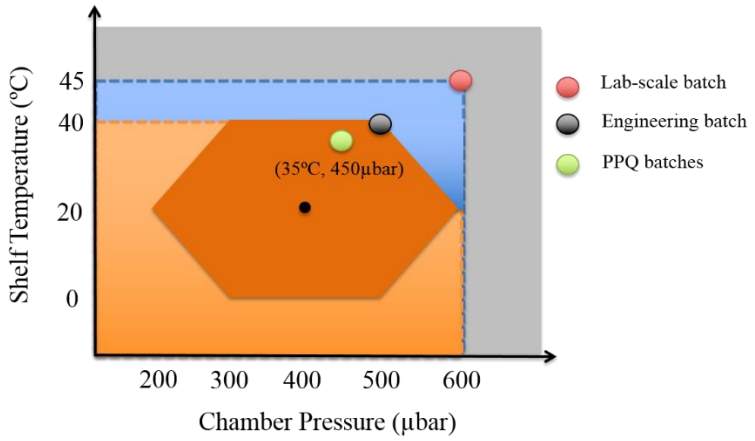

Figure 7.36. Representation of the primary drying design space IFDA 1 g freeze-drying cycle as a function of T_{shelf} and chamber pressure. DoE region is highlighted in dark orange.

[k] The stability of a drug product is described as the ability to maintain its original properties for a certain time within the quality specifications.[70]

After scale-up, the sampling plan for freeze-drying process qualification was established using a risk-based and statistical approach. An assessment of the risk associated with the freeze-drying process transfer from laboratory to industrial scale was performed through failure mode and effect analysis. As a result of this analysis, RMC was considered a medium risk CQA. Then, extensive sampling to evaluate this quality attribute was performed with two main objectives:

a) Determine freeze-drying process qualification based on capability results for RMC.
b) Perform a freeze-dryer moisture mapping of RMC (explained in Chapter 8 Part IV).

Then, the required number of process qualification batches were placed in an ICH stability program, along with the engineering batch and the lab-scale batch. The expiry data of the product was estimated using regression analysis. All data analysis and results of Stage 2 were summarized in a qualification report and were included in a variation application form of the current Spanish dossier which was approved six month later.

It is important to emphasize that the advantages of extending QbD principles from laboratory scale to industry translate in a higher level of assurance of product quality, increasing manufacturing efficiency, time and cost saving and efficiency, for both industry and regulators.[71]

2. Materials and methods

2.1. Samples

IFDA 1 g drug product. The procedure for solution manufacturing is detailed in Chapter 6. A total of 5 batches were performed: L101E (scale-up or engineering batch), LB20 (laboratory scale batch), L1001V, L1003V and L1004V (PPQ batches). Industrial batch size was 253l, which corresponded to 20750 vials. Laboratory scale batch were performed with 280 vials from industrial batches, which were stoppered and transported in trays to the laboratory freeze-dryer.

2.2. Quality control of freeze-dried product

The quality control of the freeze-dried product comprised the following tests: a visual inspection of appearance of the product; determination of the RT; determination of purity (assay and impurities, both by HPLC analysis); estimation of microbiological potency, measurement of RMC with KF titration (for batch release analysis included in the certificate of analysis) and NIR method developed in Chapter 8 (to analyse the extensive sampling in PPQ batches). Table 7.37 shows the freeze-drying product specifications at release and at shelf-life. Additionally, uniformity of mass and dosage units, bacterial endotoxins, sterility, extraneous particulate contamination and hermeticity were analyzed as well, but the results are not shown in the present study.

Table 7.37. Release and shelf-life specifications for IFDA 1 g drug product.

CQAs	Release Specifications	Shelf-life specifications
Appearance	White or almost white porous freeze-dried cake	White or almost white porous freeze-dried cake
Reconstitution time	≤ 1 min	≤ 1 min
Residual Moisture Content	≤ 5%	≤ 5%
Assay	≥ 93.0%	≥ 88.0%
Any individual known impurity	≤ 4.0%	≤ 4.0%
Any individual unknown impurity	≤ 1.5%	≤ 2.0%
Total impurities	≤ 7.0%	≤ 12.0%
Estimated microbiological potency	95% - 115%	95% - 115%

2.3. Freeze-drying equipment and process

Industrial Edwards freeze-dryers 1 and 2 (IMA Life, Italy) described in Chapter 6. Equipment capabilities were investigated, and a qualification test batch was performed to verify that no overloading[l] was observed at most aggressive conditions (40ºC and 500 µbar) of primary drying. This test was performed with maximum batch size (20750 units) of vials filled with WFI, using the same volume (12 ml), and the same primary packaging material as IFDA 1 g drug product.

All cycles were performed keeping constant the freezing and secondary drying conditions of the selected freeze-drying cycle for industrial manufacturing but varying the primary drying setpoints. Freezing was performed at -40ºC for a minimum of 4.5 h. Secondary drying was set at 40ºC for 3 h. The LB20 batch was performed at 45ºC and 600 µbar of primary drying, to expand the studied region and try to find the edge of failure. The scale-up or engineering batch was executed at the upper margin of the design space of the primary drying stage (40ºC and 500 µbar) and three PPQ batches at 35ºC and 450 µbar of T_{shelf} and P_c respectively. All temperature ramp rates were set at the maximum allowable rate for each freeze-dyer (≤ 1ºC/min). The endpoints of each freeze-drying stage had to be adjusted at industrial scale based on the following endpoint determination criteria:

- Primary drying: when the product temperature stabilises at the temperature close to the T_{shelf}, and when the pressure values measured by the two gauges (Pirani and capacitance vacuum gauges) reach very comparable values (Pirani/Baratron = 1.3).
- Secondary drying: when two consecutive PRTs yield with similar values and comparable to the scale-up PRTs results. A PRT had a duration of 15 min and 30 min were left between consecutive PRTs.

[l] The overloading could be caused by small dimensions for the connection between the freeze-dryer chamber and condenser or by limited heat removal capacity of the refrigeration system.[76]

2.4. Risk-based PPQ methodology

First of all, an FMEA was performed to evaluate the risk associated with the freeze-drying unit operation at industrial scale (data not shown). Based on this risk analysis, RMC has a medium risk due to potential lack of batch uniformity with the proposed secondary drying duration.

Then, 350 vials were sampled according to ISO ISO-2859-1-2012 [72] (inspection level II, single sampling for normal inspection) to analyse the RMC of each PPQ batch. All RMC results must comply with the corresponding specification (≤ 5%). Then, to determine the qualification status of the freeze-drying process, process performance capability (P_{pU}) was calculated for RMC according to Wiles proposal.[68]

$$P_{pU} = \frac{USL - \bar{\bar{X}}}{k_2 \hat{\sigma}} \qquad \textit{Equation 7.1}$$

Where P_{pU} is the long-term process performance capability index (for one-side specification), USL is the upper specification limit, $\bar{\bar{X}}$ is the gran mean of the process data, $\hat{\sigma}$ is the long-term process sigma and k_2 is a variable multiple of sigma. Due to the limited number of initial runs, "k_2"[m] was used instead of 3, and it is calculated with the following equation:

$$k_2 = r\sqrt{\frac{mn-1}{X^2_{\gamma,mn-1}}} \qquad \textit{Equation 7.2}$$

Where n is the batch sample size, m is the number of PPQ batches, $X^2_{\gamma,mn-1}$ is the critical value of the chi-square distribution with $mn-1$ degrees of freedom and probability γ=0.95 (statistical confidence of medium risk CQAs according to internal company procedure), and r is the interval covering p=0.990 (statistical coverage[n] of medium risk CQAs according to internal company procedure) of normal distribution found by iteration of the following equation:

$$p = \frac{1}{\sqrt{2\pi}} \int_{\frac{1}{\sqrt{mn}}-r}^{\frac{1}{\sqrt{mn}}+r} e^{\frac{-t^2}{2}} dt \qquad \textit{Equation 7.3}$$

The value of r was evaluated using the NORMDIST function in Microsoft Excel software. All equations were put into a Solver Excel spreadsheet.

[m] k_2 is a numerical factor used as a multiplier of the standard deviation in order to obtain an expanded uncertainty. The k_2 equation takes into account the statistical degrees of freedom provided by the sample size and number of PPQ batches to yield the factor, k_2, covering the desired proportion of the distribution at the desired confidence. Because the value chi-square increases with increasing degrees of freedom, k_2 decreases as the number of PPQ runs increases. Consequently, even though a process may initially yield a P_{Pu} lower than desired, the decreasing values of k_2 on subsequent PPQ runs will yield successively improved P_{Pu} values.

[n] Coverage is the proportion of the expected future data to be contained within acceptable limits.[68]

Prior to the calculation of P_{pU}, the data was plotted to test data stability and normal distribution. For non-normal data, individual probability distribution along with two normal transformation functions (Box-cox and Johnson transformation[73]) were tested prior to P_{pU} calculation.

To release these batches, the P_{pk} must reach at least the value of 1, when calculated after at least three consecutive batches that comply with all specifications. The process qualification exercise, with extensive sampling for RMC should continue until the lower capability confidence interval (LCCB) reaches at least the value of 1. LCCB was calculated with the following equation:

$$LCCB = P_{pU} - Z_{1-\frac{\alpha}{2}}\sqrt{\frac{1}{k_2^2 mn} + \frac{P_{pu}^2}{2(mn-1)}} \qquad \textit{Equation 7.4}$$

Once both, P_{pU} and LCCB reach at least the value of 1, the process is capable and in a state of statistical control. Therefore, the sampling criteria can be reduced to the level corresponding to conventional routine production, and the process can be declared as "Qualified".

2.5. Stability study

According to ICH Q1E[74], regression analysis was used to analyse quantitative stability data for shelf life estimation with a statistical level of significance of 0.25. The factor studied were batch and month. A minimum of 3 batches should be tested to establish a shelf life and storage conditions. If there is no significant difference in slope and intercepts among the batches at $\alpha = 0.25$, the data from all batches can be combined. A single shelf life was estimated from the combined data. If there is significant difference in slope and/or intercepts among batches, the shortest estimate among the individual batches was chosen as the shelf life for all batches.

An appropriate approach to shelf life estimation is to determine the earliest time at which 95% confidence limit for the mean of a CQA intersects the proposed acceptance criterion. CQAs results were tested for normality using histograms and distribution probability plots. None of CQAs results were transformed. An $R^2 \geq 80\%$ was considered an acceptable fit. When the mean response slope was not significantly larger than zero ($p>0.05$), shelf life estimate was not calculated.

2.6. Data processing

Minitab®17 Software (Minitab Ltd, Coventry, UK) was used to perform the capability analysis and regression analysis. Microsoft Excel were used for calculation of P_{pu} and LCCB with the Solver tool.

3. Results and discussion

3.1. Scale-up: industrial equipment performance and engineering batch

First of all, it was verified that the sublimation rate at the most aggressive primary drying conditions (40ºC and 500 µbar) was below industrial freeze-dryers overload. A freeze-dryer cycle was performed with vials filled with WFI and, neither T_{shelf} nor P_c exceeded the setpoint during primary drying. In conclusion, it was demonstrated that there was no risk to run a freeze-drying cycle at industrial scale with these conditions.

Afterwards, the same aggressive conditions were tested using the full-batch size of IFDA 1 g drug product (20750 vials), to verify the upper margin of the design space developed at laboratory scale. It should be noted that, if the lab-scale cycle was properly designed and with adequate safety margin, no adjustments to the T_{shelf} and P_c set points and ramping rates for production-scale cycle might be necessary. Only adjustments to the drying durations may be required because of the scale-dependent factors.[60]

In addition, this engineering cycle was used to determine the duration of each freeze-drying stage (freezing, primary drying, and secondary drying) at industrial scale, and to assess the CQAs of the obtained freeze-dried product.

The evaluation of the lyophilization process includes two complementary aspects: the examination of the freeze-drying parameters and the examination of product characteristics.

As shown in Figure 7.37, the engineering batch (L101E) was executed satisfactorily in 42 h. The product temperature stabilized close to 40ºC after 28-30 h of primary drying, but pressure values did not converge at that time. More time was left to try to observe pressure probes convergence, but it did not completely happen.

At the beginning of primary drying, some fluctuations in P_c were observed due to the high concentration of water vapour in the chamber which hinders the maintenance of the pressure set-point value. Nevertheless, pressure values were stabilized at around 19 h of primary drying (when the registered values followed a straight line) until both probes started to decrease below the set point value at the end of this stage. This indicated that there were not enough water molecules in the chamber to maintain the pressure at the set point value, because the sublimation was finished.

Moreover, the condenser temperature clearly decreased until -70ºC indicating again that there were no more water molecules in the freeze-dryer chamber. Then, the primary drying endpoint was reached after 32 h of drying. At the end of the primary drying stage, the pressure values measured by the two vacuum gauges reached Pirani/Baratron = 1,363. In addition, after 3 h of secondary drying, the two PRTs were comparable (differential pressure of $4x10^{-3}$ and $3x10^{-3}$, respectively).

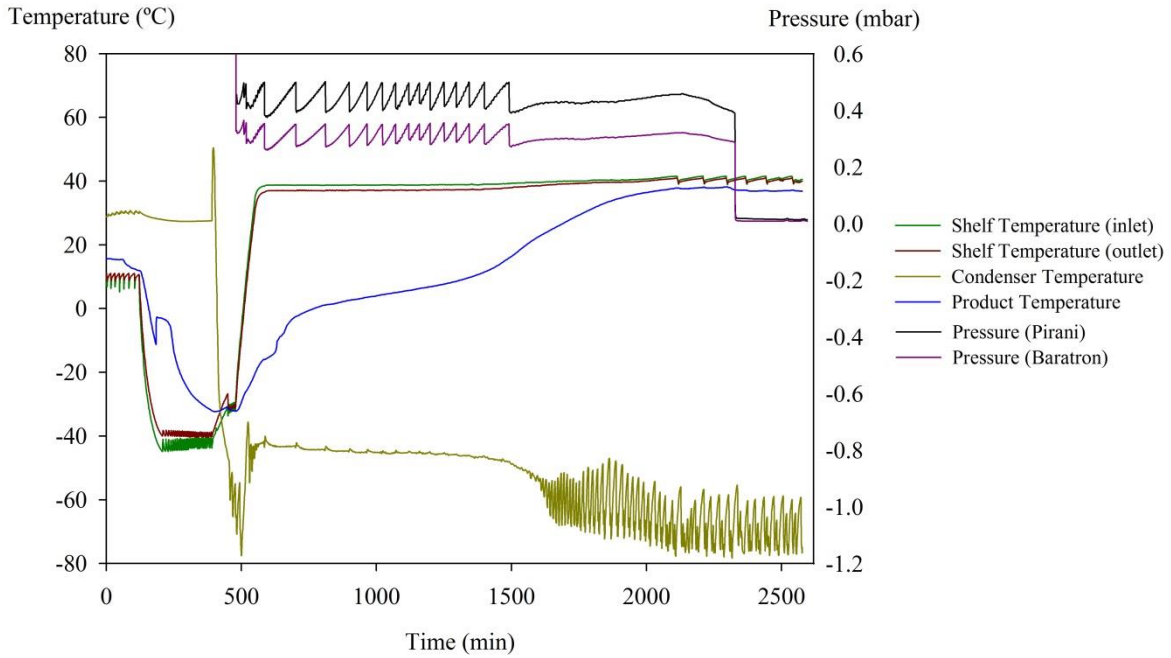

Figure 7.37. Graphical representation of the engineering freeze-drying cycle (L101E).

Finally, all the analysed CQAs complied with the specifications. An acceptable cake structure was observed from the resulting vials, and the rest of analytical tests showed product quality attributes results well within the acceptance criteria and aligned with historical trends (Table 7.38). Hence, it could be concluded that the parameters of the upper margin of the design space developed at laboratory scale were correct and suitable for industrial scale production (at least, at the time of batch release).

Table 7.38. Product quality results of the engineering batch (L101E).

CQAs	**Release Specifications**	**L101E**
Appearance	White or almost white porous freeze-dried cake	White or almost white porous freeze-dried cake
Reconstitution time	≤ 1 min	≤ 1 min
Residual Moisture Content	≤ 5%	0.4%
Assay	≥ 93.0%	*95.0%*
Any individual known impurity	≤ 4.0%	2.15%
Any individual unknown impurity	≤ 1.5%	0.71%
Total impurities	≤ 7.0%	5.04%
Estimated microbiological potency	95% - 115%	104.8%

3.2. Freeze-drying process performance qualification

The purpose of carrying out a performance qualification of the freeze-drying cycle was to demonstrate that the product could be manufactured in a reliable and reproducible manner using the selected freeze-drying process.[47] In order to demonstrate process reproducibility, it is commonly accepted that three

consecutive successful runs are adequate. Then, a statistical approach was implemented to evaluate if more runs were necessary to qualify the freeze-drying process based on the RMC results.

While examination of the final product is essential to ensure that the freeze-drying process performs consistently and as intended, the monitoring of freeze-drying parameters also ensures that they are maintained within an acceptable range, and provides an additional degree of assurance that the process is under control.[47] Hence, first of all, the suitability of the freeze-drying process was evaluated.

According to the control strategy, the following criteria were met during in the three PPQ batches (L1001V, L1003V and L1004V):

- Product temperature during freezing below T_{ts} (do not completely reach -40ºC of but all product probes were below T_{ts} (approx. -25ºC).
- T_{shelf} during primary and secondary drying within defined operating range (0ºC to 40ºC and 30ºC to 50ºC, with setpoints at 35ºC and 40ºC, respectively).
- P_c during primary drying within defined operating range (200 µbar-600 µbar, set point 450 µbar).
- Primary drying endpoint: all product probes reached the T_{shelf} value 30 h after the start of the primary drying. When all the product temperature probes reached the T_{shelf}, the condenser temperature dropped slightly, indicating a decrease in the quantity of condensed water vapour. This suggests that the sublimation was practically finished. Nevertheless, the vacuum gauges did not get together, as it was observed in the engineering batch L101E. At the end of primary drying, pressure values decreased confirming that there was practically no ice left for sublimation. All values of the Pirani/Baratron ratio were lower than the ratio obtained in the engineering batch (1.363) (Table 7.39). Hence, it was considered that the endpoint of sublimation was reached after 34 h of primary drying.
- Two consecutive PRT yielded comparable values (Table 7.39) at the end of the secondary drying stage.

Table 7.39. Pirani/Baratron ratio at the end of primary drying and PRTs at the end of secondary drying.

Batches	Pirani/Baratron ratio	1st PRT	2nd PRT
L1001V	1.31	5.0×10^{-3} mbar	4.0×10^{-3} mbar
L1003V	1.27	3.6×10^{-3} mbar	2.8×10^{-3} mbar
L1004V	1.32	4.0×10^{-3} mbar	4.0×10^{-3} mbar

Figure 7.38 shows a representative example of a freeze-drying graph of one of the PPQ batches (L1003V).

In addition, a full quality control testing of in-process samples and the final product was performed according to the standard operating procedures and release specifications.

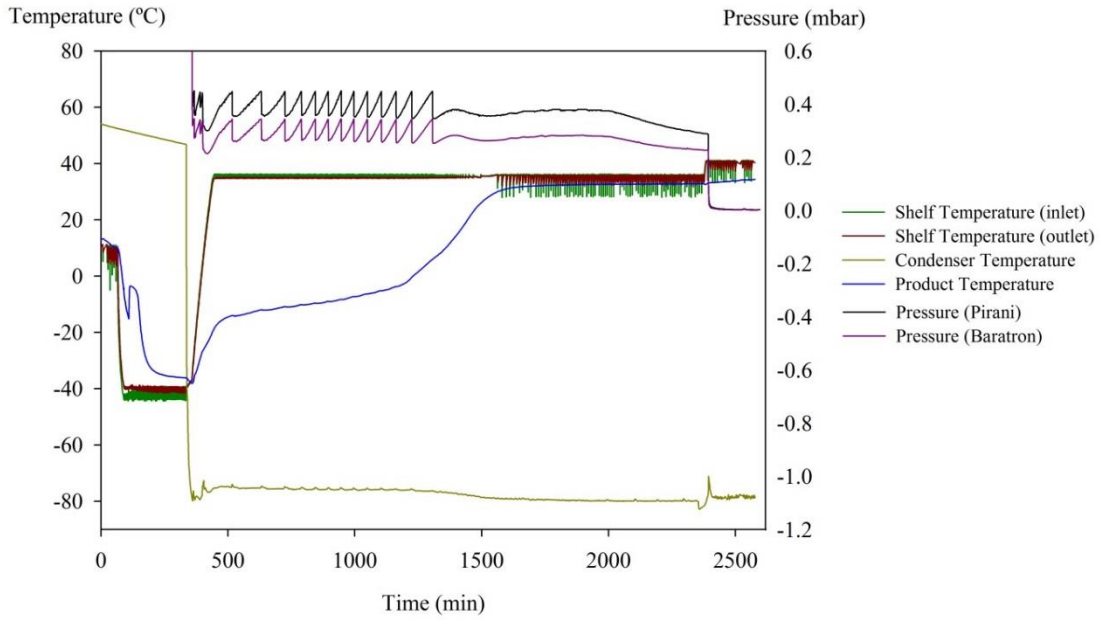

Figure 7.38. Freeze-drying graph of IFDA 1 g batch L1003V.

Liquid samples were taken at the critical stages of the process (e.g., bulk material, formulated solution before and after filtration, filled vials at the beginning, middle, and end of filling) following a sampling strategy based on the FMEA risk analysis (data not shown). The possible impact of each of the changes on the product quality was assessed, and the corresponding risk level was defined. In accordance with the risk level, a specific sampling plan (number of samples to be analysed) was defined.

Regarding the freeze-drying process unit operation, a medium risk level was found on secondary drying time due to the increment of batch size and change of equipment, which could lead with inhomogeneous RMC among vials. Then, extensive sampling was performed to verify batch uniformity, and determine the qualification status of the freeze-drying process for this attribute.

3.2.1. Freeze-drying process qualification for RMC

The RMC of 350 vials/batch was analysed by NIR method and results are shown in Table 7.40. All of them complied with the specification (≤5%) with low intra-batch variability (std <0.10%). Figure 7.39 represents the individual RMC results of each IFDA 1 g PPQ batch.

Table 7.40. Summary of the predicted RMC results for the PPQ batches of IFDA 500 mg and 1 g.

Batch	NIR predicted RMC% (average value)	std (n=350)	Minimum value	Maximum value
L1001V	0.54%	0.03%	0.46%	0.75%
L1003V	0.38%	0.03%	0.27%	0.47%
L1004V	0.48%	0.02%	0.42%	0.56%

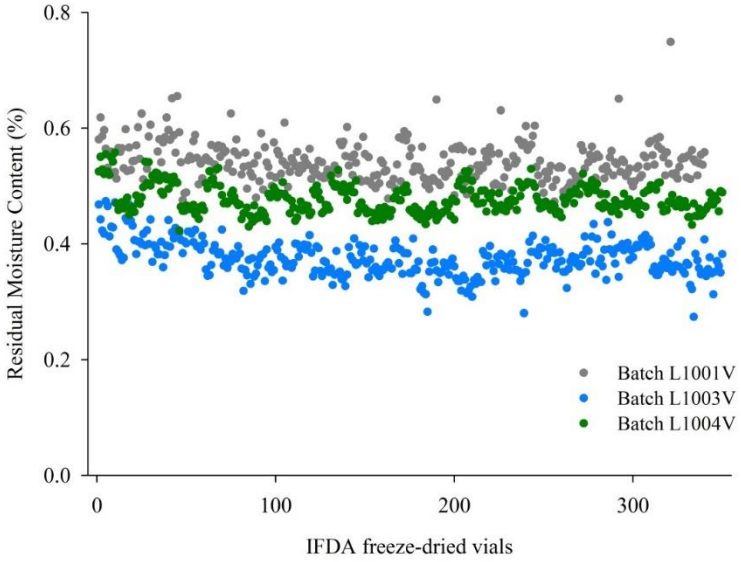

Figure 7.39. Line plot of the RMC results of IFDA 1 g PPQ batches.

First, before conducting process capability analyses, normal distribution and stability of the data was assessed. The first pre-requisite is to verify data stability, i.e. that there are no special causes of variation. In a stable process, all values must be within the control limits (mean ± 3 std). For RMC, as the standard deviation was extremely low (0.03%), the control limits were very narrow < 0.10% and some results felt outside these limits in all PPQ batches.

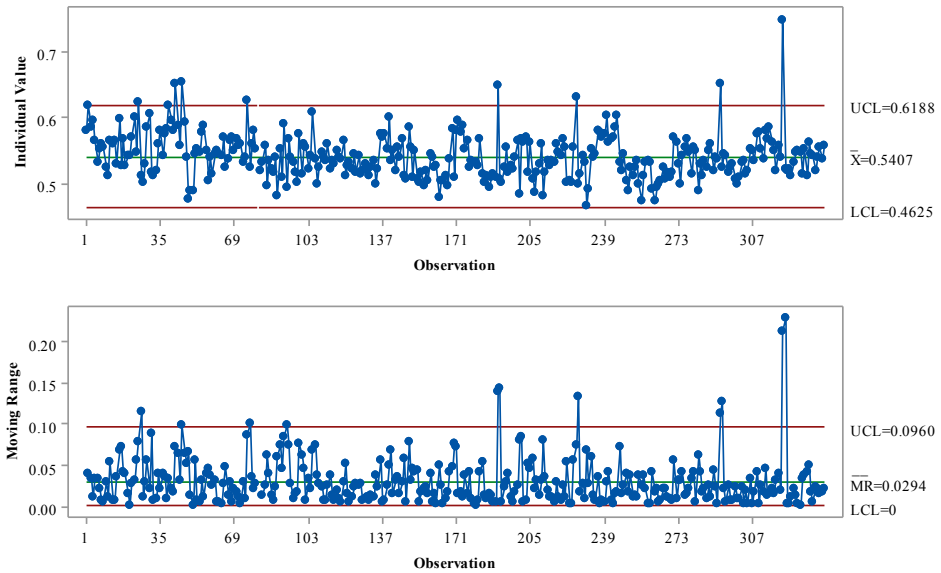

Figure 7.40. I-MR Chart of RMC of batch L1001V.

However, in general terms, the majority of the values laid between UCL and LCL. In addition, the impact of the outside results was studied in the freeze-dryer RMC mapping study (Chapter 8) to investigate if any position or shelf of the freeze-dryer was causing the observed special variations.

However, it should be note that stability analysis assumes that the data is collected across time and that it is done in a chronological order, and it is not the case of RMC sampling.

After that, the assumption of normally distributed data was tested. As shown in Table 7.41, the RMC results of the three batches did not fit to a normal distribution (AD test $p < 0.05$).

Table 7.41. AD normality test of RMC results of the three PPQ batches.

AD normality test	L1001V	L1003V	L1004V
A-square	2.33	0.95	3.77
p-value	<0.005	0.016	<0.005

Nevertheless, as observed in Figure 7.41, the histogram and probability plot showed that the loss of normality was due to a small number of vials that were either drier or wetter compared to the others. The consequence was a slightly skewed distribution.

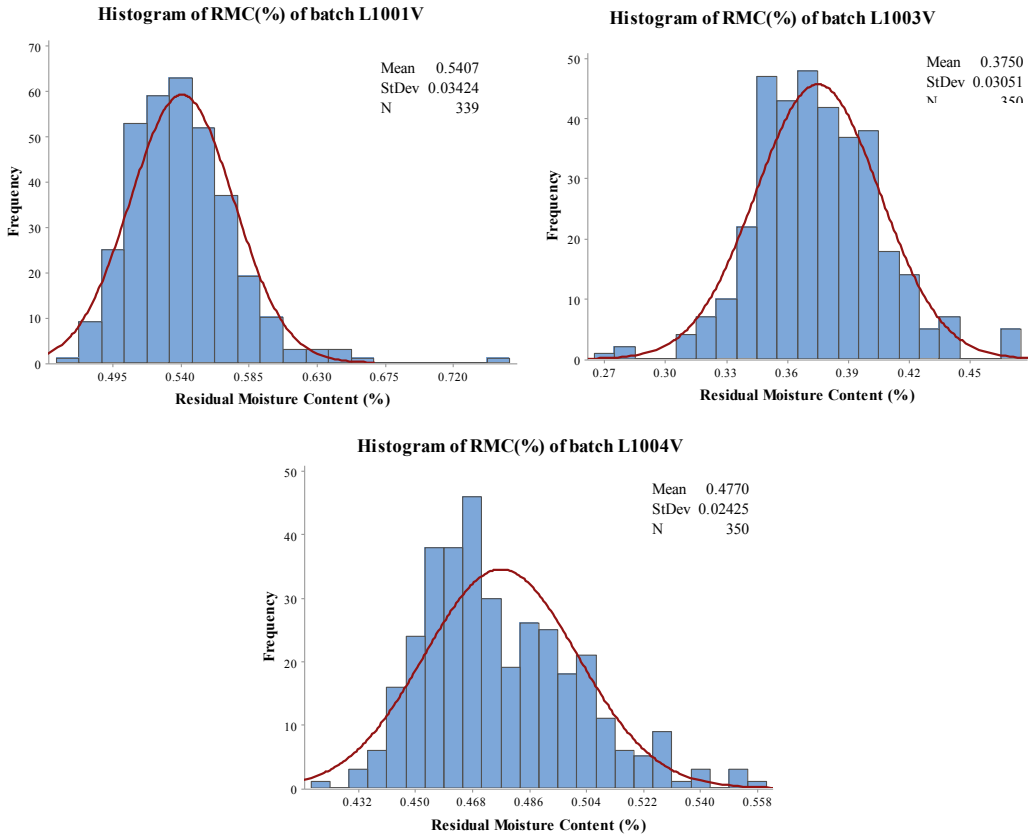

Figure 7.41. Histograms of the RMC results of the three PPQ batches. Mean, std and number of samples per batch are indicated.

Moreover, several individual distributions (lognormal, exponential, Weibull, gamma, logistic and loglogistic) were tested with Minitab, but none of them fitted with the RMC data in all the three batches.

Then, if the deviation from a normal distribution is not too severe, there are transformations[o] that can be applied to make the data emulate a normal distribution. Table 7.42 shows the results of two popular transformations (Box-cox and Johnson Transformation).

Table 7.42. Normality test results of transformed RMC data using Box-cox and Johnson transformation.

Batches	**L1001V**		**L1003V**		**L1004V**	
AD test	AD	p-value	AD	p-value	AD	p-value
Box-Cox transformation	0.173 (λ=-3)	0.927	0.953 (λ=1)	0.016	1.706 (λ=-2)	<0.005
Johnson transformation	0.152	0.960	0.411	0.340	0.514	0.191

Johnson transformation seemed to be suitable for the three PPQ batches of IFDA 1 g. However, the proposed Johnson equation for L1004V did not include the RMC specification limit (5%) in the interval of x values, so capability indices could not be calculated with the transformed data. Finally, as any of the alternative options was completely suitable, the capability indices were calculated with the original data and assuming normality (Table 7.43).

Table 7.43. Capability indices calculation for RMC in IFDA 1 g drug product.

Batches	**r**	**k_2**	**P_{pU}**	**$LCCB_u$**
L1001V	2.58	-	-	-
L1003V	2.58	2.70	18.93	17.93
L1004V	2.58	2.67	22.80	21.82

As observed in Table 7.43, both P_{pU} and $LCCB_U$ results were >> 1. Therefore, the freeze-drying process could be declared as qualified. Despite the result may not be accurate due to the assumption of stability and normality in the RMC data, the freeze-drying cycle was considered capable of yielding with a product that complied with the RMC specification. Consequently, the sampling criteria was reduced to the level corresponding to routine control strategy for batch release.

Finally, it was further verified that the product manufactured at the proposed process conditions was stable throughout product's shelf life.

3.3. Stability study

The IFDA 1 g freeze-dried product was stored in climatic chambers at different temperature and relative humidity (RH) conditions following ICH Q1A(R2)[70] recommendations. Table 7.44 shows the full-design study performed where all samples for all factors combinations were evaluated.

[o] Transformation involves finding a mathematical function that, when applied to the non-normal data, yield a data distribution more closely following that of the normal distribution.

According to ICH Q1A(R2) for room temperature storage condition, the long-term testing of a minimum of 12 months and accelerated testing at 6 months on at least three batches should be delivered at the time of submission and be continued for a period of time sufficient to cover the proposed shelf life.

Table 7.44. Stability program for IFDA 1 g drug product.

Condition*	Temperature (ºC)	RH (%)	Batches	Time-points (M)
Long-term storage	25 ± 2	60 ± 5	L101E, LB20 L1001V, L1003V L1004V	0M, 3M, 6M, 9M, 12M, 18M, 24M and 36M
Intermediate testing	30 ± 2	65 ± 5	L1001V, L1003V L1004V	0M, 3M, 6M, 9M, 12M, 18M, 24M and 36M
Accelerated storage	40 ± 2	75 ± 5	L101E, LB20 L1001V, L1003V L1004V	0M, 3M and 6M

* Long-term at 30ºC 75% for IV zone was also included for dossier registration in other countries. Nevertheless, this experimental is based on the Spain register and the results 30ºC 75% are not needed.

The results of some of the analysed CQAs (RMC, microbiological potency, assay and impurities) after 12 months of stability at all conditions studied for the three PPQ batches are shown in Table 7.45, Table 7.46 and Table 7.47.

Table 7.45. Stability results for batch L1001V.

Parameters		Appearance	RT (min)	RMC (%)	Potency (%)	Assay (%)	Individual known impurity (%)	Unknown individual impurities (%)	Total impurities (%)
Specifications		Whitish porous cake	Indicate result	≤ 5 %	95%-115%	≥ 88.0 %	≤ 4.0 %	≤ 2.0 %	≤ 12.0 %
25 ± 2ºC 60 ± 5 % RH	**0**	Complies	< 1 min	0.5	105.5	94.4	2.11	0.56	5.60
	3 M	Complies	< 1 min	0.5	105.9	93.5	2.01	0.98	6.49
	6 M	Complies	< 1 min	0.6	103.0	92.4	2.15	1.19	7.61
	9 M	Complies	< 1 min	0.6	103.4	92.7	2.09	1.06	7.28
	12 M	Complies	< 1 min	0.6	104.0	92.3	2.10	1.13	7.71
30 ± 2ºC 65 ± 5 % RH	**0**	Complies	< 1 min	0.5	105.5	94.4	2.11	0.56	5.60
	3 M	Complies	< 1 min	0.6	105.1	92.9	2.05	1.05	7.06
	6 M	Complies	< 1 min	0.6	103.6	91.2	2.22	1.33	8.82
	9 M	Complies	< 1 min	0.7	101.3	91.8	2.13	1.17	8.15
	12 M	Complies	< 1 min	0.6	102.2	91.4	2.16	1.18	8.63
40 ± 2ºC 75 ± 5 % RH	**0**	Complies	< 1 min	0.5	105.5	94.4	2.11	0.56	5.60
	3 M	Complies	< 1 min	0.6	101.6	91.0	2.15	1.30	9.00
	6 M	Complies	< 1 min	0.7	101.4	88.2	2.35	1.68	11.80

Table 7.46. Stability results for batch L1003V.

Parameters		Appearance	RT (min)	RMC (%)	Potency (%)	Assay (%)	Individual known impurity (%)	Unknown individual impurities (%)	Total impurities(%)
Specifications		Whitish porous cake	Indicate result	≤ 5 %	95%-115%	≥ 88.0 %	≤ 4.0 %	≤ 2.0 %	≤ 12.0 %
25 ± 2ºC 60 ± 5 % RH	0	Complies	< 1 min	0.4	104.6	94.6	2.10	0.49	5.44
	3 M	Complies	< 1 min	0.4	108.8	92.7	2.18	1.02	7.27
	6 M	Complies	< 1 min	0.4	107.2	92.6	2.21	1.01	7.45
	9 M	Complies	< 1 min	0.5	104.1	92.1	2.25	1.07	7.85
	12 M	Complies	< 1 min	0.5	104.1	91.7	2.21	1.18	8.30
30 ± 2ºC 65 ± 5 % RH	0	Complies	< 1 min	0.4	104.6	94.6	2.10	0.49	5.44
	3 M	Complies	< 1 min	0.4	105.6	92.3	2.19	1.08	7.67
	6 M	Complies	< 1 min	0.5	104.1	91.5	2.23	1.14	8.53
	9 M	Complies	< 1 min	0.5	105.3	91.4	2.25	1.17	8.56
	12 M	Complies	< 1 min	0.5	104.1	90.8	2.22	1.30	9.24
40 ± 2ºC 75 ± 5 % RH	0	Complies	< 1 min	0.4	104.6	94.6	2.10	0.49	5.44
	3 M	Complies	< 1 min	0.5	103.0	89.6	2.32	1.38	10.37
	6 M	Complies	< 1 min	0.6	99.7	88.4	2.39	1.43	11.56

Table 7.47. Stability results for batch L1004V.

Parameters		Appearance	RT (min)	RMC (%)	Potency (%)	Assay (%)	Individual known impurity (%)	Unknown individual impurities (%)	Total impurities(%)
Specifications		Whitish porous cake	Indicate result	≤ 5 %	95%-115%	≥ 88.0 %	≤ 4.0 %	≤ 2.0 %	≤ 12.0 %
25 ± 2ºC 60 ± 5 % RH	0	Complies	< 1 min	0.5	103.3	94.6	2.10	0.75	5.43
	3 M	Complies	< 1 min	0.5	104.8	93.1	2.14	0.99	6.94
	6 M	Complies	< 1 min	0.5	104.0	92.5	2.16	1.06	7.48
	9 M	Complies	< 1 min	0.6	104.1	92.3	2.16	1.19	7.66
	12 M	Complies	< 1 min	0.6	104.2	91.9	2.18	1.21	8.06
30 ± 2ºC 65 ± 5 % RH	0	Complies	< 1 min	0.5	103.3	94.6	2.10	0.75	5.43
	3 M	Complies	< 1 min	0.6	103.7	92.7	2.16	1.03	7.27
	6 M	Complies	< 1 min	0.6	104.5	91.9	2.20	1.11	8.09
	9 M	Complies	< 1 min	0.6	103.4	91.5	2.20	1.31	8.53
	12 M	Complies	< 1 min	0.6	100.8	90.7	2.20	1.33	9.28
40 ± 2ºC 75 ± 5 % RH	0	Complies	< 1 min	0.5	103.3	94.6	2.10	0.75	5.43
	3 M	Complies	< 1 min	0.6	101.3	90.2	2.24	1.35	9.76
	6 M	Complies	< 1 min	0.6	100.9	88.7	2.32	1.42	11.29

It was found that the product quality attributes from the three PPQ batches were well within the acceptable ranges upon the studied storage, suggesting process robustness. Nevertheless, according to ICH Q1E, when long-term and accelerated results show a change over time, statistical analysis of the long-term data can be useful in establishing a shelf life.

Therefore, based on the results of long-term condition (25ºC± 2ºC / 60%± 5%), an estimate of the shelf life of the product (only for quantitative responses) was made, to confirm that it will fulfil the 3 years proposed in the dossier application. The statistical analysis recommended by the ICH Q1E[74] was applied. Quality attributes were fitted to a regression model and the estimated shelf lives are indicated in Table 7.48.

The studied factors were batch, month and the interaction batch-month. When the batch factor was significant ($p<0.25$), a regression model was generated for each batch and the worst shelf life estimation was chosen for all batches. However, when month was not statistically significant ($p>0.25$), it was concluded that the mean response slope was not significantly different from zero. According to the above criteria, no shelf life estimate for microbiological potency was available.

Table 7.48. Estimation of the shelf life of IFDA 1 g using long-term data and regression analysis.

	Estimated shelf life (M)	**R^2**	**Regression Equation**	**Predicted at 36 M**	**Specification**
RMC (%)	344.2	88.36%	RMC = 0.50 + 0.010 M	0.86%	5%
Assay (%)	26.1	80.61%	Assay = 94.067 - 0.1956 M	87.03%	88%
Potency (%)	-	33.84%	-	-	95%-115%
Known individual impurity (%)	182.8	65.84%	Known Imp = 2.1547 + 0.00589 M	2.37%	4%
Unknown individual impurities (%)	23.9	68.81%	Unknown Imp = 0.7413 + 0.04189 M	2.25%	2%
Total impurities (%)	26.4	80.43%	Total imp. = 5.952 + 0.1921 M	12.87%	12%

In addition, Figure 7.42 shows the fitted line with the 95% confidence interval for each quality attribute.

R^2 were >80% except for the individual known and unknown impurities. Nevertheless, the most surprising observation was that the obtained shelf life estimate for assay, unknown individual impurities and total impurities was < 36 months.

It was found that data points for these three CQAs were better suited to a quadratic model, but this model is not suitable to estimate the product's shelf life. Then, a comprehensive examination of the shelf life plots revealed that the cause for such curvature in the data was an abrupt change from t = 0 M to t = 3 M in the three CQAs. Later, from 3 months to 12 months, results seemed to stabilize. Therefore, as an indicative estimate, the shelf life time was estimated eliminating the point t = 0 M for these responses.

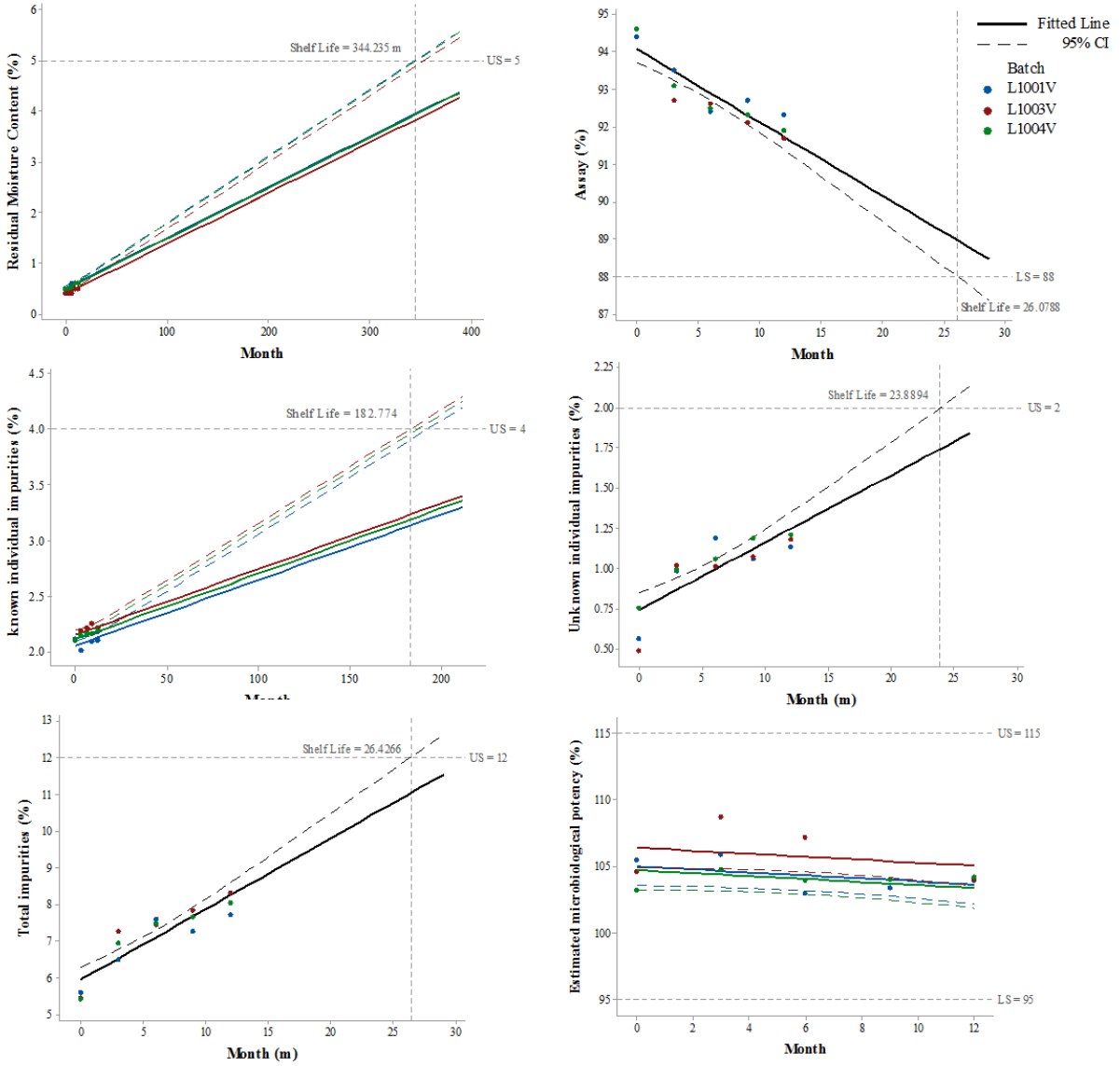

Figure 7.42. Shelf life plot for each CQA with the results of all PPQ batches of IFDA 1 g drug product after 12 months of storage.

The updated regression analysis results are presented in Table 7.49.

Table 7.49. Regression analysis of assay, unknown individual impurities and total impurities after removing the results at t=0M.

CQAs	Estimated Shelf life (M)	R^2	Regression Equation	Predicted at 36M	Specification
Assay (%)	-	84.71%	-	-.	88%
Unknown individual impurities (%)	40.5	56.94%	Unknown Imp = 0.9533 + 0.01833 M	1.61%	2.0%
Total impurities (%)	35.7	84.36%	Total impurities = 6.854 + 0.1151 M	11.0%	12.0%

As shown in Table 7.49, when performing the regression analysis without the result at t = 0 M, the obtained estimations were higher, and closer the proposed shelf life (36 months). Then, based on these results, the proposed shelf life of 36 months can be supported by statistical analysis of all analysed CQAs

except for total impurities, which are very close to the specification limit after 36 months of stability. Nevertheless, this study should be repeated when more stability points are obtained.

Finally, to check the suitability of the design space proposed for the primary drying stage, the 12 months results of the three PPQ batches were compared with the results of the engineering batch L101E (more extreme conditions of the design space) and the laboratory batch (with conditions outside the space of design) at the same storage conditions (Table 7.50). Appearance and RT were within specifications in all batches (white powder and <1 min respectively).

Table 7.50. Comparative table of the 12m stability results of L101E, LB20 and PPQ batches.

12 months	RMC (%)	Assay (%)	Known imp (%)	Unknown impurities (%)	Total impurities (%)	Estimated potency (%)
L101E	0.5	92.4	2.31	1.12	7.56	103.4
LB20	0.6	91.7	2.23	1.18	8.27	103.6
L1001V	0.6	92.3	2.10	1.13	7.71	104.0
L1003V	0.5	91.7	2.21	1.18	8.30	104.1
L1004V	0.6	91.9	2.18	1.21	8.06	104.2

The results of the most aggressive batches (L101E and LB20) at 12 months were comparable with the results of the PPQ batches. At the end of the stability study, it will be verified that all the quality attributes studied meet their respective specifications and the trends of the extreme batches will be compared with those of PPQ, to fully verify the design space of the primary drying stage of the freeze-drying process.

In addition, if the batches produced under extreme conditions are shown to be stable on storage, this is a good assurance that a small deviation from the PPQ cycle will not compromise the stability of the product.[47]

In this study, the presented results belong to IFDA 1 g drug product, however, the same procedure was performed for the other strength, IFDA 500 mg, showing similar results. The full study was presented as a variation of the manufacturing process of the current dossier in the AEMPS. After some meetings with the scientific committee, the variation was approved in approximately 6 months after its presentation. Then, in the last trimester of 2017, the manufacturing of commercial batches of IFDA drug product with the new approved dossier was initiated.

3.4. Next steps

Nowadays, Stage 3 of the process validation lifecycle approach is being under study. Different monitoring strategies will be tested and implemented with the manufacturing batches of this first year

after product approval. Some statistical process control tools, based on batch modelling, are being investigated. The goals of Stage 3 will be:

- Process understanding and/or troubleshooting using variable trajectory data from many batches.
- Infer the final product quality from process conditions during production at the end of a batch.
- Establish a "process signature" and monitor it in real-time, to determine that the batch progresses similar to previous batches.

4. Conclusions

It has been shown that the sublimation rate of the most extreme DoE freeze-drying process took place within the capabilities of mass transfer and heat energy of the industrial freeze-dryer. In addition, the performance of the scale-up batch was satisfactory, and the finished product complied with CQAs at t=0 M and at t=12M. As the upper margin of the design space for primary drying process was confirmed, theoretically, all the combinations of primary drying conditions included within the design space can be used for the application at industrial scale. But, in each individual case, the endpoint should be adjusted according to the previously defined criteria.

For PPQ Batches, the pre-defined values for the freeze-drying parameters, and the duration of all phases complied with the target value or range established during the process design. In addition, the P_{pU} and LCCB parameters were calculated for RMC after the third batch, and both parameters complied with the acceptance criteria (>1). Furthermore, the proposed risk-based methodology for process qualification allows the number of PPQ runs to be derived mathematically based on an assessment of the risks associated with the manufacturing process, thereby satisfying agency expectations for process validation under the new process validation guidance.

To confirm that the proposed shelf life of 36 months can be supported by all CQAs (including total impurities), the regression analysis should be repeated when more stability data are available. Finally, it can be concluded that the manufacturing process, as described and executed, was considered suitable for the implementation in routine production.

References

(1) Awotwe-Otoo, D.; Agarabi, C.; Wu, G. K.; Casey, E.; Read, E.; Lute, S.; Brorson, K. A.; Khan, M. A.; Shah, R. B. Quality by Design: Impact of Formulation Variables and Their Interactions on Quality Attributes of a Lyophilized Monoclonal Antibody. *Int. J. Pharm.* **2012**, *438* (1–2), 167–175.

(2) Jameel, F.; Khan, M. Quality-by-Design as Applied to the Development and Manufacturing of a Lyophilized Protein Product. *American Pharmaceutical Review*. 2009.

(3) ICH. Harmonised Tripartite Guideline Q8(R2) Pharmaceutical Development.2009.

(4) ICH. Harmonised Tripartite Guideline Q9: Quality Risk Management. 2005.

(5) ICH. Harmonised Tripartite Guideline Q10: Pharmaceutical Quality System. 2008.

(6) Mockus, L. N.; Paul, T. W.; Pease, N. A.; Harper, N. J.; Basu, P. K.; Oslos, E. A.; Sacha, G. A.; Kuu, W. Y.; Hardwick, L. M.; Karty, J. J.; et al. Quality by Design in Formulation and Process Development for a Freeze-Dried, Small Molecule Parenteral Product: A Case Study. *Pharm. Dev. Technol.* **2011**, *16* (6), 549–576.

(7) Franks, F. Freeze-Drying of Bioproducts: Putting Principles into Practice. *Eur. J. Pharm. Biopharm.* **1998**, *45*, 221–229.

(8) Patel, S. M.; Jameel, F.; Sane, S. U.; Kamat, M. Lyophilization Process Design and Development Using QbD Principles. In *Quality by Design for Biopharmaceutical Drug Product Development*; Jameel, F., Hershenson, S., Khan, M. A., Martin-Moe, S., Eds.; Springer: New York, 2015; pp 303–329.

(9) Searles, J. A.; Carpenter, J. F.; Randolph, T. W. Annealing to Optimize the Primary Drying Rate, Reduce Freezing-induced Drying Rate Heterogeneity, and Determine Tg′ in Pharmaceutical Lyophilization. *J. Pharm. Sci.* **2001**, *90* (7), 872–887.

(10) Pikal, M.; Shah, S.; Roy, M.; Putman, R. The Secondary Drying Stage of Freeze Drying: Drying Kinetics as a Function of Temperature and Chamber Pressure. *Int. J. Pharm.* **1990**, *60* (3), 203–207.

(11) Jo, E. Thermal Fingerprinting: A Way to Optimise Lyophilisation. *PharmTech*. 2010, pp 1–8.

(12) Kasper, J. C.; Friess, W. The Freezing Step in Lyophilization: Physico-Chemical Fundamentals, Freezing Methods and Consequences on Process Performance and Quality Attributes of Biopharmaceuticals. *Eur. J. Pharm. Biopharm.* **2011**, *78* (2), 248–263.

(13) Searles, J. A. Freezing and Annealing Phenomena in Lyophilization. In *Freeze Drying/Lyophilization of Pharmaceutical and Biological Products*; Rey, L., May, J. C., Eds.; Informa Healthcare: London, UK, 2010; pp 52–81.

(14) Izutsu, K.; Yoshioka, S.; Terao, T. Decreased Protein-Stabilizing Effects of Cryoprotectants Due to Crystallization. *Pharm. Res.* **1993**, *10* (8), 1232–1237.

(15) Izutsu, K.; Yoshioka, S.; Terao, T. Effect of Mannitol Crystallinity on the Stabilization of Enzymes during Freeze-Drying. *Chem. Pharm. Bull. (Tokyo)*. **1994**, *42* (1), 5–8.

(16) Kim, A. I.; Akers, M. J.; Nail, S. L. The Physical State of Mannitol after Freeze-Drying: Effects of Mannitol Concentration, Freezing Rate, and a Noncrystallizing Cosolute. *J. Pharm. Sci.* **1998**, *87* (8), 931–935.

(17) Liao, X.; Krishnamurthy, R.; Suryanarayanan, R. Influence of Processing Conditions on the Physical State of Mannitol - Implications in Freeze-Drying. *Pharm. Res.* **2007**, *24* (2), 370–376.

(18) Schwegman, J. J.; Hardwick, L. M.; Akers, M. J. Practical Formulation and Process Development of Freeze-Dried Products. *Pharm. Dev. Technol.* **2005**, *10* (2), 151–173.

(19) Yu, L.; Milton, N.; Groleau, E. G.; Mishra, D. S.; Vansickle, R. E. Existence of a Mannitol Hydrate during Freeze-Drying and Practical Implications. *J. Pharm. Sci.* **1999**, *88* (2), 196–195.

(20) Larsen, H. M. L.; Trnka, H.; Grohganz, H. Formation of Mannitol Hemihydrate in Freeze-Dried Protein Formulations - A Design of Experiment Approach. *Int. J. Pharm.* **2014**, *460* (1–2), 45–52.

(21) Johnson, R. E.; Kirchhoff, C. F.; Gaud, H. T. Mannitol-Sucrose Mixtures--Versatile Formulations for Protein Lyophilization. *J. Pharm. Sci.* **2002**, *91* (4), 914–922.

(22) Beer, T. R. M. De; Wiggenhorn, M.; Hawe, A.; Kasper, J. C.; Almeida, A.; Quinten, T.; Friess, W.; Winter, G.; Vervaet, C.; Remond, J. P. Optimization of a Pharmaceutical Freeze-Dried Product and Its Process Using an Experimental Design Approach and Innovative Process Analyzers. *Talanta* **2011**, *83*, 1623–1633.

(23) Mehta, M.; Bhardwaj, S. P.; Suryanarayanan, R. Controlling the Physical Form of Mannitol in Freeze-Dried Systems. *Eur. J. Pharm. Biopharm.* **2013**, *85* (2), 207–213.

(24) Ohtake, S.; Shalaev, E. Effect ofWater on the Chemical Stability of Amorphous Pharmaceuticals: I. Small Molecules. *J. Pharm. Sci.* **2013**, *102* (4), 1139–1154.

(25) International Centre for Diffraction Data: Newtown Square, PA, Pattern Numbers: 00-022-1793 (α-Mannitol), 00-022-1794 (δ-Mannitol) and 00-022-1797 (β-Mannitol).

(26) Pyne, A.; Surana, R.; Suryanarayanan, R. Crystallization of Mannitol below Tg during Freeze-Drying in Binary and Ternary Aqueous Systems. *Pharm. Res.* **2002**, *19* (6), 901–908.

(27) Hawe, A.; Frieß, W. Impact of Freezing Procedure and Annealing on the Physico-Chemical Properties and the Formation of Mannitol Hydrate in mannitol–sucrose–NaCl Formulations. *Eur. J. Pharm. Biopharm.* **2006**, *64* (3), 316–325.

(28) Cavatur, R. K.; Vemuri, N. M.; Pyne, A.; Chrzan, Z.; Toledo-Velasquez, D.; Suryanarayanan, R. Crystallization Behavior of Mannitol in Frozen Aqueous Solutions. *Pharm. Res.* **2002**, *19* (6), 894–900.

(29) Cannon, A.; Trappler, E. The Influence of Lyophilization on the Polymorphic Behavior of Mannitol. *PDA J. Pharm. Sci.* **1999**, *54* (1), 13–22.

(30) Hawe, A.; Friess, W. Physicochemical Characterization of the Freezing Behavior of Mannitol – Human Serum Albumin Formulations. *AAPS PharmSciTech* **2006**, *7* (4), E1-9.

(31) Liao, X.; Krishnamurthy, R.; Suryanarayanan, R. Influence of the Active Pharmaceutical Ingredient Concentration on the Physical State of Mannitol-Implications in Freeze-Drying. *Pharm. Res.* **2005**, *22* (11), 1978–1985.

(32) Cao, W.; Xie, Y.; Krishnan, S.; Lin, H.; Ricci, M. Influence of Process Conditions on the Crystallization and Transition of Metastable Mannitol Forms in Protein Formulations During Lyophilization. *Pharm. Res.* **2013**, *30* (1), 131–139.

(33) Kett, V. Development of Freeze-Dried Formulations Using Thermal Analysis and Microscopy. *Am. Pharm. Rev.* **2010**, *13* (6), 80–87.

(34) Kett, V.; McMahon, D.; Ward, K. Thermoanalytical Techniques for the Investigation of the Freeze Drying Process and Freeze-Dried Products. *Curr. Pharm. Biotechnol.* **2005**, *6* (3), 239–250.

(35) Beattie, J. R.; Barrett, L. J.; Malone, J. F.; McGarvey, J. J.; Nieuwenhuyzen, M.; Kett, V. L. Investigation into the Subambient Behavior of Aqueous Mannitol Solutions Using Temperature-Controlled Raman Microscopy. *Eur. J. Pharm. Biopharm.* **2007**, *67* (2), 569–578.

(36) Aubuchon, S. R.; Thomas, L. C. TA 340. Detection and Quantification of Amorphous Content in Pharmaceutical Materials. United States.

(37) Lu, X.; Pikal, M. J. Freeze-Drying of Mannitol–Trehalose–Sodium Chloride-Based Formulations: The Impact of Annealing on Dry Layer Resistance to Mass Transfer and Cake Structure. *Pharm. Dev. Technol.* **2004**, *9* (1), 85–95.

(38) Burger, A.; Henck, J.-O.; Hetz, S.; Rollinger, J. M.; Weissnicht, A. A.; Stöttner, H. Energy/Temperature Diagram and Compression Behavior of the Polymorphs of D-Mannitol. *J. Pharm. Sci.* **2000**, *89* (4), 457–468.

(39) Webb, S. D.; Cleland, J. L.; Carpenter, J. F.; Randolph, T. W. Effects of Annealing Lyophilized and Spray-lyophilized Formulations of Recombinant Human Interferon-γ. *J. Pharm. Sci.* **2003**, *92* (4), 715–729.

(40) Tang, X.; Pikal, M. J. Design of Freeze-Drying Processes for Pharmaceuticals: Practical Advice. *Pharm. Res.* **2004**, *21* (2), 191–200.

(41) Carpenter, J. F.; Chang, B. S.; Garzon-Rodriguez, W.; Randolph, T. W. Rational Design of Stable Lyophilized Protein: Theory and Practice. In *Rationale Design of Stable Protein Formulations: Theory and Practice*; Carpenter, J. F., Manning, M. C., Eds.; Kluwer Academic/Plenum: New York, 2002; pp 109–133.

(42) Hardwick, B. L. M.; Paunicka, C.; Akers, M. J.; Solutions, B. Critical Factors in the Design and Optimisation of Lyophilisation Processes. *Innov. Pharm. Technol.* **2008**, 26–29.

(43) Jennings, T. *Lyophilization: Introduction and Basic Principles*; Informa Healthcare: New York, 2008.

(44) Pikal, M. J. Freeze Drying of Proteins. Part I: Process Design. *BioPharm*. 1990, pp 18–28.

(45) Nail, S. L.; Gatlin, L. A. Advances in Control of Production Freeze-Dryers. *J. Parenter. Sci. Technol.* **1985**, *39* (1),

16–27.

(46) Chang, B. S.; Fischer, N. L. Development of an Efficient Single-Step Freeze-Drying Cycle for Protein Formulations. *Pharm. Res.* **1995**, *12* (6), 831–837.

(47) Bindschaedler, C. Lyophilization Process Validation. In *Freeze-Drying/Lyophilization Of Pharmaceutical & Biological Products*; Rey, L., May, J. C., Eds.; Marcel Dekker, Inc: London, UK, 2004; p 535.

(48) Overcashier, D. E.; Patapoff, T. W.; Hsu, C. C. Lyophilization of Protein Formulations in Vials: Investigation of the Relationship between Resistance to Vapor Flow during Primary Drying and Small-Scale Product Collapse. *J. Pharm. Sci.* **1999**, *88* (7), 688–695.

(49) Trappler, E. Strategies in Development of Lyophilized Parenterals. *Am. Pharm. Rev.* **2007**, 54–58.

(50) Wang, W. Lyophilization and Development of Solid Protein Pharmaceuticals. *Int. J. Pharm.* **2000**, *203*, 1–60.

(51) Sundaram, J.; Shay, Y. H. M.; Hsu, C. C.; Sane, S. U. Design Space Development for Lyophilization Using DoE and Process Modeling. *BioPharm Int.* **2010**, *23* (9), 26–36.

(52) Grant, Y. Dalby , PA. Matejtschuk, P. Use of Design of Experiment and Microscale down Strategies in Formulation and Cycle Development for Lyophilization. *Am. Pharm. Rev.* **2012**.

(53) De Beer, T. R. M.; Wiggenhorn, M.; Hawe, A.; Kasper, J. C.; Almeida, A.; Quinten, T.; Friess, W.; Winter, G.; Vervaet, C.; Remon, J. P. Optimization of a Pharmaceutical Freeze-Dried Product and Its Process Using an Experimental Design Approach and Innovative Process Analyzers. *Talanta* **2010**, *83*, 1623–1633.

(54) Wang, B. S.; Mccoy, T. R.; Pikal, M. J.; Varshney, D. Lyophilization of Therapeutic Proteins in Vials: Process Scale-Up and Advances in Quality by Design. In *Lyophilized Biologics and Vaccines Modality-Based Approaches*; Varshney, D., Singh, M., Eds.; Springer: New York, 2015; pp 121–156.

(55) Doehlert DH. Uniform Shell Designs. *Appl Stat* **1970**, *19*, 231–9.

(56) Burns, R.; Scarminio, I.; Neto, B. de B. *Statistical Design — Chemometrics. Data Handling in Science and Technology*; Rutan, S., Walczak, B., Eds.; Elsevier: Amsterdam, The Netherlands, 2006.

(57) Dejaegher, B.; Heyden, Y. Vander. Experimental Designs and Their Recent Advances in Set-Up, Data Interpretation, and Analytical Applications. *J. Pharm. Biomed. Anal.* **2011**, *56*, 141–158.

(58) Eriksson, L.; Johansson, E.; Kettaneh-Wold, N.; Wikström, C.; Wold, S. *Design of Experiments: Principles and Applications*, 3rd ed.; MKS Umetrics AB: Umea, Sweden, 2008.

(59) Xiang, J.; Hey, J. M.; Liedtke, V.; Wang, D. Q. Investigation of Freeze–drying Sublimation Rates Using a Freeze–drying Microbalance Technique. *Int. J. Pharm.* **2004**, *279*, 95–105.

(60) Sane, S. U.; Hsu, C. C. Considerations for Successful Lyophilization Process Scale-Up, Technology Transfer, and Routine Production. In *Formulation and Process Development Strategies for Manufacturing Biopharmaceuticals*; Jameel, F., Hershenson, S., Eds.; John Wiley & Sons, Inc: New Jersey, 2010; pp 797–826.

(61) Schneid, S. C.; Gieseler, H. Rational Approaches and Transfer Strategies for the Scale-up of Freeze-Drying Cycles. *Chim. Oggi/Chemistry Today* **2012**, *30* (2), 9–12.

(62) Biopharma. Applying Quality by Design to Lyophilization. *BioPharm Int.* **2012**, 22–29.

(63) Patel, S. M.; Pikal, M. Process Analytical Technologies (PAT) in Freeze-Drying of Parenteral Products. *Pharm. Dev. Technol.* **2009**, *14* (6), 567–587.

(64) Searles, J. Observation and Implications of Sonic Water Vapor Flow during Freeze-Drying. *American Pharmaceutical Review*. 2004, pp 1–14.

(65) *Lyophilization of Biopharmaceuticals.*; Costantino, H., Pikal, M. J., Eds.; AAPS Press: Arlington, VA, 2005.

(66) FDA. Guidance for Industry, Process Validation: General Principles and Practices. U.S. Department of Health and Human Services Food and Drug Administration: Silver Spring, MD, 2011.

(67) PDA. Technical Report No. 60: Process Validation: A Lifecycle Approach. *1* (60).

(68) Wiles, F. Risk-Based Methodology for Validation of Pharmaceutical Batch Processes. *PDA J. Pharm. Sci. Technol.* **2013**, *67*, 387–398.

(69) Mitchell, M. Determining Criticality–Process Parameters and Quality Attributes Part III: Process Control Strategies—Criticality throughout the Lifecycle. *BioPharm Int.* **2014**, *27* (3).

(70) ICH. Harmonised Tripartite Guideline Q1A(R2) Stability Testing of New Drug Substances and Products. 2003.

(71) Sylvester, B.; Porfire, A.; Achim, M.; Rus, L.; Tomuta, I. A Step Forward towards the Development of Stable Freeze-Dried Liposomes: A Quality by Design Approach (QbD). *Drug Dev. Ind. Pharm.* **2018**, *44* (3), 385–397.

(72) UNE-ISO 2859-1: Sampling Procedures for Inspection by Attributes -- Part 1: Sampling Schemes Indexed by

Acceptance Quality Limit (AQL) for Lot-by-Lot Inspection: 2012.

(73) Chou, Y.-M.; Polansky, A. M.; Mason, R. L. Transforming Non-Normal Data to Normality in Statistical Process Control. *J. Qual. Technol.* **1998**, *30* (2), 133–141.

(74) ICH. Harmonised Tripartite Guideline. Q1E Evaluation for Stability Data. 2003.

(75) Patel, S. M.; Chaudhuri, S.; Pikal, M. J. Choked Flow and Importance of Mach I in Freeze-Drying Process Design. *Chem. Eng. Sci.* **2010**, *65* (21), 5716–5727.

(76) Tang, X.; Nail, S. L.; Pikal, M. J. Freeze-Drying Process Design by Manometric Temperature Measurement: Design of a Smart Freeze-Dryer. *Pharm. Res.* **2005**, *22* (4), 685–700.

Chapter 8

Development, Validation and Application of a Near Infrared Spectroscopic Procedure for Residual Moisture Content Determination in IFDA Drug Product

Part 1. Risk analysis and feasibility study

1. Introduction

NIRS is an analytical procedure with a wide and varied use in pharmaceutical analysis for both, qualitative and quantitative applications. Regarding its quantitative applications, NIRS is commonly used to determine water content in pharmaceutical drug products. In fact, in the manufacturing sector of freeze-dried injectable products, NIRS has been used as an alternative method to the conventional KF titration to determine RMC in finished products.[1]

The molecular principle that allows considering the use of NIRS for water content prediction is that OH bonds absorb energy in the NIR wavelength range. The most intense absorption bands are located around 1450 nm and 1940 nm. Then, moisture is determined using a regression model developed with a set of calibration spectra with known RMC determined by a reference method. Once this NIR model has been developed and validated, moisture can be predicted directly from NIR spectra resulting in a fast, non-destructive and low-cost determination.[2]

The development and implementation of a NIRS procedure is iterative and adaptable to the application of lifecycle concepts. In this context, the application of QbD principles is considered appropriate within the development and/or validation of the NIRS procedure. The proper use of NIRS requires a sound understanding of the physicochemical basis on which its measurements rely, the instrument and the chemometric principles involved.[3]

In this sense, EMA recommends that the feasibility of using NIRS for the intended purpose should be considered in the method development phase to demonstrate its suitability. The feasibility study should be coupled with a comprehensive evaluation of those risks that may adversely affect the performance of the NIRS method in delivering valid results, which may then lead to an incorrect assessment of quality.[3] Some factors affecting the spectral response are described in *Ph. Eur.* Chapter 2.2.40.[4]

ICH Q9 [5] recommends the use of risk assessment tools to analyse and evaluate those risks. FMEA has become a very popular risk analysis method to evaluate the impact of equipment, facilities and manufacturing operation variables on products or processes. FMEA provides for an evaluation of potential failure modes of method operating parameters and the likely effect of these failures on the performance of NIRS for the intended purpose.[6] FMEA prioritise risks according to a RPN which is the product of severity, probability of occurrence and detectability of the failure effect.

In this study, the feasibility of using NIRS to predict RMC in freeze-dried vials of IFDA 1 g and 500 mg drug products were assessed using risk analysis tools and experimental studies to mitigate the estimated risks, when needed.

2. Materials and methods

2.1. Samples

Freeze-dried vials of IFDA 500 mg and 1 g from production and laboratory scale batches with different RMC were used. The glass type of the vials (type II), solution concentration (8.33%), RMC specification (≤ 5%) and freeze-drying cycle were the same for IFDA 500 mg and IFDA 1 g drug products. Sample thickness was the same; 12 ml of solution in 20 ml glass vial for IFDA 1 g and 6 ml in 10 ml glass vials for IFDA 500 mg. However, they differed in the filled volume and vial size which may cause variations in the energy transmission as well as the resistance to desorption. Therefore, water distribution inside the freeze-dried cake was the only parameter that could be different between IFDA 500 mg and 1 g. Hence, this parameter was assessed with both doses whereas the other experiments were performed only with IFDA 1 g. Polystyrene powder (Sigma Aldrich, St. Louis, MO, USA) was used as well.

2.2. Analytical methods

The laboratory and industrial freeze-drying equipment, LabSpec5000 NIR spectrometer and spectral acquisition procedure, and KF instrument and method are explained in Chapter 6.

2.3. Risk analysis

A FMEA was chosen as the risk analysis tool. The risk analysis, according to the principles given in ICH Q9[5], was addressed to the variables affecting the development of the NIRS procedure and its scope, the response, and the sample presentation. The risk analysis included: the key elements that enable the determination of a suitable NIR response, examination of the effects of sample handling and preparation, and identification of spectral response interfering elements (environment in which measurements take place, sample presentation area, sample temperature, sample thickness, age of samples, solid-state forms, etc.).

Instrument parameters were not included in the risk analysis because the LabSpec5000 spectrometer were previously qualified according to *Ph. Eur.* 2.2.40 [4]. In addition, a system suitability test before sample scanning was performed to evaluate the photometric noise and wavelength accuracy.

The overall risk level was calculated as the product of Severity, Probability and Detectability of the failure modes. The three factors were ranked from 1 to 10 using the qualitative scale described in Table 8.1.

Table 8.1. Definitions and categorical rankings of failure modes for Severity, Probability and Detectability.

Severity *A measure of the possible consequences of a hazard*		
Ranking	**Description**	**Comments**
1	Low	No relevant effect on the development of NIRS model for moisture determination
5	Moderate	Potential effect on the development of NIRS model for moisture determination.
10	High	Severe effect on the development of NIRS model for moisture determination.

Probability *A measure of the likelihood of the possible hazard*			**Detectability** *The ability to discover or determine the existence of a hazard*		
Ranking	**Description**	**Comments**	**Ranking**	**Description**	**Comments**
1	Low	Not likely to occur	*1*	High	Has a good chance of catching failure
5	Moderate	Could occur	*5*	Moderate	May catch failure
10	High	Likely to occur at some time	*10*	Low	Poor chance of finding failure

When the RPN was >25, the risk was considered significant and mitigations actions were proposed, if possible, to eliminate, reduce or control the potential failures. Some risk mitigation actions required experimental studies, which are summarized in Sections 3.2 to 3.7 of the present work.

2.4. Data analysis

All spectra are displayed in absorbance mode and imported to Unscrambler® X10.3 (CAMO, Norway). Spectra were corrected by SG smoothing (Polynomial Order: 2. Smoothing points: 29) in the region of 1810 nm - 1850 nm to reduce the slope variation due to the change of the detector. Afterwards, spectra were corrected using SNV in the range from 1100 nm -2500 nm as a standard pre-treatment. Detailed information of other specific pre-treatments and multivariate analysis of spectra is enclosed in the description of each experiment.

3. Results and discussion

3.1. Risk analysis of the NIRS procedure

Table 8.2 and Table 8.3 show the scores of the FMEA risk analysis of the NIRS procedure.

Table 8.2. FMEA risk analysis of sample presentation to develop a suitable NIRS procedure. Abbreviations: S (severity), P (probability) and D (detectability).

Parameter		Failure Mode	Failure Effect	S	P	D	RPN	Mitigating actions	S	P	D	RPN
Sample production	Freeze-drying cycle	The freeze-drying cycle design is not suitable for IFDA drug product	Samples have a collapsed structure.	**10**	**5**	**5**	**250**	The cycle is well-established and controlled (as explained in Chapter 7). Samples with high RMC that present shrinkage or loss of porous cake structure won't be analysed by NIRS.	**10**	**1**	**1**	**10**
Sample form	Type of material: Freeze-dried powder in specific vial	The powder is too porous, the surface of the lyophilized cake is irregular, and it is not stuck to the bottom of the vial or the cake is broken.	Spectra replicates are not reproducible. Vials with disrupted cake structure have noisy spectra.	**5**	**5**	**5**	**125**	IFDA freeze-dried powders are presented inside a glass vial. No sample preparation is required because the spectrum is collected directly through the closed glass vial. Data pre-treatment techniques will be applied to reduce the noise signals due to physical interferences of the freeze-dried cake and exacerbate the signals of interest (water absorption bands). The bottom surface of the freeze-dried cake should be uniform and stuck to the glass vial.	**5**	**5**	**1**	**25**
Sample source	Laboratory or industrial	Freeze-dried powders obtained from various sources show structural differences in the NIR spectra. Laboratory scale samples present wider variability than that shown for production samples	Poor calibration model with bad predictability.	**5**	**5**	**5**	**125**	The laboratory solution will be manufactured following the manufacturing batch record of the industrial batches and with the same source of API. Lab-scale samples are required to expand the RMC range beyond the variability found in production samples. Hence, spectral variability will be considered by including spectra of samples from industrial batches and lab-scale batches in the NIR model. Differences between both sources of samples will be studied by PCA during model development.	**5**	**5**	**5**	**125**
Sample presentation	Container	The proposed container absorbs NIR radiation	Interferences with samples spectra.	**1**	**1**	**1**	**1**	No mitigation actions required. NIR radiation is not absorbed by glass vials. Then, the measurement can be performed through the glass vial without samples manipulation	**1**	**1**	**1**	**1**
	Sample temperature	The freeze-dried product are not warmed up or stored at a constant temperature conditions.	Spectral changes in the water absorption bands caused by differences in sample temperature.	**10**	**5**	**1**	**50**	Sample temperature is more important for aqueous solutions than for solids and powders containing water. Nevertheless, the effect of the sample temperature will be studied **(Experiment 1)**. Samples will be heated and cooled 5ºC above or below room temperature (25ºC) and changes in the spectra will be analysed.	**10**	**5**	**1**	**50**
Sample position	Orientation (samples presentation area)	Variation in sample placement on the spectrometer, for example, the sample is not totally exposed to the light source.	Uncontrollable noise increment or bad reproducibility which could generate poor calibration models.	**10**	**5**	**1**	**50**	The spectrum is collected through the bottom of the vial covering the sampling window of the ASD Muglight accessory which is smaller than the bottom of the IFDA powder for solution for infusion glass vial. The bottom of the vial is flat and, thus, has a higher contact surface than the lateral of the vial. Using this orientation there is no risk of moving or breaking the freeze-dried cake and all samples are measured in a very reproducible way.	**10**	**1**	**1**	**10**

Parameter		Failure Mode	Failure Effect	S	P	D	RPN	Mitigating actions	S	P	D	RPN
Sample thickness	Light transmission	The sample is not compact enough and some light is transmitted through the freeze-dried powder. Samples height is very thin.	NIR spectral variability between different points of the same vial and between vials of the same product. It causes loss of NIRS signal and it perturbs the calculation of the reflectance factor.	**10**	**5**	**5**	**250**	Sample thickness is constant (1.8 cm approx.). However, the minimum sample thickness not to cause spectral distortion is dependent on the physical and chemical nature of the substance. An experimental study is required to investigate the existence of light transmission. Polystyrene will be added above the freeze-dried cake and NIR spectra will be collected from the bottom of the vial. Polystyrene peaks should not appear in the sample spectrum to guarantee that light is not transmitted through the freeze-dried cake **(Experiment 2)**	**10**	**5**	**5**	**250**
Age of samples	Chemical variation	Samples are unstable. Some impurities, residual water or API increase or decrease its concentration over time.	External variation is introduced in spectra of the same freeze-dried powder which can cause higher levels of error in any quantitative calibration model.	**5**	**5**	**10**	**250**	Moisture content in freeze-dried product may increase with storage time and temperature. Thus, this issue should be investigated. Some vials will be stored at room temperature and its spectra will be collected in different intervals of time. Variability in the NIR spectra of the same freeze-dried powder will be studied **(Experiment 3).**	**5**	**5**	**10**	**250**
	Sample storage conditions	The storage environmental conditions or the storage time change samples composition. It takes a long time between NIRS measurement and KF determination.										

Table 8.3. FMEA risk analysis of NIR spectra acquisition to develop a suitable NIRS procedure. Abbreviations: S (severity), P (probability) and D (detectability).

Parameter		Failure Mode	Failure Effect	S	P	D	RPN	Mitigating actions	S	P	D	RPN
Scanning	Reflectance mode	Sample type is not appropriate for the reflectance mode.	Not representative spectral data which could affect the accuracy and precision of the NIR method.	**5**	**5**	**5**	**125**	Diffuse reflectance (log(1/R)) measurements are performed on solids. NIR radiation penetrates several millimetres allowing sample direct measurement without manipulation. A standard procedure of spectral scanning is described in a SOP to guarantee a correct and reproducible scanning. Spectra are plotted in absorbance by log(1/R) for quantitative applications.	**5**	**1**	**1**	**5**
	Matrix composition (sample optical properties)	Interference of spectral features related to individual chemical components.	Overlapping bands between sample components and water.	**5**	**5**	**5**	**125**	Theoretically, the only variation between production and laboratory vials is the RMC, and the calibration and validation sets will be composed of solely IFDA vials. Therefore, same components and concentration is expected in the finished products.	**5**	**1**	**5**	**25**
	RMC range	Water concentration range is too small to observe relevant differences by the NIR method. Or it is too large	NIR method is not suitable to detect the desired RMC level in IFDA drug product.	**10**	**1**	**5**	**50**	Differences in the intensity of water absorption bands between samples with low and high RMC will be demonstrated in **Experiment 4**. It is also a test to evaluate if high RMC vials could be obtained with good cake appearance. Then, and the % of RMC will be determined by KF	**10**	**1**	**5**	**50**
	Reference standards for background	The % of reflectance does not coincide with the % declared in the certificate. Damage or instability of reference standard,	Calculation errors in sample reflectance values.	**10**	**5**	**5**	**250**	Certified reference standards, according to USP <1119>, are used. The Spectralon blank will be used as white reference measurement. Only spectra measured against the same reference background will be directly compared among them. The standard is stored inside a box. The procedure of background scanning is described in the SOP and includes 5 minutes of continuous collection to evaluate background reproducibility and stability over time.	**10**	**1**	**1**	**10**
	Duration of measurement	Possible sample heating due to long exposition to the lamp (spectral scanning without removing the vial from the sample device)	Spectral changes or loss of water signal due to sample heating.	**5**	**5**	**5**	**125**	This parameter should be investigated in IFDA vials with high and low RMC. Different exposition time intervals to the lamp will be studied. A maximum duration of exposition will be determined **(Experiment 5).**	**5**	**5**	**5**	**125**
	Number of replicates	Some of the spectra replicates are not representative.	The averaged spectrum is biased.	**5**	**5**	**5**	**125**	As a standard rule, three replicates will be acquired and averaged for each sample.	**5**	**1**	**1**	**5**
	Operator	Sample presentation and handling variability.	Another external variation, different from physical and chemical variability, is included in the model.	**5**	**5**	**5**	**125**	Common practices for spectra collection are explained in the SOP. Moreover, sample presentation and scanning procedures specific for IFDA freeze-dried products will be described in the NIRS model calibration and validation protocol according to the feasibility study. There is no sample preparation; hence variability introduced by operators is reduced.	**5**	**1**	**1**	**5**

Parameter		Failure Mode	Failure Effect	S	P	D	RPN	Mitigating actions	S	P	D	RPN
Environment	Temperature	Working outside the operating temperature range of the spectrometer.	Incorrect spectra collection, equipment malfunction.	**10**	**5**	**1**	**50**	This parameter is more important for aqueous solutions than for solids and powders containing water. NIR measurements will be performed in a controlled environment at around 25ºC which complies with Labspec5000 spectrometer operating range (0ºC to 40°C).	**10**	**1**	**1**	**10**
	Ambient Light	Changes in the type and intensity of light.	Additional variability in NIR spectra.	**10**	**5**	**1**	**50**	Spectra collection will always be performed inside the lab in a stable ambient light.	**10**	**1**	**1**	**10**
	Vibration	Spectrum collection is performed under vibration conditions	Spectral noise increment.	**10**	**5**	**1**	**50**	The Lapbspec5000 spectrometer and the sample device are located on a bench in a fix position. The sample is placed above the sample device, there is no sample handling.	**10**	**1**	**1**	**10**
	Humidity	Working outside the operating humidity range of the spectrometer.	NIR spectral changes (e.g. interferences by adding trace moisture absorptions to the spectra).	**10**	**5**	**1**	**50**	The temperature and the relative humidity of the room where the NIR spectrum collection is performed are maintained constant and low (non-condensing conditions).	**10**	**1**	**1**	**10**
Physical Variation	Polymorphism	Presence of polymorphism in the freeze-dried powder.	Difference in the NIR spectrum bands position and/or intensity	**5**	**5**	**10**	**250**	A freeze-dried vial of IFDA 1 g was analysed by X-ray powder diffraction. The X-ray diffraction pattern showed that the product was amorphous.	**5**	**1**	**1**	**5**
	Particle size	Particle size variation in the freeze-dried powder.	The particle size variation influences the light scattering.	**5**	**5**	**10**	**250**	Different particle size could be generated spontaneously during the freezing step. This parameter is uncontrollable; therefore, it is important to account for variation of particle size in the calibration model by using different batches in the model samples sets. Spectra pre-treatment can reasonably reduce most of the particle size effects. It should be checked that the variability explained by the obtained NIR model due to scattering effects is low.	**5**	**1**	**5**	**25**
	Water distribution within the freeze-dried cake	Water is not uniformly distributed throughout the freeze-dried cake.	Bad correlation between water absorption bands in the spectra and the real RMC content in the whole freeze-dried cake	**10**	**5**	**10**	**500**	A uniform water distribution is expected if complete drying is achieved, but it cannot be guaranteed or controlled. In fact, Pikal and Shah [7] demonstrated that during the secondary drying process, a large variation in moisture content can exist throughout cakes**.** These authors found the lowest amounts of moisture existed at the top of the cake and near the walls of the vial. Then, freeze-dried cakes will be first scanned and then grinded up and scanned again. Both spectra will be analysed and compared **(Experiment 6).**	**10**	**5**	**10**	**500**

The parameters with RPN >25 after the proposed mitigation actions were investigated with different experimental studies.

3.2. Experiment 1: Sample temperature

The aim was to study if any detectable variation in the NIR spectrum occurs after storing the samples at different temperatures. Three vials of IFDA 1 g freeze-dried product (laboratory batch LB2020150727, vials 9e, 5b and 2f) with presumably high percentages of RMC were placed inside the laboratory freeze-dryer chamber at a constant temperature for one hour. Immediately after that, spectra were obtained in triplicate. This procedure was performed at three different temperatures 20˚C, 25˚C and 30˚C. Lab-scale vials with high RMC were chosen because, if there is an effect on water content, it will be enhanced and easily detected.

The spectra of each vial at different temperatures were overlapped and no great differences were observed across the whole NIR range. Figure 8.1A shows an example for sample 9e. In addition, the scores plot of the PCA showed clear and separate groups for each vial. Spectra collected at different sample temperatures of the same vials do not show any tendency in the first two PCs which explain 98% of the spectra variability (Figure 8.1B).

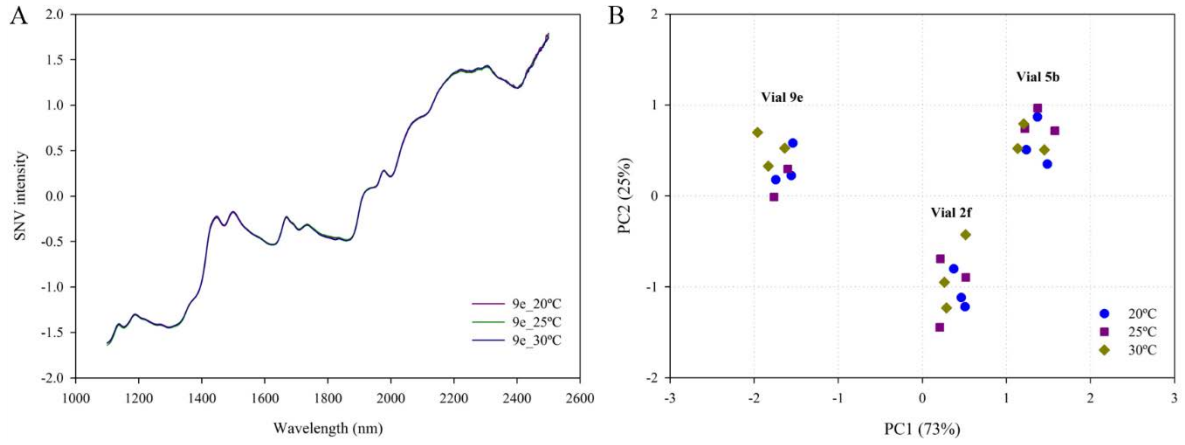

Figure 8.1. Smoothed and SNV-corrected spectra of vial 9e at 20ºC, 25ºC and 30ºC (A) and scores plot of the PCA (B).

It can be concluded that sample temperature in the range of 20-30ºC did not change the spectra as much as the variability normally observed among replicated spectra of the same vial. Nevertheless, once the model was validated, the results were corroborated in the robustness study by predicting the RMC to provide a quantitative result.

3.3. Experiment 2: Sample thickness

The aim of this experiment was to demonstrate that sample was sufficiently thick, and light was not transmitted through the freeze-dried cake. Under these circumstances, absorbance values could be linearly correlated with RMC.

Polystyrene powder, which has specific peaks in the NIR spectrum, was used to evaluate the light transmission similarly to the study performed by Padalkar et al.[8]. Two vials were prepared: one vial of IFDA 1 g freeze-dried product (industrial batch L911) and another vial filled with sufficient amount of polystyrene powder to occupy the volume of the IFDA 1 g freeze-dried cake. Spectra of both samples were collected in triplicate. Afterwards, a layer of polystyrene was added on the surface of the IFDA 1 g vial from the industrial batch and, again, its spectrum was collected in triplicate. Figure 8.2 shows the spectra obtained for each condition.

As observed in Figure 8.2, polystyrene sharp bands (at around 1140 nm, 1680 nm, 2170 nm, 2300 nm, 2350 nm and 2475 nm) are not present in the IFDA 1 g freeze-dried product with a layer of polystyrene above (green spectrum in Figure 8.2). Then, it can be concluded that sample was sufficiently thick and, therefore, the absorbance measurement was suitable to construct the NIR model for RMC determination in IFDA drug product.

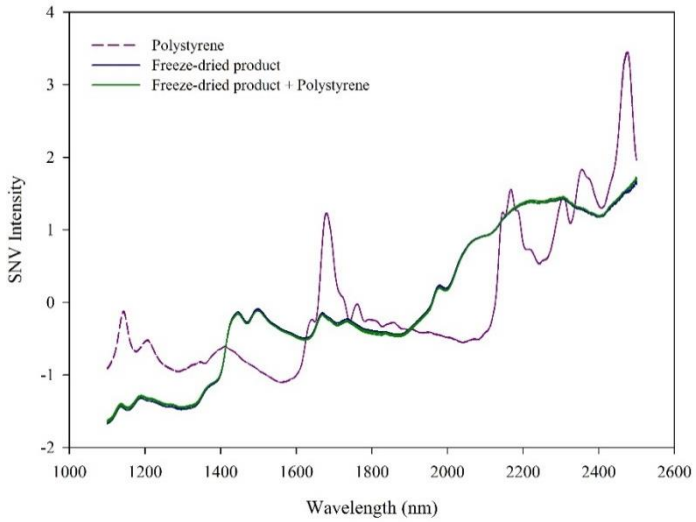

Figure 8.2. Smoothed and SNV-corrected spectra of polystyrene (violet), IFDA 1 g freeze-dried product (blue), and IFDA 1 g freeze-dried product with a layer of polystyrene on the surface of the cake (green).

3.4. Experiment 3: Age of samples

The objective was to study if any detectable variation in the NIR spectrum occurs after sample storage at different periods of time at room temperature. Spectra of five vials of IFDA 1 g freeze-dried product from laboratory batches (laboratory batch LB2020150727, vials 1b, 1c, 4b, 5b and 6b) were acquired in different storage times: 0 h (immediately after the end of the freeze-drying cycle), 1 day, 4 days, 8 days,

2 months and 9 months. Lab-scale samples were used to obtain high RMC values which allow seeing the differences during the storage time more easily.

Figure 8.3 shows only a slight increment in the water absorption band at 1940 nm after 9 months of samples storage. Nevertheless, the same band intensity is observed in the spectra obtained at 0 h and after 8 days of sample storage.

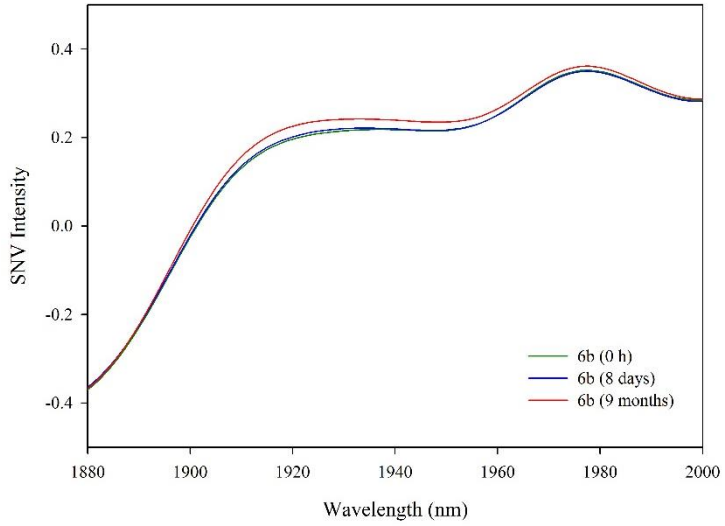

Figure 8.3. Smoothed and SNV-corrected spectra of vial 6b immediately after freeze-drying (0 h, green spectrum) and after 8 days and 9 months of storage (blue and red spectra respectively).

The observed variability was expected and could be explained by the humidity desorption from the stoppers during samples storage. In addition, the same tendency was observed in the 5 vials analysed (all with relatively high RMC values compared to production vials).

Therefore, it was proposed to scan the sample and analyse it by KF method as soon as possible (with a difference of no more than 7 days) to reduce the error due to the age of sample. Lately, during NIR model validation, this factor will be studied further to determine the robustness of the model (Chapter 8 Part 2).

3.5. Experiment 4: RMC range

The aim was to prove that samples with different RMC, could be qualitatively differentiated and that a higher RMC value corresponds to a higher intensity in water absorption bands. Spectra of two vials; one from a lab-scale batch (LB20121215) with high RMC and one from industrial batch (L912) with low RMC were recorded in triplicate and, later, they were analysed by KF method to know the exact value of RMC. The KF result for the laboratory vial was 6.98% and 0.64% for the production vial. The magnitude of the differences observed in the intensity of the water absorption band within the range between 1880 nm and 1950 nm was significant and in agreement with the results obtained by the reference method (Figure 8.4). However, no significant differences are observed in the band at 1450 nm.

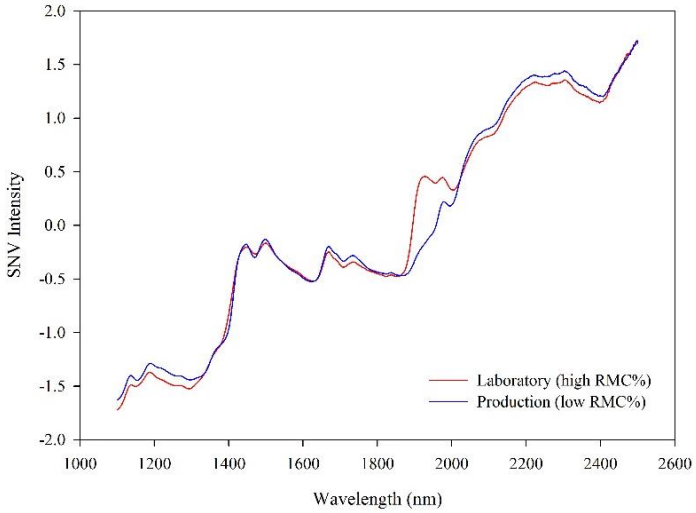

Figure 8.4. Smoothed and SNV-corrected spectra of IFDA 1 g freeze-dried product with high RMC (laboratory batch, red spectrum) and low RMC (industrial batch, blue spectrum).

Hence, the results observed suggested a correlation between the intensity of the water absorption band within the range between 1880 nm and 1950 nm and the % of RMC in IFDA drug product.

3.6. Experiment 5: Measurement procedure

The objective was to determine the maximum time for spectra acquisition by studying various times of exposition to the lamp and the impact of sample heating on the spectrum. According to the literature[9], an increment of the sample temperature may impact on the position and/or intensity of water absorption bands.

The experimental approach consisted in placing a vial on the ASD Muglight sample device. A spectrum was acquired immediately (0 s) and, after that, the vial was removed. This procedure was repeated three times waiting at least 30 s among repetitions. Then, the vial was placed again on the sample device and a spectrum was collected after 30 s, 60 s and 120 s exposition times without removing the vial. This procedure was performed with six vials of IFDA 1 g freeze-dried product: five vials from laboratory batch LB2020150727 (vials 1c, 6c, 7a, 9d and 10b) with different RMC and one vial with low RMC from the industrial batch L911.

No changes in the intensity of the water band were observed within the triplicates at 0 s when vials were removed from the sample device between NIR spectra measurements. However, when the three replicates were collected separately (without continuous exposition to the lamp), they were completely overlapped. Nevertheless, in vials with high RMC, the intensity of the water peak decreased as a function of the duration of exposition to the lamp, and it was already noticeable after 30 s of exposition Figure 8.5A. On the contrary, in vials with low RMC (either from production or laboratory), the intensity of

the water absorption band remained unchanged over the duration of exposition to the lamp (Figure 8.5B).

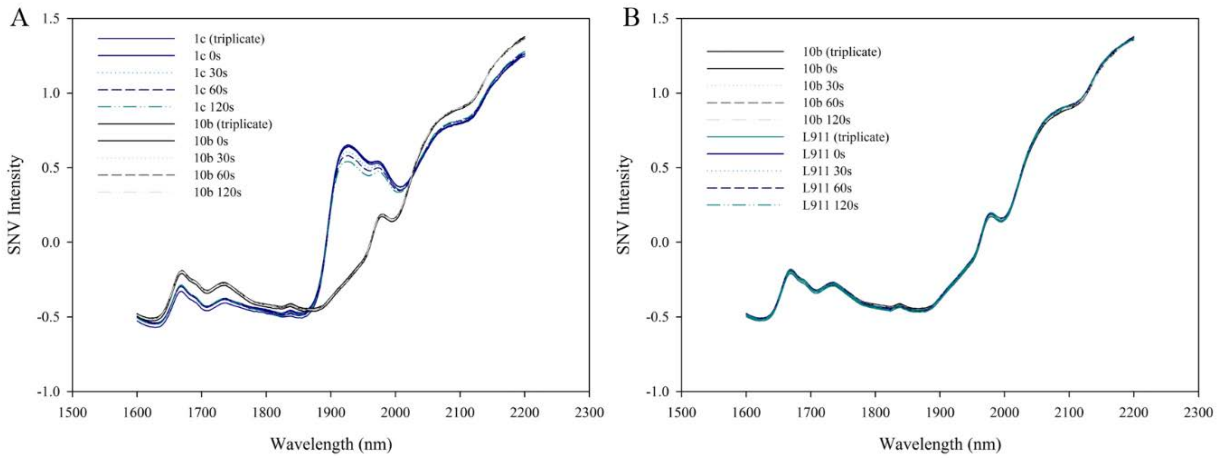

Figure 8.5. Smoothed and SNV-corrected averaged spectra of vial 1c overlapped with vial 10b (A) and vial 10b overlapped with vial L911 (B). Vial 1c had a high RMC while vials 10b and L911 had low RMC.

In conclusion, the spectra collection in the proposed NIRS procedure should be performed by taking away the vial from the lamp after each scanning.

3.7. Experiment 6: Water distribution within the cake

The aim was to study the distribution of water molecules in the freeze-dried cake. Water should be uniformly distributed throughout the freeze-dried cake to compare the results of KF with the NIR spectrum (which only detects few mm of the bottom layer of the cake). Samples used for this study were: three vials of IFDA 500 mg (laboratory batch LB2020160509, vials 3b,4a and 6a) and three vials of IFDA 1 g (laboratory batch LB2020150727, vials 2d,7c and 10c).

Vials were scanned in triplicate, then pulverized, and scanned again. It should be note that it was not possible to open the vial since the sample was highly hygroscopic. Spectra of both groups (before and after pulverization) were analysed by PCA. Some differences in the raw spectra were observed among vials before and after pulverization. For instance, higher baseline offset, and multiplicative effects were observed in the spectra of pulverized samples. To reduce these differences, spectra were pre-treated with a 2nd Derivative SG followed by a SNV, over the NIR range from 1100 nm to 2500 nm.

In Figure 8.6A, the PCA scores plot showed a clear separation between cake structures and powder structures in the PC2. Pulverized and cake samples are placed in the upper and lower part of the PC2 respectively. As observed in the loading plot in Figure 8.6B, PC2 contributed to a 6% of variability among samples which may be related to scattering variations between cake structures and powder structures that were not removed with the applied pre-treatment.

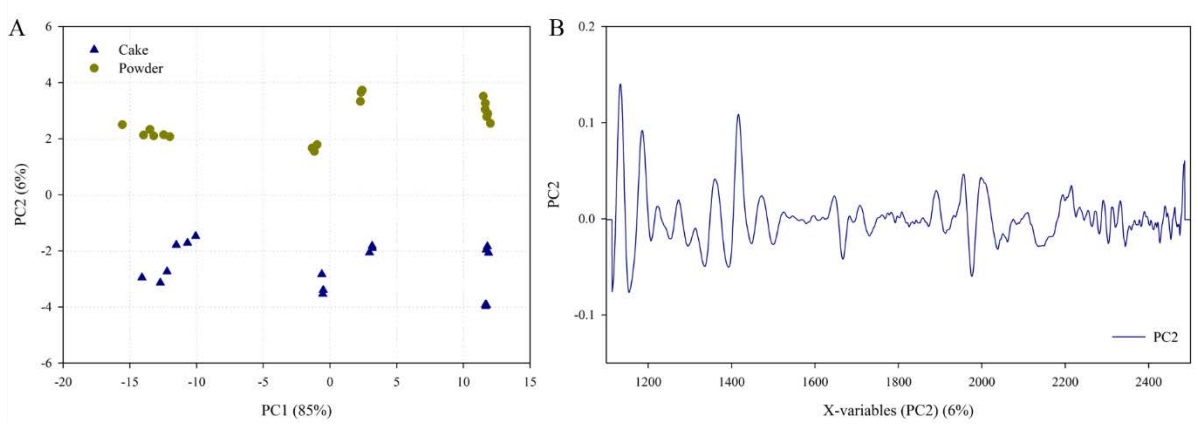

Figure 8.6. Scores plot of the PCA where PC-2 differentiates between cake (blue triangle) and powder (yellow dot) forms (A). The Loading plot of PC-2 is represented in plot B.

The same scores plot is represented in Figure 8.7A, but samples spectra are differentiated as a function of the vial code, instead of the physical appearance of the product. It is shown that the three spectra of each vial are positioned in the same location through the PC1. In addition, the loading plot in Figure 8.7B revealed that the major contribution to the variability explained by this PC is principally located in the water absorption band (1400 nm - 1500 nm and 1900 nm – 1940 nm).

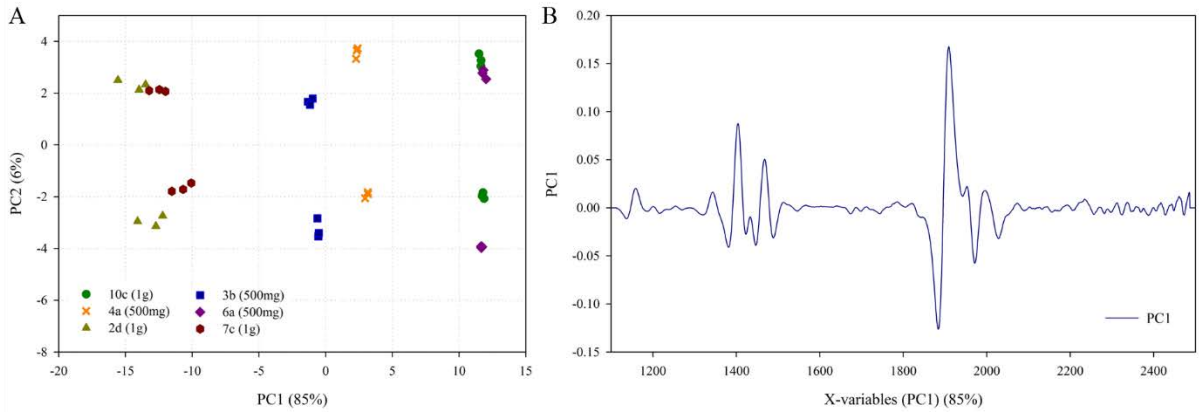

Figure 8.7. Scores plot of the PCA. The three replicates of each vial in both conditions (before and after pulverization) are represented in different symbols and colours (A). The loading plot of PC-1 is represented in plot B.

In conclusion, as no difference are observed among vials either in the intact cake structure or pulverized in PC1, it can be concluded that the intensity of the water absorption bands in the spectra of the vials before and after pulverization did not change. Hence, water seemed to be uniformly distributed through all the freeze-dried cake.

4. Conclusions

Risks related to the NIRS procedure proposed for RMC determination in IFDA 1 g drug product were evaluated by FMEA analysis. According to the results of the risk assessment, further experiments were

needed to mitigate some risks in the following parameters: sample temperature, sample thickness, age of samples, water concentration, duration of exposition to the lamp, and water distribution. Six experimental studies were proposed, and the results revealed that no risks were observed in the majority of the parameters except for two: the duration of exposition to the lamp and the age of samples. Some actions were proposed to control and reduce the risks during the execution of the NIRS procedure:

- Scan the sample and analyse it by KF method with a difference of not more than 7 days.
- Perform the collection of the three spectra of each vial following the procedure in which the vials are taken away from the lamp after each scanning.

Consequently, and in accordance with regulations guidelines, the initial risk analysis was reviewed considering the results of the mitigation studies, to observe if the overall risk level was minimized (Table 8.4).

Table 8.4. FMEA analysis after the evaluation of the experimental results for the NIRS parameters which had RPN <25 in initial risk analyses. RPN or ORL <25 are shaded in green. Abbreviation: ORL (Overall risk level).

Parameters		S	P	D	RPN	Mitigating actions	S	P	D	ORL
Sample presentation	Sample temperature	**10**	**5**	**1**	**50**	According to the results obtained in the sample temperature experiment, no detectable variation in the NIR spectrum occurs at sample temperatures of 20ºC, 25ºC and 30ºC.	**10**	**1**	**1**	**10**
Sample thickness & density	Light transmission	**10**	**5**	**5**	**250**	Sample thickness is constant (1.8cm approx.) because all vials contain the same fill volume. Polystyrene peaks do not appear in the sample spectrum which guarantees that light transmission is null.	**10**	**1**	**1**	**10**
Age of samples	Chemical variation Sample storage	**5**	**5**	**10**	**250**	Data showed a slight increment in water absorption band at around 1940 nm throughout the storage time. To reduce this error, it was proposed to scan the sample and analyse it by KF with a difference of no more than 7 days (the sooner, the better).	**5**	**1**	**1**	**5**
Scanning	RMC range	**10**	**1**	**5**	**50**	Relevant differences in absorbance intensity between samples with low and high amount of water were demonstrated (from 0.6% to 6% RMC, which includes the specification limit (≤ 5%)).	**10**	**1**	**1**	**10**
	Duration of measurement	**5**	**5**	**5**	**125**	Results showed that a long exposition time on the lamp affects the intensity of the water absorption band at around 1940 nm. To mitigate this effect, spectra collection should be performed by taking away the vials from the sample device after each scan.	**5**	**1**	**1**	**5**
Physical Variation	Water distribution	**10**	**5**	**10**	**500**	According to the results obtained, water is uniformly distributed through the freeze-dried cake.	**10**	**1**	**1**	**10**

Finally, it was demonstrated that the NIRS procedure proposed for RMC determination in IFDA drug product was feasible according to the parameters studied.

Part 2. Quantitative near infrared models development and validation

1. Introduction

RMC is a CQA for injectable freeze-dried products. In fact, the removal of moisture from the final product is considered to be a proven approach to improve stability in the final product. Currently, KF titration is widely used for RMC determination in routine analysis. However, this method is time-consuming and destructive. Thus, only a small number of samples are analysed in routine QC analysis. Moreover, variations in environmental humidity and the use of pooled samples are often a challenge, especially for determination of low RMC levels.[10] As an alternative to KF titration, the use of NIRS is increasing as the method is non-destructive, non-invasive and requires minimal sample preparation.[11] As an example, Clavaud et al.[12,13], have recently proposed NIRS as an off-line tool in quality control for release and stability testing under cGMPs.

The introduction of NIRS in the pharmaceutical field was supported by EMA[3] and FDA[14,15] more than fifteen years ago. In addition, there are several documents dealing with the requirements for the validation of analytical methods, such as ICH Q2(R1)[16], and, more specifically, for the validation of NIRS methods, like the *Ph. Eur.* General Chapter on Chemometric[17] or the standard practice document of the American Society for Testing and Materials (ASTM)[18].

In this study, NIRS was used to determine the RMC in the two strengths (500 mg and 1 g) of the IFDA drug product. First, it was necessary to optimise and validate the KF reference method to obtain accurate, precise and reliable results of individual vials and not pooled samples. Then, the feasibility of using this method was demonstrated, as shown in Part 1 of Chapter 8. After that, calibration models were developed. This step involves processing the analytical signal to establish the most accurate and precise relationship with the RMC in the freeze-dried samples.

PLS regression was used to construct calibration models. Specific models for each strength were first developed and later, for practical reasons, a single model useful for both strengths was built up. During calibration, spectra pre-treatment, wavelength range and the number of factors were chosen in an empirical manner, with the final aim of obtaining the most simple and robust model with an acceptable predictive ability.[19,20]

The aim of this project was to submit the validated NIR method to the regulatory authorities of different countries (Module 3.2.P.5.3 of the Common Technical Document for the registration of pharmaceuticals for human use). Its application was restricted to the development and qualification of the freeze-drying process, as an alternative method to KF. Independently to the submission process, the application of this NIR procedure for stability studies was investigated to broaden its application in other fields. Applications of the validated NIRS methods are shown in Part 4 of this chapter.

2. Material and methods

2.1. Description and preparation of samples

11 laboratory and 8 production batches of IFDA drug product were used to develop and validate the calibration models. A total of 232 vials were measured covering the range of 0.14% - 12.66% RMC. Table 8.5 summarizes the source and number of samples used for this study, and Table 8.6 describes more detailed information about them. All batches were manufactured between July 2015 and June 2016.

Table 8.5. Range of RMC% and number of samples for each IFDA drug product strength.

	IFDA 1 g	**IFDA 500 mg**
Batches	10	9
Laboratory batches (total nº of vials)	7 (103 vials)	4 (92 vials)
Industrial batches (total nº of vials)	3 (12 vials)	5 (25 vials)
Total RMC range	0.15%-9.24%	0.23%-12.66%
Nº of available vials	232 vials	

Table 8.6. Detailed information of the studied samples (batch number, codification and number of vials analysed).

IFDA Strength	**Batch nº**	**Solution code**	**Batch code**	**Nº of vials**
500 mg	01	L606	L606	5
	02	L607	L607	5
	03	L608	L608	5
	04	L609	L609	5
	05	L610	L610	5
	06	L929	LB2020160509	25
	07	S0009	LB2020160609	24
	08	L621	LB2020160612	17
	09	L622	LB2020160617	26
1 g	01	K606	LB2020150725	3
	02	K904	LB2020150727	19
	03	K905	LB2020150729	16
	04	K911	K911	1
	05	L908	L908	4
	06	S0007	LB2020160301	15
	07	L502	LB2020160307	13
	08	L911	L911	7
	09	L926	LB2020160430	12
	10	L927	LB2020160506	25

Note: Solution codes starting with S were manufactured in the laboratory while solution code starting with K or L were manufactured in the production plant. Batch codes starting with LB20"date" were freeze-dried in the Laboratory, the others (which have the same code as the solution) were freeze-dried in the production plant.

NIRS does not require sample preparation for routine analysis. Nevertheless, laboratory samples were required to cover the whole RMC range needed to develop a robust model. The same freeze-drying conditions were applied in laboratory and production scale batches. Equipment description and freeze-drying process conditions were described in Chapter 6, along with the strategy to obtain samples with different RMC directly during the freeze-drying cycles. Vials containing high RMC were extracted at the end of the primary drying phase, when both vacuum gauges (Pirani and Baratron) started to converge. The lower limit of the RMC range was the minimum value obtained after drying the samples several hours (up to 24 h). However, freeze-dried vials from production batches were always collected at the end of the freeze-drying cycle. Then, all production vials had low RMC. The registered specification for RMC of IFDA freeze-dried product is ≤5% in both strengths.

2.2. Near infrared spectral acquisition

Sample spectra were measured in reflectance through the bottom of the glass vial using a LabSpe5000 VIS/NIR Benchtop Spectrometer (instrument description and spectral acquisition procedure are enclosed in Chapter 6).

2.3. Karl Fischer titration method

The RMC of IFDA drug product was determined by KF titration using a 852 Karl Fischer Titrator as a reference method (instrument description in Chapter 6). Only one replicate was obtained for each vial. Reference measurements were done in less than 7 days after NIR acquisition. A brief summary of the KF validation is described in Section 3.2.

2.4. Data processing

Unscrambler 10.5X software (CAMOs Software AS, Oslo, Norway) was used for spectra acquisition and multivariate analysis. As a standard procedure, all spectra were smoothed (SG, 29 points window and polynomial order 2). Specific pre-treatments are explained in Results and Discussion section.

In all cases, the three spectra per sample were averaged to obtain a single spectrum for each RMC result before calculating the PLS model. NIPALS algorithm was used for computing PLS factors. Segmented cross validation with 10 samples per segment (corresponding to approx. 10% of total samples in calibration), selected randomly, was used to build up and assess the calibration model. Independent batches were used to validate the NIRS procedure. Minitab 17 Software (Minitab Ltd, Coventry, UK)

and Excel 2010 (Microsoft office professional) were used for statistical tests for model validation (ANOVA, F-tests and Student's t-tests). The significance of all the statistical tests was α=0.05.

3. Results and discussion

3.1. Near infrared raw spectra

Raw spectra of the 232 samples of both IFDA drug products are shown in Figure 8.8.

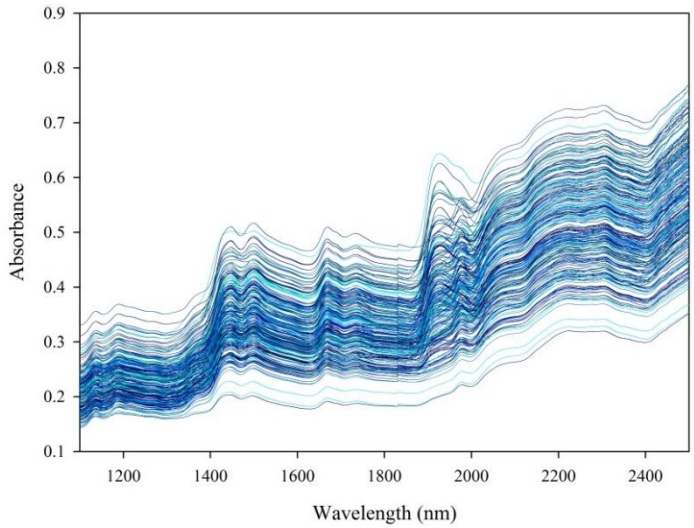

Figure 8.8. Raw spectra of 232 vials of IFDA 500 mg and 1 g drug products in the NIR range (1100 nm - 2500 nm).

Raw spectra presented a clear baseline drift due to the scattering effects. This spectral variability was reduced before the development of the regression model applying different mathematical pre-treatments. Variations were also detected in the water absorption band at approx.1920 nm, that corresponds to the combination band of OH-stretching and bending.[12] The differences in the intensity of those peaks show that the sample preparation strategy to obtain samples with different RMC was achieved successfully.

3.2. Distribution of residual moisture content results determined by Karl Fischer

Figure 8.9 shows box-whisker plot for both IFDA strengths and the histogram for the complete set of vials. The RMC distribution was highly skewed, with many samples below 1% and, in a decreasing trend, up to a maximum of 12%. For both strengths, the median was found to be around 1.5% and 2% RMC, and only a small number of samples had a percentage of RMC > 6%. In fact, it is much more difficult to obtain samples with high RMC because they ended up losing its porous structure, forming a shrunk cake or even melt.

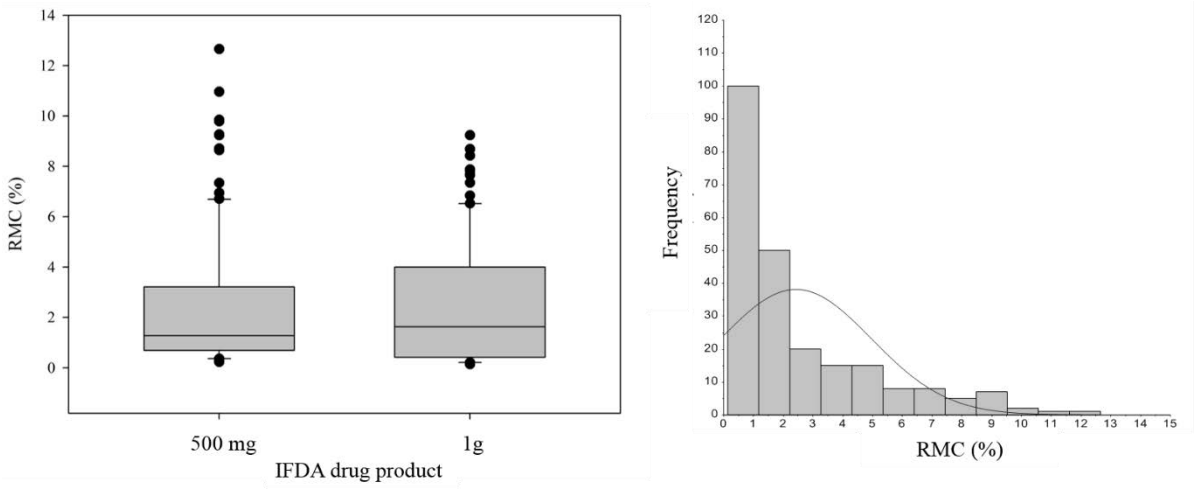

Figure 8.9. Graphical representation of the individual RMC values in all IFDA samples.

3.2.1. Volumetric Karl Fischer method validation

The original KF method for IFDA drug products consisted in pooling 6 vials, weighing 500 mg of the pool and, finally, determining the RMC. As each spectrum corresponds to an individual vial, the original KF method was optimized to determine the RMC in a single vial, avoiding the pooling and weighing steps.

The powder was pulverized inside the vial (closed and capped) and it was added to the KF titration cell directly from the vial. The mass of drug product analysed was determined by weight difference. In addition, Formamide was added to the KF titration cell to improve solubility of IFDA drug product in KF solvent (mainly methanol) and to increase the speed of KF reaction.[21]

To validate the new KF method, the absence of a matrix effect was initially proved. For this purpose, a sample was added to the KF cell, titrated, and after that and, in a consecutive way, 5 standards were added and titrated. The recovery values complied with the acceptance criteria described in the System Suitability Test of *Ph. Eur.* monograph 2.5.12 [22].

Considering the expected RMC that can be found in production samples, the accuracy and linearity of KF was demonstrated throughout the range from 1.5 mg to 30 mg of water (which correspond to 0.15% - 3% of RMC in IFDA 1 g).

Figure 8.10 depicts the results obtained vs the theoretical water content when different amounts of a water standard were titrated. It shows that a straight line with a slope close to 1 was obtained.

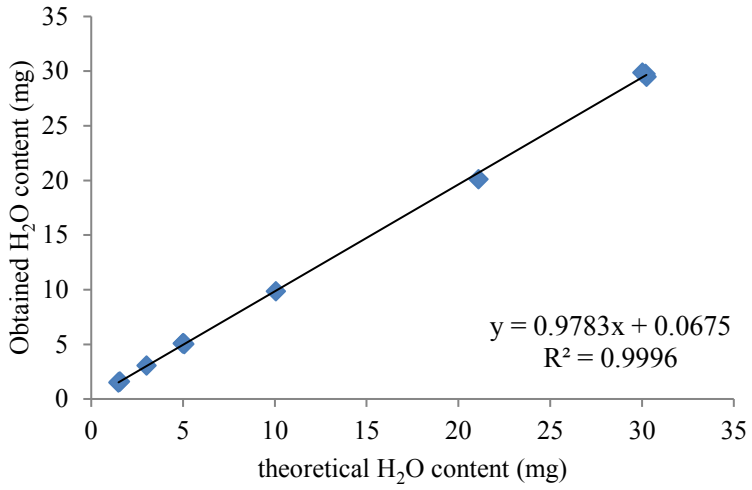

Figure 8.10. Regression line plot of obtained vs theoretical H_2O content in the standards for KF method validation. Confidence intervals for the slope and intercept were [0.940, 1.004] and [-0.431, 0.571] respectively.

Its precision was estimated by the calculation of the repeatability and intermediate precision considering two factors: the equipment and the analyst. Results obtained are described in Table 8.7. The std of the intermediate precision (0.05%) was assumed as the SEL.

Table 8.7. Repeatability and Intermediate precision results of KF method validation.

	Repeatability (n=6)	**Intermediate precision (n=12)**
Mean	0.65%	0.65%
std	0.05%	0.05%
RSD (%)	7.75%	8.26%

When applied to the RMC determination of production samples (with expected low RMC), the procedure implied the addition to the KF cell of the whole mass of the sample vial of each strength, to reduce the risk of water absorption by the highly hygroscopic API. However, when applied to the determination of RMC in highly humid samples, this procedure would imply an amount of water above the KF range. In these cases, a small portion of the powdered sample, approximately half of the total mass of product, was added. Anyway, when the titration exceeded the 30 mg of water, the results were considered invalid.

3.3. Development of quantitative models for individual strengths

At first glance, raw spectra showed a baseline shift and drift due to the scattering effect (Figure 8.8). The application of SNV transformation reduced the scattering effect and highlighted, even more, the differences in the intensity of the water absorption band. Figure 8.11 shows the relationship between absorbance at 1909 nm (located at the maximum values of the water absorption band) and RMC determined by the reference KF method.

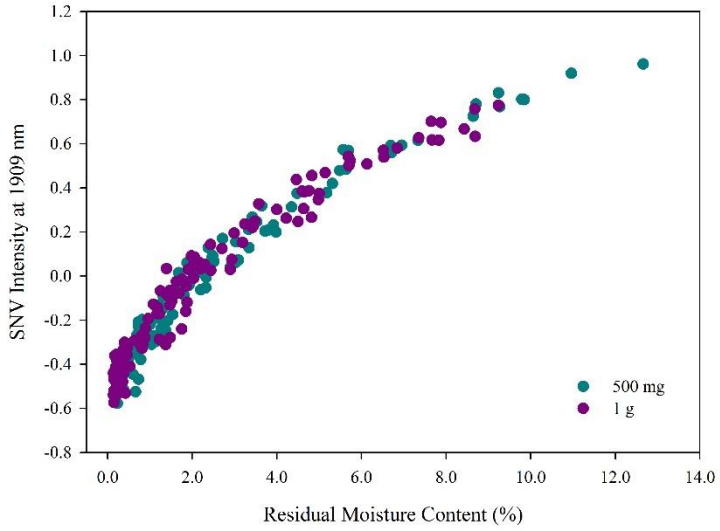

Figure 8.11. Representation of the RMC values obtained with the reference method versus the SNV intensity at 1909 nm.

As can be seen in Figure 8.11, this relationship is clearly non-linear, with a sharp slope up to around 1%, and a progressive slope decrease, especially for RMC values higher than 4-5%. In fact, PLS regression can correct certain non-linearity by increasing the number of factors, but at the expense of a reduction in the model's accuracy. Therefore, as expected, initial PLS models showed low accuracy and high errors of prediction.

Then, it was decided to restrict the range studied to the value of the product specification (5%) to avoid overfitting due to non-linearity corrections. In practice, according to the historical production data, the RMC average in industrial samples was 1% and, therefore, the superior limit at 5% was still far away. Then, samples with RMC> 5% were eliminated and, finally, 197 vials (99 of 500 mg and 98 of 1 g) were used for the individual NIRS models development.

3.3.1. Pre-treatments

The choice of the optimal pre-treatment was done in parallel with the selection of the spectral range and the number of factors of the PLS model. Initially, all spectra were smoothed through the whole NIR range, 1100 nm-2500 nm, to reduce the random noise and increasing the signal-to-noise ratio.

After that, different pre-treatments were evaluated (Absorbance (Abs), Derivatives (Der) and SNV) individually or combined, throughout three spectral ranges (1100 nm – 2500 nm, 1350 nm – 2350 nm and 1350 nm – 2100 nm). For derivatives, windows sizes from 11 to 31 were assayed. The best results were obtained by applying a 2nd Der (31 window points) followed by SNV from 1350 nm to 2100 nm.

As an example, the pre-treated spectra of the IFDA 1 g samples are displayed in Figure 8.12.

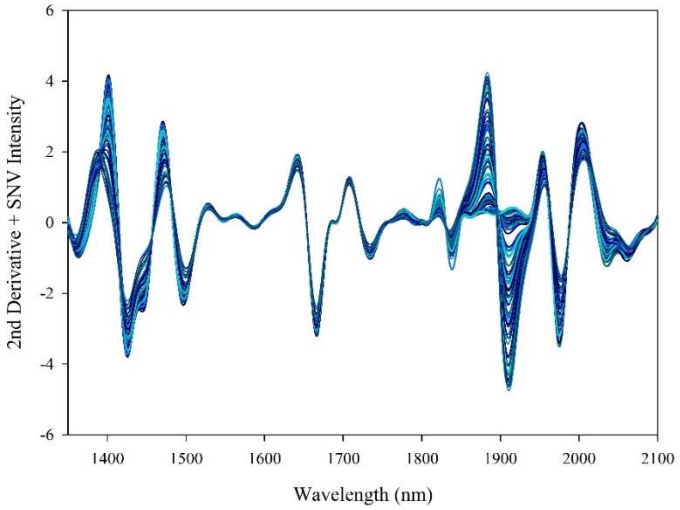

Figure 8.12. Second derivative and SNV corrected spectra of IFDA 1 g samples. Main differences in intensity are in 1400 nm and 1900 nm regions.

3.3.2. Exploratory data analysis and selection of sample sets

To complete the exploratory analysis of the spectra, a PCA was done with the pre-treated spectra of each strength independently. PC1 explained more than 90% of the variability observed in the spectra for both product strengths: 92% in the IFDA 500 mg strength and 94% in the IFDA 1 g (Figure 8.13). In addition**,** the main contributions in PC1 were observed in two wavelengths regions (1400 nm and 1900 nm) which correspond to the water absorption bands.

As observed in Figure 8.12, the applied pre-treatments did not completely eliminate the distortion caused by the detector change at 1830 nm. However, the PCA demonstrated that its contribution to the global variability of the spectra-is minimal, since there is no a clear band at that wavelength in the loadings plot of PC1.

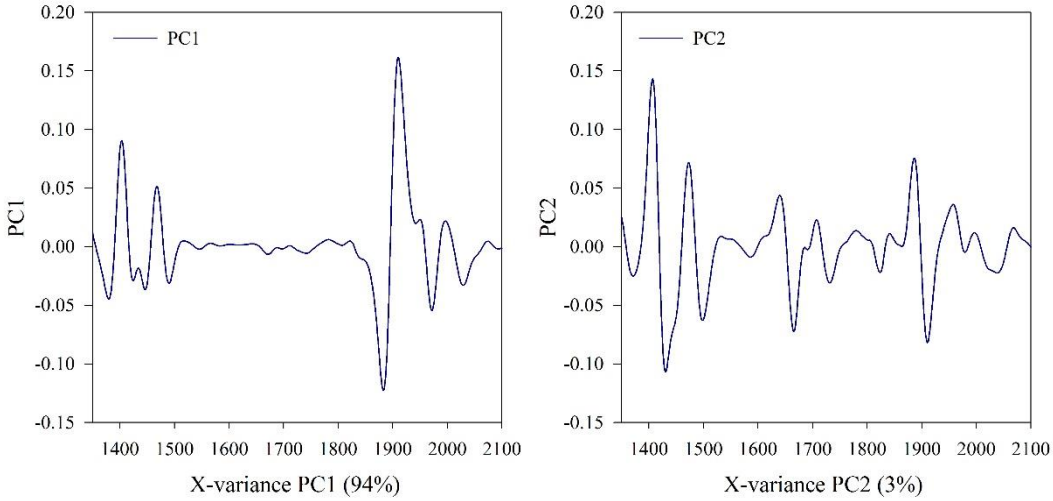

Figure 8.13. Loadings plots of PC1 and PC2 of the PCA for IFDA 1 g pre-treated spectra.

Besides, PC2 showed a random contribution of wavelengths. However, it is worth noting that water bands continue to be detected in the loading plot of PC2, but varying the relative proportion between them, which could be justified as a correction of non-linearity that affects both bands differently. PC2 only explained 3% and 4% of the variability in the spectra for IFDA 1 g and 500 mg, respectively.

The scores plot of PC1 vs PC2 showed samples grouped by their water content, in intervals of 1% from 0% to 5% (Figure 8.14). A clear separation of samples according to their RMC along PC1 is observed. Samples with warmer colours are those with a higher RMC % while samples with colder colours have lower RMC %. In addition, all samples laid inside the Hotelling's T^2 ellipse ($\alpha = 0.01$).

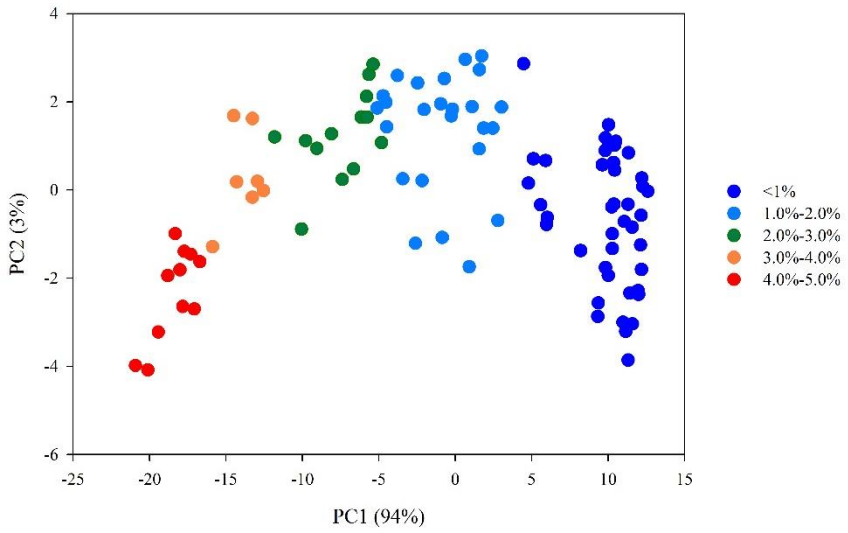

Figure 8.14. Scores plot of IFDA 1 g spectra showing sample grouping according to their % of RMC.

Samples were extracted during the freeze-drying process and, although the same extraction intervals were used, differences in RMC in vials may be observed among batches due to slightly differences in the kinetics of the drying process. Then, not all batches had a uniform distribution of the RMC parameter, and this issue limited the selection of the calibration and validation sets.

Finally, calibration and validation/prediction[a] sets were chosen considering that both sets should be representative of the variability observed in the entire population. For these reason, both sets must contain samples from laboratory and production batches. Moreover, the validation set contains samples of independent batches (i.e. different from those used to build up the model). Finally, as observed in Figure 8.15, both sample sets exhibit values of RMC uniformly spanning the selected range, with extreme values placed in the calibration set.

[a] The validation set refers to the samples from independent and external batches (not used for model calibration) predicted with the NIR models. These predictions were used to validate the calibration models.

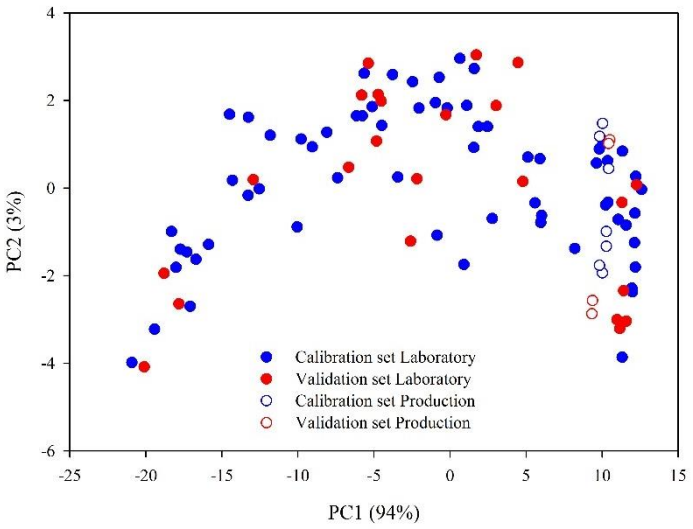

Figure 8.15. Scores plot for IFDA 1 g spectra. Calibration samples (blue dots) and validation samples (red dots) from Laboratory or Production (filled or empty dots, respectively) are marked accordingly.

3.3.3. PLS regression

After applying the spectral pre-treatments, a PLS model was computed for each IFDA drug product (500 mg and 1 g). Figure 8.16 shows a representation of the observed vs predicted RMC of IFDA 1 g drug product with a summary of the principal regression statistics. Even though the relationship between observed vs predicted values follow a lineal behaviour with good statistical regression parameters, values of RMC <0.5% were not differentiate. A similar behaviour was found for IFDA 500 mg drug product (data not shown).

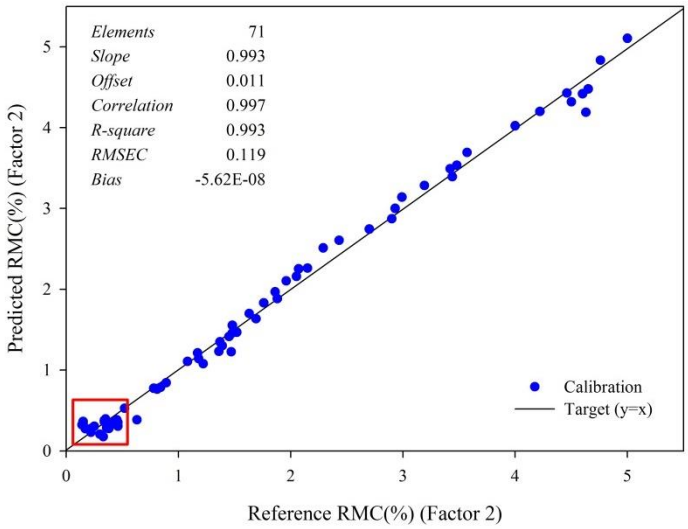

Figure 8.16. Predicted vs Observed plot of IFDA 1 g. A plateau of RMC values <0.5% is highlighted with a red square.

Furthermore, a statistical analysis of the distributions of residuals using the Wald-Wolfowitz[b] Test[23] show that residuals were not randomly distributed in any of the two NIR models, and, consequently, the assumption of linearity could not be sustained. Hence, NIR models did not comply with all validation parameters.

As historical results of production batches had a value of approx. 1% RMC determined by KF, it was decided that the drier samples could be eliminated to obtain a linear model. Samples were removed sequentially, and suitable models were built up after removing samples with a RMC < 0.3%. Then, 16 samples of the calibration set, and 7 samples of the validation set were removed for IFDA 1 g. Likewise, 23 samples of the calibration set, and 9 samples of the validation set were removed for IFDA 500 mg.

Finally, a PLS model was obtained for each IFDA drug product and its characteristics are described in Table 8.8. Calibration models were evaluated by cross-validation (10% of the calibration set of samples per segment). Two outliers[c] were detected and removed (FD0002_03_02c for IFDA 1 g and FD0002_07_01a for IFDA 500 mg). In general terms, the correlation coefficient (r) was close to 1, the slope, considering its uncertainty, included 1. The intercept value, with its uncertainty, included 0 and the bias was close to 0 in both models.

Table 8.8. Description of the main parameters of the individual PLS calibration models for IFDA drug products.

Model parameters		**IFDA 1 g**	**IFDA 500 mg**
Calibration	Calibration set	54 vials	63 vials
	Lab / Production vials	51 / 3 vials	53 / 10 vials
	RMC range	0.38% - 5.00%	0.34% - 3.98%
	Pre-treatment	2 Der (15p) + SNV	2Der (15p) + SNV
	Spectral range	1350 nm – 2100 nm	1250 nm – 2100 nm
	Nº of PLS factors	2	3
	Y-explained variance	99.56%	99.10%
	RMSEC	0.090%	0.094%
	RMSECV	0.103%	0.116%
	r	0.998	0.995
	Slope	0.996±0.018	0.991±0.024
	Intercept	0.009±0.045	0.014±0.044
	Bias	-6.35E-08	1.80E-08

Afterwards, both individual NIR models were validated satisfactorily with the RMC predictions of the validation set for each strength (results are summarized in Section 4). As observed in Figure 8.17, the

[b] In this test, if the value of r_{exp} is greater than r_{crit}, we accept the null hypothesis that the residuals are distributed randomly

[c] Samples residual limit ± 3 std.

quality of the model improved considerably when samples with very low RMC were eliminated. In addition, the linearity of both calibration models was evaluated by applying the Wald-Wolfowitz test with a confidence level of 95% [23,24]. For IFDA 1 g, r_{crit}=22 and r_{exp}=20.76 and for IFDA 500 mg r_{crit}=25 and r_{exp}=25. As $r_{crit} \geq r_{exp}$, the null hypothesis of the test cannot be rejected, so residuals were randomly distributed (Figure 8.18).

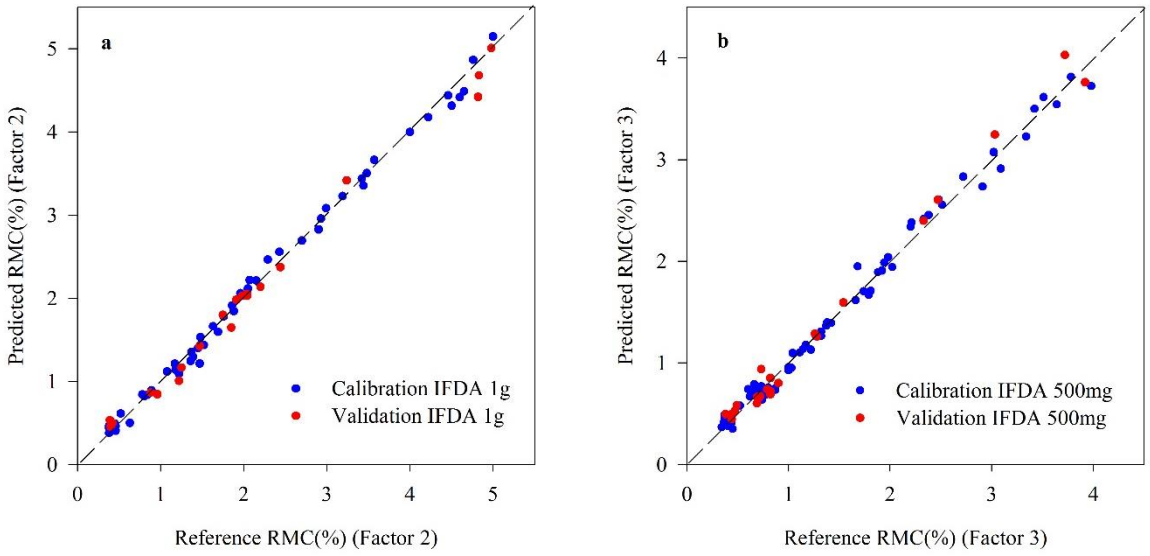

Figure 8.17. Predicted vs reference plot of IFDA 1 g (a) and IFDA 500 mg (b) PLS models. Dotted line represents the target y=x line.

However, when the RMC was predicted in vials from the new industrial process qualification batches, it was observed that there were samples with RMC <0.4% (lower limit of the validated models). Therefore, the lower limit of the PLS models had to be extended to be able to quantify all industrial samples.

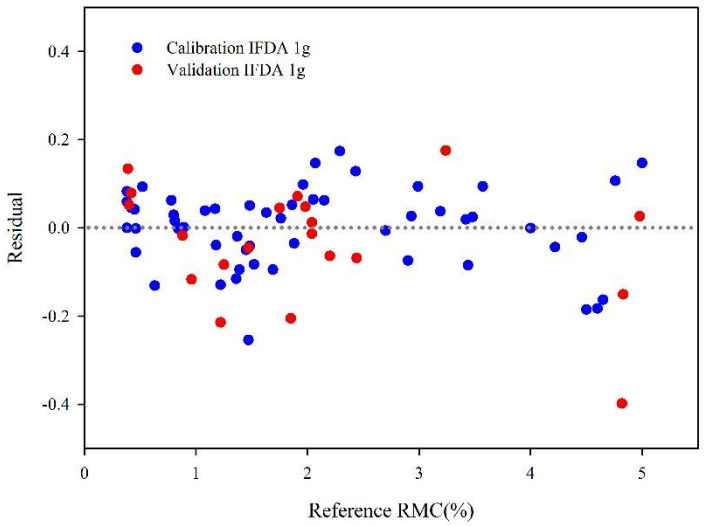

Figure 8.18. Residuals scatter plot for calibration (blue) and validation (red) samples of the PLS model for IFDA 1 g. Residual was calculated subtracting the reference KF value from the predicted NIR value.

Nevertheless, given the non-linearity of the response, to obtain a good model for the entire interval it would have been necessary to apply more complex non-linear algorithms, such as such as Artificial Neural Networks and Locally-Weighted Regression.[25] Therefore, it was decided to keep the both individuals models for quality control analysis of RMC in IFDA finished products, considering that values <0.4% will not be quantified.

However, for the application in RMC freeze-dryer moisture mapping, it was necessary to quantify every sampled vial from every position and shelf of the freeze-dryer (this application is further explained in Part 4 of this chapter). Hence, a more practical alternative was chosen, shortening the upper limit of the model to counteract the loss of linearity, and including the samples with low RMC previously excluded.

To define the maximum RMC limit of the PLS models, the average of the predictions made with the individual models (0.6-0.7%[d]) was chosen as the midpoint of the model range. This way, approximately 1.5% was chosen as the high RMC level of the PLS model. With a smaller range, it is more likely to get a good model fit with small errors in predictions. The number of samples that cover the 0.14% - 1.5% range for IFDA 1 g and IFDA 500 mg was 57 and 64 respectively.

Both individual NIR models (including the RMC range) were highly similar, which would indicate that the small difference in the matrix might cause no perceptible differences in the NIR calibrations. So, a combined model was developed. The capability to determine the RMC of both strengths with a single model optimizes the application of the model in the freeze-drying process qualification. In addition, it only involves carrying out one maintenance or revalidation plan, when needed. Hence it represented a huge benefit from the industrial point of view.

3.4. Combined model development and validation

3.4.1. Selection of the calibration set

121 samples were analysed with an RMC <1.5%. The samples for inclusion in the calibration set and validation set were chosen as previously described for the individual PLS models (Section 3.3).

First, a PCA was applied to the whole set of available spectra to obtain a uniform sample distribution throughout the RMC range.[19] Batch(es) with the minimum and maximum RMC values were included in the calibration set. Moreover, at least one laboratory and one production batch of each strength were chosen for both, the calibration and validation set to account for inter-batch variability.

[d] The change of this value with respect to the historical one (1%) is attributed to an optimization of the freeze-drying cycle and the KF method (reducing the manipulation of the sample).

The scores plot in Figure 8.19 shows the spectral variability and distribution of the chosen calibration and validation sets. The calibration set of the combined PLS model contained approximately two thirds of the dataset (96 samples) and the validation set the remaining third (25 samples). In addition, PC1 still explained the variability due to RMC, which accounts for 55% of the overall variability.

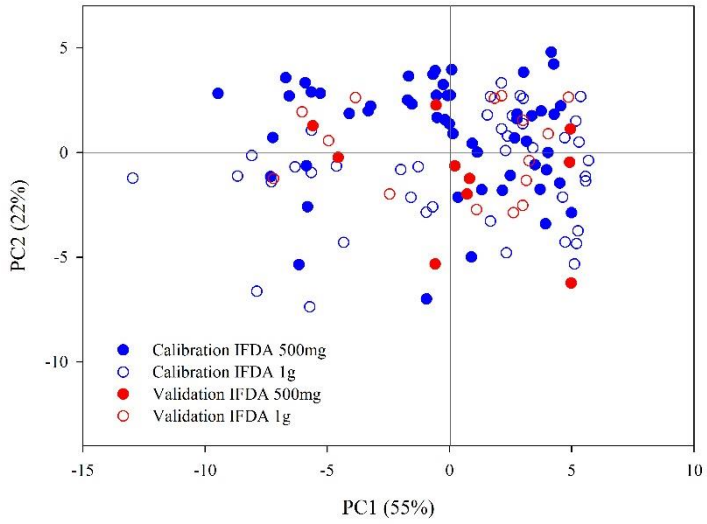

Figure 8.19. Scores Plot of the combined PLS model showing the distribution of calibration and validation samples in different colours.

3.4.2. Construction of the calibration model

A PLS regression was carried out on the pre-treated NIR spectra and the calibration models was evaluated with a segmented cross-validation (10 samples/segment) to check the goodness of fit of the model.[19] In addition, the external validation sample set was used to evaluate the predictive ability of the calibration model.

Two spectral ranges were chosen, 1100 nm -2500 nm and 1350 nm – 2100 nm, both including water absorption bands at 1450 nm and 1920 nm. The number of factors were selected by plotting SECV against each factor and choosing the one corresponding to the minimum of the curve. When it was not clear, or in the absence of a minimum, Haaland and Thomas criteria was applied.[26]

After that, several pre-treatments were applied to the smoothed spectra (including 1st and 2nd Der and SNV, individually and combined). The optimal model was chosen based in the predictive ability and model simplicity. Hence, the optimum PLS calibration model was the one that presents a lower RMSECV and RMSEP, a higher Y-variance, with as few factors as possible and complied the paired t-test of the prediction residuals (NIR-KF). It was also considered that the correlation coefficient must be as close as possible to 1. The values obtained for each parameter are described in Table 8.9.

With the Abs spectra (without pre-treatments), the variability due to the RMC appeared in the third factor of the PLS. The first two factors modelled the differences due to baseline offset and slope. However, as shown in Table 8.9, the use of 1st, 2nd Der and SNV, improved RMSEC, RMSECV and

explained Y variance, but best results were found when using the Der-SNV combination. When combined Der-SNV pre-treatments were applied, the first factor of the resulted PLS model explains >94% of model variability, that corresponded to differences in the water absorption bands.

Over all possible combinations, the 2Der + SNV, in the order indicated, presents a RMSEC and RMSECV and explained variances with acceptable values in both, the full-spectrum range (1100 nm – 2500 nm) and the shorter range (1350 nm – 2100 nm), that allowed to obtain a calibration model with 2 PLS factors, with an acceptable predictive ability. However, although the results of both ranges seemed to be practically identical, when the validation set was predicted using both models, the PLS model developed with 2Der+SNV pre-treated spectra in the short range complied the paired-t test of the residuals, whereas the model with the larger range did not comply at α=0.05.

Using the combination of both pre-treatments, it was possible to correct baseline offsets, slope variations and minimize the effects caused by scattering. However, other authors have found better results in the opposite order of pre-treatments (SNV + 2Der).[27] In this sense, Fearn published a short commentary about the importance of the order of these pre-treatments, concluding that it is recommendable to do the Derivative first.[28]

Table 8.9. Comparative table of the calibration and predictive performance of models constructed with spectra processed with different pre-treatments.

Pre-treatments	Spectral range	Calibration (n=92 samples)			Cross-validation		Prediction (n=25 samples)			
		Factors nº	Y-var (%)	RMSEC	Y-var (%)	RMSECV	RMSEP	Residuals mean	Residuals std	t_{exp}
Abs	1100-2500	5	92.6	0.111	91.2	0.123	0.112	0.05	0.11	2.20
	1350-2100	3	91.0	0.122	90.2	0.129	0.099	0.02	0.10	0.82
1Der	1100-2500	2	91.7	0.117	90.5	0.125	0.097	0.04	0.09	2.45
	1350-2100	2	91.7	0.117	91.3	0.123	0.100	0.05	0.09	2.75
2Der	1100-2500	3	91.4	0.119	90.2	0.129	0.100	0.05	0.09	2.54
	1350-2100	3	91.4	0.120	90.6	0.126	0.099	0.05	0.09	2.59
SNV	1100-2500	4	97.7	0.061	97.6	0.065	0.063	0.04	0.06	3.28
	1350-2100	5	98.3	0.053	97.9	0.059	0.055	0.03	0.05	2.83
1Der+SNV	1100-2500	1	98.0	0.058	97.6	0.063	0.054	0.03	0.05	3.03
	1350-2100	1	98.1	0.056	98.1	0.057	0.053	0.03	0.05	3.14
SNV+1Der	1100-2500	3	98.0	0.058	97.7	0.061	0.055	0.03	0.05	2.88
	1350-2100	3	98.0	0.057	97.8	0.060	0.060	0.03	0.05	2.78
2Der+SNV	1100-2500	2	98.0	0.058	97.8	0.061	0.053	0.02	0.05	2.38
	1350-2100	2	98.2	0.055	98.1	0.057	0.057	0.02	0.05	1.78
SNV+2Der	1100-2500	2	97.7	0.061	97.5	0.066	0.060	0.02	0.06	2.10
	1350-2100	2	97.8	0.060	97.7	0.063	0.060	0.02	0.06	2.02

t_{crit} (0.05, 24 df)= **2.06**. Abbreviation: Y-var (Y-variance)

In addition, four outliers were detected and removed. Table 8.10 describes the characteristics of the combined calibration model for both strengths. In addition, the combined PLS model fit is shown in Figure 8.20.

Table 8.10. Summary table of the calibration model parameters. Residuals were calculated as predicted NIR value – reference KF value.

Parameters	Results	Parameters	Results
Calibration set	92 vials	*r*	0.991
N° of factors	2	R^2	0.982
Pretreatment	2Der + SNV	*Slope*	0.982 ± 0.028
Spectral range	1350 nm – 2100 nm	*Intercept*	0.013 ± 0.023
Y-explained variance	98.20%	*Residuals*	Random distribution
RMC range	0.15% - 1.47%	*Bias*	9.23×10^{-9}
RMSEC	0.055	*Residuals mean*	-9.78×10^{-9}
RMSECV	0.057	*Residuals std*	0.055

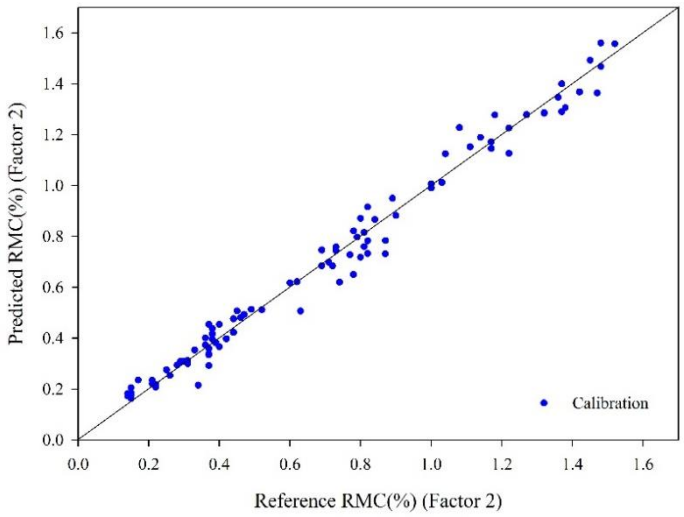

Figure 8.20. Predicted vs Reference plot of the combined PLS calibration model

3.4.3. Combined model validation

The combined PLS model was validated according to ICHQ2(R1)[16], EMA and FDA Guidelines[3,15], Ph Eur 5.21[17], and following the structure of the article published by Clavaud et al.[12]. To do this, a prediction was performed with the validation set using Unscrambler. The evaluated parameters and the results for each parameter are explained in the following subsections:

Specificity

The development and risk analysis data (Part 1 of this chapter) demonstrated a suitable NIR response for RMC. Additionally, as observed in Figure 8.21, variables that had the largest effect on the loadings plot of PC1 were the ones corresponding to the water absorption bands at 1450 nm and 1920 nm

respectively. In addition, sample distribution in the scores plot across PC1 showed a clear separation according to the RMC from left (low RMC) to right (high RMC).

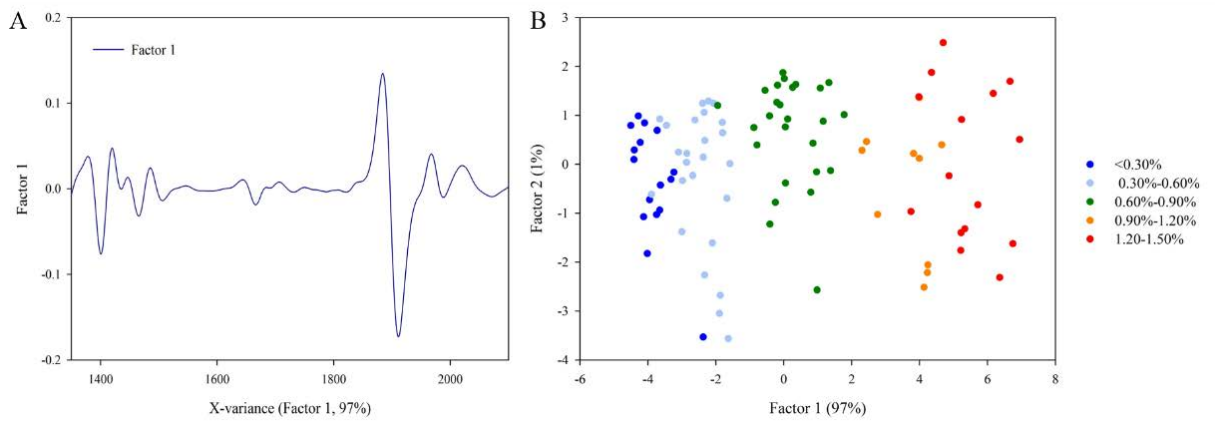

Figure 8.21. Loading plot of Factor 1 (A) and Scores plot of all IFDA 1 g and 500 mg of the combined PLS model.

Linearity and range

The calibration range was 0.14% to 1.52% while the validation range spanned from 0.20% to 1.47%. Thus, the validation range was included in the calibration range. Then, the linearity of the combined PLS calibration model and the predictions of the validation set were analysed by comparing the least squares regression line between the values found by NIR and the reference RMC values. The results were evaluated by looking at the range, the correlation coefficient, the intercept, the slope, and the bias (Table 8.11).

Table 8.11. Regression statistics of calibration and validation samples of the combined PLS model.

	Calibration	**Validation**
r	0,991	0.990
Slope	0.982 ± 0.028	0.992 ± 0.060
Intercept	0.013 ± 0.023	0.024 ± 0.045
Bias	9.23E-09	0.019

In both cases, r was close to 1. Slope and intercept were not statistically different from 1 and 0 respectively in both sample sets. Additionally, bias was close to 0 which confirmed the absence of constant systematic errors.

Figure 8.22 represents the regression line for the validation samples and the residuals plot of both sample sets. It was not possible to confirm linearity performing a "lack of fit" test in the ANOVA regression, as there were no replicates, so the Wald-Wolfowitz test was used instead.[23,24] In both cases, $r_{exp} > r_{crit}$ (Calibration: 42> 37, Validation: 12> 8), hence residuals were randomly distributed.

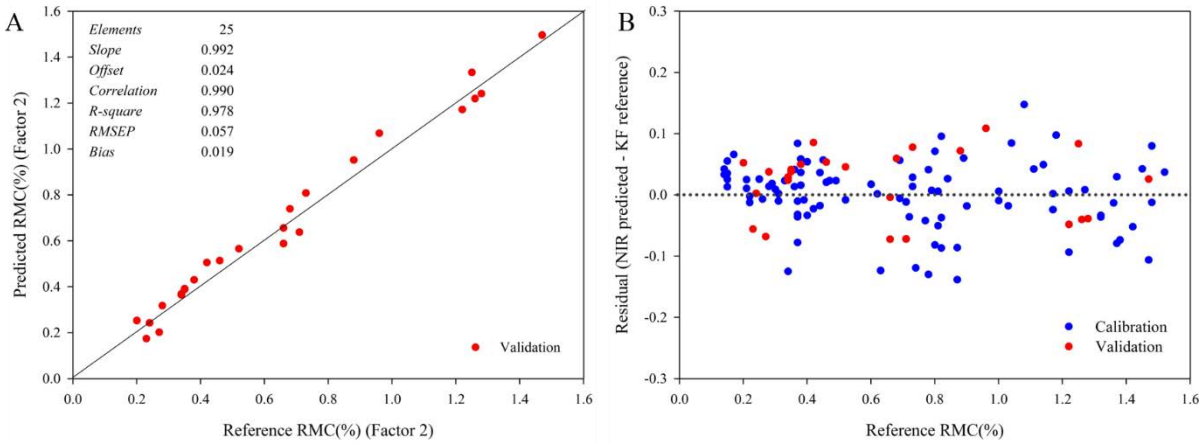

Figure 8.22. Reference vs Predicted plot of the validation samples for the combined PLS model(A). Residuals plot of the calibration and validation sets of the combined PLS model (B).

In summary, the linear relationship of the validation samples observed between the NIRS and the KF values was confirmed.

Precision

The repeatability was analysed by measuring two production vials (one of each strength) of the validation set in sextuplicate, the same day by the same analyst. Predicted RMC results are described in Table 8.12. For the repeatability test, a maximum RSD of 0.50% was observed.

Table 8.12. Repeatabilityof the combined PLS model for RMC determination in IFDA drug products.

RMC (%)	IFDA 500 mg	IFDA 1 g
Measure 1	0.60	0.67
Measure 2	0.61	0.67
Measure 3	0.61	0.68
Measure 4	0.61	0.67
Measure 5	0.61	0.68
Measure 6	0.60	0.67
Mean	0.61	0.67
std	$2.7x10^{-3}$	$3.4x10^{-3}$
RSD (%)	0.45	0.50

The intermediate precision test was performed by measuring three sample on three separate days by three different analysts in triplicate. The samples were representative of the calibration purpose covering the full range (high, medium and low RMC). Subsequently, the predicted RMC results were evaluated using the two-way ANOVA. Table 8.13 shows the results obtained as well as the most relevant data for the statistical study.

As can be seen in the Table 8.13, $F_{exp} < F_{crit}$ (6.94) was obtained in all studied conditions. Hence, neither the operators nor the days had statistically significant influence on the results. In addition, the interaction

of both factors, day and analyst, was non-significant in the three RMC levels ($p > 0.05$). As a result, the method was considered precise.

Table 8.13. Intermediate precision of the combined model for RMC determination in IFDA drug products. F_{crit}=6.94.

Sample with high RMC level (%)		*Day 1*	*Day 2*	*Day 3*	
	Analyst 1	1.38	1.41	1.42	
	Analyst 2	1.37	1.42	1.40	
	Analyst 3	1.37	1.39	1.43	
	Day	*p-value*	0.079	F_{exp}	6.78
	Analyst	*p-value*	0.291	F_{exp}	0.20
Sample with medium RMC level (%)		*Day 1*	*Day 2*	*Day 3*	
	Analyst 1	0.61	0.60	0.61	
	Analyst 2	0.60	0.61	0.60	
	Analyst 3	0.61	0.61	0.61	
	Day	*p-value*	0.814	F_{exp}	0.22
	Analyst	*p-value*	0.467	F_{exp}	0.93
Sample with low RMC level (%)		*Day 1*	*Day 2*	*Day 3*	
	Analyst 1	0.24	0.25	0.25	
	Analyst 2	0.25	0.25	0.25	
	Analyst 3	0.25	0.25	0.25	
	Day	*p-value*	0.615	F_{exp}	0.55
	Analyst	*p-value*	0.640	F_{exp}	0.50

Accuracy

A paired t-test (CI 95%) was performed to evaluate if the predicted results were significantly different to the reference values. At α=0.05 and n=25, t_{cri} was 2.06 and t_{exp} was 1.78. As $t_{exp} < t_{crit}$, the NIR mean was not significantly different from that of KF ($p > 0.088$). The values of RMSEC, RMSECV and RMSEP (0.055%, 0.057% and 0.057% respectively), were low and comparable to the error of the laboratory (SEL=0.051). In addition, the value of SEP was 0.068% which complied with two criteria proposed by EMA NIR guideline [3]: SEP < 1.4xSEL and the RMC range was more than ten times the SEP. Finally, the residues plot (Figure 8.22) showed that the samples were distributed around zero with a minimum value of –0.07% and a maximum value of 0.11% for the validation sample set. Then, excellent predictive performances were observed for the validation samples.

Robustness

To evaluate the robustness of the PLS model, the influence of sample temperature, the time between the preparation of the sample and the acquisition of spectra, and the errors of prediction of each IFDA strength individually were studied.

The RMSEPs of the validation set of samples separated as a function of the strength (10 samples for IFDA 500 mg and 15 samples for IFDA 1 g) were comparable (0.052 and 0.059 respectively). For each strength, the RMSEP values were compared with a F-test. The F_{exp} was defined with the Equation 8.1 proposed by Clavaud et al.[12]:

$$F_{exp} = \left(RMSEP_{IFDA\ 1\ g}\right)^2 / \left(RMSEP_{IFDA\ 500\ mg}\right)^2 \qquad \textit{Equation 8.1}$$

The F_{exp} was 1.29, which was lower than F_{crit} 2.65 (calculated with α=0.05, df_1= 9 and df_2=14), hence the RMSEPs were not significantly different.

To evaluate the sample temperature effect, four vials of each IFDA strength were first stored at 20°C and the NIR spectra were acquired after 2 h of storage. Then, the same vials were kept at 25°C and 30ºC, and the NIR spectra were acquired after 2 h in each case. Spectra were acquired in triplicate for each vial. For each IFDA strength, the RMC data acquired at each temperature condition were evaluated. Variances in the RMC results for the three samples temperatures were equal (Levene's test, p= 0.830). Differences among the means of the three sample temperatures at the 0.05 level were not significant (p=0.981). In addition, a paired Student's t-test (α = 0.05) was applied to the 20ºC and 30ºC RMC predictions. A bias of -0.003 was obtained which showed no systematic errors. A t_{exp} of 1.16 and a t_{crit} of 2.07 at 23 degrees of freedom were obtained ($t_{exp} < t_{crit}$). Then, a p_{value} of 0.26 (>0.05) was determined. Consequently, no significant differences between the results measured at two temperatures were observed.

Afterwards, the spectra of four vials of IFDA 1 g and four vials of IFDA 500 mg were acquired in triplicate at different days: 0, 2, 4, 5, 6, 7, 8, 9 and 10, to study the influence of the time between the preparation of the sample and the acquisition of spectra. The RMC was predicted using the combined PLS model and results are shown in Figure 8.23.

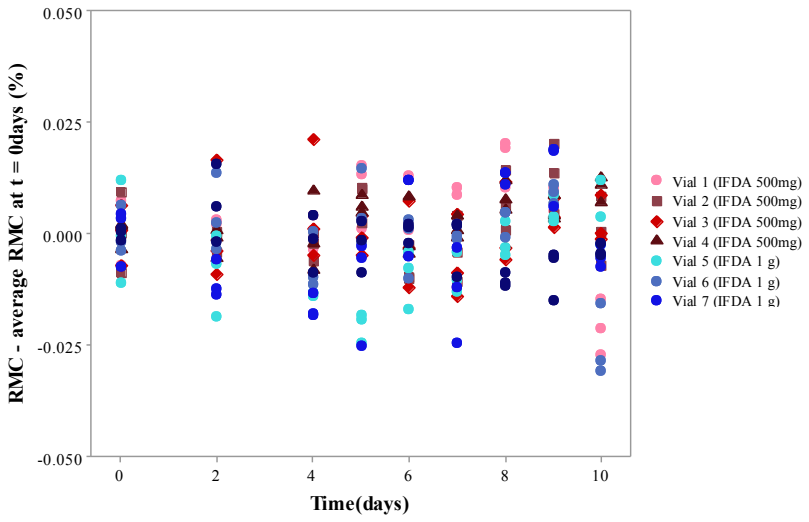

Figure 8.23. Predicted RMC value of the eight IFDA vials throughout 10 days of storage at room temperature.

As observed in Figure 8.23, all predicted values were normalized by subtracting the average value at t=0 days in each vial. All the normalized RMC results laid between ±0.03, which was considered an irrelevant variation. In addition, the regression analysis of the predicted RMC results for each vial showed the relationship between RMC and time was not statistically significant ($p>0.05$).

Limit of Detection and Limit of Quantitation

The EMA Guideline on NIRS states that LOD and LOQ for the proposed NIRS method need only to be demonstrated when the analyte is considered to be an impurity, which is the case of water in a freeze-dried product.[3] In this sense, it is recommended to calculate LOD/LOQ of the obtained NIR model for RMC determination in the IFDA drug products to complete the method validation. Due to its relevance, LOD and LOQ estimations are explained in a separate section (Part 3 of Chapter 8).

4. Validation summary table

Table 8.14 summarizes the validation parameters of the two individual models and the combined model for RMC determination in IFDA drug products.

Table 8.14. Summary table of the three NIR quantitative models for RMC determination in IFDA drug products.

Validation parameters			IFDA 1 g	IFDA 500 mg	IFDA 1 g&500 mg
Linearity and range	*n*		20	23	25
	r		0.996	0.995	0.990
	Slope		0.967±0.044	1.034±0.048	0.992 ± 0.060
	Intercept		0.032±0.109	-0.017±0.079	0.024 ± 0.045
	Wald-Wolfowitz test		Residuals random distribution		
	Range		0.39%-4.98%	0.38% - 3.92%	0.20% -1.47%
Accuracy	*RMSEP*		0.134%	0.130%	0.057%
	Bias		-0.036%	0.027%	0.019%
	Residuals STD		0.134%	0.118%	0.055%
	t_{exp}		1.215	1.08	1.78
	t_{crit}		2.861	2.07	2.06
Repeatability	*RMC Average (%)*	*Low*	0.58%	-	0.61% (1 g) 0.67% (500 mg)
		Medium	2.36%	0.73%	
		High	3.44%	-	
	RSD%	*Low*	1.40%	-	0.45% (1 g) 0.50% (500 mg)
		Medium	0.27%	0.56%	
		High	0.66%	-	

Validation parameters			IFDA 1 g	IFDA 500 mg	IFDA 1 g&500 mg
Intermediate precision (F_{crit} = 6.94)	*RMC Average (%)*	*Low*	0.50%	-	0.25%
		Medium	1.36%	0.71%	0.61%
		High	3.08%	-	1.40%
	Day (F_{exp})	*Low*	0.04	-	0.55
		Medium	2.08	2.40	0.22
		High	0.47	-	6.78
	Analyst (F_{exp})	*Low*	0.10	-	0.50
		Medium	3.51	0.48	0.93
		High	2.10	-	0.20

5. Conclusions

The results presented in this study demonstrated that NIRS can be used for RMC determination in IFDA 500 mg and 1 g drug products as an alternative method to KF.

Two individual PLS models for each strength were developed and successfully validated. The validated models were linear, accurate and precise in the studied ranges. However, when the RMC of samples from freeze-drying qualification batches was predicted, some vials had RMC values < 0.40%, which was the lower limit of the validated range for both models. Then, another model combining both IFDA strengths and including samples <0.40% RMC was developed. However, the combined model covered a narrow range (<1.5% RMC).

The pre-treatment chosen was the 2Der + SNV over the range 1350-2100nm. The validation of this method conforms to EMA requirements and ICH Q2(R1) guideline with regards to specificity, linearity, range, accuracy, precision and robustness. In addition, the use of a combined NIR model represents an optimization from an industrial point of view.

Table 8.15 summarized the main properties of the obtained NIR models.

Table 8.15. Summary table of all PLS models for RMC determination in both strengths of IFDA drug product.

Models	Comments	RMC range (%)	Spectral range (nm)
Individual models Ia and Ib	No random residuals. Not validated. Flat for RMC < 0.5%.	0.23-3.92% (500 mg) 0.15-4.98% (1 g)	1250-2100 nm (500 mg) 1350-2100 nm (1 g)
Individual models IIa and IIb	Not useful for samples with RMC < 0.4%.	0.38-3.92% (500 mg) 0.39-4.98% (1 g)	1250-2100 nm (500 mg) 1350-2100 nm (1 g)
Model III	One model for both strength. Not useful for samples with RMC > 1.5%.	0.20-1.47%	1350-2100 nm

Part 3. Determination of limit of detection and limit of quantitation

1. Introduction

The LOD is usually defined as the lowest quantity or concentration of a component that can be reliably detected with a given analytical method.[29]

In classical terms, set by the International Union of Pure and Applied Chemistry (IUPAC) in 1975, and reaffirmed by the American Chemical Society in 1980 [30], the LOD was defined as the lowest concentration of analyte which yields a signal whose magnitude is significantly different from that of the blank.[31] Conceptually, it is a very coherent definition. When the analytical signal is specific, any significant deviation from the blank value can be attributed to the analyte. Then, the LOD was estimated considering that a signal significantly different from the blank value corresponded to three times the std of the blank signals.

Detection limit is estimated in the response (or signal) domain but is usually reported in terms of concentration or amount (mass). The relationship between the response and concentration domains is the calibration function. Then, the AMC recommended to use the slope "b" of the calibration line obtained near the LOD to obtain the LOD in concentration units.[32]

$$LOD = \frac{3 \cdot s_{blank}}{b} \qquad \textit{Equation 8.2}$$

where s_{blank} is the std of blank signals and 3 corresponds approximately to the 99% confidence limit of the theoretical Gaussian distribution.[31] Sometimes 3 is expressed as a numerical factor, k, chosen in accordance with the confidence level desired.

However, a modern definition of LOD considers the uncertainty of the value obtained by interpolation in the regression line and the theories of hypothesis testing. This implies that LOD is the minimum quantity detectable with a preset probability of false positives (assuming that the analyte is present when it is absent, Type I errors) and false negatives (assuming that the analyte is absent when it is present, Type II errors).[33] Looking at the classical definition for the LOD (Equation 8.2), it only evaluates the probability of false positive but does not explicitly quantify the probability of a false negative.[34]

In this sense, the International Organization for Standardization (ISO) defined the capability of detection as "the true net concentration of the analyte in the material to be analysed which will lead with a probability of (1-ß) to the conclusion that the concentration of the component in the analysed material is greater than that of a blank sample"[35]. The need to evaluate the probability of false positive and of false negative has also been recognized by the IUPAC.[36,37] The following sections describe some LOD estimators found in the literature for univariate and multivariate calibrations.

1.1. Univariate calibration

When the analytical signal is univariate and analyte-specific, the determination of the LOD is based on the presence of false-positive and false-negative errors for the null hypothesis (H_0) "there is no analyte" and the alternative hypothesis (H_a) "there is analyte".[38] Figure 8.24 illustrates the main idea of the univariate LOD calculation. Two Gaussian bands are centered at the blank and at the LOD respectively. The decision limit (LD) helps to decide whether the analyte is detected or not with a rate α of false positives, whereas the LOD implies detection with a rate α of false positives (green-shaded area) and a rate β of false negatives (red-shaded area).[39]

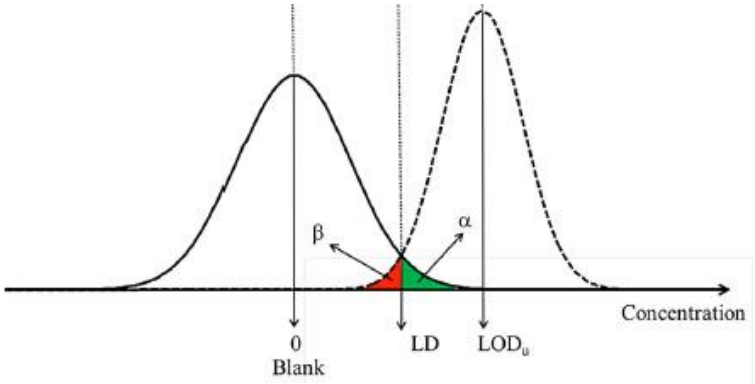

Figure 8.24. Representation of the IUPAC definition of the univariate decision limit (LD) and univariate limit of detection (LODu).Adapted from reference [39]***.***

The LOD should be expressed as a concentration, and the analytical methods give signals, thus, the calibration curve is used to transform the signal into concentration. Thus, the minimum detectable net concentration[35], x_d, or minimum detectable value can be estimated in the univariate case using the linear calibration model using the following equation[40]:

$$x_d = \frac{\Delta(\alpha,\beta) w_0 s_{y|x}}{b} \qquad \textit{Equation 8.3}$$

where Δ(α,β), is a value of the noncentral t-distribution related to the probabilities α and β (both traditionally set at 0.05), $s_{y|x}$ is the Std of the regression residuals, b, is the slope of the calibration line and w_0 is defined as:[40]

$$w_0 = \sqrt{\frac{1}{q} + \frac{1}{N} + \frac{(\bar{c})^2}{\sum_{i=1}^{N}(c_i - \bar{c})^2}} \qquad \textit{Equation 8.4}$$

being "q" the number of replicates used to obtain the mean signal in the problem sample, "N" the total number of calibration samples with individual concentrations "c_i" and mean value "$\bar{c}$".[40]

However, there are many analytical instruments which give a vector or a matrix of numbers for each sample instead of a unique signal. Therefore, the estimation of LOD should be adapted to those cases.

1.2. Multivariate calibration

The problem arises when dealing with multivariate calibration, typically NIR and PLS, although the same situation can be extended to other techniques and regression methods. In multivariate methods, instrumental signals are not specific for a given analyte and, in general, the sample matrix is complex and formed by several compounds. Therefore, and this is the chemical key to the problem, the spectrum of the target is not unique and could change depending on the components of the matrix. For these reasons, there is still no generally accepted LOD estimator for PLS calibrations although different methodologies have been published[33,38,41–46].

Lorber et al.[41] developed an approach based on the concept of net analyte signal, i.e., the part of the spectrum which is unique for the analyte in study and orthogonal to the interferents.[47] However, in multivariate calibration (classical or inverse), computation of net analyte signal is more complicated, because one or more interfering species with varying concentration may contribute to the measured response.

However, the main drawback of this estimator is that it only considers the uncertainty in the signal measurements, making its real application rather limited.[33,48] In analytical methods that use inverse calibration models, one of the main sources of uncertainty is given by the concentrations of the reference method, from which the former method has been calibrated. Consequently, every source of uncertainty from the whole method contributing to the final predicted value should be included in the calculation of multivariate detection limits.[42]

Nevertheless, an important progress in this area was performed by Ortiz et al.[38], who proposed an LOD estimator which can be directly generated by extending the ISO norm 11843 for univariate calibration to multivariate calibration. This generalization is based on the mathematical proof that the LOD, as defined by ISO and IUPAC for univariate calibration, is invariant for linear transformations of the response. [38,40]

Using this pseudounivariate approach, the analyte concentrations estimated for the calibration set of samples by the PLS model are plotted against their calibration concentrations measured by a reference technique, or nominally assigned when prepared in the laboratory from analyte standards.[38] The graph is processed as in univariate calibration which leads to an LOD value (named pseudounivariate LOD or LOD_{pu}) estimated from the classical univariate equation[33] (see Equation 8.3 and Equation 8.4).

However, this approach does not solve the basic conceptual problem, that, properly speaking, there is not a single blank of the sample, but several. Hence, several authors have proposed different alternatives, based on the fact that there is no single LOD, but a range of values, being able to estimate a minimum and maximum value of them.

Although some authors focused on this idea[44–46], the approach described by Olivieri is possibly the most recent and complete of this subject. Allegrini and Olivieri[33] suggested that the multivariate LOD for PLS should be expressed as an interval of LOD, which depends on the variation of the background composition in the calibration space. It is based on several complementary ideas: (1) each test sample has in principle a specifically associated LOD value, (2) the universe of test samples is well-represented by the calibration set of samples (3) the LOD toward a given analyte depends on various factors beyond the instrumental signals measured for a set of calibration samples.[49] The lower and upper limits of the LOD interval (LOD_{min} and LOD_{max}, respectively) correspond to the calibration samples with the lowest and largest extrapolated leverages to zero analyte concentration[e]. The lower and upper limits of the interval are given by the following equations:[33]

$$LOD_{min} = 3.3 \sqrt{\frac{var\ (x)(1 + h_{0min})}{\|\beta\|^2} + h_{0min} var(c_{cal})} \qquad \textit{Equation 8.5}$$

$$LOD_{max} = 3.3 \sqrt{\frac{var\ (x)(1 + h_{0max})}{\|\beta\|^2} + h_{0max} var(c_{cal})} \qquad \textit{Equation 8.6}$$

where β is the vector of regression coefficients, $\|\beta\|$ indicates the norm or vector length, $var\ (x)$ is the variance in the instrumental signal, $var(c_{cal})$ is the variance in calibration concentrations, and h_{0min} and h_{0max} are the minimum and maximum values of the leverage at the blank level. The interpretation of the factor 3.3 in Equation 8.5 and Equation 8.6 is the same as that given for univariate calibration. Typically, the factor $\Delta(\alpha, \beta)$ takes the approximate value of 3.3 where α and β are assigned a value of 0.05.

In multivariate calibration, h_0 assumes different values depending on the sample composition. In PLS, each test sample with zero analyte concentration, but having different levels of other components that contribute to the sample spectrum, will generate a specific set of scores onto H_o[f], and, thus, a specific value of the leverage h_0. The value of h_{0min} and h_{0max} are calculated with the following equations:[39]

$$h_{0min} = \frac{\bar{c}_{cal}^2}{\sum_{i=1}^{I}(c_i - \bar{c}_{cal})^2} \qquad \textit{Equation 8.7}$$

$$h_{0max} = \max\left(h_i + h_{0min}\left[1 - \left(\frac{c_i - \bar{c}_{cal}}{\bar{c}_{cal}}\right)^2\right]\right) \qquad \textit{Equation 8.8}$$

[e] For detailed information about this multivariate LOD estimator, refer to Allegrini and Olivieri published work[33,39,49,65,66]

where h_i and c_i are the leverage and analyte concentration of a generic calibration sample, $\bar{c}_{cal}$ is the mean of the calibration concentrations.[33] The interpretation of the LOD interval is: the analyte is absent when the predicted value is below LOD_{min}, and it is present when the predicted value is above LOD_{max}. But what is the decision for predicted values between LOD_{min} and LOD_{max} ? The authors proposed to estimate a specific LOD value for the corresponding test sample, approximating its real leverage h_i to the leverage h_0, which would correspond to its background components. The obtained LOD value can then be employed to check whether the predicted concentration is below (analyte absent) or above (analyte present) the sample-specific LOD. [49]

1.3. Pharmaceutical normative considerations

The *Ph. Eur.* has recently published a chapter on Chemometrics[17] where it is specified that the lowest value of the reference results determines the limits of detection and quantitation of the analytical method. This is a very pragmatic proposal, considering that LOD = LOQ = lowest concentration of the samples. In fact, this proposal is very consistent with the LOQ, since a multivariate calibration model cannot be extrapolated. This reasoning also serves for the LOD, considering that in its normal application, determination of the API in a preparation, the concentration levels of the API are very far from the hypothetical LOD, so its determination is not really crucial.

However, the determination of RMC in freeze-dried drug products is a very remarkable exception to this general concept, since it is performed by NIR, multivariate calibration, and it can be very close to the limits of the analytical procedure. So, the estimation of a LOD in this case would make sense from an analytical point of view. ICHQ2(R1) [50] stated that the LOD may be calculated based on the std of the response and the slope and, be expressed as:

$$LOD_{ICH} = \frac{3.3\sigma}{S} \qquad \textit{Equation 8.9}$$

where σ is the std of the response and S is the slope of the calibration curve. For LOQ, a factor of 10 is considered instead of 3.3, but the rest of the formula remains the same. The estimate of σ may be carried out based on the std of the blank measurement or based on the residual std of a regression line.

ICH method is used in several publications of NIR models for water determination in pharmaceutical freeze-dried products[51–53], as well as the concept defined in *Ph. Eur.* 5.21[17]. In addition, the Guidelines for the Development and Validation of Near-infrared Spectroscopic Methods in the Pharmaceutical Industry[54], edited by Pharmaceutical Analytical Sciences Group, considers the LOD and LOQ as described in ICHQ2(R1), but LOQ should be constrained by the lowest level available in sample calibration set. In addition, as for our knowledge, the pharmaceutical guidelines have not included methodologies for multivariate LOD determinations yet.

1.4. Proposed approach

Based on the aforementioned literature, a mixed approached was proposed to estimate LOD and LOQ of the individual and combined NIR models. When considering the LOD and LOQ of an analytical method, it is necessary to differentiate between its chemical meaning and the procedure for its estimation. From our point of view, a chemical approach to estimate LOQ, rather than a pure statistical calculation, may be advantageous. In this way, it is considered reasonable that the lowest value of the NIRS model validation range could be the LOQ, since it corresponds to the lowest amount of RMC determined by the reference method which has a quantified signal in the spectrum.

Nevertheless, regarding the LOD, it is not that *easy*. IFDA drug product is constituted solely by API and residual moisture. Then, in the absence of moisture, there is a blank spectrum, although in practice it is not possible to obtain since the API always contains a small % of water. Because of this, and taking into account that it is not possible to extrapolate a value with the regression model obtained when x = 0, it is necessary to estimate a variation "only due to water" that gives us a spectrum different from the pure matrix. In this case, the pseudounivariate approach for the calculation of the LOD in PLS calibrations describe by Ortiz et al.[38] could be applicable.

An added problem is that, at these low concentration levels, the precision in the acquisition of a NIR spectrum is comparable, or even better, than that of the reference method (KF).[17] For this reason, LOD could also be estimated by orthogonal regression which considers that both, X and Y, contain measurement error, unlike simple LSR which assumes that the error in X is negligible. Consequently, a 'reasonable' value of the std of NIR and KF (and S_{NIR} and S_{KF}, respectively) should be provided. These two values must have been estimated in conditions as similar as possible, so as not to bias the final result. Thus, S_{KF} and S_{NIR} were estimated from the parameters of the analytical validation of both analytical methods.

Minitab (Minitab Ltd, Coventry, UK) was used to calculate the orthogonal regression. Moreover, multivariate LOD was calculated as well, using a MATLAB software (mvc1) for first-order calibration created by Allegrini and Olivieri[33] Finally, the different approaches to estimate the LOD were interpreted and compared.

2. Results

2.1. Determination of S_{NIR} and S_{KF}

S_{NIR} was determined as the std calculated for the repeatability during NIRS models validation. It was carried out at a single level (medium), comparable to the RMC value obtained in industrial samples of both strengths (~0.6%). Six spectra of one vial of IFDA 500 mg and one vial of IFDA 1 g were acquired

and they were used to predict the RMC using each individual model and the combined model. Table 8.16 summarizes the results of repeatability for the combined model. The S_{NIR} was calculated as the average of the std of both doses, giving a value of $S_{NIR} = 3.8x10^{-3}$.

Table 8.16. Repeatability of the combined NIR model.

Replicates	IFDA 500 mg	IFDA 1 g
1	0.604	0.687
2	0.614	0.691
3	0.613	0.693
4	0.611	0.687
5	0.611	0.693
6	0.607	0.683
Mean	0.610	0.689
Std (n=6)	$3.7x10^{-3}$	$3.9x10^{-3}$

In the same way, for the individual NIR models, the values of S_{NIR} were $7.0x10^{-3}$ and $5.4x10^{-3}$, for IFDA 1 g and 500 mg respectively.

Since KF is a destructive method, S_{KF} was calculated from the standard recovery. Initially, the idea was to calculate the recovery of a pool of several IFDA vials, but the product is very hygroscopic, and the results of the pool presented more variability than that different determinations of individual vials of the same batch. Thus, S_{KF} was calculated based on the variability of the standard determinations used for the System Suitability Test described in *Ph. Eur.* Method 2.5.12 [22].

Basically, the procedure consists in the analysis of a sample, and, then, adding similar quantities of a standard (5 repetitions) in the same medium where the sample has been determined. This procedure was performed for each IFDA strength individually. S_{KF} was obtained from the std of the recoveries for each strength, and the average of both when used for the combined model ($S_{KF} = 8.2x10^{-3}$). Results are summarized in Table 8.17.

Table 8.17. KF system suitability test results.

Standard additions	IFDA 1 g (target RMC = 1%)	IFDA 500 mg (target RMC = 0.5%)
1	1.035	0.509
2	1.025	0.508
3	1.016	0.515
4	1.016	0.495
5	1.013	0.508
Mean	1.021	0.507
Std (n=5)	$9.2x10^{-3}$	$7.2x10^{-3}$

It should be noted that the standard error obtained from the intermediate precision was not considered because, in NIR, always the same vial was analysed while, in KF, the variability was calculated using the determinations of different vials that have very similar RMC values.

2.2. Estimation of LOD

LOD was estimated in the three NIR models (individual models and the combined model) using three approaches ICH, pseudounivariate and multivariate. In addition, for ICH and pseudounivariate approaches, LOD was calculated based on the std of the regression residuals obtain from simple LSR and orthogonal regression.

For the three NIR models, the regression models obtained by simple LSR were significant (p-value<0.05) with no significant lack of fit (p-value = 0.332). In addition, residuals were normally distributed (AD test, p-value > 0.05). Applying the ICH and pseudounivariate approaches, for α=β=0.05 and q=1, the estimated LODs are shown in Table 8.18. In both cases, the estimated LODs weree similar because the same factor, 3.3, was applied and $w_0 \approx 1$. However, both values of LOD were a little bit higher than expected (they were close to the lower limit of the NIR models range). As an example, the lower limit of the validated range for the combined PLS model was 0.20% RMC (considered the LOQ), and the estimated LOD was >0.18%. In addition, the values close to 0.20% were predicted with good precision and accuracy, as demonstrated during models validation. Hence, it indicates that it is not logical to consider that value as the LOD.

Regarding the orthogonal regression, the following errors in y/x (calculated based on S_{NIR}/S_{KF}) were considered for each model: 0.3044 for the combined model, and 0.3239 and 0.2935 for the individual models of IFDA 500 mg and 1 g respectively. When applying an orthogonal regression, the estimated LOD values were lower than the ones obtained with simple LSR (Table 8.18).

Table 8.18. Estimation of LOD of the three models using the ICH and pseudounivariate approaches.

Models	**Combined Model**		**Individual model IFDA 1 g**		**Individual model IFDA 500 mg**	
Regression	LSR	Orthogonal	LSR	Orthogonal	LSR	Orthogonal
Slope	0.982	0.994	0.996	0.998	0.991	0.996
$S_{y/x}$	0.055	0.031	0.091	0.059	0.095	0.062
N	92		54		63	
w_0	1.021		1.030		1.027	
LOD_{pu}	0.19%	0.11%	0.31%	0.20%	0.32%	0.21%
LOD_{ICH}	0.18%	0.10%	0.30%	0.20%	0.32%	0.21%

So, when the error in X was not considered negligible, the LOD estimator was lower and more meaningful from a practical point of view. Figure 8.25 shows a comparison of the regression lines using both methods.

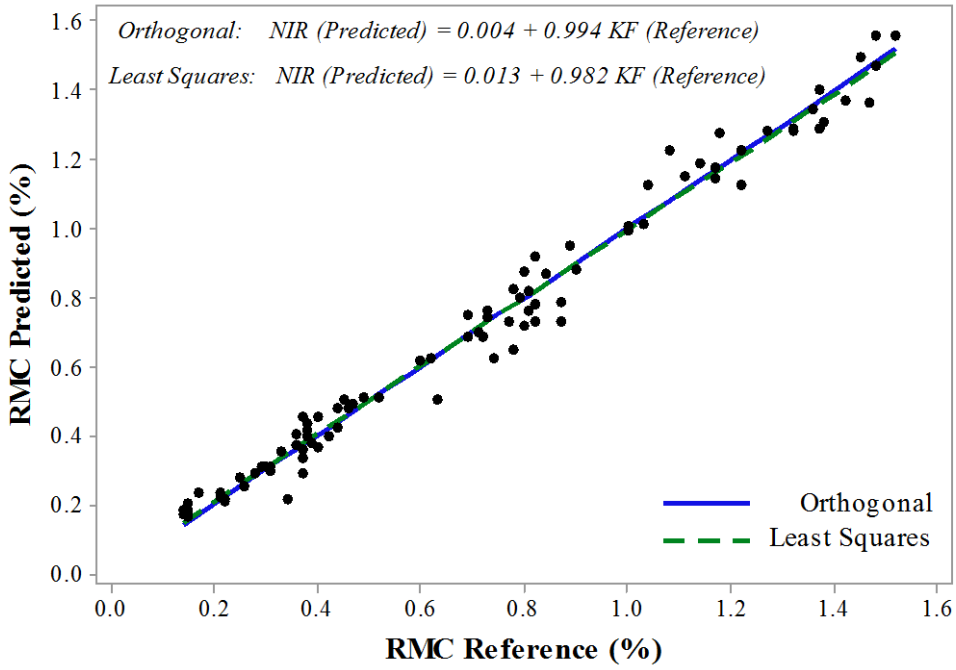

Figure 8.25. Plot of NIR (predicted) vs KF (reference) RMC values with fitted lines and regression equations.

In addition, Table 8.19 shows the LOD interval calculated using the multivariate approach. Both LOD_{min} and LOD_{max} were lower than the ones predicted using the ICH and pseudounivariate approaches.

Table 8.19. Results of LOD estimation using the multivariate approach for the three models.

	Combined Model	**Individual model IFDA 1 g**	**Individual model IFDA 500 mg**
LOD_{min}	0.04%	0.09%	0.08%
LOD_{max}	0.07%	0.13%	0.15%

2.3. Estimation of LOQ

According to the proposed approach, the LOQ of the combined NIRS model corresponds to the lowest RMC of the validated range determined by the reference method, which was 0.20% RMC. The relative residual values for the calibration set and validation set of samples were compared with the LOQ to further verify the suitability of this value (Figure 8.26). The plot shows that the LOQ limit is consistent because a significant increase in relative residuals is observed in RMC values <0.20%.

In addition, the LOQ_{min} and LOQ_{max} calculated with Allegrini and Olivieri's software gave values very similar to the proposed LOQ for the three NIR models (Table 8.20). However, the LOQ estimation using the ICH and pseudounivariate approaches (multiplying by a factor of 10 instead of 3.3) resulted in very high estimators, even with the use of orthogonal regression.

Table 8.20. Results of the LOQ estimation using the multivariate approach for the three models.

	Combined Model	Individual model IFDA 1 g	Individual model IFDA 500 mg
LOQ_{min}	0.13%	0.26%	0.24%
LOQ_{max}	0.20%	0.38%	0.46%
Proposed LOQ	0.20%	0.39%	0.38%

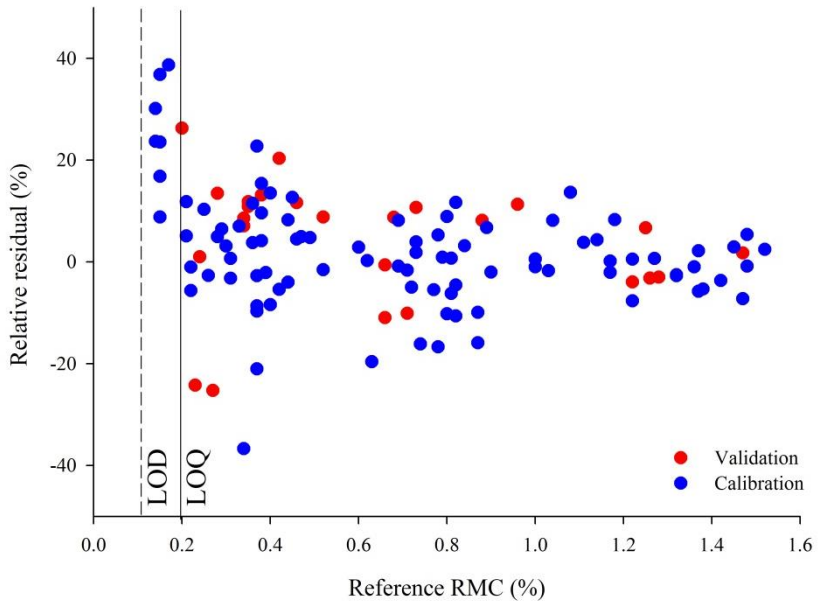

Figure 8.26. Scatter plot of the relative residuals vs reference RMC for the combined NIR model. Relative residuals were calculated as $(\boldsymbol{Predicted\ (NIR) - Reference\ (KF)/Reference\ (KF)}) \times \mathbf{100}$.

3. Discussion and conclusions

Different approaches were used to calculate the LOD of the three NIR models developed in Part 2 of this chapter, two individual models, one for each IFDA strength, and a combined model. The objective was to compare them and discuss which values were reasonable.

The estimated LOD obtained by orthogonal or multivariate regression gave reasonable values However, the limit was overestimated with simple LSR, being close to the LOQ determined from the minimum reference value of the external validation set. As an example, Table 8.21 summarizes the results for the combined PLS model, but the same pattern was observed in the individual PLS models.

In fact, the estimated error of the reference KF determination (S_{KF}) was higher than the NIR error (S_{NIR}), according to our calculations. Hence, the error on the X axis was not negligible and NIR determinations were more reproducible than those performed by KF. Therefore, it indicates that it is necessary to consider the calibration concentration uncertainties to calculate a more optimal LOD.

For this reason, the LOD calculated with the ICH approach based on orthogonal regression could represent the most useful estimate in our case, due to the simplicity of the estimation, and because it

accounts for the error in the reference measurement. As both methods, NIR and KF, must be validated, S_{NIR} and S_{KF} can be calculated in a reliable manner.

Table 8.21. Summary of LOD estimations for the combined NIR model.

LOD		**Combined NIR model**
LSR	LOD_{pu}	0.19%
	LOD_{ICH}	0.18%
Orthogonal Regression	LOD_{pu}	0.11%
	LOD_{ICH}	0.10%
Multivariate	LOD_{min}	0.04%
	LOD_{max}	0.07%

The relationship between the pseudounivariate and the multivariate approaches has been discussed by Allegrini and Olivieri[33].They found out that when concentration uncertainties compete with the instrumental noise in relative size, the mutual relationship among LOD_{pu} (calculated by LSR), LOD_{min} and LOD_{max} was less clear.[55] In fact, the authors found that the LOD_{pu} value could be even larger than the LOD_{max}, which agrees with the results obtained in this work.

Moreover, it was demonstrated that the LOQ value was acceptable since the relative error of the predictions above LOQ were small and uniform throughout the RMC range. On the contrary, the relative error of the predictions below the LOQ were at least 2-3 times higher than the ones of the RMC predictions above LOQ.

Part 4. Application of the combined NIR model

1. Introduction

As previously stated, RMC is a CQA of freeze-dried drug products that influences product's stability and shelf life. In a freeze-drying process, each individual vial within a batch could experience slightly different freezing and drying conditions. In fact, RMC is dependent on a multitude of factors including the location of the samples in the chamber, and their position in the middle or at the edge of the trays, due to differences in fluid dynamics of the vapour in the chamber as well as on the heat radiation effect.[56,57] As a consequence, drying rate and product temperature may vary between vials of the same batch leading to differences in RMC among them.[58–60]

Therefore, an extensive and well-defined sampling plan should be used to show RMC uniformity from various physical locations within the drying chamber. In extreme cases, the variations in RMC may be large enough to have dramatic repercussions on batch stability. It is therefore essential to demonstrate that the batches produced have uniform RMC, or at least that the differences observed are too small to compromise product stability.[61]

Moreover, quality attributes could evolve in the course of storage.[62] Variations in relative humidity and storage temperature can change samples' quality attributes. In fact, a change in RMC over time is expected, and those samples with high RMC may have a more compact and compressed structure, which can be translated to scattering differences in the spectra. Therefore, it is essential to verify that the NIR is still useful for this type of samples.

Conventionally, KF Titration is the most widely used analytical technique for determination of water content in the pharmaceutical industry. However, recently, NIRS has emerged as a new powerful technique due to its capability to determine large number of samples in a non-invasive and non-destructive analysis.[3] In this study, NIR spectroscopy was applied for two purposes:

1. To perform a freeze-dryer moisture mapping with the six PPQ batches of both IFDA drug products and assess the variability among different positions, shelves, and freeze dryers.
2. To verify whether the validated NIR method could be used to determine the RMC of samples under stability programs.

First, samples from different positions from all the shelves of two freeze-dryers were taken and analysed by NIR. Samples spectra were used to predict the RMC results by the combined NIR model. After, the predicted RMC results were plotted in a 3D representation of the freeze-dryers to visualize the spatial distribution of the RMC inside the freeze-dryer. Secondly, the impact of storage conditions and time was evaluated in the same batches. As the RMC determination by NIR is non-destructive, it represents a benefit allowing to reduce the number of samples in stability programs and use the same vial for other analysis, which, in turn, allows to correlate different CQAs of the same vial.

2. Materials and methods

2.1. Samples

For freeze-dryers moisture mapping, vials of IFDA 1 g and IFDA 500 mg drug products from the following PPQ batches: L1001V, L1003V and L1004V (for IFDA 1 g) and L5001V, L5002V and L5003V (for IFDA 500 mg), were used. One vial of IFDA 1 g from shelf 3-position 2 of batch L1001V and one vial of IFDA 500 mg from shelf 4-position 5 of batch L5001V were not scanned due to vial breakage during transportation. In addition, there were no vials in the positions 6 and 7 of shelf 10 of batch L1001V, because the freeze-dryer was not completely loaded. For the storage condition effect, 198 samples of the six PPQ batches stored in four different conditions were measured with the NIRS and KF methods.

2.2. Sampling procedure

The sampling criteria defined by the ISO Standard 2859-1:2012, inspection level II, single sampling for normal inspection was applied. Based on this standard, for a batch size of 20750 vials (for IFDA 1 g) and 35000 vials (for IFDA 500 mg), a minimum of 315 vials should be sampled. Consequently, 350 vials were collected to fit all sampling positions evenly distributed throughout the shelves. 5 vials were sampled in each position following the schema represented in Figure 8.27. Considering that the shelves in industrial Freeze-dryer 1 are bigger than the shelves of Freeze-dryer 2, the sampling at the central position was done in three positions (position 3, 4 and 5).

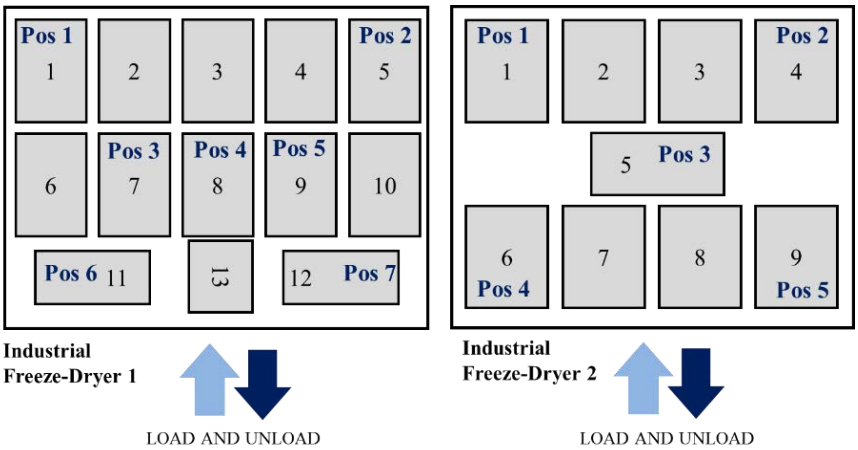

Figure 8.27. Sampling positions per shelf in both industrial freeze-dryers. The picture represents the superior view of a shelf in each freeze-dryer. Trays are represented in grey rectangles and approx. 160 vials for IFDA 1 g and 270 vials for IFDA 500 mg can be placed in a tray. Freeze-dryer 1 has 10 shelves and 13 trays per shelf while Freeze-dryer 2 has 14 shelves and 9 trays per shelf. Sampling positions are indicated with "Pos"+ a number.

2.3. Storage conditions of the stability studies

PPQ batches were stored in four different conditions, according to ICH Q1A(R2)[63] and ICH Q1F[64]. Table 8.22 summarized the evaluated storage conditions.

Table 8.22. Summary of the storage conditions used for the stability studies of IFDA drug products.

Condition	Temperature (ºC)	Relative Humidity (RH%)	Time points (M)[g]
1	25 ± 2	60 ± 5	0 3 6 9 12 18
2	30 ± 2	65 ± 5	0 3 6 9 12 18
3	30 ± 2	75 ± 5	0 3 6 9 12 18
4	40 ± 2	75 ± 5	0 3 6

Three vials of each batch were analysed by NIR and KF after freeze-drying (t = 0 M) and represented the starting point for each condition. For the rest of stability time points and conditions, 2 samples per batch were analysed by NIR and KF. In all cases, KF analyses were performed the same day or the day after NIR spectra collection.

2.4. Equipment, instruments and analytical methods

Two Industrial freeze-dryers, Edwards 1 and 2 (IMA Life, Italy) were used in the six PPQ batches. Reference RMC values were obtained by KF titration using a 852 Karl Fischer Titrator (Metrohm, Switzerland). NIR spectra in the range 1100 nm - 2500 nm were acquired by an ASDinc LabSpec5000 equipped with a High Intensity Muglight accessory. Three spectra were collected directly from the bottom of the glass vial and averaged. Vials were rotated between measurements. RMC results were predicted using the combined NIRS model. More details about instruments and methods can be found in Chapter 6.

2.5. Data analysis

JMP®7 software (SAS Institute Inc, North Carolina, USA) were used for freeze-dryers moisture mapping analyses and 3D representations. NIR spectra were processed using Unscrambler® 10.3X (CAMO Software AS, Norway). Statistical analyses were performed with Minitab 17 (Minitab Ltd, Coventry, UK) and Microsoft Excel software.

ANOVA tests were used to investigate the significance of shelves, positions and freeze-dryers in the study of RMC mapping.

[g] At time point of 9 months, the NIR spectra of the two vials of batches L1003V, L1004V, L5002V, L5003V were not acquired because they were accidentally analysed by KF before NIR spectra acquisition.

For the analysis of storage conditions and time, a graphical representation of residuals (NIR-KF) vs storage time was reported. Theoretical alert and action limits for the residuals were established as 2σ and 3σ respectively. The σ of the residuals was calculated as follows:

$$\sigma = \sqrt{\sigma_{NIR}^2 + \sigma_{KF}^2} \qquad \textit{Equation 8.10}$$

Where σ_{NIR} corresponded to the SEP of the NIR model (0.068) and σ_{KF} to the SEL (0.051). Then, the calculated 2σ and 3σ limits were 0.17 and 0.26 respectively.

The normality of the residuals of the six batches was checked using the AD test. After that, the bias and the variances of the NIRS and KF data at each storage time were evaluated using the Student's paired t-test and the F-test respectively at α = 0.05.

3. Results

3.1. Industrial freeze-dryers moisture mapping

Table 8.23 shows a summary of the RMC values predicted using the combined NIR model for each PPQ batch. All results comply with the specification of RMC ≤ 5% and the dispersion of RMC results around the mean is small (std <0.06%).

Table 8.23. Summary of the predicted RMC results for the PPQ batches of IFDA 500 mg and 1 g.

Freeze-dryer	Dose	Batch	NIR predicted RMC%) mean	std (n=350 vials)	Minimum value	Maximum value
1	1 g	L1001V	0.54%	0.03%	0.46%	0.75%
2	1 g	L1003V	0.38%	0.03%	0.27%	0.47%
1	1 g	L1004V	0.48%	0.02%	0.42%	0.56%
1	500 mg	L5001V	0.66%	0.06%	0.53%	0.89%
2	500 mg	L5002V	0.52%	0.06%	0.40%	0.66%
2	500 mg	L5003V	0.59%	0.06%	0.45%	0.93%

Figure 8.28 represents the individual RMC results for each batch of both IFDA strengths. As observed in this figure, IFDA 500 mg vials had slightly higher RMCs values than IFDA 1 g. Nevertheless, none of the vials exceeded 1% RMC and the intra-batch RMC results were very uniform.

These results suggested that the freeze-drying process for both IFDA drug products was well-controlled.

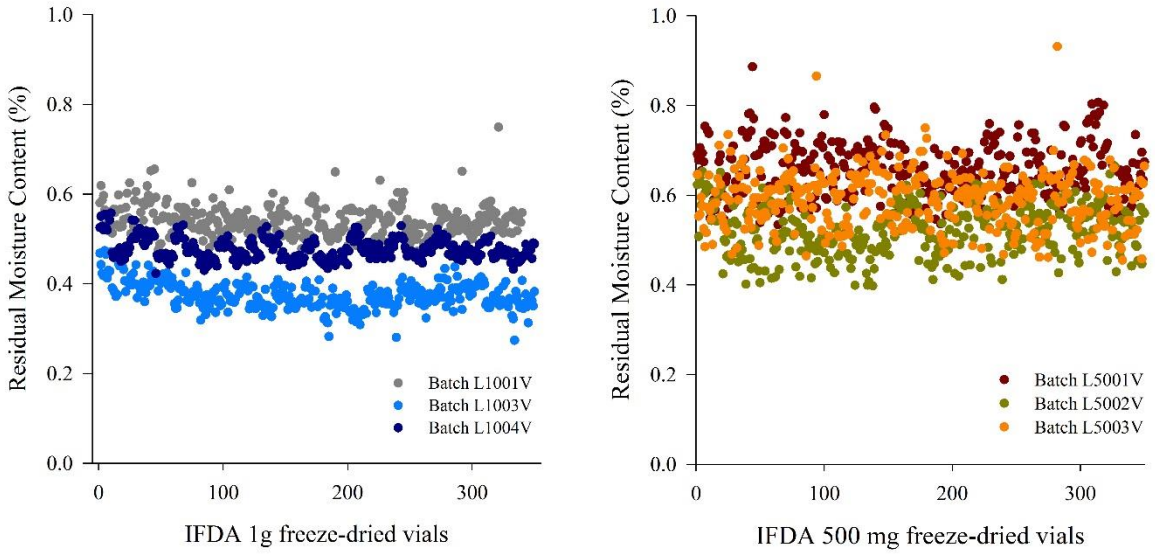

Figure 8.28. Line plot of the overall RMC results.

Afterwards, the predicted RMC results were plotted in a 3D scatter plot for each industrial freeze-dryer to visualise the geometric distribution of the RMC inside the freeze-dryer. RMC results were standardised from 0 to 1 to eliminate the inter-batch variability and to be able to use results of both strengths in the same plot with the same colour scale. The colour scale represents the driest samples in blue and the samples with the highest RMC in red. As observed in Figure 8.29 and Figure 8.30, the highest RMC results seemed to be located predominantly in the edge positions.

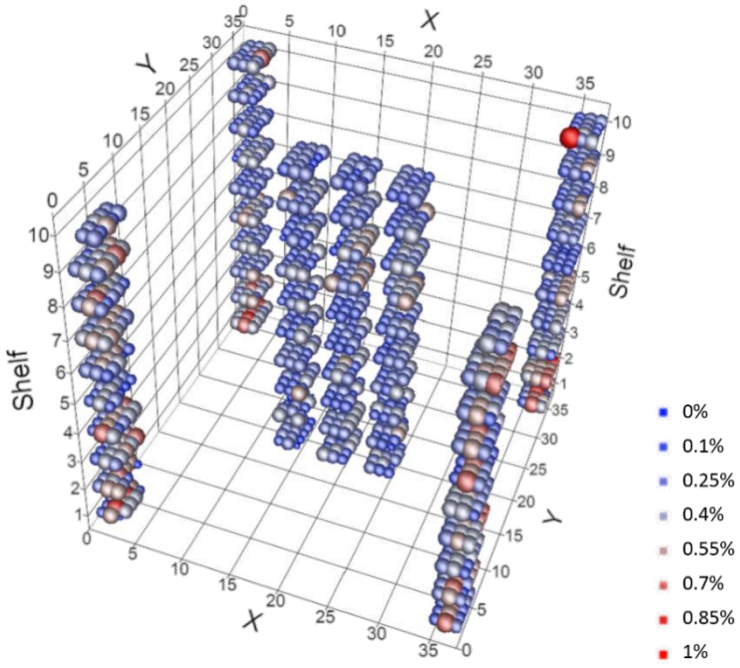

Figure 8.29. Scatter 3D plot of Freeze-dryer 1.

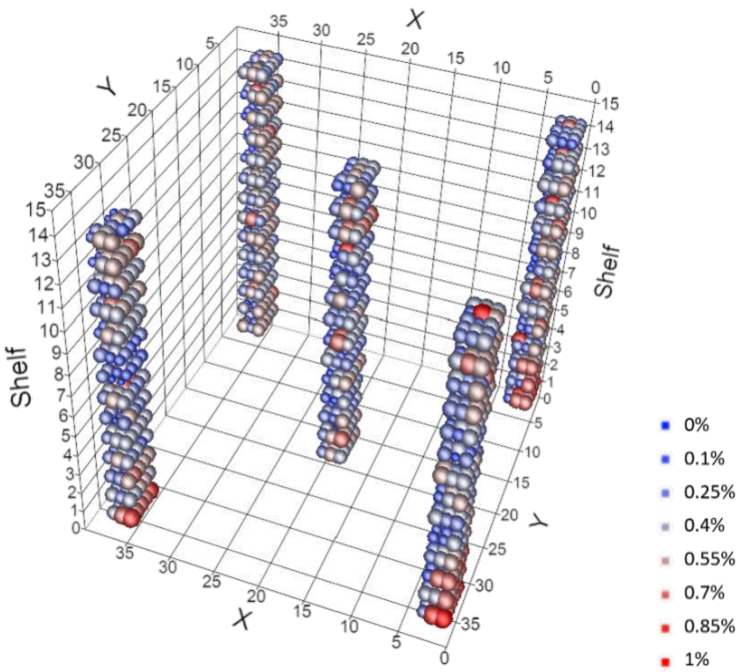

Figure 8.30. Scatter 3D plot of Freeze-dryer 2.

In addition, the variability among different shelves and positions inside the shelves of a given freeze-dryer was assessed using ANOVA. As expected, ANOVA found significant differences among batches ($p<0.05$), hence, the study of uniformity among shelves and positions was performed for each batch individually.

Due to the narrow confidence interval, there were statistically differences among RMC means of different shelves at the 0.05 level of significance. The same situation was observed for different positions inside the shelf, expect for batches L5002V and L5003V where no differences were observed among different positions.

Alternatively, the mean of the standardized results was used to study if there are differences among shelves and positions in each freeze-dryer. In Industrial freeze-dryer 1, there were differences between shelves 1-2 and 6 (lower and central shelves) at $\alpha=0.05$. Likewise, shelf 1 of Industrial Freeze-dryer 2 had a RMC mean higher than the rest of the shelves. When comparing the results of different positions, the ANOVA test found statistically significant differences among positions in both freeze-dryers ($p<0.05$). In both cases, central positions presented lower RMC values compared to the external positions. Surprisingly, this result is opposite to the vial edge effect described in the literature.

Nevertheless, it should be noted that the std of the 350 RMC results for each batch was similar to the SEP of the combined NIR model (0.068%). Therefore, the observed differences were of the same magnitude as the measurement error.

Finally, the influence of the strength and the freeze-dryer in the RMC values was studied using a two-way ANOVA. It should be noted that for one freeze-dryer there are 2 batches of one strength and 1 batch of the other strength. Both factors were significant (p=0.000), and the effect of them in RMC is described in Figure 8.31.

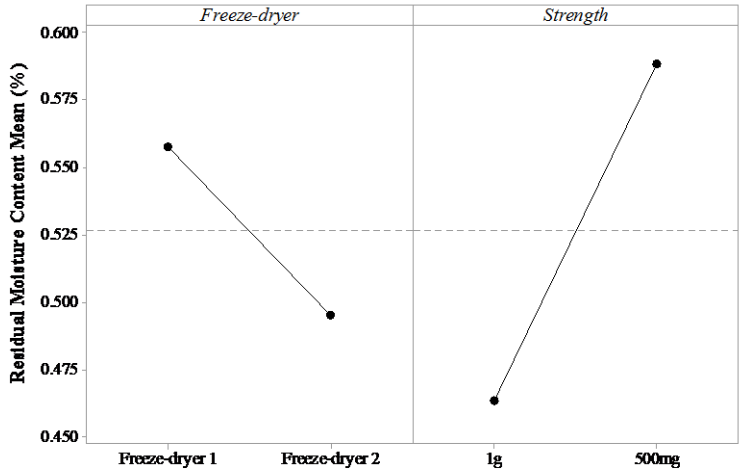

Figure 8.31. Main effects plot for RMC in IFDA drug product as a function of the freeze-dryer and the strength.

As observed in Figure 8.31, the average RMC of batches manufactured in Freeze-dryer 2 was lower that of the batches manufactured in Freeze-dryer 1. Moreover, the average of the three PPQ batches of IFDA 1 g was lower than that of IFDA 500 mg batches. Finally, Figure 8.32 represents a summary of the statistical analysis in a graphical representation of the average RMC and its 95% confidence interval for each batch as a function of the freeze-dryer and the strength.

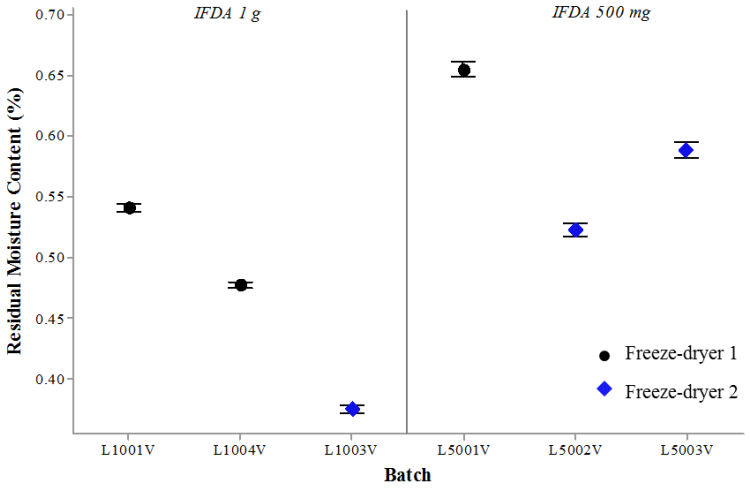

Figure 8.32. Interval plot of RMC %. Error bars correspond to 95% CI for the mean.

Then, under the same process conditions, Freeze-dryer 2 was able to dry vials a little bit more. One potential explanation of this finding could be that Freeze-dryer 2 is newer than Freeze-dryer 1. In this

case, the obtained result emphasizes that a regular and systematic application of engineering maintenance to equipment is extremely necessary to ensure their proper functionality and to reduce their rate of deterioration.

Finally, based on the obtained statistical results, routine sampling should be performed in lower shelves (1 or 2) and in the external positions, in both freeze-dryers. However, in practical terms, all RMC results were <1%, with a very small intra-batch variability. Therefore, there risk of providing an inaccurate result if sampling is performed randomly in both freeze-dryers is almost null.

3.2. Analysis of residual moisture content in stability samples

First, the RMC results determined by KF at different stability time points are represented in Figure 8.33. It can be observed that RMC slightly increases across time, and higher RMC are obtained at 40ºC – 75% compared to 25ºC – 60%. Therefore, the storage condition may have an effect on RMC.

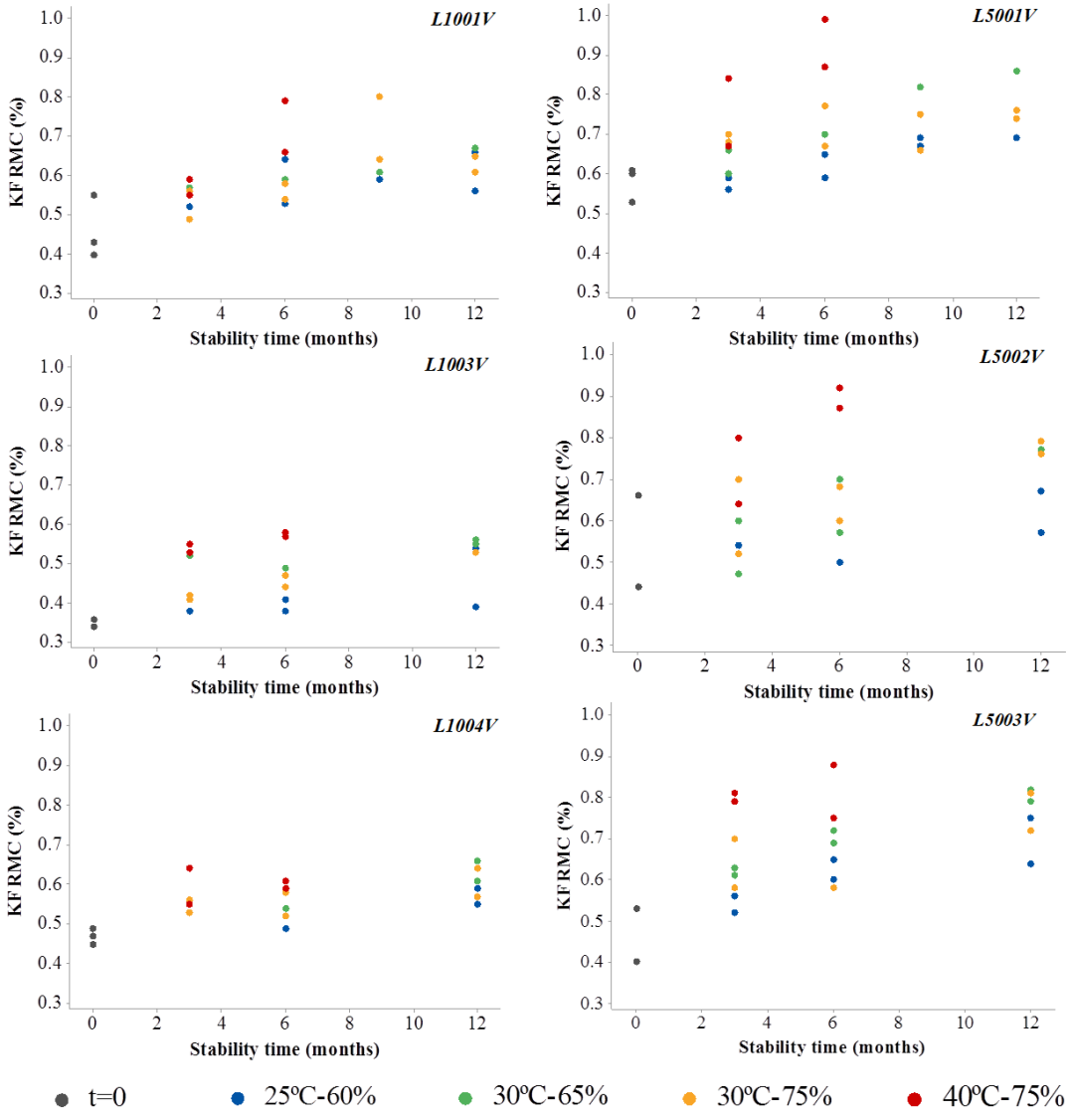

Figure 8.33. Scatterplot of KF vs stability time in IFDA 500 mg and 1 g drug product.

However, all samples represented in Figure 8.33 were analysed by the NIR model as well, to evaluate the ability of the NIR method to predict the RMC of stability samples.

First, potential differences in NIR spectra of samples stored at different conditions and time with respect to the calibration set of samples (used to develop the NIR model) were evaluated by PCA. Stability samples were projected to the scores plot of the calibration samples set of the combined NIR model. As observed in Figure 8.34, both sample sets completely overlapped in the scores plot, hence they belong to the same population.

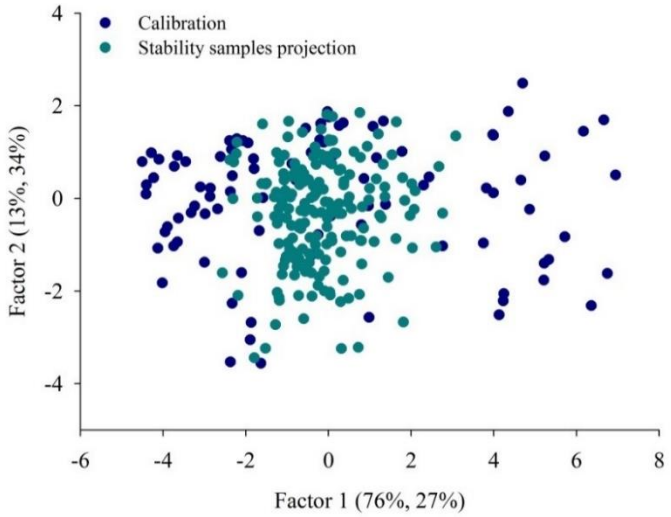

Figure 8.34. Scores plot of the calibration set of the combined NIR model (blue) with the projection of the stability samples (green)

In addition, no outliers were detected in the RMC predictions of the stability samples using the combined model. Consequently, these results suggest that there were no relevant changes in the NIR spectra. After that, the residuals were evaluated. Figure 8.35 and Figure 8.36 show the graphical representation of the residuals.

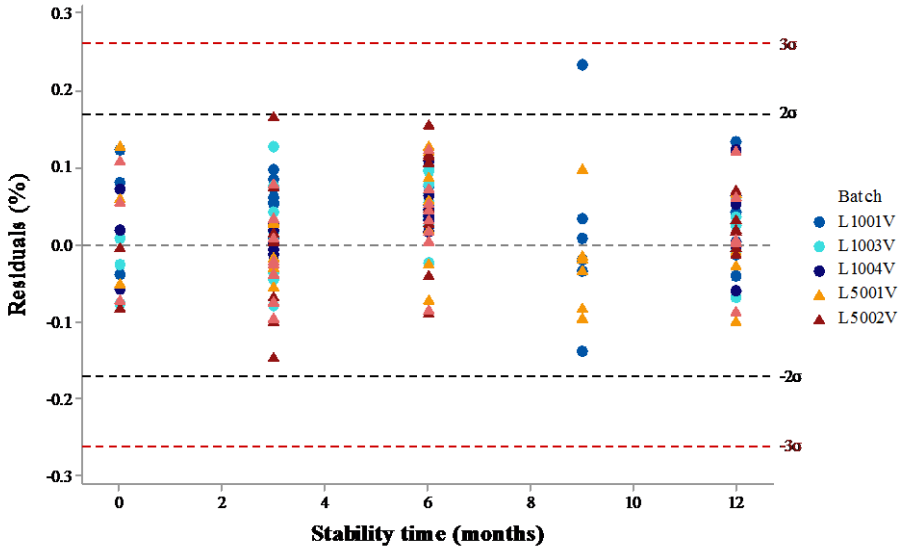

Figure 8.35. Graphical representation of the residuals (NIR-KF) vs storage time as a function of batch number.

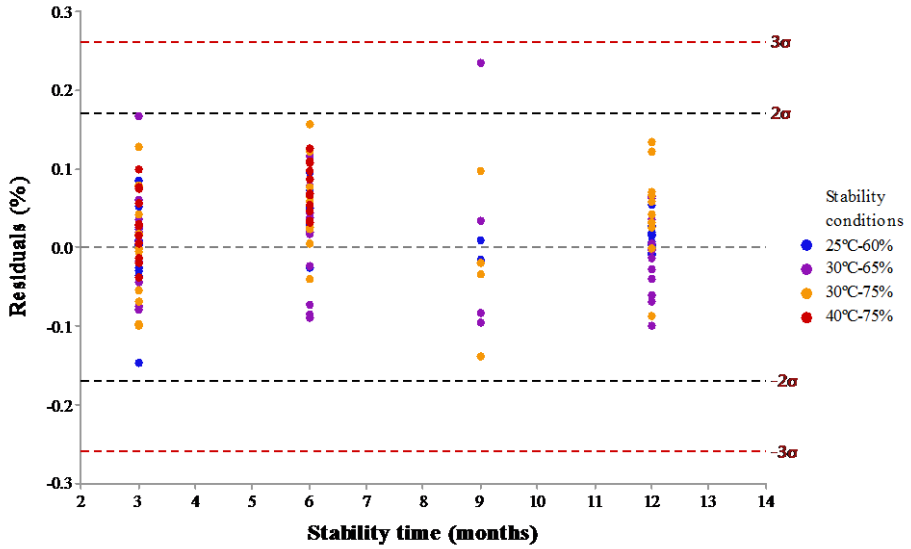

Figure 8.36. Graphical representation of the residuals (NIR-KF) vs storage time as a function of stability conditions.

First, the normal distribution of the residuals was verified (AD test, p=0.218). As observed in Figure 8.35 and Figure 8.36, all residuals laid within ±3σ. Hence, NIR showed a good agreement with the KF results in stability samples until 12 months at different storage conditions.

Finally, RMC results of stability samples were statistically analysed. For the 198 samples, a bias of 0.02 was determined, which showed no systematic errors. Afterwards, NIRS and KF results of each of the five time points were taken separately and analysed by Student's paired t-tests, to evaluate if significant differences between both methods were observed across time. Previously, F-test for variances of two samples were performed for each storage time and, in all cases, p>0.05, thus, both variances were equal.

Table 8.24. RMC means and std of samples from different stability time points determined by NIR and KF methods. The experimental t-values of the paired t-tests are included along with the p-values.

Time	n	RMC_{NIR} mean (%)	RMC_{KF} mean (%)	NIR std	KF std	t-value	p-value
0 M	17	0.48	0.47	0.108	0.097	0.82	0.425
3 M	48	0.59	0.58	0.113	0.104	1.19	0.240
6 M	48	0.68	0.63	0.145	0.138	6.26	0.000
9 M	12	0.68	0.69	0.075	0.077	-0.19	0.853
12 M	36	0.68	0.66	0.106	0.106	1.71	0.096

As observed in Table 8.24, NIR and KF means were not significantly different in all time points except at 6 months. To further evaluate this difference, a paired t-test was applied to 6 months' samples as a function of the storage condition. Statistical significant differences were observed in samples stored at 25ºC and 40ºC, while no differences were observed between the RMC mean of NIR and KF in samples stored at 30ºC. At 25ºC and 40ºC, almost all predicted RMC results by NIR were slightly higher than the RMC determined by KF. Unfortunately, no justification was found to explain this tendency.

Therefore, this statistical analysis will continue until the end of the stability studies to confirm the suitability of NIR for the determination of RMC in stability samples and try to find a potential justification of the difference between NIR and KF observed at 6 months.

4. Conclusions

It has been demonstrated that NIRS can be used as a primary method for RMC analyses in freeze-dried products, especially when it requires extensive sampling. In the six IFDA drug product PPQ batches, RMC results complied with the specification limit (≤ 5.0%)

The results of the freeze-dryers moisture mapping indicated that no practical differences were observed among shelves and positions, demonstrating RMC uniformity and freeze-drying process consistency in large-scale cGMP production. Hence, vials can be sampled from any of the shelves or positions in industrial batches.

However, RMC results of batches from industrial Freeze-dryer 2 were slightly lower than the RMC results obtained in batches from Freeze-dryer 1. Statistical significant differences were also found between IFDA strengths, where batches of IFDA 500 mg had higher RMC than that of IFDA 1 g. Nevertheless, the std of the 350 RMC results for each batch was similar to the SEP of the combined NIR model. Therefore, the observed differences were of the same magnitude as the measurement error.

Stability samples can be well predicted with the combined NIR model until 12 months of storage at the studied conditions. But, more stability points will be analysed by NIR and KF until product expiry date, to support this preliminary conclusion.

References

(1) Reich, G. Near-Infrared Spectroscopy and Imaging: Basic Principles and Pharmaceutical Applications. *Adv. Drug Deliv. Rev.* **2005**, *57* (8), 1109–1143.

(2) Bedi, S.; Balabathula, P.; Mandal, B.; Mittal, I.; Bhattacharjee, H. NIR Applications for Lyophilization of Biopharmaceuticals. *Am. Pharm. Rev.* **2012**, 1–7.

(3) EMA. Guideline on the Use of Near Infrared Spectroscopy (NIRS) by the Pharmaceutical Industry and the Data Requirements for New Submissions and Variations. European Medicines Agency; London, UK, 2014.

(4) European Pharmacopoeia. Ph. Eur. 8.0. Chapter 2.2.40. Near-Infraed Spectrophotometry. Council of Europe, Strasbourg, France, 2014.

(5) ICH. Harmonised Tripartite Guideline Q9 Quality Risk Management. 2011.

(6) Morton, M. A Quality-by-Design (QbD) Approach to Quantitative near-Infrared Continuous Pharmaceutical Manufacturing. *Am. Pharm. Rev.* **2011**, *14* (6), 106–113.

(7) Pikal, M. J.; Shah, S. Intravial Distribution of Moisture during the Secondary Drying Stage of Freeze Drying. *PDA J. Pharm. Sci. Technol.* **1997**, *51* (1), 17–24.

(8) Padalkar, M. V; Pleshko, N. Wavelength-Dependent Penetration Depth of Near Infrared Radiation into Cartilage. *Analyst* **2015**, *140* (7), 2093–2100.

(9) Delwiche, S. R.; Norris, K. H.; Pitt, R. E. Temperature Sensitivity of Near-Infrared Scattering Transmittance Spectra of Water-Adsorbed Starch and Cellulose. *Appl. Spectrosocopy* **1992**, *46* (5), 782–789.

(10) Jennings, T. *Lyophilization: Introduction and Basic Principles*; Informa Healthcare: New York, 2008.

(11) Roggo, Y.; Chalus, P.; Maurer, L.; Lema-Martinez, C.; Edmond, A.; Jent, N. A Review of Near Infrared Spectroscopy and Chemometrics in Pharmaceutical Technologies. *J. Pharm. Biomed. Anal.* **2007**, *44*, 683–700.

(12) Clavaud, M.; Roggo, Y.; Dégardin, K.; Sacré, P.-Y.; Hubert, P.; Ziemons, E. Moisture Content Determination in an Antibody-Drug Conjugate Freeze-Dried Medicine by near-Infrared Spectroscopy: A Case Study for Release Testing. *J. Pharm. Biomed. Anal.* **2016**, *131*, 380–390.

(13) Clavaud, M.; Roggo, Y.; Dégardin, K.; Sacré, P.; Hubert, P.; Ziemons, E. Global Regression Model for Moisture Content Determination Using near-Infrared Spectroscopy. *Eur. J. Pharm. Biopharm.* **2017**, *119*, 343–352.

(14) FDA. Guidance for Industry, PAT- A Framework for Innovative Pharmaceutical Development, Manufacturing, and Quality Assurance. U.S. Department of Health and Human Services Food and Drug Administration: Rockville, MD, 2004.

(15) FDA. Guidance for Industry, Development and Submission of Near Infrared Analytical Procedures Guidance for Industry. U.S. Department of Health and Human Services Food and Drug Administration: Silver Spring, MD, 2015.

(16) ICH. Harmonised Tripartite Guideline Q2(R1) Validation of Analytical Procedures: Text and Methodology. 2005.

(17) European Pharmacopoeia. Ph. Eur. 8.7. Chapter 5.21. Chemometric Methods Applied to Analytical Data. Council of Europe, Strasbourg, France, 2016.

(18) ASTM E1655-05, Standard Practices for Infrared Multivariate Quantitative Analysis, ASTM International, West Conshohocken, PA, 2005, Www.astm.org.

(19) Blanco, M.; Alcalà, M. Multivariate Calibration for Quantitative Analysis. In *Infrared Spectroscopy for Food Quality*

Analysis and Control; Sun, D.-W., Ed.; Academic Press: USA, 2009; pp 51–82.

(20) Zheng, Y.; Lai, X.; Wrang Bruun, S.; Ipsen, H.; Larsen, J. N.; Løwenstein, H.; Søndergaard, I.; Jacobsen, S. Determination of Moisture Content of Lyophilized Allergen Vaccines by NIR Spectroscopy. *J. Pharm. Biomed. Anal.* **2008**, *46*, 592–596.

(21) Ronkart, S. N.; Paquot, M.; Fougnies, C.; Deroanne, C.; Van Herck, J. C.; Blecker, C. Determination of Total Water Content in Inulin Using the Volumetric Karl Fischer Titration. *Talanta* **2006**, *70* (5), 1006–1010.

(22) European Pharmacopoeia. Ph. Eur. 8.0. Chapter 2.5.12. Water: Semi-Micro Determination. Council of Europe, Strasbourg, France, 2014.

(23) Miller, J. N.; Miller, J. C. *Statistics and Chemometrics for Analytical Chemistry*, 6th ed.; Pearson Education Limited: Harlow, England, 2010.

(24) Bhar, L. Non-Parametric Tests. In *Advances in Data Analytical Techniques. Module III Diagnostics and Remedial Measures*; pp 57–68.

(25) Miller, C. E.; Box, P. O.; Law, B. Sources of Non-Linearity in near Infrared Methods. *NIR news* **1993**, *4* (6), 3–5.

(26) Haaland, D. M.; Thomas, E. V. Partial Least-Squares Methods for Spectral Analyses. 1. Relation to Other Quantitative Calibration Methods and the Extraction of Qualitative Information. *Anal. Chem.* **1988**, *60* (11), 1193–1202.

(27) Arruabarrena, J.; Coello, J.; Maspoch, S. Enhancing Sensitivity and Precision on Nir Reflectance Determination of an Api at Low Concentration: Application to an Hormonal Preparation. *J. Pharm. Biomed. Anal.* **2012**, *60*, 59–64.

(28) Fearn, T. The Interaction between Standard Normal Variate and Derivatives. *NIR news* **2008**, *19* (7), 16.

(29) Boqué, R.; Vander Heyden, Y. The Limit of Detection. *LCGC Eur.* **2009**, *22* (2), 82–85.

(30) MacDougall, D.; Amore, F. J.; Cox, G. V; Lai, J.; Langner, R. R.; Crosby, D. G.; Estes, F. L.; Mcclelland, N. I.; Phillips, W. F.; Freeman, D. H.; et al. Guidelines for Data Acquisition and Data Quality Evaluation in Environmental Chemistry. *Anal. Chem.* **1980**, *52* (14), 2242–2249.

(31) Andrade-Garda, J.; Carlosena-Zubieta, A.; Gómez-Carracedo, M.; Maestro-Saavedra, M.; Prieto-Blanco, M.; Soto-Ferreiro, R. *Problems of Instrumental Analytical Chemistry A Hands-On Guide*; World Scientific: Covent Garden, London, 2017.

(32) Analytical Methods Committee. Recommendations for the Definition, Estimation and Use of the Detection Limit. *Analyst* **1987**, *112*, 199–204.

(33) Allegrini, F.; Olivieri, A. C. IUPAC-Consistent Approach to the Limit of Detection in Partial Least-Squares Calibration. *Anal. Chem.* **2014**, *86*, 7858–7866.

(34) Ortiz, M. C.; Sánchez, M. S.; Sarabia, L. A. 1.05 Quality of Analytical Measurements: Univariate Regression. In *Comprehensive Chemometrics. Chemical and Biochemical Data Analysis*; Brown, S. D., Tauler, R., Walczak, B., Eds.; Elsevier B.V., 2009; pp 127–169.

(35) International Organization for Standardization. ISO 11843-1. Capability of Detection. Part 1: Terms and Definitions. *Genève* **1997**.

(36) IUPAC. Nomenclature in Evaluation of Analytical Methods Including Detection and Quantification Capabilities. *Pure Appl. Chem.* **1995**, *67*, 1699–1723.

(37) Currie, L. A. Detection and Quantification Limits: Origins and Historical Overview. *Anal. Chim. Acta* **1999**, *391*, 127–134.

(38) Ortiz, M. C.; Sarabia, L. A.; Herrero, A.; Sánchez, M. S.; Sanz, M. B.; Rueda, M. E.; Giménez, D.; Meléndez, M. E. Capability of Detection of an Analytical Method Evaluating False Positive and False Negative (ISO 11843) with Partial Least Squares. *Chemom. Intell. Lab. Syst.* **2003**, *69*, 21–33.

(39) Olivieri, A. C. Practical Guidelines for Reporting Results in Single- and Multi-Component Analytical Calibration: A Tutorial. *Anal. Chim. Acta* **2015**, *868*, 10–22.

(40) Ortiz, M. C.; Sarabia, L. A.; Sánchez, M. S. Tutorial on Evaluation of Type I and Type II Errors in Chemical Analyses: From the Analytical Detection to Authentication of Products and Process Control. *Anal. Chim. Acta* **2010**, *674* (2), 123–142.

(41) Lorber, A.; Faber, K.; Kowalski, B. R. Net Analyte Signal Calculation in Multivariate Calibration. *Anal. Chem.* **1997**,

69, 1620–1626.

(42) Boqué, R.; Larrechi, M. S.; Rius, F. X. Multivariate Detection Limits with Fixed Probabilities of Error. *Chemom. Intell. Lab. Syst.* **1999**, *45*, 397–408.

(43) Ostra, M.; Ubide, C.; Vidal, M.; Zuriarrain, J. Detection Limit Estimator for Multivariate Calibration by an Extension of the IUPAC Recommendations for Univariate Methods. *Analyst* **2008**, *133*, 532–539.

(44) Klaas, N.; Faber, M.; Bro, R. Standard Error of Prediction for Multiway PLS 1. Background and a Simulation Study. *Chemom. Intell. Lab. Syst.* **2002**, *61*, 133–149.

(45) Blanco, M.; Castillo, M.; Peinado, A.; Beneyto, R. Determination of Low Analyte Concentrations by near-Infrared Spectroscopy: Effect of Spectral Pretreatments and Estimation of Multivariate Detection Limits. *Anal. Chim. Acta* **2007**, *581*, 318–323.

(46) Alcalà, M.; León, J.; Ropero, J.; Blanco, M.; Romañach, R. J. Analysis of Low Content Drug Tablets by Transmission near Infrared Spectroscopy: Selection of Calibration Ranges according to Multivariate Detection and Quantitation Limits of PLS Models. *J. Pharm. Sci.* **2008**, *97* (12), 5318–5327.

(47) Lorber, A. Error Propagation and Figures of Merit for Quantification by Solving Matrix Equations. *Anal. Chem.* **1986**, *58*, 1167–1172.

(48) Brown, C. D. Discordance between Net Analyte Signal Theory and Practical Multivariate Calibration. *Anal. Chem.* **2004**, *76* (15), 4364–4373.

(49) Olivieri, A. C.; Bortolato, S.; Allegrini, F. Figures of Merit in Multiway Calibration. In *Data Handling in Science and Technology, Vol 29.*; Elsevier B.V., 2015; pp 541–575.

(50) ICH. Harmonised Tripartite Guideline Q2(R1) Validation of Analytical Procedures: Text and Methodology. 2009.

(51) Muzzio, C. R.; Dini, N. G.; Simionato, L. D. Determination of Moisture Content in Lyophilized Mannitol through Intact Glass Vials Using NIR Micro-Spectrometers. *Brazilian J. Pharm. Sci.* **2011**, *47* (2), 289–297.

(52) Grohganz, H.; Gildemyn, D.; Skibsted, E.; Flink, J. M.; Rantanen, J. Towards a Robust Water Content Determination of Freeze-Dried Samples by near-Infrared Spectroscopy. *Anal. Chim. Acta* **2010**, *676*, 34–40.

(53) Stokvold, A.; Dyrstad, K.; Libnau, F. O. Sensitive NIRS Measurement of Increased Moisture in Stored Hygroscopic Freeze Dried Product. *J. Pharm. Biomed. Anal.* **2002**, *28*, 867–873.

(54) Broad, N.; Graham, P.; Hailey, P.; Hardy, A.; Holland, S.; Hughes, S.; Lee, D.; Prebble, K.; Salton, N.; Warren, P. Guidelines for the Development and Validation of Near-Infrared Spectroscopic Methods in the Pharmaceutical Industry. In *Handbook of Vibrational Spectroscopy*; Chalmers, J. M., Griffiths, P. R., Eds.; John Wiley & Sons Ltd: Chichester, UK, 2002.

(55) Olivieri, A. C.; Bortolato, S.; Allegrini, F. Figures of Merit in Multiway Calibration. In *Fundamentals and Analytical Applications of Multi-way Calibration*; Elsevier B.V., 2015; Vol. 29, pp 541–575.

(56) Rasetto, V.; Marchisio, D. L.; Fissore, D.; Barresi, A. A. On the Use of a Dual-Scale Model to Improve Understanding of a Pharmaceutical Freeze-Drying Process. *J. Pharm. Sci.* **2010**, *99* (10), 4337–4350.

(57) Gan, K. H.; Bruttini, R.; Crosser, O. K.; Liapis, A. I. Freeze-Drying of Pharmaceuticals in Vials on Trays: Effects of Drying Chamber Wall Temperature and Tray Side on Lyophilization Performance. *Int. J. Heat Mass Transf.* **2005**, *48*, 1675–1687.

(58) Barresi, A. A.; Velardi, S. A.; Pisano, R.; Rasetto, V.; Vallan, A.; Galan, M. In-Line Control of the Lyophilization Process. A Gentle PAT Approach Using Software Sensors. *Int. J. Refrig.* **2009**, *32* (5), 1003–1014.

(59) Sane, S. U.; Hsu, C. C. Considerations for Successful Lyophilization Process Scale-Up, Technology Transfer, and Routine Production. In *Formulation and Process Development Strategies for Manufacturing Biopharmaceuticals*; Jameel, F., Hershenson, S., Eds.; John Wiley & Sons, Inc: New Jersey, 2010; pp 797–826.

(60) Greiff, D. Factors Affecting the Statistical Parameters and Patterns of Distribution of Residual Moistures in Arrays of Samples Following Lyophilization. *J. Parenter. Sci. Technol. 44* (3), 118–129.

(61) Bindschaedler, C. Lyophilization Process Validation. In *Freeze-Drying/Lyophilization Of Pharmaceutical & Biological Products*; Rey, L., May, J. C., Eds.; Marcel Dekker, Inc: London, UK, 2004; p 535.

(62) Rey, L. Glimpses into the Realm of Freeze-Drying: Classical Issues and New Ventures. In *Freeze-Drying/Lyophilization of Pharmaceutical and Biological Products*; Rey, L., May, J. C., Eds.; Informa Healthcare:

London, UK, 2010; pp 1–28.

(63) ICH. Harmonised Tripartite Guideline Q1A(R2) Stability Testing of New Drug Substances and Products. 2003.

(64) ICH. Harmonised Tripartite Guideline Q1F. Stability Data Package for Registration Applications in Climatic Zones III and IV. 2006.

(65) Olivieri, A. C. Analytical Figures of Merit: From Univariate to Multiway Calibration. *Chem. Rev.* **2014**, *114*, 5358−5378.

(66) Allegrini, F.; Olivieri, A. C. Recent Advances in Analytical Figures of Merit: Heteroscedasticity Strikes Back. *Anal. Methods* **2017**, *9*, 739–743.

CONCLUSIONS

Conclusions

Specific conclusions of the work carried out have been detailed at the end of each chapter and section. The following are the general conclusions that can be drawn from the experimental work performed in this Doctoral Thesis, in relation to the objectives presented at the beginning of the manuscript.

1. It was demonstrated that optimum freeze-drying processes for two drug products (IFDA and IFDB) can be developed at laboratory scale using a quality by design approach. The use of risk-based approaches provided more knowledge about the product and the process allowing for a successful scale-up and qualification of the freeze-drying process at industrial scale.
    a. The use of risk assessment tools, like cause and effect matrix and FMEA, had proven to be very useful to establish the experimental strategy for the freeze-drying processes development and qualification.
    b. The thermal fingerprint of both formulations was determined using different analytical techniques (DSC, FDM, and X-ray). In IFDA solutions, no critical temperature was found by either DSC or FDM. In IFDB solutions, low cooling rates (1ºC/min) allowed mannitol crystallization while keeping the API in an amorphous state. The introduction of annealing did not improve either the process efficiency or the quality of the IFDB drug product.
    c. Based on the understanding of the formulation and the use of design of experiments and risk analysis tools, the operating ranges for shelf temperature, chamber pressure and time were established, resulting in a more flexible freeze-drying process.
    d. Regarding the secondary drying, the results of the CQAs of the drug product obtained using different secondary drying temperatures and durations complied with the specifications in all extraction times. There were no great differences in RMC results over the studied ranges of temperature and durations. Therefore, the chosen secondary drying conditions were 40ºC and 3 h for IFDA, and 35ºC and 4h for IFDB.
    e. For the study of the primary drying stage, a Doehlert design was executed with two factors, shelf temperature and chamber pressure, and four responses: primary drying time, appearance, RMC and RT for each product. Statistical significant MLR models were obtained for RMC and primary drying time in IFDA drug product, and RT and primary drying time for IFDB. The best fit and predictive ability was observed in the MLR models for primary drying time, in which temperature was the predominant factor to predict its duration. Based on the obtained models for each product, optimal primary drying conditions were selected with the focus on minimizing the duration of primary drying while preserving the quality of the product. The chosen conditions for IFDA formulation were 35°C and 0.450 mbar, while 5ºC and 0.280 mbar resulted in proper conditions for IFDB. In both cases, the expected total

cycle duration at industrial scale was less than 2 days. Finally, a design space for this stage was defined, where the fulfilment of all quality attributes was confirmed.

f. Before the freeze-drying process transfer to industrial scale, it has been confirmed that the sublimation rate of freeze-drying process with the most extreme primary drying conditions took place within the capabilities of mass transfer and heat energy of the industrial freeze-dryer. In addition, the performance of the scale-up batch and PPQ batches were satisfactory, and the finished product complied with all CQAs specifications at t=0 and t=12 months of the stability studies, performed following ICH guidelines. It was demonstrated that with only three batches per strength, the process was qualified for RMC giving capability indices (P_{pU} and LCCB) > 1. Finally, it was concluded that the manufacturing process, as described and executed, can be considered suitable for the implementation in routine production. Furthermore, using the QbD approach, deviations in the set-points conditions can be tolerated as long as they remain within the design space.

2. It was evidenced that NIR spectroscopy can be used as an alternative method for RMC analyses in IFDA 500 mg and 1 g drug products.
   - During the feasibility study, some risk was found in two parameters: the duration of exposition to the lamp and age of samples. Conclusions were that vials must be taken away from the lamp after each scanning. Moreover, KF analyses must be carried out with no more than 7 days after NIR spectra acquisition.
   - Two individual PLS models for each strength were developed and successfully validated. In addition, another PLS model combining both IFDA strengths was developed and validated over the RMC range of 0.2%-1.5%, which represented a benefit from an industrial point of view. For the combined model, the pre-treatment chosen was the 2Der + SNV over the range from 1350 nm to 2100 nm. The model explained 98% of RMC variability with 2 factors with a low RMSEP (0.057%). An intercept value of 0.013 ± 0.023 and a slope of 0.982 ± 0.028 were observed for reference *vs* predicted NIR.
   - The estimation of LOD using the ICH formula and the $S_{y/x}$ from least squares orthogonal regression is suggested because it gives an estimation by using a very simple calculation procedure that has been proved to be in good agreement with the experimental results. This approach highlights the need of estimating the calibration concentration uncertainties in a reliable manner. Moreover, it was demonstrated that the LOQ value was acceptable since the relative error of the predictions above LOQ were small and uniform throughout the RMC range.
   - It has been shown that the drying stage of the freeze-drying process was homogeneous by analysing 350 vials per batch from different shelves and positions within the freeze-dryer. The results of the two industrial freeze-dryers moisture mappings indicated that no practical

differences are observed among shelves and positions. Therefore, the routine sampling was reduced, and it could be performed randomly. Although the difference between RMC averages of the two freeze-dryers was very small, statistical significant differences were found, which demonstrates the relevance of equipment maintenance plans for the design of robust processes.

- It was demonstrated that stability samples can be well predicted with the combined NIR model up to 12 months of storage at the studied conditions.

3. This freeze-drying development and qualification study, including the NIR method, was presented in a QbD-variation of the IFDA dossier to the Spanish Agency (AEMPS). The most important outcomes were the reduction of the variation type (from II to IB) and a significant reduction in the variation approval time.